



Florian Wolfgang Krainer, Bakk.rer.nat. MSc

**Production and characterization
of recombinant plant peroxidases
in *Pichia pastoris***

DOCTORAL THESIS

to achieve the university degree of

Doktor der Naturwissenschaften

submitted to

Graz University of Technology

Supervisor

Ao.Univ.-Prof. Mag. Dr.rer.nat. Anton Glieder

Institute of Molecular Biotechnology

AFFIDAVIT

I declare that I have authored this thesis independently, that I have not used other than the declared sources/resources, and that I have explicitly indicated all material which has been quoted either literally or by content from the sources used. The text document uploaded to TUGRAZonline is identical to the present doctoral thesis.

23.04.15

Date

Alice Kri

Signature

- Danksagung -

Am Ende meines Studiums möchte ich mich bei einigen Menschen herzlich bedanken:

Meinen Eltern, die mich ausnahmslos in all meinen Unternehmungen unterstützten, förderten und bestärkten, und meiner Schwester, die mir immer zur Seite stand und wohnte (haha) und stets zur Erweiterung meines Horizonts beitrug.

Meiner Freundin Ziska, deren unvergleichliche Geduld und Rückhalt die größte Unterstützung waren, die ich mir vorstellen kann.

Meinem Betreuer Toni (Ao. Univ.-Prof. Dr. Mag. rer. nat. Anton Glieder), der mir diese faszinierende und vielseitige Dissertation ermöglicht hat und mir die Freiheit ließ, selbstständig und weitestgehend unabhängig Wissenschaft zu erleben.

Allen Generationen der Gliedergruppe, die mich während meiner Dissertation begleiteten und die der Arbeit (und daneben) die nötige Menge Spaß hinzufügten. Ganz besonders möchte ich meiner Masterstudentin Michi Gerstmann, meiner studentischen Mitarbeiterin Astrid Weninger und den Projektstudentinnen Caro Kunz, Jasmin Fischer und Patricia Knabl für ihre Beiträge danken. Weiters möchte ich Christian Schmid danken, dessen großartiges Labormanagement den Laden am Laufen hält und der immer weiß, wo was ist und wann was nachkommt. Außerdem möchte ich der unermüdlichen Amneris Schlager-Weidinger danken, deren Hilfe gar nicht genug geschätzt werden kann. Ich möchte auch Institutsvorstand Prof. Helmut Schwab, Sissy Schmerzeck, Eveline Schemitsch-Hirmke und allen anderen Angestellten des IMBT für ihre Hilfe und eine einzigartige Zeit danken.

Oliver Spadiut und seinem Team von der TU Wien für eine großartige Kollaboration, die maßgeblich zum Erfolg dieser Arbeit beigetragen hat.

Andy Munro und seinem Team, insbesondere Kirsty McLean, die mir einen großartigen Aufenthalt in Manchester ermöglichten, der mir noch lange in Erinnerung bleiben wird.

Vielen Dank :)

- Abstract -

Horseradish peroxidases (HRPs) are enzymes of high demand for applications in diagnostics and immunohistochemistry, biotechnology and medicine until now and ongoing. However, current HRP preparations are typically isolated from plant roots as varying mixtures of isoenzymes and previous attempts for recombinant HRP production in common host organisms were limited at low yields.

In the course of this thesis, successive optimization studies were employed to establish a competitive recombinant production system using the methylotrophic yeast *Pichia pastoris*, and to enable new applications of HRP by its recombinant production. Inactivation of a key mannosyltransferase activity allowed the production of homogeneously glycosylated recombinant HRP, facilitating downstream processing. Optimization of cultivation media by supplementation with hemin was shown to effectively saturate secreted apo-HRP with the essential heme cofactor. A combination of a signal peptide mutant for enhanced secretion with strong methanol-independent production of HRP and coproduction of Hac1 to activate the unfolded protein response were found to enhance the yields of volumetric and specific HRP activities. Recombinant production of the well-studied isoenzyme C1A, the acidic isoenzyme A2A and the basic isoenzyme E5 enabled comprehensive comparative characterizations thereof, revealing distinct features of the isoenzymes which can now be exploited in novel and improved applications. In order to demonstrate the broad applicability of recombinant HRP, it was further applied as reporter enzyme in a metabolic engineering study and in a HRP-protein G fusion protein forming a well-defined construct for applications in diagnostics and immunohistochemistry.

Keywords

Horseradish peroxidase, plant peroxidase, heme cofactor, *Pichia pastoris*, recombinant protein production, protein purification, enzyme characterization, strain engineering, fusion protein, protein G, immunohistochemistry

- Kurzfassung -

Meerrettich Peroxidasen (HRPs) sind nach wie vor Enzyme mit großer Nachfrage in Anwendungen der Diagnostik und Immunhistochemie, der Biotechnologie und der Medizin. Allerdings werden aktuelle HRP Präparationen üblicherweise als uneinheitliche Mischungen von Isoenzymen aus Pflanzenwurzeln isoliert und bisherige rekombinante Produktionsversuche in gängigen Wirtsorganismen waren durch niedrige Ausbeuten limitiert.

Im Zuge dieser Dissertation wurden sukzessive Optimierungsstudien durchgeführt, um ein wettbewerbsfähiges rekombinantes Produktionssystem in der methylophilen Hefe *Pichia pastoris* zu etablieren, und um mit dessen Hilfe neue Anwendungen der HRP zu ermöglichen. Das Downstream Processing konnte durch Inaktivierung einer Schlüsselmannosyltransferaseaktivität erleichtert werden, wodurch die Produktion homogen glycosylierter rekombinanter HRP möglich wurde. Eine erfolgreiche Sättigung sekretierter apo-HRP mit dem essentiellen Häm Kofaktor konnte mit einer Optimierung der Kultumedien durch Heminzugabe gezeigt werden. Die Kombination einer Signalpeptidmutante für gesteigerte Sekretion mit starker Methanol-unabhängiger HRP Produktion und Hac1-Koproduktion zur Aktivierung der Unfolded Protein Response führte zu erhöhten Ausbeuten der volumetrischen und spezifischen HRP Aktivitäten. Rekombinante Produktion des gut untersuchten Isoenzym C1A, des sauren Isoenzym A2A und des basischen Isoenzym E5 ermöglichte deren umfassende vergleichende Charakterisierung, welche die ausgeprägten individuellen Eigenschaften der Isoenzyme offenbarte, die nun in neuen und verbesserten Anwendungen eingesetzt werden können. Um die breite Anwendbarkeit rekombinanter HRP zu zeigen, wurde das Enzym überdies als Reporter in einer Studie zu Metabolic Engineering und in einem HRP-Protein G Fusionsprotein verwendet. Letzteres findet als hochdefiniertes Konstrukt Anwendung in der Diagnostik und Immunhistochemie.

Keywords

Meerrettich Peroxidase, Pflanzenperoxidase, Häm Kofaktor, *Pichia pastoris*, rekombinante Proteinproduktion, Proteinaufreinigung, Enzymcharakterisierung, Stamm Engineering, Fusionsprotein, Protein G, Immunhistochemie

- Table of contents -

Danksagung	I
Abstract	II
Kurzfassung	III
Table of contents.....	IV
Introduction & aims of this thesis	1
Chapter 1 An updated view on horseradish peroxidases: recombinant production and biotechnological applications	9
Chapter 2 Purification and basic biochemical characterization of 19 recombinant plant peroxidase isoenzymes produced in <i>Pichia pastoris</i>	25
Chapter 3 Knockout of an endogenous mannosyltransferase increases the homogeneity of glycoproteins produced in <i>Pichia pastoris</i>	35
Chapter 4 Optimizing cofactor availability for the production of recombinant heme peroxidase in <i>Pichia pastoris</i>	49
Chapter 5 Systematic assessment of strategies for improved production of recombinant plant peroxidase in <i>Pichia pastoris</i>	59
Chapter 6 Characterization of recombinant horseradish peroxidase isoenzymes from <i>Pichia pastoris</i>	82
Chapter 7 Recombinant protein expression in <i>Pichia pastoris</i> strains with an engineered methanol utilization pathway	122
Chapter 8 Biotechnological production of a peroxidase-protein G fusion protein in <i>Pichia pastoris</i>	137
Chapter 9 Protocol for the production and purification of recombinant horseradish peroxidase from <i>Pichia pastoris</i>	150
Conclusions and outlook	168
Appendix	172
<i>Curriculum vitae</i>	184

- Introduction and aims of this thesis -

Horseradish peroxidases (HRPs) are class III plant peroxidases [1] found in *Armoracia rusticana*, horseradish. They are assigned to the EC number 1.11.1.7 and typically catalyze the oxidation of reducing substrates upon reduction of a peroxide species [2]. HRPs are predominantly alpha-helical globular proteins [3] with a carbohydrate content of up to 22% [4, 5] when isolated from plant. The formation of four disulfide bridges [6] as well as a covalently bound heme cofactor [7] are essential in order to form functionally active enzyme. Similar to class III peroxidases from the model plant *Arabidopsis thaliana* [8], *A. rusticana* possesses a large gene family encoding HRP isoenzymes with different biochemical properties [9, 10]. So far however, only a small number of these isoenzymes had been characterized in detail and the vast majority of studies focused on a single isoenzyme, C1A. HRPs are nowadays employed in a broad range of applications in the fields of life sciences, biotechnology and medicine. Particularly the well-characterized isoenzyme C1A is a high-demand enzyme due to its long-lasting use in "classical" HRP applications such as in immunohistochemistry and diagnostic kits. Current commercial HRP preparations are usually derived from plant root isolates consisting of varying mixtures of HRP isoenzymes. The actual isoenzyme content of such isolates varies in response to uncontrollable environmental factors [11], considerably affecting reproducibility and quality of the preparations. The production of a particular HRP isoenzyme of choice in a controllable and reproducible recombinant process therefore presents an attractive alternative. However, recombinant HRP production processes in well-established host organisms such as *Escherichia coli* [12, 13] or *Saccharomyces cerevisiae* [14, 15] were limited at non-competitive yields in the lower mg/L range at most.

The major aims of this thesis were:

- 1) The establishment of a competitive recombinant production system for HRP including suitable production strains and a thorough production process.
- 2) An in-depth comparative enzymological characterization of different recombinantly produced HRP isoenzymes.
- 3) The use of recombinantly produced HRP activity in applications of present-day relevance.

A comprehensive overview on previous HRP research is given in **Chapter 1**. The review highlights most current discoveries and enzymological features that are of particular biotechnological relevance. The main focus of the review lies on strategies for recombinant HRP production and on the broad diversity of traditional and upcoming applications for HRP.

To date, the methylotrophic yeast *P. pastoris* (formally *Komagataella pastoris* or *K. phaffii* [16]) is one of the most commonly used eukaryotic production host organisms in industry and research, as reviewed previously, *e.g.* [17–19]. Most notably, the Food and Drug Administration (FDA) of the United States Department of Health and Human Services declared *P. pastoris* as "Generally Recognized As Safe" (GRAS)* due to the general absence of hazardous biological compounds such as endotoxins or viral DNA in products from this yeast. Moreover, proteins passing through the secretory pathway can be subjected to typical modifications of eukaryotic proteins such as disulfide bridge formation or glycosylation, which might be essential for the stability and activity of target enzymes. *P. pastoris* can be grown to high cell densities (*i.e.* 160 g/L dry cell weight [20]) in bioreactor cultivations enabling high volumetric productivities. Yields of secreted target protein of more than 18 g/L have been described recently [21], demonstrating the remarkable production capacities of this host. However, the actual production performance depends on the target protein and a rationale on pivotal product parameters remained elusive so far. Therefore, recombinant protein production in *P. pastoris* requires assessment on a case-by-case basis and may necessitate individual optimization endeavors such as engineering of the production strain and process for maximum yield of a particular target protein. In the case of recombinant HRP production in *P. pastoris*, reported yields were higher than from *S. cerevisiae*, albeit still in the lower mg/L range [15, 22, 23]. Thus, recombinant HRP production in *P. pastoris* has been predominantly limited to its use as reporter enzyme in studies on strain development and process design, *e.g.* [24–27]. In order to develop *P. pastoris* further towards an effective host system for competitive production of recombinant HRP, a series of studies was performed.

Apart from low yields, the downstream processing of recombinant HRP from *P. pastoris* presents a particular challenge. The applicability of classical purification approaches such as

* http://www.accessdata.fda.gov/scripts/fdcc/?set=GRASNotices&id=204&sort=GRN_No&order=DESC&startrow=1&type=basic&search=pichia%20pastoris (accessed Apr 2015)

ion exchange chromatography or hydrophobic interaction chromatography is limited by yeast-type hyperglycosylation of recombinant HRP. Nevertheless, a substantial purification of the HRP isoenzyme C1A could be shown previously [28] when hydrophobic charge induction chromatography was performed in flowthrough mode. In **Chapter 2**, a two-step purification protocol is described, combining the previously published flowthrough purification strategy with a subsequent anion exchange flowthrough step. This strategy was applied to 19 recombinant HRP isoenzymes, that were produced in *P. pastoris* from synthetic codon-optimized genes based on HRP sequences found in the transcriptome of *A. rusticana* [10]. A correlation was found between the degree of glycosylation of the HRP isoenzymes and the success of the described double-flowthrough purification strategy in terms of purification factor and enzyme recovery. Consequently, the obtained preparations of the studied recombinant HRP isoenzymes were of varying purity. Nevertheless, in basic characterizations of the obtained preparations, the recombinant HRP isoenzymes could be shown to possess distinct substrate specificities, emphasizing the importance of a recombinant production system which allows the production of individual isoenzymes as opposed to the inconsistent mixture of isoenzymes that is isolated from plant roots.

The heterogeneous hyperglycosylation mentioned above is typical for secretory proteins derived from yeast. In some cases, glycosylation was found to affect protein properties such as folding, stability or enzymatic activity whereas in others no effect could be observed [29]. Previous studies on deglycosylated HRP described ambiguous results [30–32] with respect to the effect of deglycosylation on enzyme structure or activity. Generally, the presence of glycans on HRP can be assumed to either have a neutral or even positive effect, considering the carbohydrate content of native HRP from plant [5]. However, the high degree of heterogeneity of yeast-type hyperglycosylation considerably impedes downstream processing. Thus, strain engineering had to be performed in order to produce homogeneously glycosylated recombinant HRP in *P. pastoris*, as described in **Chapter 3**. The *OCH1* encoded α -1,6-mannosyltransferase of the yeast Golgi apparatus is a key glycotransferase in the initiation of yeast-type N-hyperglycosylation [33]. A *P. pastoris* strain with deleted *OCH1* ORF showed an altered growth and colony phenotype accompanied by rearrangements of cell wall components. Most importantly however, recombinant HRP from this strain was homogeneously glycosylated, facilitating its downstream processing considerably.

A covalently bound heme cofactor is essential for the enzymatic activity of HRP. However, the limited availability of endogenous heme in *P. pastoris* is considered a major bottleneck in recombinant HRP production. **Chapter 4** deals with endeavors to maximize cofactor availability throughout the production of recombinant HRP. In contrast to previous results in *S. cerevisiae* [34], overexpression of genes of the heme biosynthesis pathway in *P. pastoris* could not improve the yield of active heme enzyme. However, supplementation of production media with hemin proved to be an easy-to-do strategy to effectively saturate secreted apo-HRP with cofactor, yielding considerably increased target enzyme activities.

With the methodological tools described in the Chapters 3 and 4 at hand, a set of strategies was systematically assessed to maximize recombinant HRP yields from *P. pastoris* (**Chapter 5**). Secretion directed by the *S. cerevisiae* mating factor alpha prepro signal peptide could not be enhanced by cooverexpression of either of the signal peptidase-encoding genes *KEX2* or *STE13*, or by removal of the Ste13 cleavage site at the C-terminus of the signal peptide. However, use of a recently published deletion mutant of the signal peptide [27] could be confirmed to yield augmented enzyme activity. Cooverexpression of the protein disulfide isomerase-encoding *PDI1* gene did not increase recombinant enzyme yields indicating that correct formation of the four disulfide bridges of HRP C1A is not limiting its production in *P. pastoris*. On the other hand, by activation of the systemic unfolded protein response upon inducible cooverexpression of the transcription factor-encoding *HAC1* gene [35], improved recombinant HRP production could be observed in microscale and bioreactor cultivations. Ultimately, coproduction of HRP and Hac1 by the bidirectional promoter *PHTX1* allowed competitive HRP yields of approximately 130 mg/L in bioreactor cultivation.

Improved recombinant production of HRP also facilitates the biochemical characterization of individual HRP isoenzymes. In order to broaden our understanding on different HRP isoenzymes, the well-studied isoenzyme C1A, an acidic isoenzyme A2A and a basic isoenzyme E5 were recombinantly produced in *P. pastoris* and used for comprehensive comparative characterizations, as described in **Chapter 6**. Biophysical characterizations involved electron paramagnetic resonance spectroscopy to describe the magnetic properties, and redox potentiometry to compare the reduction potentials of the $\text{Fe}^{3+}/\text{Fe}^{2+}$ redox couples of the different isoenzymes. Additional characterizations involved the determination of stabilities in response to pH, temperature and hydrogen peroxide, the

binding of a common ligand, benzhydroxamic acid, and steady-state kinetics using substrates of diagnostic relevance. Moreover, steady-state and stopped-flow kinetics were recorded using indole acetic acid, which has been suggested as substrate in an enzyme-prodrug system for cancer treatment. In conclusion, the performed comparative characterization of the recombinantly produced natural HRP isoenzymes revealed distinct enzyme properties. This study contributes to the generation of a toolbox of recombinant HRP isoenzymes from which an isoenzyme can be selected that meets the specific requirements of any application best.

In the study described in **Chapter 7**, recombinant HRP was used as reporter enzyme in *P. pastoris* strains cooverexpressing genes of the methanol utilization pathway. The Mut^S phenotype of *P. pastoris* could be shown conclusively to be superior over the Mut⁺ phenotype in terms of specific and volumetric HRP productivities as well as HRP production efficiency under *PAOX1*-regulation. Among all cooverexpressed genes, the formaldehyde dehydrogenase-encoding *FLD1* gene was identified as most promising due to a two-fold more efficient conversion of substrate methanol to target protein and even slightly increased specific and volumetric productivities compared to a control strain.

HRP is not only used as reporter enzyme in strain engineering studies, but most commonly in diagnostics and immunohistochemical applications such as Western Blots or enzyme-linked immunosorbent assays (ELISA). Currently, a HRP preparation from plant is linked to streptococcal protein G or to secondary antibodies by chemical conjugation, *e.g.* [36]. These conjugates can be used to bind and hereby quantify primary antibodies which again bind to target antigens. However, chemical conjugations not only require the use of hazardous chemicals and risk enzyme inactivation but also lead to heterogeneous conjugate preparations, in addition to the heterogeneity that is already introduced by the use of plant-derived HRP. In **Chapter 8**, the production of a recombinant HRP-protein G fusion protein in *P. pastoris* is described. In contrast to current conjugate preparations, the produced fusion protein is homogeneous with regard to the identity of the HRP isoenzyme and the stoichiometry of the two fusion partners. Functional binding of the recombinant HRP-protein G fusion protein could be shown when antibodies from either human or rabbit serum were used as antigens in ELISA.

In **Chapter 9**, the currently most effective methodology for recombinant HRP production and purification is described in the form of a protocol. The protocol presents an easily accessible résumé of successful strategies described in the chapters above. Recombinant HRP production procedures are described for microscale cultivations in 96-deep well plates as well as in bioreactor cultivations for expression from either of the promoters *PAOX1*, *PGAP* or *PHTX1*. A purification protocol comprising immobilized metal affinity chromatography, optional ligand affinity chromatography and size exclusion chromatography is described in detail. Finally, assay procedures are described to allow an adequate characterization of the obtained samples and preparations.

Ultimately, I would like to acknowledge coworkers that contributed to this thesis. The studies described in the Chapters 2, 3, 4 and 7 were performed in close collaboration with the team of Oliver Spadiut from the Vienna University of Technology, Institute of Chemical Engineering, Research Area Biochemical Engineering, Gumpendorfer Strasse 1a, A-1060 Vienna, Austria. Results from the master's thesis of Michaela A. Gerstmann from the Graz University of Technology, Institute of Molecular Biotechnology, NAWI Graz, Petersgasse 14, 8010 Graz, Austria, contributed to the content of the study described in Chapter 5. The characterizations of recombinant HRP isoenzymes described in Chapter 6 were performed in the lab of Andrew W. Munro from the University of Manchester, Manchester Institute of Biotechnology, 131 Princess Street, Manchester M1 7DN, UK. All contributing coworkers are listed as coauthors in the respective Chapters. The nature and extent of my contributions to the various manuscripts of this thesis as well as generated IP are stated in the Appendix.

References

1. Welinder K: **Superfamily of plant, fungal and bacterial peroxidases**. *Curr. Opin. Struct. Biol.* 1992, **2**:388–393.
2. Veitch NC: **Horseradish peroxidase: a modern view of a classic enzyme**. *Phytochemistry* 2004, **65**:249–59.
3. Gajhede M, Schuller DJ, Henriksen A, Smith AT, Poulos TL: **Crystal structure of horseradish peroxidase C at 2.15 Å resolution**. *Nat. Struct. Biol.* 1997, **4**:1032–8.
4. Aibara S, Kobayashi T, Morita Y: **Isolation and properties of basic isoenzymes of horseradish peroxidase**. *J. Biochem.* 1981, **90**:489–96.
5. Yang BY, Gray JS, Montgomery R: **The glycans of horseradish peroxidase**. *Carbohydr. Res.* 1996, **287**:203–12.
6. Welinder KG: **Covalent structure of the glycoprotein horseradish peroxidase (EC 1.11.1.7)**. *FEBS Lett.* 1976, **72**:19–23.

7. Veitch NC, Smith AT: **Horseradish peroxidase**. *Adv. Inorg. Chem. Vol. 51* 2001, **51**:107–162.
8. Tognolli M, Penel C, Greppin H, Simon P: **Analysis and expression of the class III peroxidase large gene family in *Arabidopsis thaliana***. *Gene* 2002, **288**:129–38.
9. Hoyle MC: **High resolution of peroxidase-indoleacetic acid oxidase isoenzymes from horseradish by isoelectric focusing**. *Plant Physiol.* 1977, **60**:787–93.
10. Näätsaari L, Krainer FW, Schubert M, Glieder A, Thallinger GG: **Peroxidase gene discovery from the horseradish transcriptome**. *BMC Genomics* 2014, **15**:227.
11. Jermyn MA, Thomas R: **Multiple components in horseradish peroxidase**. *Biochem. J.* 1954, **56**:631–9.
12. Smith AT, Santama N, Dacey S, Edwards M, Bray RC, Thorneley RN, Burke JF: **Expression of a synthetic gene for horseradish peroxidase C in *Escherichia coli* and folding and activation of the recombinant enzyme with Ca²⁺ and heme**. *J. Biol. Chem.* 1990, **265**:13335–43.
13. Grigorenko V, Chubar T, Kapeliuch Y, Borchers T, Spener F, Egorov A: **New approaches for functional expression of recombinant horseradish peroxidase C in *Escherichia coli***. *Biocatal. Biotransformation* 1999, **17**:359–379.
14. Vlamis-Gardikas A, Smith AT, Clements JM, Burke JF: **Expression of active horseradish peroxidase in *Saccharomyces cerevisiae***. *Biochem. Soc. Trans.* 1992, **20**:111S.
15. Morawski B, Lin Z, Cirino P, Joo H, Bandara G, Arnold FH: **Functional expression of horseradish peroxidase in *Saccharomyces cerevisiae* and *Pichia pastoris***. *Protein Eng.* 2000, **13**:377–84.
16. Kurtzman CP: **Biotechnological strains of *Komagataella (Pichia) pastoris* are *Komagataella phaffii* as determined from multigene sequence analysis**. *J. Ind. Microbiol. Biotechnol.* 2009, **36**:1435–8.
17. Cregg JM, Lin-Cereghino J, Shi J, Higgins DR: **Recombinant Protein Expression in *Pichia pastoris***. *Mol. Biotechnol.* 2000, **16**:23–52.
18. Macauley-Patrick S, Fazenda ML, McNeil B, Harvey LM: **Heterologous protein production using the *Pichia pastoris* expression system**. *Yeast* 2005, **22**:249–70.
19. Vogl T, Hartner FS, Glieder A: **New opportunities by synthetic biology for biopharmaceutical production in *Pichia pastoris***. *Curr. Opin. Biotechnol.* 2013:Article in Press.
20. Jahic M, Rotticci-Mulder JC, Martinelle M, Hult K, Enfors S-O: **Modeling of growth and energy metabolism of *Pichia pastoris* producing a fusion protein**. *Bioprocess Biosyst. Eng.* 2002, **24**:385–393.
21. Mellitzer A, Ruth C, Gustafsson C, Welch M, Birner-Grünberger R, Weis R, Purkarthofer T, Glieder A: **Synergistic modular promoter and gene optimization to push cellulase secretion by *Pichia pastoris* beyond existing benchmarks**. *J. Biotechnol.* 2014:1–9.
22. Morawski B, Quan S, Arnold FH: **Functional expression and stabilization of horseradish peroxidase by directed evolution in *Saccharomyces cerevisiae***. *Biotechnol. Bioeng.* 2001, **76**:99–107.
23. Hartner FS, Ruth C, Langenegger D, Johnson SN, Hyka P, Lin-Cereghino GP, Lin-Cereghino J, Kovar K, Cregg JM, Glieder A: **Promoter library designed for fine-tuned gene expression in *Pichia pastoris***. *Nucleic Acids Res.* 2008, **36**:e76.
24. Dietzsch C, Spadiut O, Herwig C: **A fast approach to determine a fed batch feeding profile for recombinant *Pichia pastoris* strains**. *Microb. Cell Fact.* 2011, **10**:85–94.
25. Zalai D, Dietzsch C, Herwig C, Spadiut O: **A dynamic fed batch strategy for a *Pichia pastoris* mixed feed system to increase process understanding**. *Biotechnol. Prog.* 2012, **28**:878–86.
26. Spadiut O, Zalai D, Dietzsch C, Herwig C: **Quantitative comparison of dynamic physiological feeding profiles for recombinant protein production with *Pichia pastoris***. *Bioprocess Biosyst. Eng.* 2014, **37**:1163–72.
27. Lin-Cereghino GP, Stark CM, Kim D, Chang J, Shaheen N, Poerwanto H, Agari K, Moua P, Low LK, Tran N, Huang AD, Nattestad M, Oshiro KT, Chang JW, Chavan A, Tsai JW, Lin-Cereghino J: **The effect of α -mating factor secretion signal mutations on recombinant protein expression in *Pichia pastoris***. *Gene* 2013, **519**:311–7.
28. Spadiut O, Rossetti L, Dietzsch C, Herwig C: **Purification of a recombinant plant peroxidase produced in *Pichia pastoris* by a simple 2-step strategy**. *Protein Expr. Purif.* 2012, **86**:89–97.

29. Parekh RB: **Effects of glycosylation on protein function.** *Curr. Opin. Struct. Biol.* 1991, **1**:750–754.
30. Silva E, Edwards AM, Faljoni-Alario A: **Enzymatic generation of triplet acetone by deglycosylated horseradish peroxidase.** *Arch. Biochem. Biophys.* 1990, **276**:527–30.
31. Tams JW, Welinder KG: **Mild chemical deglycosylation of horseradish peroxidase yields a fully active, homogeneous enzyme.** *Anal. Biochem.* 1995, **228**:48–55.
32. Tams JW, Welinder KG: **Glycosylation and thermodynamic versus kinetic stability of horseradish peroxidase.** *FEBS Lett.* 1998, **421**:234–6.
33. Nakanishi-Shindo Y, Nakayama K, Tanaka A, Toda Y, Jigami Y: **Structure of the N-linked oligosaccharides that show the complete loss of alpha-1,6-polymannose outer chain from *och1*, *och1 mnn1*, and *och1 mnn1 alg3* mutants of *Saccharomyces cerevisiae*.** *J. Biol. Chem.* 1993, **268**:26338–26345.
34. Michener JK, Nielsen J, Smolke CD: **Identification and treatment of heme depletion attributed to overexpression of a lineage of evolved P450 monooxygenases.** *Proc. Natl. Acad. Sci. U. S. A.* 2012, **109**:19504–9.
35. Guerfal M, Ryckaert S, Jacobs PP, Ameloot P, Van Craenenbroeck K, Derycke R, Callewaert N: **The *HAC1* gene from *Pichia pastoris*: characterization and effect of its overexpression on the production of secreted, surface displayed and membrane proteins.** *Microb. Cell Fact.* 2010, **9**:49.
36. O'Sullivan MJ, Gnemmi E, Morris D, Chierigatti G, Simmons M, Simmonds AD, Bridges JW, Marks V: **A simple method for the preparation of enzyme-antibody conjugates.** *FEBS Lett.* 1978, **95**:311–3.

- Chapter 1 -

An updated view on horseradish peroxidases: recombinant production and biotechnological applications

Florian W. Krainer^{1*} and Anton Glieder¹

¹ Graz University of Technology, Institute of Molecular Biotechnology, NAWI Graz, Petersgasse 14, 8010 Graz, Austria

* Corresponding author: Florian Krainer, Graz University of Technology, Institute of Molecular Biotechnology, NAWI Graz, Petersgasse 14, 8010 Graz, Austria; florian.krainer@tugraz.at; Tel: +43 316 873 4077; Fax: +43 316 873 4071

An updated view on horseradish peroxidases: recombinant production and biotechnological applications

Florian W. Krainer · Anton Glieder

Received: 19 September 2014 / Revised: 19 December 2014 / Accepted: 21 December 2014 / Published online: 11 January 2015
© The Author(s) 2015. This article is published with open access at Springerlink.com

Abstract Horseradish peroxidase has been the subject of scientific research for centuries. It has been used exhaustively as reporter enzyme in diagnostics and histochemistry and still plays a major role in these applications. Numerous studies have been conducted on the role of horseradish peroxidase in the plant and its catalytic mechanism. However, little progress has been made in its recombinant production. Until now, commercial preparations of horseradish peroxidase are still isolated from plant roots. These preparations are commonly mixtures of various isoenzymes of which only a small fraction has been described so far. The composition of isoenzymes in these mixed isolates is subjected to uncontrollable environmental conditions. Nowadays, horseradish peroxidase regains interest due to its broad applicability in the fields of medicine, life sciences, and biotechnology in cancer therapy, biosensor systems, bioremediation, and biocatalysis. These medically and commercially relevant applications, the recent discovery of new natural isoenzymes with different biochemical properties, as well as the challenges in recombinant production render this enzyme particularly interesting for future biotechnological solutions. Therefore, we reviewed previous studies as well as current developments with biotechnological emphasis on new applications and the major remaining biotechnological challenge—the efficient recombinant production of horseradish peroxidase enzymes.

Keywords Horseradish peroxidase · Plant peroxidase · Recombinant protein production · Diagnostics · Biosensor · Indole-3-acetic acid · Cancer treatment

Introduction

Peroxidases catalyze various oxidative reactions in which electrons are transferred to peroxide species (often H_2O_2) and substrate molecules are oxidized. These enzymes have been found in all living organisms, involved in a variety of biological processes. Peroxidase activity has been detected in a number of enzymes, predominantly classified to EC 1.11.1.7. Horseradish peroxidase (HRP) first appeared in scientific literature more than 200 years ago and has been the subject of numerous studies until now and ongoing. Scientific interest in HRP spiked in the late 1980s and early 1990s with the breakthrough of molecular diagnostics, molecular biology tool kits, and the publication of the first HRP gene (Fujiyama et al. 1988). Over the past 20 years, the number of publications involving HRP declined. Recently however, this decline not only flattened out but the number of publications rose by more than one third compared to the last 10 years, indicating new interest in this enzyme (Fig. 1).

HRP research typically deals with enzymological characterization, recombinant production in various expression systems, and to a large part with applications and their improvement by mutagenesis and chemical engineering. Until now, the vast majority of HRP research focused on one isoenzyme, C1A, neglecting the potential of other natural isoenzymes. Due to the discovery of new natural HRP isoenzymes (Näätsaari et al. 2014), an additional increase in the studies on HRP can be anticipated. In this review, we concisely highlight the crucial aspects of HRP research to give an overview of the state-of-the-art and particularly focus on the most recent strategies and developments of biotechnological relevance to provide access to the current challenges and opportunities.

F. W. Krainer (✉) · A. Glieder
Institute of Molecular Biotechnology, NAWI Graz, Graz University
of Technology, Petersgasse 14, 8010 Graz, Austria
e-mail: florian.krainer@tugraz.at

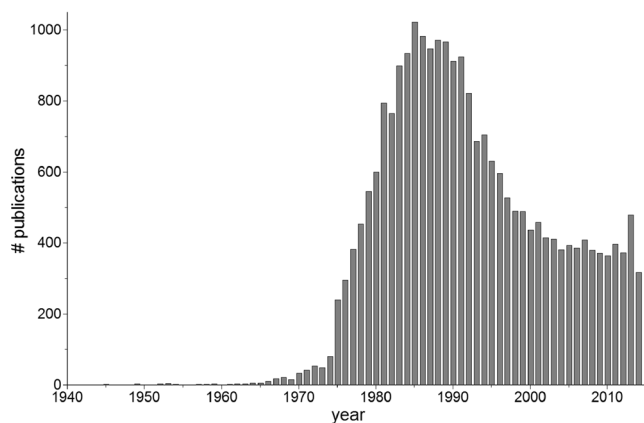


Fig. 1 Scientific output on horseradish peroxidase over time. Publications involving horseradish peroxidase from 1940 to 2014 in the PubMed database (Aug 2014)

New horseradish peroxidase isoenzymes

The studies on peroxidase from horseradish date back as early as to the beginning of the nineteenth century. Already back in 1810, Planche reported the resin of *Guaiacum* plants turning blue upon contact with horseradish roots (Planche 1810). In the early 1950s, multiple components with peroxidase activity were found in horseradish, extending the number of peroxidase isoenzymes to 5 (Jermyn 1952; Jermyn and Thomas 1954). Moreover, seasonal variation in the relative amounts of these peroxidase components and differences in their reactivities towards different substrates were observed, underlining the hypothesis that the detected components were in fact separate isoenzymes rather than artifacts of a single peroxidase enzyme (Jermyn and Thomas 1954). In 1966, in the first of four papers on “peroxidase isoenzymes from horseradish roots” (Shannon et al. 1966; Kay et al. 1967; Strickland et al. 1968; Shih et al. 1971), the authors reported on the isolation, purification, and physical properties of seven distinct isoenzymes from horseradish. In the second publication of that same series, differences in pH optima, specific activities, and substrate affinities were described for these isoenzymes (Kay et al. 1967). In analogy to these previous findings, differences in kinetics and substrate profiles were found by comparing an acidic HRP isoenzyme with a basic one (Marklund et al. 1974). In 1977, a total of 42 HRP isoenzymes were detected by separating the peroxidase activities of three commercial preparations from horseradish by isoelectric focusing (Hoyle 1977). In the early 1980s, the isoenzymes E1–E6 and the five isoenzymes B1–B3, C1, and C2 were biochemically characterized (Aibara et al. 1981, 1982). Until recently however, only six nucleotide sequences of HRP isoenzymes were available from public databases. In 2014, we published a total of 28 sequences encoding enzymes with a secretory plant peroxidase domain that were found in a pyrosequenced

transcriptome of *A Armoracia rusticana*, horseradish, and showed diverging substrate profiles (Näätsaari et al. 2014). Natural HRP isoenzyme sequences that are currently available from public databases are shown in Table 1.

When the gene structures of 73 class III peroxidases from the model plant *Arabidopsis thaliana* were studied, a conserved exon/intron structure of four exons and three introns was described (Tognolli et al. 2002). Similarly, we found this gene structure in 75 % of class III peroxidase sequences by comparing transcriptome and genome sequences of horseradish (Näätsaari et al. 2014).

The numerous peroxidase isoenzymes are thought to play specific physiological roles *in planta*. Peroxidase activity is detectable throughout the whole lifespan of a plant with a broad variety of reactions, which have been reviewed elsewhere (Passardi et al. 2005). However, only little information is available on the regulation of the expression of HRP isoenzymes. The recently identified HRP isoenzyme sequences (Näätsaari et al. 2014) will facilitate future studies on the expression patterns of individual isoenzymes in different plant tissues and in response to external stimuli. Also, due to their biochemical diversity, the large number of HRP isoenzymes constitutes a convenient toolbox of plant peroxidases from which an isoenzyme can be chosen that meets the requirements of an application best. For instance, the enzyme stability towards external factors (e.g. peroxide species, temperature) plays an essential role in biocatalysis and bioremediation (e.g. Kim et al. 2014a). An acidic HRP isoenzyme A2 has been found more stable towards H_2O_2 inactivation than an isoenzyme C (Hiner et al. 2001a). However, an isoenzyme E showed higher specific activity in oxalacetate oxidation than the isoenzymes A2 and C (Kay et al. 1967). Recombinant technology enables us to exploit and combine such features within the HRP toolbox, allowing for novel and improved biocatalysts in the near future.

Structure and catalytic mechanism

Since enzymological features of HRP have been reviewed before exhaustively (e.g. Veitch and Smith 2001), we focus on the most recent studies and those features that are of relevance from a biotechnological perspective. So far, the majority of studies on HRPs have been performed on isoenzyme C1A; if not stated otherwise, all data mentioned here refer to this isoenzyme.

Structural features of biotechnological relevance

HRP is a globular molecule with a predominantly α -helical secondary structure with the exception of one short β -sheet region (Fig. 2) (Gajhede et al. 1997). The HRP molecule is separated into a distal and a proximal region by an iron

Table 1 Horseradish peroxidase isoenzymes

Isoenzyme	pI	MW kDa	GenBank	UniProt	References	
C1A	5.7	38.8	M37156.1	P00433	(Fujiyama et al. 1988; Gajhede et al. 1997; Henriksen et al. 1998; Welinder 1976)	
C1A	5.7	38.8	HE963800.1	K7ZWW6	(Näätsaari et al. 2014)	
C1B	5.7	38.6	M37157.1	P15232	(Fujiyama et al. 1988)	
C1B	5.7	38.6	HE963801.1	K7ZW26	(Näätsaari et al. 2014)	
C1C	6.2	36.5	M60729.1	P15233	(Fujiyama et al. 1988)	
25148.1 (C1C)	6.6	38.8	HE963802.1	K7ZWQ1	(Näätsaari et al. 2014)	
25148.2 (C1D)	7.0	38.8	HE963803.1	K7ZW56	(Näätsaari et al. 2014)	
C2	8.7	38.0	D90115.1	P17179	(Fujiyama et al. 1990)	
04627 (C2)	8.7	38.0	HE963804.1	K7ZW02	(Näätsaari et al. 2014)	
C3	7.5	38.2	D90116.1	P17180	(Fujiyama et al. 1990)	
C3	7.5	38.2	HE963805.1	K7ZWW7	(Näätsaari et al. 2014)	
A2	4.7	31.9	—	P80679	(Nielsen et al. 2001)	
A2A	4.8	35.0	HE963806.1	K7ZW28	(Näätsaari et al. 2014)	
A2B	4.8	35.1	HE963807.1	K7ZWQ2	(Näätsaari et al. 2014)	
E5	9.1	33.7	—	P59121	(Morita et al. 1991)	
E5	8.7	37.9	HE963808.1	K7ZW57	(Näätsaari et al. 2014)	
N	7.5	35.1	X57564.1	Q42517	(Bartonek-Roxå et al. 1991)	
01805	6.4	39.1	HE963809.1	K7ZW05	(Näätsaari et al. 2014)	
Natural HRP isoenzymes are shown with their corresponding GenBank and UniProt database accession numbers and references. Isoelectric points and molecular weights were predicted with the Compute pI/Mw tool (Bjellqvist et al. 1993, 1994; Gasteiger et al. 2005) using unprocessed amino acid sequences (if available; the isoenzymes A2, P80689, and E5, P59121, were only available as processed peptides). For isoenzyme C1A, the amino acid at position 37 is Ile according to the GenBank entry M37156.1 but Tyr according to the GenBank entry HE963800.1 and the UniProt entries P00433 and K7ZWW6; calculations of pI and MW were performed with the latter sequence	22684.1	6.8	37.7	HE963810.1	K7ZWW8	(Näätsaari et al. 2014)
	22684.2	6.3	37.8	HE963811.1	K7ZW29	(Näätsaari et al. 2014)
	01350	8.7	34.3	HE963812.1	K7ZWQ3	(Näätsaari et al. 2014)
	02021	9.6	35.8	HE963813.1	K7ZW58	(Näätsaari et al. 2014)
	23190	8.4	39.4	HE963817.1	K7ZWQ4	(Näätsaari et al. 2014)
	04663	4.4	37.2	HE963814.1	K7ZW09	(Näätsaari et al. 2014)
	06351	6.9	34.6	HE963816.1	K7ZW31	(Näätsaari et al. 2014)
	03523	8.9	35.6	HE963820.1	K7ZWX0	(Näätsaari et al. 2014)
	05508	8.6	34.3	HE963815.1	K7ZWW9	(Näätsaari et al. 2014)
	22489.1	8.8	34.8	HE963818.1	K7ZW59	(Näätsaari et al. 2014)
	22489.2	8.8	34.8	HE963819.1	K7ZW11	(Näätsaari et al. 2014)
	06117	5.7	36.4	HE963821.1	K7ZW32	(Näätsaari et al. 2014)
	17517.1	9.6	35.1	HE963822.1	K7ZWQ5	(Näätsaari et al. 2014)
	17517.2	9.6	35.1	HE963823.1	K7ZW60	(Näätsaari et al. 2014)
	08562.1	9.0	36.1	HE963824.1	K7ZW15	(Näätsaari et al. 2014)
	08562.4	9.0	36.1	HE963825.1	K7ZWX1	(Näätsaari et al. 2014)

protoporphyrin IX cofactor, commonly referred to as the heme group. Heme is typically linked to HRP by a coordinate bond of the heme iron with a conserved His170 residue, facilitating the evaluation of the purity of a preparation by the ratio of A403 over A280, i.e. the absorbances of heme at the Soret band and of aromatic amino acids, respectively. This ratio is commonly referred to as the *Rz* value (originating from the German word *Reinheitszahl* which translates to “number of purity”) (Theorell et al. 1950). A *Rz*>3.0 indicates a high relative heme content correlating with a high degree of

enzyme purity. However, it has to be pointed out that different isoenzymes may yield different *Rz* values at comparable degrees of purity (Shannon et al. 1966). The availability of sufficient heme cofactor is a matter of consideration in recombinant production and can be tackled by media supplementation (e.g. de las Segura et al. 2005, Ryan and O’Fágáin (2008).

C1A contains nine Asn-X-Ser/Thr-X motives (X being any amino acid but Pro) as potential N glycosylation sites. *In planta*, all Asn residues of HRP C1A except for Asn286 are subjected to glycosylation (Welinder 1979). All glycosylated

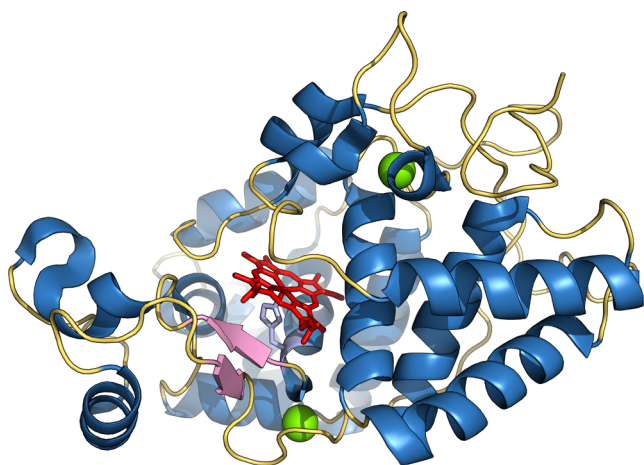


Fig. 2 Structure of HRP C1A (PDB ID 1H5A). Helices and loops are shown in *blue* and *yellow*, respectively; one short β -sheet region is shown in *pink*. The two calcium ions are shown as *green spheres*. The heme group is shown in *red* and lies between the distal and the proximal domain; the proximal His170 residue (*light blue*) coordinates to the heme iron

Asn residues are located on the surface of C1A (Gajhede et al. 1997). A total carbohydrate content of 21.8 % was reported for C1A; however, basic isoenzymes were found to have lower glycan contents (e.g. 0.8–4.2 % for the isoenzymes E3–E6) (Aibara et al. 1981; Yang et al. 1996). Chemical deglycosylation of C1A to a carbohydrate content of 5.5 % did not seem to affect the heme group but was described to cause structural changes and impaired enzymatic activity (Silva et al. 1990). In another study, all enzyme-linked carbohydrate structures were reduced by mild chemical deglycosylation to GlcNAc₂, which remained attached to Asn. Both glycosylated and deglycosylated HRP showed the same isoelectric point and absorbance spectrum and unaltered specific activity towards *o*-dianisidine, contrasting the previous findings. Only solubility in ammonium sulfate was found to be decreased upon deglycosylation (Tams and Welinder 1995). Further stability studies on deglycosylated HRP showed unaltered thermal stability, but threefold decreased kinetic stability in unfolding studies with guanidinium chloride (Tams and Welinder 1998). Additional studies will have to be conducted to conclusively determine the role of glycans on the biochemical properties of HRP. The recombinant production of individual isoenzymes from glycosylating expression hosts such as yeasts and non-glycosylating hosts such as *Escherichia coli* could be particularly useful for studies on HRP glycosylation.

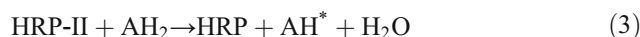
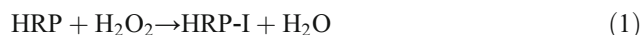
Surface lysine residues are of particular interest for directed enzyme immobilization via covalent linkages. On the surface of HRP C1A, three (Lys174, Lys232, Lys241) out of six lysine residues were found accessible to chemical modifications (O'Brien et al. 2001).

In C1A, four disulfide bridges are formed between Cys41–121, Cys74–79, Cys127–331, and Cys207–239 (Welinder 1976), yet another feature that has to be kept in mind when

it comes to choosing a host organism for recombinant production. Recombinant HRP from eukaryotic hosts such as *Pichia pastoris* does not require refolding to yield active enzyme, as opposed to HRP from *E. coli* which is typically produced as inclusion bodies (e.g. Smith et al. 1990).

HRP catalysis and redox states

Peroxidative HRP catalysis can be roughly described by three consecutive reactions (Eqs. 1, 2, and 3) as established by Chance (1952) and George (1952, 1953).



HRP, HRP-I, and HRP-II represent the enzyme in its resting state, a first intermediate state, compound I, and a second intermediate state, compound II, respectively. AH₂ and AH* are a reducing substrate and its oxidized radical species, respectively. The first step of the peroxidative cycle, compound I formation, was described by the Poulos-Kraut mechanism (Poulos and Kraut 1980). Recently, this step was suggested to happen as a “wet” mechanism via a single water molecule that allows formation of a ferric hydroperoxide intermediate, compound 0, based on QM/MM calculations (Derat and Shaik 2006; Derat et al. 2007; Vidossich et al. 2010). The O-O bond of compound 0 is then cleaved in accordance to the Poulos-Kraut mechanism, resulting in formation of compound I, which is reduced back to the enzyme’s resting state in two consecutive one-electron transfer reactions with two molecules of reducing substrate, as depicted above.

Aside the three described oxidation states of HRP in the peroxidative cycle, two more oxidation states have been described: a ferrous species and compound III which can be described as either a dioxygen-binding ferrous species or an isoelectric ferric species binding a superoxide anion. The structures of these five intermediate states were solved in 2002 (Berglund et al. 2002) and are schematically depicted in Fig. 3.

In the absence of reducing substrates, excess peroxides react as reductants with compound I, giving rise to several spectroscopically distinct species (Keilin and Hartree 1951). In the case of H₂O₂, three pathways have to be considered subsequent to the formation of a compound I-H₂O₂ complex: (1) a catalase-like (i.e. pseudocatalase) two-electron reduction reaction that restores the enzyme to the resting state, (2) another catalytic pathway that leads to the formation of

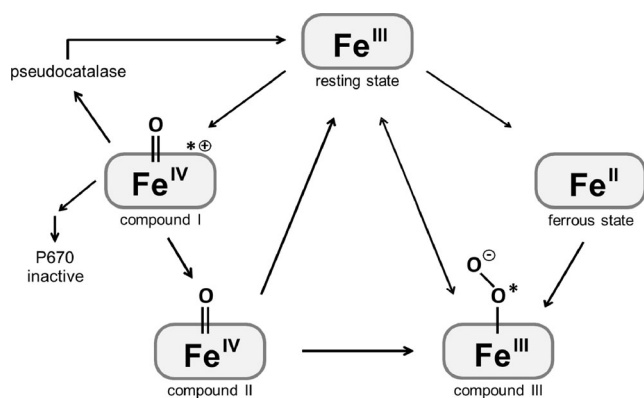


Fig. 3 Schematic overview of HRP intermediate states. The peroxidative cycle starts with oxidation of the ferric resting state to an oxoferryl species plus a porphyrin-based π cation radical, compound I. Reduction of compound I by elimination of the π cation radical forms compound II which is reduced to return the enzyme to the resting state. Compound III (here shown as superoxide anion-binding ferric species) can be formed from a ferrous species, compound II, or directly from the resting state and slowly decays back to the latter. Upon peroxide excess, compound I can either react back to the resting state via a pseudocatalase activity, react further to compound II, or react to the inactive P670 species

compound III which decays back to the resting state, (3) and a competing pathway that leads to the irreversible inactivation of the enzyme. The presence of a reducing substrate, as well as the two catalytic pathways, plays important roles in preventing enzyme inactivation by H_2O_2 (Arnao et al. 1990a, b). The enzymatic production of molecular oxygen via the pseudocatalase activity of HRP was described as a major protective mechanism against H_2O_2 inactivation (Hernández-Ruiz et al. 2001; Hiner et al. 2001b). However, this protective pathway is ineffective against peroxides other than H_2O_2 . The inactivation pathway was described to first yield an intermediate with an absorbance band at 940 nm (P940) which further decays to an inactive verdohemoprotein species with an absorbance peak at 670 nm (P670) (Bagger et al. 1971; Vlasits et al. 2010). Studies comparing different isoenzymes showed basic isoenzymes to be more sensitive to inactivation than acidic isoenzymes under the tested conditions (Hiner et al. 1996, 2001a). Further studies on H_2O_2 susceptibility of natural HRP isoenzymes might yield valuable information for improving the oxidative stability of HRPs by rational design. A glycosylated isoenzyme C1A from plant was found to be twofold more resistant towards H_2O_2 inactivation compared to non-glycosylated recombinant C1A from *E. coli* and mutants thereof (Hiner et al. 1995), raising the issue on the role of HRP glycans once again. As a consequence, the recombinant HRP preparations from glycosylating hosts might be preferable over preparations from *E. coli* for applications requiring stable enzyme. However, the mutants Thr110Val, Lys232Asn, and Lys241Phe produced in another study in *E. coli* (Ryan and O’Fágáin 2007a) were found to be 25-, 18-, and 12-fold more stable towards H_2O_2 inactivation, respectively, than wild-type

C1A. Suggested explanations for the findings were the removal of oxidizable groups or enhanced protective pseudocatalase activity. At this point, further studies are necessary to demonstrate a possible potentiation of the positive effects of these mutants from *E. coli* with the seemingly protective function of carbohydrate structures from a glycosylating production host.

Recombinant production of horseradish peroxidases

Current commercial HRP preparations are typically isolated from horseradish roots as mixtures of several isoenzymes. The amount of individual isoenzymes in such a mixture depends on the *in planta* expression patterns of the respective isoenzymes (Jermyn and Thomas 1954). In general, it can be assumed that the quality and actual isoenzyme composition of any plant isolate depend on hard-to-predict and barely controllable environmental influences. To avoid this dependency on nature’s unpredictability and laborious steps to separate isoenzymes from one another, several organisms have been tested for their applicability as expression hosts for the recombinant production of HRP.

Recombinant HRP production in *E. coli*

In 1988, a patent application was filed relating to the synthesis of a DNA sequence encoding HRP C (Chiswell and Ortlepp 1988). The HRP gene was cloned into a vector and transformed to *E. coli* for expression. The staining of HRP expressing colonies with *N,N,N',N'*-tetramethylphenylene diamine was performed to demonstrate the successful production of active HRP by *E. coli*. An anti-HRP antibody confirmed the identity of the produced peptide. In 1989, two further studies were published in which a recombinant HRP was successfully produced in *E. coli* (Burke et al. 1989; Ortlepp et al. 1989). In 1990, a procedure for intracellular expression of a synthetic C1A gene in *E. coli* and a protocol for refolding were described (Smith et al. 1990). The gene was based on a C1A sequence of 308 amino acids lacking the N-terminal signal peptide and the C-terminal propeptide (Welinder 1976; Fujiyama et al. 1988). To date, variations of this protocol for refolding of intracellularly produced HRP from inclusion bodies in *E. coli* are most commonly used for recombinant HRP production. Alternatively, some efforts have been taken to improve the recombinant production of active HRP in *E. coli* without the need for refolding. For instance, N-terminal fusion to a pelB leader peptide was performed for periplasmic targeting to yield active enzyme (e.g. Grigorenko et al. 1999; Ryan and O’Fágáin 2008). However, the yield of holo-HRP was as low as 0.5 mg/L (Grigorenko et al. 1999). The coproduction of the DsbABCD proteins was suggested to support the correct formation of protein disulfide bonds when HRP was targeted to

the periplasm of *E. coli* and to enhance the yield of active enzyme (Kurokawa et al. 2000). Nevertheless, it has to be pointed out that the production of secreted HRP in *E. coli* is still by far not suitable for biotechnological applications due to the extremely low yields. A general issue in recombinant production of active hemoproteins is heme availability. A common approach to improve heme supply is media supplementation with δ -aminolevulinic acid, a precursor molecule of the heme biosynthesis pathway (e.g. Ryan and O’Fágáin 2008). As an alternative, the coproduction of a heme receptor was reported to allow direct uptake of exogenously added heme by *E. coli* (Varnado and Goodwin 2004). Several more studies on improved HRP yields from *E. coli* have been published (e.g. Egorov et al. 1991; Grigorenko et al. 1999; Asad et al. 2013). However, the ultimately achievable yields from *E. coli* did not surpass 10 mg/L so far (Grigorenko et al. 1999), which cannot compete with the current isolation from plant and are thus not suitable for biotechnological applications. Therefore, most studies on recombinant HRP from *E. coli* deal with the production of C1A mutant variants to study the influence of specific amino acids on catalysis or stability. For instance, mutations of surface lysines resulted in augmented stabilities towards heat and solvent and higher enzymatic activity (Ryan and O’Fágáin 2008). In another study, arginine residues opposite the active site were mutated to lysines to form a batch of reactive groups suitable for increased and directed enzyme immobilization (Ryan and O’Fágáin 2007b). Notably, the stabilities of the studied mutants were found affected and a combination with stabilizing mutations will be required to link the favorable immobilization behavior with high enzyme stability. In order to stabilize recombinant HRP, selected residues were subjected to site-directed mutagenesis based on a sequence alignment of class III peroxidases (Ryan et al. 2008). However, the mutated consensus residues did not significantly improve thermal stability, indicating that this strategy could not be applied to class III peroxidases. In a recent follow-up study, an ancestral class III peroxidase was produced in *E. coli* and characterized (Loughran et al. 2014). This ancestral peroxidase was found twofold more resistant towards H_2O_2 inactivation than HRP C1A but less thermostable. In addition to the data on this ancestral peroxidase platform, comparative characterizations of the recently published extant HRP isoenzymes (Näätsaari et al. 2014) would provide additional data that could allow rational HRP design in the future after all. An overview of site-directed HRP mutants that have been characterized before 2006 was given in a previous review (Ryan et al. 2006). Thus, these studies will not be discussed here. It has to be pointed out that recombinantly produced HRP mutants from *E. coli* are commonly compared to recombinant wild-type enzyme from the same host but rarely to the plant-derived wild-type enzyme which might have yet again different characteristics, e.g. due its native glycosylation (Hiner et al. 1995). Hence, observed mutations on an unglycosylated

mutant from *E. coli* might not be transferable to a glycosylated enzyme from a plant or yeast host (Hiner et al. 1995) and may require additional experimental data. Reevaluation of the advantageous mutations found in recombinant HRPs from *E. coli* in the context of a glycosylating production system might reveal a potentially additive benefit from enzyme-linked glycan structures.

Recombinant HRP production in yeast systems

Mainly due to the presence of disulfide bridges, as well as to the considerable degree of glycosylation of native plant HRP, several studies have been performed on the production of recombinant HRP in eukaryotic expression systems. In 1992, *Saccharomyces cerevisiae* was used as a host for the secretory production of active hyperglycosylated HRP (Vlamiš-Gardikas et al. 1992). Not only *S. cerevisiae* but also the methylotrophic yeast *P. pastoris* was used to study C1A mutants, generated by directed evolution to yield higher enzymatic activity and thermal stability (Morawski et al. 2000, 2001). An Asn175Ser mutation was found to increase thermal stability, presumably due to an additional hydrogen bond which was hypothesized to stabilize the enzyme’s heme cavity (Morawski et al. 2001). Conjugates of HRP with Fab fragments against atrazine were produced in *P. pastoris* and found to show functional antigen-binding properties (Koliashnikov et al. 2011). Hereby, the authors demonstrated the feasibility of recombinant HRP-antibody fusion proteins and provided an alternative to chemical conjugation procedures. Also, the use of HRP as a reporter enzyme in strain engineering and bioprocess studies with *P. pastoris* has been reported repeatedly (e.g. Hartner et al. 2008; Dietzsch et al. 2011a, b; Krainer et al. 2012, 2013a). Lately, we focused on the development and evaluation of purification protocols for different recombinant HRP isoenzyme preparations from *P. pastoris* (Spadiut et al. 2012; Krainer et al. 2013b). We performed two-step reverse chromatography purifications on 19 different isoenzymes and found considerable differences in both, purification efficiency and biochemical characteristics of the preparations. Strikingly, the number of N-glycosylation sites per isoenzyme appeared to affect both purification factor and recovery yield, indicating that yeast-type hypermannosylation of secreted HRP prevented interactions with the employed chromatography resins, thereby facilitating purification in reverse mode. A finding which is not only relevant for HRP purification but for secreted yeast-derived proteins in general (Krainer et al. 2013b).

In order to study the effect of N-glycosylation sites, recombinant C1A mutants were produced in *P. pastoris*, in which Asn residues of all N-glycosylation sites were systematically changed to either Asp, Gln, or Ser. The obtained mutant preparations were described to vary in their biochemical and physicochemical properties. Strikingly, a mutant preparation

harboring mutations in all N-glycosylation sites showed a 300-fold reduction in catalytic activity compared to wild-type C1A (Capone et al. 2014). Regarding a medical application of recombinant HRP, the use of glycoengineered *P. pastoris* strains might be considered in order to allow human-type glycosylation.

By using a Δ Asn57-Ile70 deletion mutant of the prepro signal peptide of the *S. cerevisiae* mating factor α , which is commonly employed to facilitate enzyme secretion, HRP activity yields from *P. pastoris* could be increased by almost 60 % (Lin-Cereghino et al. 2013). Apparently, the passage through the secretory pathway describes a bottleneck in recombinant HRP production in *P. pastoris*, and additional engineering thereof is likely to further augment enzyme yields (e.g. Gasser et al. 2006; Guerfal et al. 2010).

Alternatively to *S. cerevisiae* and *P. pastoris*, a basidiomycete yeast strain, *Cryptococcus* sp. S-2, was recently used to produce more than 100 mg/L recombinant C1A in a fed-batch fermentation process. Expression was regulated by a xylose-inducible xylanase promoter, and a shortened xylanase signal peptide was used to mediate efficient secretion (Utashima et al. 2014). This strategy allowed for the highest yields of recombinant HRP so far. However, the employed yeast, *Cryptococcus* sp. S-2, is not “generally recognized as safe” (GRAS)—in contrast to *P. pastoris* (US Food and Drug Administration 2006). In the light of an application of HRP in medicine and for more convenient handling, the use of the latter might be reconsidered as soon as competitive yields can be achieved.

Recombinant HRP production in insect systems

In 1992, an active secreted HRP was produced in cell cultures of insect SF9 cells (Hartmann and Ortiz de Montellano 1992). Thirteen years later, an improved protocol was published for HRP production in SF9 cells and subsequent purification. Up to 41.3 mg of active HRP was produced per liter of cell culture upon addition of hemin to the culture medium (de las Segura et al. 2005). By combining a poly-Arg and a poly-His tag fused to recombinant HRP from SF9 cells, the enzyme was purified 130-fold by cation-exchange chromatography at a yield of >98 % (Levin et al. 2005). Similar to *E. coli*, several mechanistic studies have been published on mutant HRPs produced in insect cell culture (Miller et al. 1995; Newmyer and Ortiz de Montellano 1995, 1996; Newmyer et al. 1996; Savenkova et al. 1996, 1998; Savenkova and Ortiz de Montellano 1998). Even though the yields from insect cells (40 mg/L; de las Segura et al. 2005) were fourfold higher than from *E. coli* (10 mg/L; Grigorenko et al. 1999), the yeast systems are still more promising (100 mg/L; Utashima et al. 2014) and allow more convenient handling than cell cultures. As an alternative to HRP production in insect cell cultures, an oral infective baculovirus was used for infection of

lepidopteran larvae, and *Spodoptera frugiperda* larvae were found to produce the highest amount of HRP per larva (Romero et al. 2010, 2011). However, the competitiveness of this HRP production strategy in terms of handling and production efficiency remains yet to be demonstrated.

Recombinant HRP production in plants

Plant hosts were described for the production of HRP as well, predominantly for studies on the physiological roles of peroxidases. In 1994, C1A was overexpressed in *Nicotiana tabacum*. The transformants were found to grow 20 % faster than wild-type plants (Kawaoka et al. 1994). Further studies on the impact of overexpressed HRP on growth and development of the tobacco plant emphasized the importance of subcellular peroxidase targeting (Heggie et al. 2005). For instance, tobacco plants showed increased axillary branching and decreased lignin deposition upon overexpression of C1A lacking a C-terminal vacuolar targeting peptide. However, these effects could not be observed when full length C1A was overexpressed. Additional studies (Matsui et al. 2003, 2006, 2011; Kis et al. 2004) were performed with transgenic tobacco to broaden the understanding on the regulation of vacuolar peroxidase targeting *in planta*. The expression of HRP not only in tobacco but also in hybrid aspen were found to increase growth rates in the transformed plants (Kawaoka et al. 2003). As a consequence, HRP overexpression in woody plants was suggested to increase biomass production for forestry and textile, pulp, and paper industries as a rather unconventional but nevertheless interesting application for HRP. Enhanced plant growth upon HRP overexpression might correlate with an altered metabolism of plant growth hormones such as indole-3-acetic acid (IAA) and remains to be demonstrated. In a recent publication (Walwyn et al. 2014), *Nicotiana benthamiana* was described for transient HRP expression, yielding 240 mg of HRP per kg of plant biomass. The authors calculated a yearly output of more than 5 kg of HRP by applying the described system at sufficiently large scale. Nevertheless, the handling of an appropriate microbial system might be more convenient and cost- and time-efficient, and further progress in microbial recombinant HRP production can be anticipated, considering the recent advances in recombinant HRP production in yeast systems (e.g. Lin-Cereghino et al. 2013; Utashima et al. 2014).

As an alternative to the production of HRP in a heterologous host, an *in vitro* production of HRP in horseradish hairy root cultures was reported (Uozumi et al. 1992; Flocco et al. 1998; Flocco and Giulietti 2003). However, this method takes a long time and yields a mixture of HRP isoenzymes that need to be separated from one another. Hence, it is not suitable for biotechnological application at this point.

Remarks on current recombinant production systems

In conclusion, there are several hosts available that are suitable for the production of recombinant HRP (summarized in Table 2). Unfortunately, the comparability of the various hosts is complicated by the diversity of the reported yields (i.e. protein/volume, activity/volume, and activity/biomass). Hence, an absolute assessment of the production performance of a certain host is rather difficult from current literature. Moreover, there is variation in the quality of the produced HRP (purity, isoenzyme identity, glycosylation) and in the production costs of the respective hosts. These aspects will have to be taken into consideration in order to establish a recombinant production system. Recombinant HRP production at competitive yields is crucial in order to outmatch the current natural source. However, in light of the most recent promising results obtained with yeast host systems (e.g. Lin-Cereghino et al. 2013; Utashima et al. 2014), this goal appears achievable in the near future, allowing for well-defined enzyme preparations for the broad range of applications for the first time.

Impact of recombinant technology on traditional and future HRP applications

Despite the aforementioned pitfalls in the isolation of HRP from horseradish roots and the challenges in recombinant

production, numerous applications have been described for HRP in the fields of medicine, biotechnology, and life sciences. Several former examples thereof have been reviewed previously (Azevedo et al. 2003; Regalado et al. 2004). Here, we thus highlight only the most recent reports of applied HRP and emphasize the beneficial contributions of recombinant HRP to present-day applications.

HRP as a reporter enzyme

Traditionally, HRP has been used exhaustively as a reporter enzyme, e.g. in histochemical stainings and diagnostic assays. For instance, HRP-conjugated secondary antibodies were used to detect HIV-1 envelope peptides expressed in cell culture via a cell-based ELISA (Veillette et al. 2014). HRP activity can either be detected by the formation of a chromogenic or fluorogenic product, or by an electrochemical signal due to the redox nature of HRP catalysis. The majority of studies on HRP in biosensor systems focuses on the detection of H₂O₂ (e.g. Kafi et al. 2008; Virel et al. 2010; Zhong et al. 2011; Ahammad et al. 2011). In recent years however, a considerable number of studies also dealt with the detection of other molecules, such as glucose (Alonso-Lomillo et al. 2005), ethanol (Azevedo et al. 2005), DNA and RNA (Fan et al. 2013; Tran et al. 2014; Saikrishnan et al. 2014), L-phenylalanine (Kubota et al. 2013), citrinin (Zachetti et al. 2013), pyrogallol and hydroquinone (Raghu et al. 2013), phenols (Kafi and

Table 2 Recombinant production systems for horseradish peroxidase

Expression host	Reported yields	Remarks	References
<i>Escherichia coli</i>	2–3 % of total protein	Refolded from inclusion bodies	(Smith et al. 1990)
	8–10 mg/L		(Grigorenko et al. 1999)
	0.5 mg/L	Targeted to periplasm; active	
<i>Saccharomyces cerevisiae</i> (baker's yeast)	260 U/L/OD ₆₀₀	Secreted to supernatant; active	(Morawski et al. 2000)
<i>Pichia pastoris</i>	600 U/L/OD ₆₀₀		
	15 U/mL		(Hartner et al. 2008)
	1.66 U/g DCW/h		(Kraimer et al. 2012)
<i>Cryptococcus</i> sp. S-2	110 mg/L	Optimized for codon usage and secretion	(Utashima et al. 2014)
<i>Spodoptera frugiperda</i> (fall armyworm)	41.3 mg/L	Produced in cell culture	(de las Segura et al. 2005)
	41 µg/larva	Produced in larvae	(Romero et al. 2010)
<i>Rachiplusia nu</i> (sunflower looper)	22 µg/larva		
<i>Nicotiana benthamiana</i>	240 mg/kg of plant biomass	Transient expression of isoenzyme C1A	(Walwyn et al. 2014)
<i>Nicotiana tabacum</i> (tobacco)	n/a	Growth studies	(Kawaoka et al. 1994)
<i>Populus</i> sp. (aspen)			(Kawaoka et al. 2003)
<i>Armoracia rusticana</i> (horseradish)		Produced in hairy root culture	(Flocco and Giulietti 2003)

Host organisms used for the expression of horseradish peroxidase are listed with their corresponding references. Yields from *Nicotiana tabacum*, *Populus* sp., and *Armoracia rusticana* were not available (n/a)

Chen 2009; Liu et al. 2011), the milk allergen β -lactoglobulin (Ruiz-Valdepeñas Montiel et al. 2015), rotavirus titers (Li et al. 2014), and tumor markers (Chen et al. 2009; Kim et al. 2014b; Patris et al. 2014) via H_2O_2 . Notably, studies on HRP applications of medical relevance are currently particularly prevalent. For example, HRP reporter activity was recently used for the quantification of protein kinase activity (Yin et al. 2015), which is of importance in cases of kinase-related drug discovery, therapy, and clinical diagnosis. In another study, HRP conjugates were used for the detection of DNA from the human pathogen *Mycobacterium tuberculosis* (Saikrishnan et al. 2014). A consistent enzyme quality is of particular relevance in medical diagnostics. These applications must not depend on fluctuating plant isolates and would therefore benefit greatly from a supply with consistent recombinant HRP.

To date, HRP is also a major component of high throughput assays in enzyme engineering, detecting H_2O_2 as a side product of biooxidants (Willies et al. 2012; Barber et al. 2014) or products of coupling reactions after biohydroxylations (Joo et al. 1999).

HRP in biocatalysis

The applications of HRP in organic synthesis predominantly deal with polymerization reactions. For instance, HRP-catalyzed formation of poly(methyl methacrylate), a component of optical fibers, could be performed at ambient temperature (Kalra and Gross 2000). Also, polymerization reactions to form polystyrene (which is used e.g. as packaging material) from styrene and derivatives thereof were successfully performed with HRP (Singh et al. 2000). Moreover, HRP was used to form hydrogels, using phenolic derivatives of chitosan and polyvinyl alcohol (Sakai et al. 2014). By choosing the appropriate ratio of the two starting molecules, fibroblastic cell adhesion or growth of *E. coli* was either allowed or inhibited, respectively. Recently, the intrinsically conductive polymer poly(3,4-ethylenedioxythiophene) was synthesized in a two-step process involving HRP (Wang et al. 2014). However, enzyme inactivation by phenoxy radicals describes a major limitation in oxidative polymerization reactions. A new study (Kim et al. 2014a) described a recombinantly produced quadruple mutant (Phe68Ala/Phe142Ala/Phe143Ala/Phe179Ala) to show improved stability towards radical inactivation at even faster substrate turnover than a wild-type enzyme, underlining yet again the so far largely untapped potential of recombinant HRPs in applications of industrial relevance.

Further HRP-catalyzed reactions of biocatalytical interest include oxidative dehydrogenation (Colonna et al. 1999), sulfoxidation (Colonna et al. 1992; Ozaki and Ortiz de Montellano 1994, 1995; Das et al. 2002; Yu and Klibanov 2006), and nitrogen oxidation (Kalliney and Zaks 1995;

Boucher et al. 1996). In 2009, a yeast surface display strategy was adopted to screen point mutants of recombinant C1A. An Arg178Glu mutant showing enhanced enantioselectivity for phenol oxidation was identified (Antipov et al. 2009). Presumably, the combination of an efficient recombinant production system with enzyme engineering approaches will further improve and expand the use of HRP in biocatalysis.

HRP in bioremediation systems

Beside the development of new electrochemical biosensor systems, most current publications on applied HRP deal with bioremediation systems to degrade synthetic dyes (Cheng et al. 2006; Ulson de Souza et al. 2007; da Silva et al. 2011; Bayramoglu et al. 2012; Malani et al. 2013; Preethi et al. 2013; Pereira et al. 2014) and to remove phenolic contaminants from wastewater (Bayramoğlu and Arica 2008; Bódalo et al. 2008; Alemzadeh and Nejati 2009; Vasileva et al. 2009; Li et al. 2013). Also in these applications, enzyme stability is a crucial factor. By modifying HRP with different polysaccharides, a starch-conjugated enzyme was recently found to show more than sixfold improved stability compared to unconjugated HRP. The enzymatic activity of starch-conjugated HRP was found unimpaired when applied for decolorization of bromophenol blue, demonstrating its applicability for wastewaters treatment (Kagliwal and Singhal 2014). The use of recombinant HRP mutants with improved stability behavior (e.g. Morawski et al. 2001; Ryan and O’Fágáin 2007a), as well as upcoming studies thereon are likely to yield further beneficial contributions in the near future. The broad substrate spectrum of HRP and the spontaneous polymerization of radicalized reaction products in particular facilitate the use of HRP in detoxification applications. Insoluble polymer molecules are easily separable from aqueous systems by filtration. Immobilization of HRP onto a suitable carrier surface facilitates reusability, it is known to affect enzyme activity and stability, and its optimization will certainly be the subject of future studies. In that regard, we recently filed a patent application on the use of immobilized recombinant HRP and variants thereof for the treatment of wastewater in order to remove e.g. endocrine-disrupting compounds such as synthetic estrogens (Kulterer et al. 2013). Also in terms of immobilization, the choice of an appropriate production host is crucial due to the absence or presence of glycan structures which could be exploited for convenient enzyme immobilization (Dalal and Gupta 2007) and affect enzyme stability (Hiner et al. 1995).

Recent advances in cancer treatment using HRP in an enzyme-prodrug system

Since the late 1990s (Folkes et al. 1998, 1999), HRP has been studied in an enzyme/prodrug system for cancer treatment.

The plant hormone IAA is part of the auxin metabolism and a natural substrate of HRP. It has long been known that oxidation of IAA by HRP does not require addition of H₂O₂ (Galston et al. 1953). However, due to the high number of partially unstable IAA derivatives and enzyme intermediates, the actual reaction mechanism is still not fully understood (Yamazaki and Yamazaki 1973; Kanofsky 1988; Gazarian et al. 1998). Targeting of HRP to cancer cells is crucial for the directed killing of these cells and can be achieved by either antibody-, polymer-, or gene-direct enzyme-prodrug therapy (ADEPT/PDEPT/GDEPT) (Folkes and Wardman 2001; Greco et al. 2001). The most recent explanation for the mechanism of HRP/IAA-induced cytotoxicity involves the induction of apoptosis due to the production of free radicals (Greco et al. 2002; de Melo et al. 2004; Kim et al. 2004). HRP/IAA-produced H₂O₂ was suggested to trigger the activation of the MAP kinases c-Jun N-terminal kinase and p38, caspase-3 activation, and poly(ADP-ribose) polymerase cleavage. The authors concluded that H₂O₂ is the key mediator of HRP/IAA-induced apoptosis (Kim et al. 2006a), involving the activation of a death receptor signaling pathway which is initiated by a H₂O₂-mediated increase in CD95 cell surface expression (Kim et al. 2006b). However, also other apoptotic pathways are likely to be involved in HRP/IAA-mediated cytotoxicity and additional studies will have to be conducted in order to unravel the overall molecular mechanism. In recent years, the HRP/IAA system has been tested successfully *in vitro* in various cancer cell lines of pancreatic cancer (Huang et al. 2005), lung carcinoma (Xu et al. 2011), urinary bladder carcinoma (Jeong et al. 2010), and hematopoietic tumor cells (Dalmazzo et al. 2011), as well as *in vivo* in mice (Xu et al. 2011; Dai et al. 2012). In a new study, chitosan nanoparticles encapsulating HRP were shown to induce cell death in a human breast cancer cell line. The encapsulation allowed for enhanced stability at 37 °C and in the presence of urea, compared to free enzyme (Cao et al. 2014). However, particularly with respect to this exciting medical application, a biotechnological approach would be considerably favorable over the current isolation procedure from plant roots to ensure a steady supply of recombinant HRP preparations at consistent quality via a controllable production process.

Conclusions and outlook

HRP research has come a long way over the last two centuries. To date, HRP is a model enzyme for peroxidases. The numerous studies on its structural and mechanistic properties greatly broadened our understanding on peroxidase catalysis. On the other hand, plenty of questions remain unanswered so far, such as the identities and *in planta* roles of all different natural HRP isoenzymes, their biochemical properties, and their exploitation in the vast selection of potential applications. The

use of an efficient recombinant expression system will greatly facilitate production processes of individual isoenzymes, which can then be evaluated for their suitability for any given application, an effort which is highly recommendable, regarding the diversity of the biochemical properties of the different isoenzymes. Also, further in-depth knowledge on the enzymology of different isoenzymes will facilitate rational design endeavors to generate mutant HRPs with tailor-made properties for any application, e.g. increased substrate affinity, solvent stability, peroxide resistance, or enantioselectivity. Regarding diagnostics, we now have the tools at hand to make use of modern recombinant technologies and a whole range of HRP isoenzymes with different characteristics to design tailored fusion proteins for a new and higher level of diagnostic kits with well-defined detection/reporter enzymes of consistent high quality. In light of a possible medical application of HRP in human, e.g. in ADEPT for cancer therapy, the glycan structures on the enzyme surface will have to be addressed not to interfere with the human immune system. To avoid this issue, the use of engineered yeast strains that allow human-type glycosylation could be considered. On the other hand, a rapid clearance of those HRP molecules that did not bind to cancer cells might also be a desired effect.

Despite the astonishing number of studies on HRP, it seems that we have just scratched the surface. In light of the increasing demand for HRP due to the multitude of applications in life sciences and medicine, biotechnological state-of-the-art strategies will have to be adopted to allow a steady supply of well-defined HRP preparations at high quality.

Acknowledgments The authors would like to acknowledge the support from NAWI Graz and the Austrian Science Fund FWF project W901 “DK Molecular Enzymology.” The authors declare that they have no conflict of interest.

Open Access This article is distributed under the terms of the Creative Commons Attribution License which permits any use, distribution, and reproduction in any medium, provided the original author(s) and the source are credited.

References

- Ahammad AJS, Sarker S, Lee J-J (2011) Immobilization of horseradish peroxidase onto a gold-nanoparticle-adsorbed poly(thionine) film for the construction of a hydrogen peroxide biosensor. *J Nanosci Nanotechnol* 11:5670–5
- Aibara S, Kobayashi T, Morita Y (1981) Isolation and properties of basic isoenzymes of horseradish peroxidase. *J Biochem* 90:489–96
- Aibara S, Yamashita H, Mori E, Kato M, Morita Y (1982) Isolation and characterization of five neutral isoenzymes of horseradish peroxidase. *J Biochem* 92:531–9
- Alemzadeh I, Nejati S (2009) Phenols removal by immobilized horseradish peroxidase. *J Hazard Mater* 166:1082–6. doi:10.1016/j.jhazmat.2008.12.026

- Alonso-Lomillo MA, Ruiz JG, Pascual FJM (2005) Biosensor based on platinum chips for glucose determination. *Anal Chim Acta* 547: 209–214. doi:10.1016/j.aca.2005.05.037
- Antipov E, Cho AE, Klivanov AM (2009) How a single-point mutation in horseradish peroxidase markedly enhances enantioselectivity. *J Am Chem Soc* 131:11155–60. doi:10.1021/ja903482u
- Arnao MB, Acosta M, del Río JA, García-Cánovas F (1990a) Inactivation of peroxidase by hydrogen peroxide and its protection by a reductant agent. *Biochim Biophys Acta* 1038:85–9
- Arnao MB, Acosta M, del Río JA, Varón R, García-Cánovas F (1990b) A kinetic study on the suicide inactivation of peroxidase by hydrogen peroxide. *Biochim Biophys Acta* 1041:43–7
- Asad S, Dabirmanesh B, Ghaemi N, Etezzad SM, Khajeh K (2013) Studies on the refolding process of recombinant horseradish peroxidase. *Mol Biotechnol* 54:484–92. doi:10.1007/s12033-012-9588-6
- Azevedo AM, Martins VC, Prazeres DM, Vojinović V, Cabral JM, Fonseca LP (2003) Horseradish peroxidase: a valuable tool in biotechnology. *Biotechnol Annu Rev* 9:199–247. doi:10.1016/S1387-2656(03)09003-3
- Azevedo AM, Prazeres DMF, Cabral JMS, Fonseca LP (2005) Ethanol biosensors based on alcohol oxidase. *Biosens Bioelectron* 21:235–47. doi:10.1016/j.bios.2004.09.030
- Bagger S, Williams RJP, Schroll G, Lindberg AA, Lagerlund I, Ehrenberg L (1971) Intermediates in the reaction between hydrogen peroxide and horseradish peroxidase. *Acta Chem Scand* 25:976–982. doi:10.3891/acta.chem.scand.25-0976
- Barber JEB, Damry AM, Calderini GF, Walton CJW, Chica RA (2014) Continuous colorimetric screening assay for detection of d-amino acid aminotransferase mutants displaying altered substrate specificity. *Anal Biochem* 463:23–30. doi:10.1016/j.ab.2014.06.006
- Bartonek-Roxå E, Eriksson H, Mattiasson B (1991) The cDNA sequence of a neutral horseradish peroxidase. *Biochim Biophys Acta* 1088: 245–50
- Bayramoğlu G, Arica MY (2008) Enzymatic removal of phenol and p-chlorophenol in enzyme reactor: horseradish peroxidase immobilized on magnetic beads. *J Hazard Mater* 156:148–55. doi:10.1016/j.jhazmat.2007.12.008
- Bayramoglu G, Altintas B, Yakup Arica M (2012) Cross-linking of horseradish peroxidase adsorbed on polycationic films: utilization for direct dye degradation. *Bioprocess Biosyst Eng* 35:1355–65. doi:10.1007/s00449-012-0724-2
- Berglund GI, Carlsson GH, Smith AT, Szöke H, Henriksen A, Hajdu J (2002) The catalytic pathway of horseradish peroxidase at high resolution. *Nature* 417:463–8. doi:10.1038/417463a
- Bjellqvist B, Hughes GJ, Pasquali C, Paquet N, Ravier F, Sanchez JC, Frutiger S, Hochstrasser D (1993) The focusing positions of polypeptides in immobilized pH gradients can be predicted from their amino acid sequences. *Electrophoresis* 14:1023–31
- Bjellqvist B, Basse B, Olsen E, Celis JE (1994) Reference points for comparisons of two-dimensional maps of proteins from different human cell types defined in a pH scale where isoelectric points correlate with polypeptide compositions. *Electrophoresis* 15:529–39
- Bódalo A, Bastida J, Máximo MF, Montiel MC, Gómez M, Murcia MD (2008) A comparative study of free and immobilized soybean and horseradish peroxidases for 4-chlorophenol removal: protective effects of immobilization. *Bioprocess Biosyst Eng* 31: 587–93. doi:10.1007/s00449-008-0207-7
- Boucher J, Vadon S, Tomas A, Viosat B, Mansuy D (1996) Oxidation of arylamidoximes by hydrogen peroxide and horseradish peroxidase in water: easy preparation and X-ray structure of O-(arylimidoyl)arylamidoximes. *Tetrahedron Lett* 37:3113–3116
- Burke JF, Smith A, Santama N, Bray RC, Thorneley RN, Dacey S, Griffiths J, Catlin G, Edwards M (1989) Expression of recombinant horseradish peroxidase C in *Escherichia coli*. *Biochem Soc Trans* 17:1077–8
- Cao X, Chen C, Yu H, Wang P (2014) Horseradish peroxidase-encapsulated chitosan nanoparticles for enzyme-prodrug cancer therapy. *Biotechnol Lett*. doi:10.1007/s10529-014-1664-5
- Capone S, Pletzenauer R, Maresch D, Metzger K, Altmann F, Herwig C, Spadiut O (2014) Glyco-variant library of the versatile enzyme horseradish peroxidase. *Glycobiology*. doi:10.1093/glycob/cwu047
- Chance B (1952) The kinetics and stoichiometry of the transition from the primary to the secondary peroxidase peroxide complexes. *Arch Biochem Biophys* 41:416–24
- Chen H, Jiang C, Yu C, Zhang S, Liu B, Kong J (2009) Protein chips and nanomaterials for application in tumor marker immunoassays. *Biosens Bioelectron* 24:3399–411. doi:10.1016/j.bios.2009.03.020
- Cheng J, Ming Yu S, Zuo P (2006) Horseradish peroxidase immobilized on aluminium-pillared inter-layered clay for the catalytic oxidation of phenolic wastewater. *Water Res* 40:283–90. doi:10.1016/j.watres.2005.11.017
- Chiswell DJ, Ortlepp SA (1988) DNA sequence coding for HRP enzyme. EP0299682A1
- Colonna S, Gaggero N, Carrea G, Pasta P (1992) Horseradish peroxidase catalysed sulfoxidation is enantioselective. *J Chem Soc Chem Commun* 357. doi:10.1039/c39920000357
- Colonna S, Gaggero N, Richelmi C, Pasta P (1999) Recent biotechnological developments in the use of peroxidases. *Trends Biotechnol* 17:163–8
- Da Silva MR, de Sá LRV, Russo C, Scio E, Ferreira-Leitão VS (2011) The use of HRP in decolorization of reactive dyes and toxicological evaluation of their products. *Enzym Res* 2010: 703824. doi:10.4061/2010/703824
- Dai M, Liu J, Chen D-E, Rao Y, Tang Z-J, Ho W-Z, Dong C-Y (2012) Tumor-targeted gene therapy using Adv-AFP-HRPC/IAA prodrug system suppresses growth of hepatoma xenografted in mice. *Cancer Gene Ther* 19:77–83. doi:10.1038/cgt.2011.65
- Dalal S, Gupta MN (2007) Treatment of phenolic wastewater by horseradish peroxidase immobilized by bioaffinity layering. *Chemosphere* 67:741–7. doi:10.1016/j.chemosphere.2006.10.043
- Dalmazzo LFF, Santana-Lemos BA, Jácomo RH, Garcia AB, Rego EM, da Fonseca LM, Falcão RP (2011) Antibody-targeted horseradish peroxidase associated with indole-3-acetic acid induces apoptosis in vitro in hematological malignancies. *Leuk Res* 35:657–62. doi:10.1016/j.leukres.2010.11.025
- Das PK, Caaveiro JMM, Luque S, Klivanov AM (2002) Binding of hydrophobic hydroxamic acids enhances peroxidase's stereoselectivity in nonaqueous sulfoxidations. *J Am Chem Soc* 124:782–787. doi:10.1021/ja012075o
- de las Segura M, Levin G, Miranda MV, Mendive FM, Targovnik HM, Cascone O (2005) High-level expression and purification of recombinant horseradish peroxidase isozyme C in SF-9 insect cell culture. *Process Biochem* 40:795–800. doi:10.1016/j.procbio.2004.02.009
- De Melo MP, de Lima TM, Pithon-Curi TC, Curi R (2004) The mechanism of indole acetic acid cytotoxicity. *Toxicol Lett* 148:103–11. doi:10.1016/j.toxlet.2003.12.067
- Derat E, Shaik S (2006) The Poulos-Kraut mechanism of compound I formation in horseradish peroxidase: a QM/MM study. *J Phys Chem B* 110:10526–33. doi:10.1021/jp055412e
- Derat E, Shaik S, Rovira C, Vidossich P, Alfonso-Prieto M (2007) The effect of a water molecule on the mechanism of formation of compound 0 in horseradish peroxidase. *J Am Chem Soc* 129:6346–7. doi:10.1021/ja0676861
- Dietzsch C, Spadiut O, Herwig C (2011a) A fast approach to determine a fed batch feeding profile for recombinant *Pichia pastoris* strains. *Microb Cell Factories* 10:85–94. doi:10.1186/1475-2859-10-85
- Dietzsch C, Spadiut O, Herwig C (2011b) A dynamic method based on the specific substrate uptake rate to set up a feeding strategy for *Pichia pastoris*. *Microb Cell Factories* 10:14–22. doi:10.1186/1475-2859-10-14

- Egorov AM, Gazaryan IG, Savelyev SV, Fechina VA, Veryovkin AN, Kim BB (1991) Horseradish peroxidase gene expression in *Escherichia coli*. Ann N Y Acad Sci 646:35–40
- Fan H, Jiao F, Chen H, Zhang F, Wang Q, He P, Fang Y (2013) Qualitative and quantitative detection of DNA amplified with HRP-modified SiO₂ nanoparticles using scanning electrochemical microscopy. Biosens Bioelectron 47:373–8. doi:10.1016/j.bios.2013.03.027
- Flocco CG, Giulietti M (2003) Effect of chitosan on peroxidase activity and isoenzyme profile in hairy root cultures of *Armoracia lapathifolia*. Appl Biochem Biotechnol 110:175–83
- Flocco CG, Alvarez MA, Giulietti AM (1998) Peroxidase production in vitro by *Armoracia lapathifolia* (horseradish)-transformed root cultures: effect of elicitation on level and profile of isoenzymes. Biotechnol Appl Biochem 28:33–8
- Folkes LK, Wardman P (2001) Oxidative activation of indole-3-acetic acids to cytotoxic species—a potential new role for plant auxins in cancer therapy. Biochem Pharmacol 61:129–36
- Folkes LK, Candeias LP, Wardman P (1998) Toward targeted “oxidation therapy” of cancer: peroxidase-catalysed cytotoxicity of indole-3-acetic acids. Int J Radiat Oncol Biol Phys 42:917–20. doi:10.1021/bi970384e
- Folkes LK, Dennis MF, Stratford MR, Candeias LP, Wardman P (1999) Peroxidase-catalyzed effects of indole-3-acetic acid and analogues on lipid membranes, DNA, and mammalian cells in vitro. Biochem Pharmacol 57:375–82
- Fujiyama K, Takemura H, Shibayama S, Kobayashi K, Choi JK, Shinmyo A, Takano M, Yamada Y, Okada H (1988) Structure of the horseradish peroxidase isozyme C genes. Eur J Biochem 173:681–7
- Fujiyama K, Takemura H, Shinmyo A, Okada H, Takano M (1990) Genomic DNA structure of two new horseradish-peroxidase-encoding genes. Gene 89:163–9
- Gajhede M, Schuller DJ, Henriksen A, Smith AT, Poulos TL (1997) Crystal structure of horseradish peroxidase C at 2.15 Å resolution. Nat Struct Biol 4:1032–8
- Galston AW, Bonner J, Baker RS (1953) Flavoprotein and peroxidase as components of the indoleacetic acid oxidase system of peas. Arch Biochem Biophys 42:456–70
- Gasser B, Maurer M, Gach J, Kunert R, Mattanovich D (2006) Engineering of *Pichia pastoris* for improved production of antibody fragments. Biotechnol Bioeng 94:353–61. doi:10.1002/bit.20851
- Gasteiger E, Hoogland C, Gattiker A, Duvaud S, Wilkins MR, Appel RD, Bairoch A (2005) The proteomics protocols handbook: protein identification and analysis tools on the ExPASy server, 1st ed. Biochemical 71:571–607. doi:10.1134/S0006297906060150
- Gazarian IG, Lagrimini LM, Mellon FA, Naldrett MJ, Ashby GA, Thorneley RN (1998) Identification of skatolyl hydroperoxide and its role in the peroxidase-catalysed oxidation of indol-3-yl acetic acid. Biochem J 333:223–32
- George P (1952) Chemical nature of the secondary hydrogen peroxide compound formed by cytochrome-c peroxidase and horseradish peroxidase. Nature 169:612–3
- George P (1953) The chemical nature of the second hydrogen peroxide compound formed by cytochrome c peroxidase and horseradish peroxidase. I. Titration with reducing agents. Biochem J 54:267–76
- Greco O, Rossiter S, Kanthou C, Folkes LK, Wardman P, Tozer GM, Dachs GU (2001) Horseradish peroxidase-mediated gene therapy: choice of prodrugs in oxic and anoxic tumor conditions. Mol Cancer Ther 1:151–60
- Greco O, Dachs GU, Tozer GM, Kanthou C (2002) Mechanisms of cytotoxicity induced by horseradish peroxidase/indole-3-acetic acid gene therapy. J Cell Biochem 87:221–232. doi:10.1002/jcb.10292
- Grigorenko V, Chubar T, Kapeliuch Y, Borchers T, Spener F, Egorov A (1999) New approaches for functional expression of recombinant horseradish peroxidase C in *Escherichia coli*. Biocatal Biotransformation 17:359–379
- Guerfal M, Ryckaert S, Jacobs PP, Ameloot P, Van Craenenbroeck K, Derycke R, Callewaert N (2010) The *HAC1* gene from *Pichia pastoris*: characterization and effect of its overexpression on the production of secreted, surface displayed and membrane proteins. Microb Cell Factories 9:49. doi:10.1186/1475-2859-9-49
- Hartmann C, Ortiz de Montellano PR (1992) Baculovirus expression and characterization of catalytically active horseradish peroxidase. Arch Biochem Biophys 297:61–72
- Hartner FS, Ruth C, Langenegger D, Johnson SN, Hyka P, Lin-Cereghino GP, Lin-Cereghino J, Kovar K, Cregg JM, Glieder A (2008) Promoter library designed for fine-tuned gene expression in *Pichia pastoris*. Nucleic Acids Res 36:e76. doi:10.1093/nar/gkn369
- Heggie L, Jansen MAK, Burbridge EM, Kavanagh TA, Thorneley RNF, Dix PJ (2005) Transgenic tobacco (*Nicotiana tabacum* L. cv. Samsun-NN) plants over-expressing a synthetic HRP-C gene are altered in growth, development and susceptibility to abiotic stress. Plant Physiol Biochem 43:1067–73. doi:10.1016/j.plaphy.2005.11.002
- Henriksen A, Schuller DJ, Meno K, Welinder KG, Smith AT, Gajhede M (1998) Structural interactions between horseradish peroxidase C and the substrate benzhydroxamic acid determined by X-ray crystallography. Biochemistry 37:8054–60. doi:10.1021/bi980234j
- Hernández-Ruiz J, Arnao MB, Hiner AN, García-Cánovas F, Acosta M (2001) Catalase-like activity of horseradish peroxidase: relationship to enzyme inactivation by H₂O₂. Biochem J 354:107–14
- Hiner AN, Hernández-Ruiz J, García-Cánovas F, Smith AT, Arnao MB, Acosta M (1995) A comparative study of the inactivation of wild-type, recombinant and two mutant horseradish peroxidase isoenzymes C by hydrogen peroxide and m-chloroperoxybenzoic acid. Eur J Biochem 234:506–12
- Hiner AN, Hernández-Ruiz J, Arnao MB, García-Cánovas F, Acosta M (1996) A comparative study of the purity, enzyme activity, and inactivation by hydrogen peroxide of commercially available horseradish peroxidase isoenzymes A and C. Biotechnol Bioeng 50:655–62. doi:10.1002/(SICI)1097-0290(19960620)50:6<655::AID-BIT6>3.0.CO;2-J
- Hiner ANP, Hernández-Ruiz J, Rodríguez-López JN, Arnao MB, Varón R, García-Cánovas F, Acosta M (2001a) The inactivation of horseradish peroxidase isoenzyme A2 by hydrogen peroxide: an example of partial resistance due to the formation of a stable enzyme intermediate. J Biol Inorg Chem 6:504–16. doi:10.1007/s007750100219
- Hiner AN, Hernández-Ruiz J, Williams GA, Arnao MB, García-Cánovas F, Acosta M (2001b) Catalase-like oxygen production by horseradish peroxidase must predominantly be an enzyme-catalyzed reaction. Arch Biochem Biophys 392:295–302. doi:10.1006/abbi.2001.2460
- Hoyle MC (1977) High resolution of peroxidase-indoleacetic acid oxidase isoenzymes from horseradish by isoelectric focusing. Plant Physiol 60:787–93
- Huang C, Liu L-Y, Song T-S, Ni L, Yang L, Hu X-Y, Hu J-S, Song L-P, Luo Y, Si L-S (2005) Apoptosis of pancreatic cancer BXPc-3 cells induced by indole-3-acetic acid in combination with horseradish peroxidase. World J Gastroenterol 11:4519–23
- Jeong Y-M, Oh MH, Kim SY, Li H, Yun H-Y, Baek KJ, Kwon NS, Kim WY, Kim D-S (2010) Indole-3-acetic acid/horseradish peroxidase induces apoptosis in TCCSUP human urinary bladder carcinoma cells. Pharmazie 65:122–6
- Jermyn MA (1952) Horseradish peroxidase. Nature 169:488–9
- Jermyn MA, Thomas R (1954) Multiple components in horseradish peroxidase. Biochem J 56:631–9
- Joo H, Lin Z, Arnold FH (1999) Laboratory evolution of peroxide-mediated cytochrome P450 hydroxylation. Nature 399:670–3. doi:10.1038/21395
- Kafi AKM, Chen A (2009) A novel amperometric biosensor for the detection of nitrophenol. Talanta 79:97–102. doi:10.1016/j.talanta.2009.03.015

- Kafi AKM, Wu G, Chen A (2008) A novel hydrogen peroxide biosensor based on the immobilization of horseradish peroxidase onto Au-modified titanium dioxide nanotube arrays. *Biosens Bioelectron* 24:566–71. doi:10.1016/j.bios.2008.06.004
- Kagliwal LD, Singhal RS (2014) Enzyme-polysaccharide interaction: a method for improved stability of horseradish peroxidase. *Int J Biol Macromol* 69:329–35. doi:10.1016/j.ijbiomac.2014.05.065
- Kalliney S, Zaks A (1995) An efficient peroxidase-catalyzed oxidation of hydroxylaminoeverminomicin in aqueous-organic media. *Tetrahedron Lett* 36:4163–4166. doi:10.1016/0040-4039(95)00713-M
- Kalra B, Gross RA (2000) Horseradish peroxidase mediated free radical polymerization of methyl methacrylate. *Biomacromolecules* 1:501–5
- Kanofsky JR (1988) Singlet oxygen production from the peroxidase-catalyzed oxidation of indole-3-acetic acid. *J Biol Chem* 263:14171–5
- Kawaoka A, Kawamoto T, Moriki H, Murakami A, Murakami K, Yoshida K, Sekine M, Takano M, Shinmyo A (1994) Growth-stimulation of tobacco plant introduced the horseradish peroxidase gene *prxC1a*. *J Ferment Bioeng* 78:49–53. doi:10.1016/0922-338X(94)90177-5
- Kawaoka A, Matsunaga E, Endo S, Kondo S, Yoshida K, Shinmyo A, Ebinuma H (2003) Ectopic expression of a horseradish peroxidase enhances growth rate and increases oxidative stress resistance in hybrid aspen. *Plant Physiol* 132:1177–85
- Kay E, Shannon LM, Lew JY (1967) Peroxidase isozymes from horseradish roots. II. Catalytic properties. *J Biol Chem* 242:2470–3
- Keilin D, Hartree EF (1951) Purification of horse-radish peroxidase and comparison of its properties with those of catalase and methaemoglobin. *Biochem J* 49:88–104
- Kim D-S, Jeon S-E, Park K-C (2004) Oxidation of indole-3-acetic acid by horseradish peroxidase induces apoptosis in G361 human melanoma cells. *Cell Signal* 16:81–8. doi:10.1016/S0898-6568(03)00091-3
- Kim D-S, Jeon S-E, Jeong Y-M, Kim S-Y, Kwon S-B, Park K-C (2006a) Hydrogen peroxide is a mediator of indole-3-acetic acid/horseradish peroxidase-induced apoptosis. *FEBS Lett* 580:1439–46. doi:10.1016/j.febslet.2006.01.073
- Kim D-S, Kim S-Y, Jeong Y-M, Jeon S-E, Kim M-K, Kwon S-B, Park K-C (2006b) Indole-3-acetic acid/horseradish peroxidase-induced apoptosis involves cell surface CD95 (Fas/APO-1) expression. *Biol Pharm Bull* 29:1625–9
- Kim SJ, Joo JC, Song BK, Yoo YJ, Kim YH (2014a) Engineering a horseradish peroxidase C stable to radical attacks by mutating multiple radical coupling sites. *Biotechnol Bioeng* 1–28. doi:10.1002/bit.25483
- Kim J, Kim J, Rho THD, Lee JH (2014b) Rapid chemiluminescent sandwich enzyme immunoassay capable of consecutively quantifying multiple tumor markers in a sample. *Talanta* 129:106–12. doi:10.1016/j.talanta.2014.05.020
- Kis M, Burbridge E, Brock IW, Heggie L, Dix PJ, Kavanagh TA (2004) An N-terminal peptide extension results in efficient expression, but not secretion, of a synthetic horseradish peroxidase gene in transgenic tobacco. *Ann Bot* 93:303–10. doi:10.1093/aob/mch045
- Koliasnikov OV, Grigorenko VG, Egorov AM, Lange S, Schmid RD (2011) Recombinant production of horseradish peroxidase conjugates with Fab antibodies in *Pichia pastoris* for analytical applications. *Acta Nat* 3:85–92
- Krainer FW, Dietzsch C, Hajek T, Herwig C, Spadiut O, Glieder A (2012) Recombinant protein expression in *Pichia pastoris* strains with an engineered methanol utilization pathway. *Microb Cell Factories* 11:22–35. doi:10.1186/1475-2859-11-22
- Krainer FW, Gmeiner C, Neutsch L, Windwarder M, Pletzenauer R, Herwig C, Altmann F, Glieder A, Spadiut O (2013a) Knockout of an endogenous mannosyltransferase increases the homogeneity of glycoproteins produced in *Pichia pastoris*. *Sci Rep* 3:3279–91. doi:10.1038/srep03279
- Krainer FW, Pletzenauer R, Rossetti L, Herwig C, Glieder A, Spadiut O (2013b) Purification and basic biochemical characterization of 19 recombinant plant peroxidase isoenzymes produced in *Pichia pastoris*. *Protein Expr Purif* 95C:104–112. doi:10.1016/j.pep.2013.12.003
- Kubota K, Mizukoshi T, Miyano H (2013) A new approach for quantitative analysis of L-phenylalanine using a novel semi-sandwich immunometric assay. *Anal Bioanal Chem* 405:8093–103. doi:10.1007/s00216-013-7081-0
- Kulterer M, Reichel V, Ribitsch V, Glieder A, Krainer F (2013) Degradation of hormones using recombinant HRP isoenzymes. EP2628713A1
- Kurokawa Y, Yanagi H, Yura T (2000) Overexpression of protein disulfide isomerase DsbC stabilizes multiple-disulfide-bonded recombinant protein produced and transported to the periplasm in *Escherichia coli*. *Appl Environ Microbiol* 66:3960–5. doi:10.1128/AEM.66.9.3960-3965.2000
- Levin G, Mendive F, Targovnik HM, Cascone O, Miranda MV (2005) Genetically engineered horseradish peroxidase for facilitated purification from baculovirus cultures by cation-exchange chromatography. *J Biotechnol* 118:363–9. doi:10.1016/j.jbiotec.2005.05.015
- Li H, Zhao H, Liu C, Li Y, Cao H, Zhang Y (2013) A novel mechanism of bisphenol A removal during electro-enzymatic oxidative process: chain reactions from self-polymerization to cross-coupling oxidation. *Chemosphere* 92:1294–300. doi:10.1016/j.chemosphere.2013.04.071
- Li T, Lin H, Yu L, Xue M, Ge S, Zhao Q, Zhang J, Xia N (2014) Development of an enzyme-linked immunospot assay for determination of rotavirus infectivity. *J Virol Methods* 209:7–14. doi:10.1016/j.jviromet.2014.08.012
- Lin-Cereghino GP, Stark CM, Kim D, Chang J, Shaheen N, Poerwanto H, Agari K, Moua P, Low LK, Tran N, Huang AD, Nattestad M, Oshiro KT, Chang JW, Chavan A, Tsai JW, Lin-Cereghino J (2013) The effect of α -mating factor secretion signal mutations on recombinant protein expression in *Pichia pastoris*. *Gene* 519:311–7. doi:10.1016/j.gene.2013.01.062
- Liu X, Luo L, Ding Y, Xu Y (2011) Amperometric biosensors based on alumina nanoparticles-chitosan-horseradish peroxidase nanobiocomposites for the determination of phenolic compounds. *Analyst* 136:696–701. doi:10.1039/c0an00752h
- Loughran NB, O'Connell MJ, O'Connor B, O'Fágáin C (2014) Stability properties of an ancient plant peroxidase. *Biochimie* 104:156–9. doi:10.1016/j.biochi.2014.05.012
- Malani RS, Khanna S, Moholkar VS (2013) Sonoenzymatic decolorization of an azo dye employing immobilized horse radish peroxidase (HRP): a mechanistic study. *J Hazard Mater* 256–257:90–7. doi:10.1016/j.jhazmat.2013.04.023
- Marklund S, Ohlsson PI, Opara A, Paul KG (1974) The substrate profiles of the acidic and slightly basic horseradish peroxidases. *Biochim Biophys Acta* 350:304–13
- Matsui T, Nakayama H, Yoshida K, Shinmyo A (2003) Vesicular transport route of horseradish C1a peroxidase is regulated by N- and C-terminal propeptides in tobacco cells. *Appl Microbiol Biotechnol* 62:517–22. doi:10.1007/s00253-003-1273-z
- Matsui T, Hori M, Shizawa N, Nakayama H, Shinmyo A, Yoshida K (2006) High-efficiency secretory production of peroxidase C1a using vesicular transport engineering in transgenic tobacco. *J Biosci Bioeng* 102:102–9. doi:10.1263/jbb.102.102
- Matsui T, Tabayashi A, Iwano M, Shinmyo A, Kato K, Nakayama H (2011) Activity of the C-terminal-dependent vacuolar sorting signal of horseradish peroxidase C1a is enhanced by its secondary structure. *Plant Cell Physiol* 52:413–20. doi:10.1093/pcp/pcq205
- Miller VP, Goodin DB, Friedman AE, Hartmann C, Ortiz de Montellano PR (1995) Horseradish peroxidase Phe172 \rightarrow Tyr mutant. Sequential formation of compound I with a porphyrin radical cation and a protein radical. *J Biol Chem* 270:18413–9

- Morawski B, Lin Z, Cirino P, Joo H, Bandara G, Arnold FH (2000) Functional expression of horseradish peroxidase in *Saccharomyces cerevisiae* and *Pichia pastoris*. *Protein Eng* 13:377–84
- Morawski B, Quan S, Arnold FH (2001) Functional expression and stabilization of horseradish peroxidase by directed evolution in *Saccharomyces cerevisiae*. *Biotechnol Bioeng* 76:99–107
- Morita Y, Mikami B, H. Y, Lee JY, Aibara S, Sato M, Katsube Y, Tanaka N (1991) Biochemical, molecular, and physiological aspects of plant peroxidases: primary and crystal structures of horseradish peroxidase isozyme E5. 81–88
- Näätsaari L, Krainer FW, Schubert M, Glieder A, Thallinger GG (2014) Peroxidase gene discovery from the horseradish transcriptome. *BMC Genomics* 15:227. doi:10.1186/1471-2164-15-227
- Newmyer SL, Ortiz de Montellano PR (1995) Horseradish peroxidase His-42 → Ala, His-42 → Val, and Phe-41 → Ala mutants. Histidine catalysis and control of substrate access to the heme iron. *J Biol Chem* 270:19430–8
- Newmyer SL, Ortiz de Montellano PR (1996) Rescue of the catalytic activity of an H42A mutant of horseradish peroxidase by exogenous imidazoles. *J Biol Chem* 271:14891–6
- Newmyer SL, Sun J, Loehr TM, Ortiz de Montellano PR (1996) Rescue of the horseradish peroxidase His-170 → Ala mutant activity by imidazole: importance of proximal ligand tethering. *Biochemistry* 35:12788–95. doi:10.1021/bi9609331
- Nielsen KL, Indiani C, Henriksen A, Feis A, Becucci M, Gajhede M, Smulevich G, Welinder KG (2001) Differential activity and structure of highly similar peroxidases. Spectroscopic, crystallographic, and enzymatic analyses of lignifying *Arabidopsis thaliana* peroxidase A2 and horseradish peroxidase A2. *Biochemistry* 40:11013–21
- O'Brien AM, O'Fágáin C, Nielsen PF, Welinder KG (2001) Location of crosslinks in chemically stabilized horseradish peroxidase: implications for design of crosslinks. *Biotechnol Bioeng* 76:277–84. doi:10.1002/bit.1194
- Ortlepp SA, Pollard-Knight D, Chiswell DJ (1989) Expression and characterisation of a protein specified by a synthetic horseradish peroxidase gene in *Escherichia coli*. *J Biotechnol* 11:353–364. doi:10.1016/0168-1656(89)90019-9
- Ozaki S, Ortiz de Montellano PR (1994) Molecular engineering of horseradish peroxidase. Highly enantioselective sulfoxidation of aryl alkyl sulfides by the Phe-41 → Leu mutant. *J Am Chem Soc* 116:4487–4488. doi:10.1021/ja00089a052
- Ozaki S, Ortiz de Montellano PR (1995) Molecular engineering of horseradish peroxidase: thioether sulfoxidation and styrene epoxidation by Phe-41 leucine and threonine mutants. *J Am Chem Soc* 117:7056–7064. doi:10.1021/ja00132a003
- Passardi F, Cosio C, Penel C, Dunand C (2005) Peroxidases have more functions than a Swiss army knife. *Plant Cell Rep* 24:255–65. doi:10.1007/s00299-005-0972-6
- Patris S, De Pauw P, Vandepuut M, Huet J, Van Antwerpen P, Muyldermans S, Kauffmann J-M (2014) Nanoimmunoassay onto a screen printed electrode for HER2 breast cancer biomarker determination. *Talanta* 130:164–70. doi:10.1016/j.talanta.2014.06.069
- Pereira AR, da Costa RS, Yokoyama L, Alhadeff EM, Teixeira LAC (2014) Evaluation of textile dye degradation due to the combined action of enzyme horseradish peroxidase and hydrogen peroxide. *Appl Biochem Biotechnol* 174:2741–7. doi:10.1007/s12010-014-1222-6
- Planche LA (1810) Note sur la sophistication de la résine de jalap et sur les moyens de la reconnaître. *Bull Pharm* 2:578–580
- Poulos TL, Kraut J (1980) The stereochemistry of peroxidase catalysis. *J Biol Chem* 255:8199–205
- Preethi S, Anumary A, Ashokkumar M, Thanikaivelan P (2013) Probing horseradish peroxidase catalyzed degradation of azo dye from tannery wastewater. *Springerplus* 2:341. doi:10.1186/2193-1801-2-341
- Raghu P, Madhusudana Reddy T, Reddaiah K, Jaidev LR, Narasimha G (2013) A novel electrochemical biosensor based on horseradish peroxidase immobilized on Ag-nanoparticles/poly(l-arginine) modified carbon paste electrode toward the determination of pyrogallol/hydroquinone. *Enzym Microb Technol* 52:377–385. doi:10.1016/j.enzmictec.2013.02.010
- Regalado C, García-Almendárez BE, Duarte-Vázquez MA (2004) Biotechnological applications of peroxidases. *Phytochem Rev* 3:243–256. doi:10.1023/B:PHYT.0000047797.81958.69
- Romero L, Targovnik A, Wolman F, Fogar M, Simonella M, Cascone O, Miranda M (2010) Recombinant peroxidase production in species of lepidoptera frequently found in Argentina. *N Biotechnol* 27:857–61. doi:10.1016/j.nbt.2010.06.019
- Romero LV, Targovnik AM, Wolman FJ, Cascone O, Miranda MV (2011) *Rachiphusia nu* larva as a biofactory to achieve high level expression of horseradish peroxidase. *Biotechnol Lett* 33:947–56. doi:10.1007/s10529-011-0540-9
- Ruiz-Valdepeñas Montiel V, Campuzano S, Conzuelo F, Torrente-Rodríguez RM, Gamella M, Reviejo AJ, Pingarrón JM (2015) Electrochemical magnetoimmunosensing platform for determination of the milk allergen β-lactoglobulin. *Talanta* 131:156–62. doi:10.1016/j.talanta.2014.07.076
- Ryan BJ, O'Fágáin C (2007a) Effects of single mutations on the stability of horseradish peroxidase to hydrogen peroxide. *Biochimie* 89:1029–32. doi:10.1016/j.biochi.2007.03.013
- Ryan BJ, O'Fágáin C (2007b) Arginine-to-lysine substitutions influence recombinant horseradish peroxidase stability and immobilisation effectiveness. *BMC Biotechnol* 7:86. doi:10.1186/1472-6750-7-86
- Ryan BJ, O'Fágáin C (2008) Effects of mutations in the helix G region of horseradish peroxidase. *Biochimie* 90:1414–21. doi:10.1016/j.biochi.2008.05.008
- Ryan BJ, Carolan N, O'Fágáin C (2006) Horseradish and soybean peroxidases: comparable tools for alternative niches? *Trends Biotechnol* 24:355–63. doi:10.1016/j.tibtech.2006.06.007
- Ryan BJ, O'Connell MJ, O'Fágáin C (2008) Consensus mutagenesis reveals that non-helical regions influence thermal stability of horseradish peroxidase. *Biochimie* 90:1389–96. doi:10.1016/j.biochi.2008.04.009
- Saikrishnan D, Goyal M, Rossiter S, Kukol A (2014) A cellulose-based bioassay for the colorimetric detection of pathogen DNA. *Anal Bioanal Chem* 406:7887–98. doi:10.1007/s00216-014-8257-y
- Sakai S, Khanmohammadi M, Khoshfetrat AB, Taya M (2014) Horseradish peroxidase-catalyzed formation of hydrogels from chitosan and poly(vinyl alcohol) derivatives both possessing phenolic hydroxyl groups. *Carbohydr Polym* 111:404–9. doi:10.1016/j.carbpol.2014.05.010
- Savenkova MI, Ortiz de Montellano PR (1998) Horseradish peroxidase: partial rescue of the His-42 → Ala mutant by a concurrent Asn-70 → Asp mutation. *Arch Biochem Biophys* 351:286–93. doi:10.1006/abbi.1997.0559
- Savenkova MI, Newmyer SL, Ortiz de Montellano PR (1996) Rescue of His-42 → Ala horseradish peroxidase by a Phe-41 → His mutation. Engineering of a surrogate catalytic histidine. *J Biol Chem* 271:24598–603
- Savenkova MI, Kuo JM, Ortiz de Montellano PR (1998) Improvement of peroxygenase activity by relocation of a catalytic histidine within the active site of horseradish peroxidase. *Biochemistry* 37:10828–36. doi:10.1021/bi9725780
- Shannon LM, Kay E, Lew JY (1966) Peroxidase isozymes from horseradish roots. I. Isolation and physical properties. *J Biol Chem* 241:2166–72
- Shih JHC, Shannon LM, Kay E, Lew JY (1971) Peroxidase isoenzymes from horseradish roots. IV. Structural relationships. *J Biol Chem* 246:4546–4551
- Silva E, Edwards AM, Faljoni-Alario A (1990) Enzymatic generation of triplet acetone by deglycosylated horseradish peroxidase. *Arch Biochem Biophys* 276:527–30
- Singh A, Ma D, Kaplan DL (2000) Enzyme-mediated free radical polymerization of styrene. *Biomacromolecules* 1:592–6

- Smith AT, Santama N, Dacey S, Edwards M, Bray RC, Thorneley RN, Burke JF (1990) Expression of a synthetic gene for horseradish peroxidase C in *Escherichia coli* and folding and activation of the recombinant enzyme with Ca²⁺ and heme. *J Biol Chem* 265:13335–43
- Spadiut O, Rossetti L, Dietzsch C, Herwig C (2012) Purification of a recombinant plant peroxidase produced in *Pichia pastoris* by a simple 2-step strategy. *Protein Expr Purif* 86: 89–97. doi:10.1016/j.pep.2012.09.008
- Strickland EH, Kay E, Shannon LM, Horwitz J (1968) Peroxidase isoenzymes from horseradish roots. 3. Circular dichroism of isoenzymes and apoisoenzymes. *J Biol Chem* 243:3560–5
- Tams JW, Welinder KG (1995) Mild chemical deglycosylation of horseradish peroxidase yields a fully active, homogeneous enzyme. *Anal Biochem* 228:48–55. doi:10.1006/abio.1995.1313
- Tams JW, Welinder KG (1998) Glycosylation and thermodynamic versus kinetic stability of horseradish peroxidase. *FEBS Lett* 421:234–6
- Theorell H, Maehly AC, Dam H, Kinell P-O (1950) Untersuchungen an künstlichen Peroxydasen. *Acta Chem Scand* 4:422–434. doi: 10.3891/acta.chem.scand. 04-0422
- Tognolli M, Penel C, Greppin H, Simon P (2002) Analysis and expression of the class III peroxidase large gene family in *Arabidopsis thaliana*. *Gene* 288:129–38
- Tran HV, Piro B, Reisberg S, Huy Nguyen L, Dung Nguyen T, Duc HT, Pham MC (2014) An electrochemical ELISA-like immunosensor for miRNAs detection based on screen-printed gold electrodes modified with reduced graphene oxide and carbon nanotubes. *Biosens Bioelectron* 62:25–30. doi:10.1016/j.bios.2014.06.014
- US Food and Drug Administration (2006) Phospholipase C enzyme preparation from *Pichia pastoris* expressing a heterologous phospholipase C gene. <http://www.accessdata.fda.gov/scripts/fdccc/?set=GRASNotices&id=204> (Accessed Dec 2014)
- Ulson de Souza SMAG, Forgari E, Ulson de Souza AA (2007) Toxicity of textile dyes and their degradation by the enzyme horseradish peroxidase (HRP). *J Hazard Mater* 147:1073–8. doi:10.1016/j.jhazmat.2007.06.003
- Uozumi N, Kato Y, Nakashimada Y, Kobayashi T (1992) Excretion of peroxidase from horseradish hairy root in combination with ion supplementation. *Appl Microbiol Biotechnol* 37:560–565. doi:10.1007/BF00240725
- Utashima Y, Matsumoto H, Masaki K, Iefuji H (2014) Heterologous production of horseradish peroxidase C1a by the basidiomycete yeast *Cryptococcus sp.* S-2 using codon and signal optimizations. *Appl Microbiol Biotechnol* 98:7893–900. doi:10.1007/s00253-014-5856-7
- Varnado CL, Goodwin DC (2004) System for the expression of recombinant hemoproteins in *Escherichia coli*. *Protein Expr Purif* 35:76–83. doi:10.1016/j.pep.2003.12.001
- Vasileva N, Godjevargova T, Ivanova D, Gabrovska K (2009) Application of immobilized horseradish peroxidase onto modified acrylonitrile copolymer membrane in removing of phenol from water. *Int J Biol Macromol* 44:190–4. doi:10.1016/j.ijbiomac.2008.12.002
- Veillette M, Coutu M, Richard J, Batrville L-A, Désormeaux A, Roger M, Finzi A (2014) Conformational evaluation of HIV-1 trimeric envelope glycoproteins using a cell-based ELISA assay. *J Vis Exp* 91:51995. doi:10.3791/51995
- Veitch NC, Smith AT (2001) Horseradish peroxidase. *Adv Inorg Chem* 51(51):107–162
- Vidossich P, Fiorin G, Alfonso-Prieto M, Derat E, Shaik S, Rovira C (2010) On the role of water in peroxidase catalysis: a theoretical investigation of HRP compound I formation. *J Phys Chem B* 114: 5161–9. doi:10.1021/jp911170b
- Virel A, Saa L, Köster SD, Pavlov V (2010) Ultrasensitive optical detection of hydrogen peroxide by triggered activation of horseradish peroxidase. *Analyst* 135:2291–5. doi:10.1039/c0an00095g
- Vlamiš-Gardikas A, Smith AT, Clements JM, Burke JF (1992) Expression of active horseradish peroxidase in *Saccharomyces cerevisiae*. *Biochem Soc Trans* 20:111S
- Vlasits J, Jakopitsch C, Bernroither M, Zamocky M, Furtmüller PG, Obinger C (2010) Mechanisms of catalase activity of heme peroxidases. *Arch Biochem Biophys* 500:74–81. doi: 10.1016/j.abb.2010.04.018
- Walwyn DR, Huddy SM, Rybicki EP (2014) Techno-economic analysis of horseradish peroxidase production using a transient expression system in *Nicotiana benthamiana*. *Appl Biochem Biotechnol*. doi: 10.1007/s12010-014-1320-5
- Wang J, Fang B-S, Chou K-Y, Chen C-C, Gu Y (2014) A two-stage enzymatic synthesis of conductive poly(3,4-ethylenedioxythiophene). *Enzym Microb Technol* 54:45–50. doi:10.1016/j.enzmictec. 2013.10.002
- Welinder KG (1976) Covalent structure of the glycoprotein horseradish peroxidase (EC 1.11.1.7). *FEBS Lett* 72:19–23
- Welinder KG (1979) Amino acid sequence studies of horseradish peroxidase. Amino and carboxyl termini, cyanogen bromide and tryptic fragments, the complete sequence, and some structural characteristics of horseradish peroxidase C. *Eur J Biochem* 96:483–502
- Willies SC, White JL, Turner NJ (2012) Development of a high-throughput screening method for racemase activity and its application to the identification of alanine racemase variants with activity towards L-arginine. *Tetrahedron* 68:7564–7567. doi:10.1016/j.tet. 2012.06.062
- Xu Y, Hou J, Liu Z, Yu H, Sun W, Xiong J, Liao Z, Zhou F, Xie C, Zhou Y (2011) Gene therapy with tumor-specific promoter mediated suicide gene plus IL-12 gene enhanced tumor inhibition and prolonged host survival in a murine model of Lewis lung carcinoma. *J Transl Med* 9:39. doi:10.1186/1479-5876-9-39
- Yamazaki H, Yamazaki I (1973) The reaction between indole 3-acetic acid and horseradish peroxidase. *Arch Biochem Biophys* 154:147–59
- Yang BY, Gray JS, Montgomery R (1996) The glycans of horseradish peroxidase. *Carbohydr Res* 287:203–12
- Yin H, Wang M, Li B, Yang Z, Zhou Y, Ai S (2015) A sensitive electrochemical biosensor for detection of protein kinase A activity and inhibitors based on Phos-tag and enzymatic signal amplification. *Biosens Bioelectron* 63:26–32. doi:10.1016/j.bios.2014.07.016
- Yu J-H, Klivanov AM (2006) Co-lyophilization with D-proline greatly enhances peroxidase's stereoselectivity in a non-aqueous medium. *Biotechnol Lett* 28:555–8. doi:10.1007/s10529-006-0018-3
- Zachetti VGL, Granero AM, Robledo SN, Zon MA, Fernández H (2013) Development of an amperometric biosensor based on peroxidases to quantify citrinin in rice samples. *Bioelectrochemistry* 91:37–43. doi: 10.1016/j.bioelechem.2012.12.004
- Zhong H, Yuan R, Chai Y, Li W, Zhang Y, Wang C (2011) Amperometric biosensor for hydrogen peroxide based on horseradish peroxidase onto gold nanowires and TiO₂ nanoparticles. *Bioprocess Biosyst Eng* 34:923–930. doi:10.1007/s00449-011-0543-x

- Chapter 2 -

Purification and basic biochemical characterization of 19 recombinant plant peroxidase isoenzymes produced in *Pichia pastoris*

Florian W. Krainer^{1*}, Robert Pletzenauer^{2*}, Laura Rossetti², Christoph Herwig², Anton Glieder³ and Oliver Spadiut^{2§}

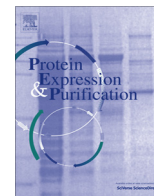
¹ Graz University of Technology, Institute of Molecular Biotechnology, Graz, Austria

² Vienna University of Technology, Institute of Chemical Engineering, Research Area Biochemical Engineering, Vienna, Austria

³ Austrian Centre of Industrial Biotechnology (ACIB GmbH), Graz, Austria

* these authors contributed equally

[§] Corresponding author: Oliver Spadiut, Vienna University of Technology, Institute of Chemical Engineering, Research Area Biochemical Engineering, Gumpendorfer Strasse 1a, A-1060 Vienna, Austria; oliver.spadiut@tuwien.ac.at; Tel: +43 (0)1 58801 166473



Purification and basic biochemical characterization of 19 recombinant plant peroxidase isoenzymes produced in *Pichia pastoris* [☆]



Florian W. Krainer ^{a,1}, Robert Pletzenauer ^{b,1}, Laura Rossetti ^b, Christoph Herwig ^b, Anton Glieder ^c, Oliver Spadiut ^{b,*}

^a Graz University of Technology, Institute of Molecular Biotechnology, Graz, Austria

^b Vienna University of Technology, Institute of Chemical Engineering, Research Area Biochemical Engineering, Vienna, Austria

^c Austrian Centre of Industrial Biotechnology (ACIB, GmbH), Graz, Austria

ARTICLE INFO

Article history:

Received 30 October 2013

and in revised form 27 November 2013

Available online 14 December 2013

Keywords:

Horseradish peroxidase

Pichia pastoris

Glycosylation

Protein purification

Negative chromatography

Monolith

ABSTRACT

The plant enzyme horseradish peroxidase (HRP) is used in several important industrial and medical applications, of which especially biosensors and diagnostic kits describe an emerging field. Although there is an increasing demand for high amounts of pure enzyme preparations, HRP is still isolated from the plant as a mixture of different isoenzymes with different biochemical properties. Based on a recent next generation sequencing approach of the horseradish transcriptome, we produced 19 individual HRP isoenzymes recombinantly in the yeast *Pichia pastoris*. After optimizing a previously reported 2-step purification strategy for the recombinant isoenzyme HRP C1A by substituting an unfavorable size exclusion chromatography step with an anion exchange step using a monolithic column, we purified the 19 HRP isoenzymes with varying success. Subsequent basic biochemical characterization revealed differences in catalytic activity, substrate specificity and thermal stability of the purified HRP preparations. The preparations of the isoenzymes HRP A2A and HRP A2B were found to be highly interesting candidates for future applications in diagnostic kits with increased sensitivity.

© 2013 The Authors. Published by Elsevier Inc. All rights reserved.

Introduction

Horseradish peroxidase (HRP²; EC 1.11.1.7) is a class III peroxidase or classical secretory plant peroxidase which oxidizes different substrates (e.g. aromatic phenols, indoles, phenolic acids, amines, sulfonates) using peroxides, commonly H₂O₂, as initial electron acceptors [1–3]. This enzyme has been studied for more than 200 years. Already in 1810, horseradish roots were observed to cause a color reaction when mixed with the resin of *Guaiacum* plants [4],

probably the oxidation of α -guaiaconic acid to guaiacum blue by HRP [5]. In plants, HRP is involved in numerous reactions, such as the crosslinking of phenolic molecules and the regulation of H₂O₂ levels, the cell wall network and auxin catabolism [6–8]. Correlating with the large number of different *in vivo* functions, horseradish was found to contain a multitude of different HRP isoenzymes. Up to 42 isoenzymes were detected by isoelectric focusing of commercial HRP preparations [9]. Jermyn et al. observed multiple proteins in the horseradish plant with peroxidase activity and found seasonal variation in their relative amounts as well as differences in substrate affinity [10,11]. This biochemical versatility of HRP isoenzymes was further demonstrated in several subsequent studies (e.g. [12–16]).

Until now, however, most studies have focused on the isoenzyme C1A [17], which is the only isoenzyme with a solved structure [18]. HRP C1A contains nine potential N-glycosylation sites, defined by the N-X-S/T motif, with X being any amino acid but proline, of which eight are glycosylated when isolated from plant [19]. Plant-derived HRP C1A has a total carbohydrate content of 21.8% [20]. Interestingly, plant-derived HRP isoenzymes with a basic isoelectric point (pI) of >12 were found to be less glycosylated, e.g. only 0.8–4.2% carbohydrate content for isoenzymes E3–E6 [15]. Tams et al. studied the effect of the N-glycans on the biochemical properties of HRP C1A and found that pI, absorption spectrum,

[☆] This is an open-access article distributed under the terms of the Creative Commons Attribution-NonCommercial-No Derivative Works License, which permits non-commercial use, distribution, and reproduction in any medium, provided the original author and source are credited.

* Corresponding author. Address: Vienna University of Technology, Institute of Chemical Engineering, Research Area Biochemical Engineering, Gumpendorfer Strasse 1a, A-1060 Vienna, Austria. Tel.: +43 1 58801 166473.

E-mail address: oliver.spadiut@tuwien.ac.at (O. Spadiut).

¹ These authors contributed equally to this work.

² Abbreviations used: HRP, horseradish peroxidase; pI, isoelectric point; HCIC, hydrophobic charge induction chromatography; HIC, hydrophobic interaction chromatography; SEC, size exclusion chromatography; AEC, anion exchange chromatography; ONC, overnight culture; YPD, yeast extract-peptone-dextrose; CV, column volumes; PF, purification factor; R%, recovery yield of HRP activity in percentage; ELISA, enzyme-linked immunosorbent assays; ABTS, 2,2'-azino-bis(3-ethylbenzthiazoline-6-sulfonic acid) diammonium salt; TMB, 3,3',5,5'-tetramethylbenzidine HCl.

peroxidase activity towards *o*-dianisidine and thermal stability remained the same, whereas the kinetic stability and the solubility in ammonium sulfate were decreased upon deglycosylation [21,22]. Thus, the presence of glycan structures on the enzyme surface has a considerable impact on HRP.

Today, the roots of the horseradish plant are the main source for commercially available HRP preparations. These preparations commonly describe mixtures of isoenzymes whose expression patterns change seasonally and in response to uncontrollable environmental factors [8]. The yields of HRP are rather low with less than 10 mg of total HRP protein, which presents a mixture of different isoenzymes, from 100 g of horseradish roots [23]. Thus, the yield of specific isoenzymes purified from such a mixture is extremely low, e.g. Aibara et al. reported as little as 40 mg of isoenzyme E1 from 200 kg of horseradish roots [15]. Unfortunately, due to intrinsic enzyme properties such as intramolecular disulfide bridges [18], the recombinant production of HRP is challenging. Recombinant production as inclusion bodies in *Escherichia coli* is possible (e.g. [24,25]), but refolding yields are as low as 10 mg L⁻¹ [25]. Beside the recombinant production of HRP in insect cell cultures (e.g. [26,27]), the currently most promising production systems are yeasts such as *Saccharomyces cerevisiae* [28–30] and *Pichia pastoris* [29,31]. However, HRP produced in *P. pastoris* is heterogeneously hyperglycosylated, causing the enzyme to appear as a smear on a SDS polyacrylamide gel at a size of approximately 65 kDa instead of its unglycosylated size of 35 kDa [29,32,33]. These excessive yeast-type glycans considerably impede classical downstream processing approaches. Whereas plant-derived HRP can be purified either by several consecutive steps of column chromatography (e.g. [12,15,16]) or by affinity chromatography using the lectin concanavalin A (e.g. [34–37]) as an isoenzyme mixture in a quite simple way, yeast-derived HRP cannot be purified by these strategies [33].

One obvious advantage of the recombinant production of single HRP isoenzymes in *P. pastoris* is the fact that this isoenzyme does not need to be isolated from an isoenzyme mixture, an otherwise time-intensive and tedious purification effort. Consequently, all HRP activity can be ascribed to the produced individual isoenzyme, allowing its specific enzymatic characterization. However, for that purpose, the HRP isoenzyme still has to be purified from yeast proteins. Hyperglycosylated HRP isoenzyme C1A from *P. pastoris* was previously purified by subsequent steps of hydrophobic interaction chromatography (HIC), size exclusion chromatography (SEC) and anion exchange chromatography (AEC) [29,30]. Recently, we addressed the issue of this cumbersome purification strategy by even making use of the high carbohydrate content of recombinant HRP C1A. We applied hydrophobic charge induction chromatography (HCIC) operated in flowthrough mode to remove contaminating proteins that bound to the resin, whereas the hyperglycosylated HRP eluted in the flowthrough. The glycan coat surrounding HRP C1A seemed to mask the physicochemical properties of the enzyme, allowing this rather unconventional, negative chromatography approach. An additional polishing step by SEC gave a preparation of HRP C1A with a specific activity comparable to the purest commercially available HRP preparation from plant [33].

Recently, we performed a next generation sequencing approach of the horseradish transcriptome which greatly increased the amount of available HRP isoenzyme sequences [38], and thus allowed more detailed studies of single isoenzymes. Considering the numerous applications of HRP as a reporter enzyme in diagnostic assays and histochemical staining as well as in strain engineering studies (e.g. [31,39,40]), biocatalysis (e.g. [41]), wastewater cleanup systems (e.g. [42]) and antibody-directed enzyme-prodrug cancer therapy (e.g. [43]), it is highly interesting to biochemically characterize the different HRP isoenzymes to find the most suitable one for a certain application.

Here, we report the production, purification and basic biochemical characterization of 19 individual HRP isoenzyme preparations. We significantly improved our recently reported 2-step purification procedure [33], replacing the rather inefficient and slow SEC polishing step by using a tube monolithic AEC column. Finally, we performed a basic enzymatic characterization of the final HRP preparations to determine potential differences in their catalytic activities, substrate specificities and thermal stabilities.

Materials and methods

Chemicals

Enzymes were obtained from Thermo Scientific (formerly Fermentas, Germany). 2,2'-Azino-bis(3-ethylbenzthiazoline-6-sulfonic acid) diammonium salt (ABTS), 3,3',5,5'-tetramethylbenzidine HCl (TMB) and D(+)-biotin were purchased from Sigma-Aldrich (Austria). Difco™ yeast nitrogen base w/o amino acids (YNB), Bacto™ tryptone and Bacto™ yeast extract were obtained from Becton Dickinson (Austria). Zeocin™ was obtained from *in vivo* Gen (France). Other chemicals were obtained from Carl Roth (Germany).

P. pastoris strains for HRP production

All *P. pastoris* strains in this study were based on the *P. pastoris* wildtype strain CBS 7435 (identical to NRRL Y-11430 and ATCC 76273). The Mut^s (methanol utilization slow) phenotype of *P. pastoris* was shown to be superior over the Mut⁺ phenotype in terms of volumetric productivity and production efficiency of HRP [31]. Thus, all HRP production strains in this study were strains with Mut^s phenotype [44]. A detailed description of the identification of new HRP isoenzyme sequences and the generation of the *P. pastoris* strains producing the various HRP isoenzymes was given elsewhere [38]. Calculated basic protein parameters and the corresponding database accession codes are shown in Table 1. Synthetic codon-optimized genes encoding mature HRP isoenzymes were N-terminally fused to the prepro signal peptide of the *S. cerevisiae* mating factor alpha to facilitate efficient secretion of the recombinant HRP to the cultivation supernatant. The expression of the HRP

Table 1

Calculated basic characteristics of HRP isoenzymes. The isoelectric point (pI) and the molecular weight (MW) were calculated using the Compute pI/Mw tool of the ExpASY server [55,56] and the number of potential N-glycosylation sites (N-X-S/T) was deduced from the NetNGlyc 1.0 Server [57]. All calculations were based on a cleavage of the prepro signal peptide of the *S. cerevisiae* mating factor alpha between A87 and E88, upstream of the mature HRP peptide.

HRP isoenzyme	pI	MW [kDa]	N-X-S/T	GenBank	UniProt
C1A	5.41	35.82	9	HE963800.1	K7ZWW6
25148.1 (C1C)	6.13	35.86	7	HE963802.1	K7ZWQ1
25148.2 (C1D)	6.50	35.89	7	HE963803.1	K7ZW56
04627 (C2)	8.38	35.67	4	HE963804.1	K7ZW02
C3	7.05	35.48	3	HE963805.1	K7ZWW7
A2A	4.84	32.09	9	HE963806.1	K7ZW28
A2B	4.84	32.12	9	HE963807.1	K7ZWQ2
E5	8.99	33.92	3	HE963808.1	K7ZW57
1805	5.75	35.96	5	HE963809.1	K7ZW05
22684.1	6.39	35.06	4	HE963810.1	K7ZWW8
22684.2	6.00	35.15	4	HE963811.1	K7ZW29
1350	8.47	31.42	3	HE963812.1	K7ZWQ3
5508	8.22	31.35	3	HE963815.1	K7ZWW9
6351	5.99	32.89	2	HE963816.1	K7ZW31
22489.1	8.24	31.37	2	HE963818.1	K7ZW59
22489.2	8.24	31.39	2	HE963819.1	K7ZW11
17517.2	9.30	32.69	4	HE963823.1	K7ZW60
08562.4	8.91	33.26	3	HE963825.1	K7ZWX1
08562.1	8.89	33.81	3	HE963824.1	K7ZW15

encoding genes was regulated by the methanol-inducible promoter of the *P. pastoris* AOX1 gene.

Production of recombinant HRP isoenzymes

Recombinant production of 19 different HRP isoenzymes in *P. pastoris* was performed in 2.5 L Ultra Yield Flasks from BioSilta (Finland), applying a protocol based on [45] with the following modifications: An overnight culture (ONC) of 30 mL YPD (yeast extract-peptone-dextrose) in 250 mL baffled shake flasks was inoculated with a single colony of a *P. pastoris* strain producing a specific HRP isoenzyme and incubated at 28 °C, 90 rpm and approximately 50% humidity for at least 12 h. 1.5 mL of this ONC were transferred to 270 mL of iron-supplemented BMD1% (11 g L⁻¹ α-D(+)-glucose monohydrate, 13.4 g L⁻¹ YNB, 0.4 mg L⁻¹ D(+)-biotin, 278 mg L⁻¹ FeSO₄·7H₂O, 0.1 M potassium phosphate buffer, pH 6.0) per Ultra Yield Flask and cultivated under the same conditions for approximately 60 h. A first induction pulse was performed by addition of 30 mL BMM10 (5% (v/v) methanol, 13.4 g L⁻¹ YNB, 0.4 mg L⁻¹ D(+)-biotin, 0.1 M potassium phosphate buffer, pH 6.0). 3.0 mL of pure methanol were added approximately 12 h and 36 h after the first induction pulse, 1.5 mL of pure methanol were added approximately 24 h and 48 h after the first induction pulse. 72 h after the first induction pulse, the culture broth was centrifuged (15,000×g, 30 min, 4 °C) and the supernatant was filtered through a 0.2 μm cellulose acetate filter (Sartorius Stedim Biotech, Germany).

Purification of recombinant HRP isoenzymes

In accordance to our previous study, the supernatant was concentrated using the Vivaflow 50 system (Sartorius Stedim Biotech, Germany) with a 10 kDa MWCO membrane prior to hydrophobic charge induction chromatography (HCIC; [33]). The buffer was changed to HCIC-A (500 mM NaCl, 20 mM NaOAc, pH 6.0) and concentrated to a final volume of 10–15 mL. All further steps of concentration and buffer change were performed using Vivaspin 20 tubes (Sartorius Stedim Biotech, Germany) with 10 kDa MWCO. The HCIC resin MEP HyperCel™ was obtained from Pall (Austria), and HCIC was performed in flowthrough mode based on [33]: A column containing approximately 25 mL of MEP HyperCel™ resin was equilibrated with at least 4 column volumes (CV) of buffer HCIC-A. 10–15 mL concentrated HRP solution in HCIC-A were loaded onto the column and washed with at least 220 mL of HCIC-A at a flow rate of approximately 55 cm h⁻¹. Fractions of 10 mL were collected. Fractions containing HRP activity were pooled and concentrated to 500–1000 μL. The column was washed with 5 CV of 800 mM NaOH, then re-equilibrated with HCIC-A for subsequent runs.

Univariate screenings for a potential application of CIM® tube monolithic columns (BIA separations, Slovenia) as a second chromatographic purification step were performed with the partially purified isoenzyme C1A after HCIC. Flowthrough fractions from HCIC purifications were pooled, concentrated and rebuffed in either of the loading buffers: 50 mM Tris-HCl, pH 7.4, 50 mM Tris-HCl, pH 8.0 or 50 mM potassium phosphate, pH 6.0. The respective elution buffers contained 1 M NaCl. The tube monolithic columns tested were 1 mL CIM®-DEAE, 1 mL CIM®-QA and 1 mL CIM®-OH (BIA separations, Slovenia), which were equilibrated in the respective loading buffer at a flow rate of 156 cm h⁻¹. A post-load wash of 4 CV binding buffer was performed before elution was conducted by either increasing the elution buffer in a single step to 100% or in a linear gradient to 100% over 30 CV.

Ultimately, anion exchange chromatography (AEC) with an 8 mL CIM®-DEAE tube monolithic column was performed as a second purification step for all the HRP isoenzymes. The column was equilibrated in loading buffer AEC-A (50 mM Tris-HCl, pH 8.0) at a flow rate of 16.8 cm h⁻¹. Post-HCIC pools of each HRP isoenzyme

were subjected to diafiltration in AEC-A and were subsequently loaded onto the AEC column at an average linear flow rate of 16.8 cm h⁻¹. Elution was performed in a single step from 0% to 100% AEC-B (50 mM Tris-HCl, 1 M NaCl, pH 8.0). For column recovery the column was washed with 5 CV of a 1 M NaOH/1 M NaCl solution at an average linear flow rate of 33.6 cm h⁻¹.

Electrophoresis

To check the electrophoretic purity of HRP isoenzyme preparations SDS-PAGE was performed using a 5% stacking gel and a 10% separating gel in 1× Tris-glycine buffer. Unless otherwise stated, samples were diluted to a protein concentration between 0.1 and 0.5 mg mL⁻¹ before loading. Gels were run in a vertical electrophoresis Mini-PROTEAN Tetra Cell apparatus (Biorad, Austria) and stained with Coomassie blue. The protein mass standard used was the PageRuler Prestained Ladder (Fermentas, Austria).

Data analysis and basic enzymatic characterization of purified recombinant HRP isoenzymes

Protein concentrations were determined at 595 nm by the Bradford assay using the Sigma-Aldrich (Austria) Protein Assay Kit with bovine serum albumin as standard in the range of 0.2–1.2 mg mL⁻¹.

The enzymatic activity of HRP was measured using an ABTS assay in a CuBiAn XC enzymatic robot (Innovatis, Germany). 10 μL of sample were mixed with 140 μL 1 mM ABTS solution (50 mM potassium phosphate buffer, pH 6.5). The reaction mixture was incubated at 37 °C for 5 min before the reaction was started by the addition of 20 μL 0.078% (w/w) H₂O₂. Changes in absorption at 415 nm were measured for 80 s and rates were calculated. The standard curve was prepared using a commercially available HRP preparation (Type VI-A, Sigma-Aldrich, Austria) in the range from 0.02 to 2.0 U mL⁻¹.

The efficiency of the applied purification approach was evaluated by determining the purification factor (PF) and the recovery yield of HRP activity in percentage (R%). PF and R% were calculated by Eqs. (1) and (2):

$$PF = \frac{\text{specific activity}_{\text{post}}}{\text{specific activity}_{\text{pre}}} \quad (1)$$

$$R(\%) = 100 \times \frac{\text{volumetric activity}_{\text{post}} \times \text{volume}_{\text{post}}}{\text{volumetric activity}_{\text{pre}} \times \text{volume}_{\text{pre}}} \quad (2)$$

The suffixes “pre” and “post” indicate the respective values before and after a purification step. To obtain an overall PF and R% for the 2-step purification approach, we combined the values we determined for the single purification steps (Table 2). In case one purification step did not work or could not be evaluated, e.g. due to too low HRP activity, we only presented the successful purification step. The pooled active fractions after AEC were concentrated using Amicon Ultra-15 Centrifugal Filter Units with 10 kDa MWCO (Merck-Millipore, Austria) to the final enzyme preparation of a volume of approximately 1.5 mL.

Characterization of the purified HRP isoenzyme preparations included the determination of the basic kinetic parameters, V_{max} and K_M , for the electron acceptors ABTS and TMB in a spectrophotometer UV-1601 from Shimadzu (Austria). These peroxidase substrates are commonly used in enzyme-linked immunosorbent assays (ELISA). The reaction mixture with a final volume of 1.0 mL contained a concentration of 1 mM H₂O₂, 10 μL of HRP isoenzyme preparation and varying concentrations of ABTS (0.05–10 mM) or TMB (0.005–0.5 mM) in 50 mM potassium phosphate buffer, pH 6.5. The increase in absorption was followed at 420 nm for ABTS and at 653 nm for

Table 2

Summary of the 2-step purification approach of 19 recombinant HRP isoenzymes. The purification factor (PF) and the recovery of HRP activity in percentage (R%) of the applied HCIC and AEC flowthrough steps, as well as the combined purification results are shown. Some isoenzymes did not show any detectable peroxidase activity. In these cases, no values for PF or R% are available (n/a). The combined PF value is a product of the PFs of the HCIC and AEC step; in case no values were available for one purification step (n/a), the combined value only describes the working step.

HRP isoenzyme	HCIC		AEC		Combined	
	PF	R%	PF	R%	PF	R%
C1A	7.02	95.4	10.92	58.5	76.66	55.8
25148.1 (C1C)	6.80	95.5	2.28	66.4	15.50	63.4
25148.2 (C1D)	8.96	32.9	2.42	66.5	21.68	21.9
04627 (C2)	10.08	100.0	6.17	45.7	62.19	45.7
C3	2.17	17.6	2.50	100.0	5.43	17.6
A2A	15.85	100.0	43.18	15.6	684.40	15.6
A2B	5.82	92.0	6.64	80.0	38.64	73.6
E5	3.89	33.1	0.54	81.0	2.10	26.8
1805	n/a	n/a	15.68	38.4	15.68	38.4
22684.1	0.11	1.4	n/a	n/a	n/a	n/a
22684.2	n/a	n/a	n/a	n/a	n/a	n/a
1350	n/a	n/a	n/a	n/a	n/a	n/a
5508	2.18	33.2	66.25	31.5	144.43	10.5
6351	3.01	32.6	n/a	n/a	n/a	n/a
22489.1	0.42	3.8	n/a	n/a	n/a	n/a
22489.2	0.02	0.3	2.09	74.6	0.04	0.2
17517.2	3.48	38.9	0.98	75.0	3.41	29.2
08562.4	n/a	n/a	0.89	32.6	0.89	32.6
08562.1	1.18	16.5	0.27	45.5	0.32	7.5

TMB at 30 °C for 180 s, respectively. Absorption curves were recorded with an adapted software program (UVPC Optional Kinetics software, Shimadzu). The maximum reaction rate (V_{\max}) and the Michaelis constant (K_m) were calculated with the Sigma Plot software (Version 11.0, Systat Software Inc., USA).

The thermal stability of individual HRP isoenzyme preparations was tested at 60 °C. The residual activity towards ABTS was measured after 5, 10, 15, 20, 30 and 60 min of incubation at 60 °C. The residual activities were plotted versus the incubation time and the half life times of thermal inactivation at 60 °C ($\tau_{1/2}$) were calculated using Eq. (3) [46]:

$$\tau^{1/2} = \frac{\ln 2}{k_{in}}, \quad (3)$$

k_{in} rate of inactivation (slope of the logarithmic residual activity).

Results and discussion

HRP is a well-studied enzyme which is used in numerous industrial and medical applications (e.g. [31,39–43]). Due to certain intrinsic enzyme features, the recombinant production and purification of this important enzyme is quite cumbersome, and HRP is still isolated from horseradish roots as a mixture of isoenzymes at low yields. A recombinant production process in combination with an efficient purification strategy would allow the reliable production of individual HRP isoenzymes for the various applications in large amounts.

HRP production

In this study, 19 HRP isoenzymes were recombinantly produced in the methylotrophic yeast *P. pastoris* in shake flask cultivations. By fusing the genes to the prepro signal sequence of the *S. cerevisiae* mating factor alpha, the HRP isoenzymes were secreted to the cultivation broth. Due to the fact that *P. pastoris* actively secretes only few endogenous proteins [47,48], the subsequent downstream process was thereby considerably facilitated already. After centrifugation and diafiltration, the HRP isoenzymes could

already be subjected to chromatography. Typical total protein concentrations in the cultivation broth at the time of harvesting were in the range of 200–500 mg L⁻¹. The amount of obtainable purified HRP isoenzyme preparation differed vastly; for the isoenzymes which could be purified best using the here presented 2-step strategy the following protein contents per liter cultivation broth were obtained: 1.0 mg C1A, 0.6 mg C2, 0.1 mg A2A and 0.15 mg 5508. Also volumetric HRP activities with ABTS as reducing substrate varied considerably from isoenzyme to isoenzyme. For instance, the HRP isoenzymes 8562.1, 22489.1, A2A, C1A and E5 gave approximately 3, 70, 220, 440 and 670 U L⁻¹, respectively.

Hydrophobic charge induction chromatography (HCIC)

In a recent multivariate Design of Experiments screening study, we found HCIC operated in the flowthrough mode to be very effective for the purification of the hyperglycosylated recombinant HRP C1A, allowing a 5-fold purification at almost 100% recovery [33]. However, in the present study the application of this flowthrough purification step to the 19 different HRP isoenzymes produced in *P. pastoris* led to quite diverse results in terms of purification factor (PF) and recovery yield (R%; Table 2), indicating significant differences in the physicochemical properties, to some extent probably caused by the different degrees of glycosylation of the individual HRP isoenzymes. However, the HCIC elution profile of the HRP isoenzyme C1A that was shown previously [33], could be reproduced under the conditions applied in the present study as the whole HRP activity was found in the flowthrough (Fig. 1). The higher PF for HRP C1A in this study compared to our previous results [33] (i.e. 7-fold versus 5-fold, respectively) might be explained by the different cultivation approaches. In the present study, we produced HRP C1A in shake flask cultivations, whereas previous cultivations were done in the controlled environment of a bioreactor [33]. The latter allowed cultivation under optimized conditions, thus limiting cell lysis and contamination of the cultivation broth by intracellular proteins. Presumably, the amount of contaminating proteins in the starting solution was therefore lower, causing an overall lower PF for the C1A preparation from the bioreactor.

Elution profiles similar to the one shown in Fig. 1 were found for ten other HRP isoenzymes (graphs not shown), indicating the applicability of the HCIC flowthrough purification for these isoenzymes (Table 2). Remarkably, a 16-fold purification at 100% recovery was achieved for isoenzyme HRP A2A (Table 2). However, for some isoenzymes the flowthrough based HCIC step could not be applied successfully as no purification was achieved (e.g. HRP 22489.1; Table 2). To find an explanation for that phenomenon, we looked at the single isoenzymes in more detail. Predictions of potential N-glycosylation sites, based on the identification of the conserved N-X-S/T motif, were performed using the NetNGlyc 1.0 Server (Table 1). Interestingly, the number of predicted potential N-glycosylation sites correlated well with both the PF and the recovery yield (R%; Fig. 2). This observation strongly underlines our previous hypothesis that extensive glycosylation prevents the interaction of recombinant HRP from *P. pastoris* with the HCIC material, hence allowing the negative chromatography purification step [33]. For example, HRP C1A and HRP A2A each contain nine N-X-S/T motifs and could be purified 7.0- and 15.9-fold at 95.4 and 100.0% recovery, respectively. HRP 6351 and HRP C3, on the other hand, contain only 2 and 3 N-X-S/T motifs and could only be purified 3.0- and 2.2-fold at 32.6 and 17.6% recovery, respectively (Tables 1 and 2). Outliers from that correlation, e.g. HRP 22684.1, which could not be purified via HCIC (PF of 0.1; Table 2) despite containing four N-X-S/T motifs, might be explained by varying degrees in glycosylation due to steric hindrance at certain N-glycosylation sites. However, the generally high correlation between the number of glycosylation sites and both the PF and

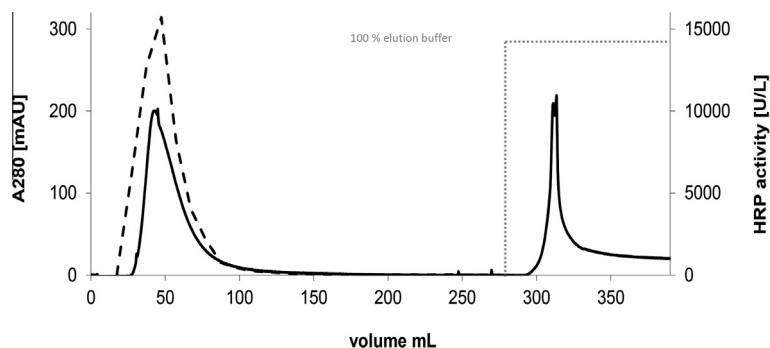


Fig. 1. HIC chromatogram of the recombinant HRP isoenzyme C1A. The HRP activity (dashed line) was determined by using ABTS as reducing substrate. Protein content was followed throughout the run by recording the absorption at 280 nm (solid line).

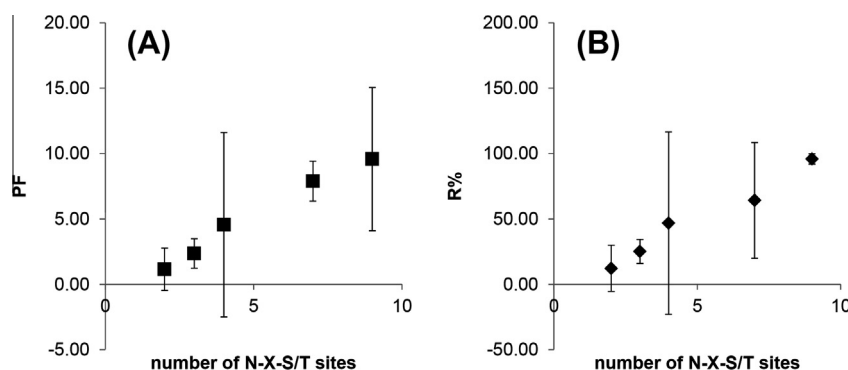


Fig. 2. Correlation of the number of N-glycosylation sites and HIC purification parameters. A, purification factor (PF); B, recovery yield of HRP activity in percentage (R%). The average PF and R% for HRPs with n N-X-S/T sites are shown with the corresponding calculated standard deviations; $n_2 = 3$, $n_3 = 4$, $n_4 = 3$, $n_7 = 2$, $n_9 = 3$.

the R%, as evident in Fig. 2, allows the design of an appropriate purification strategy for extensively glycosylated enzymes produced in *P. pastoris*.

Anion exchange chromatography (AEC)

Recently, monolithic columns were discovered as a powerful tool for both analytical purposes and preparative protein purification [49–51]. The solid support, a uniform monolithic porous material (e.g. glycidyl methacrylate-based materials), is simple to handle and to scale up, allows elevated operating flow rates and pressures (e.g. flow rates of up to 336 cm h^{-1} and a back pressure of up to 20 bar for an 8 mL tube monolithic column from BIA separations), and provides high binding capacity ($>20 \text{ mg mL}^{-1}$). These beneficial features are mainly enabled by the convective mass transfer of the target molecule through the highly interconnected channel structure of the porous polymer block. In convective processes, both resolution and binding capacity are not affected by the flow rate, an effect that is emphasized when large biomolecules such as proteins are separated due to their high diffusion coefficients [49]. On the other hand, porous particles which are applied in conventional chromatographic media require diffusive transport of the molecules which have to enter the pores to get in contact with the active surface. This diffusive transport results in increased separation times and void volumes.

In our previous study, we polished partially purified recombinant HRP C1A after HIC by SEC [33]. Although this strategy gave a good PF of >2.0 and a recovery yield of 100%, SEC has several uneconomical disadvantages such as low flow rates, sample dilution, temperature effects due to long process times, limited sample volumes and limited scalability. Thus, we tested monolithic columns as an alternative to SEC. A wide range of monolithic formats

and ligands is available today [52]. In this study, we tested two AEC resins and a HIC resin, since these two purification principles had shown promising results using particle-based resins for recombinant HRP C1A before [33]. We used different buffer systems and elution profiles for the potential application of CIM[®] tube monolithic columns as polishing step for recombinant HRP C1A, partially purified after HIC. Active flowthrough fractions from HIC purifications were pooled, concentrated via diafiltration and loaded on the different CIM[®] tube columns. The HIC resin CIM[®]-OH was not able to purify recombinant HRP C1A after HIC any further, regardless of the buffers applied. We believe that this was due to the fact that the vast majority of hydrophobic proteins had already been retained on the HIC resin. Using the strong AEC resin CIM[®]-QA, the enzyme preparation could not be purified more than 1.3-fold regardless of the buffer, a phenomenon which we also observed with particle-based strong AEC materials before [33]. However, the weak AEC tube monolithic column CIM[®]-DEAE gave satisfactory results. Using Tris-HCl (50 mM, pH 8.0) as loading buffer, a PF of nearly 11.0 was obtained for recombinant HRP C1A when the negative chromatography approach was applied.

Interestingly, similar to the HIC flowthrough step, operation of AEC in the flowthrough mode also gave diverse results in terms of PF and R% for the different recombinant HRP isoenzymes (Table 2). Some isoenzymes could not be purified by this strategy, whereas other isoenzymes were purified up to 66-fold. Remarkably, for isoenzymes 1805, 5508 and 22489.2 only the second purification step via the CIM[®]-DEAE monolithic column worked, whereas HIC could not improve the preparations in terms of enzyme purity; in fact, PFs of more than 30 showed that for some HRP isoenzymes the AEC step alone already described an efficient purification strategy (Table 2). The HRP isoenzymes 22684.1, 6351 and 22489.1 did not show any detectable peroxidase activity after diafiltration

indicating instability under the conditions applied. Furthermore, no HRP activity was detected prior to AEC for 22684.2 and 1350 due to the high dilution of the enzyme at that stage (Table 2). Therefore, we cannot comment on the applicability of the AEC strategy for these five isoenzymes.

Summarizing, the CIM[®]-DEAE tube monolith describes a highly interesting alternative to SEC as a polishing step for partially purified recombinant HRP isoenzymes. Compared to the PF of around 2.0 which we achieved for the recombinant HRP isoenzyme C1A using SEC before [33], the flowthrough step applying an anion exchange monolith presented here is not only advantageous in terms of flow rates, sample volumes and thus process time, but also gave a 5-fold higher PF of nearly 11.0. In Fig. 3 we exemplarily show a SDS gel of the different steps during AEC purification of the HRP isoenzyme C1A. Although there are no striking bands indicating contaminant proteins in the flowthrough fraction of AEC, the specific activity of the purified HRP C1A preparation in this study was remarkably lower than in our previous study [33]: The preparation of HRP C1A in this study yielded a specific activity of only approximately 100 U mg⁻¹, whereas the C1A preparation in our previous study yielded a specific activity of approximately 1000 U mg⁻¹ [33]. We ascribe this phenomenon to the different cultivation procedures. Whereas HRP C1A was produced in the controlled environment of a bioreactor constantly providing optimal conditions for *P. pastoris* in our previous work [33], in the present study the HRP isoenzymes, including HRP C1A, were produced in shake flasks where conditions were not controlled. Limitations in oxygen and nutrients as well as gradients, which can occur in shake flasks, apparently influence the physiology of the cells and hence their ability to produce catalytically active enzyme. In fact, this is a very good example how the upstream process might influence the downstream process and the final product quality.

Basic biochemical characterization of HRP isoenzyme preparations

After the chromatographic 2-step purification procedure, the flowthrough fractions of the single HRP isoenzymes were pooled and concentrated by ultrafiltration before basic biochemical characterization was done. Especially, for HRP isoenzymes 22684.2 and 1350, where the concentration of HRP in the collected fractions was very low, this step was essential to be able to obtain reliable kinetic data.

As anticipated from our preliminary data [38], the preparations of the recombinant HRP isoenzymes featured significantly different biochemical properties. Not only physicochemical parameters, such as the predicted pI (Table 1), covered a broad range, but also the enzymatic activity towards the two tested electron donors ABTS and TMB were found to be highly versatile (Table 3; examples for Michaelis–Menten plots shown in Fig. 4).

For the oxidation of ABTS, the highest V_{max} values were obtained for the preparations of the isoenzymes A2A and A2B. These two isoenzyme preparations were able to oxidize ABTS 4- to 5-fold better than the preparation of the well-studied isoenzyme C1A (Table 3), rendering our preparations of HRP A2A and A2B particularly interesting for diagnostic bioassays with increased sensitivity. In a previous study on commercial preparations of acidic HRP isoenzymes from the plant, a comparatively high K_M value of 4.0 mM was reported for ABTS as the reducing substrate [53]. In contrast, the here reported K_M values of recombinant preparations of the acidic isoenzymes A2A and A2B were significantly lower with 1.95 and 1.73 mM, respectively. An explanation for this difference in substrate affinity remains speculative, but might be ascribed to the slightly different amino acid sequences of isoenzymes A2A and A2B used in this study compared to the commercial isoenzymes.

The here presented apparent K_M of 1.01 mM for ABTS for the HRP C1A preparation was higher than the previously published K_M values of 0.27 mM and 0.18 mM for C1A preparations from plant and *E. coli*, respectively [54]. In a previous study on recombinant HRP C1A from *P. pastoris* a K_M of 0.68 mM was reported [30]. Apparently, yeast-derived HRP C1A preparations generally have a tendency for a lowered affinity for ABTS, probably related to the yeast-type hyperglycosylation compared to preparations from plant and *E. coli*.

Interestingly, some HRP isoenzyme preparations did not show any (e.g. 22684.1) or only very low (e.g. 08562.4) catalytic activity with H₂O₂ and ABTS. Nevertheless, bearing the biochemical diversity of HRP isoenzymes in mind, these isoenzymes might be more active towards other substrates that were not tested in this study.

The oxidation of TMB was catalyzed best by the HRP C1A preparation, followed by HRP A2A and A2B (Table 3). Interestingly, HRP A2A oxidized TMB slower than ABTS, whereas most other isoenzymes – including C1A and A2B – oxidized TMB faster than ABTS (Table 3). Once more, these kinetic differences demonstrate the diverse substrate affinities and biochemical properties of the individual HRP isoenzymes. Keeping this variance in mind, it is of

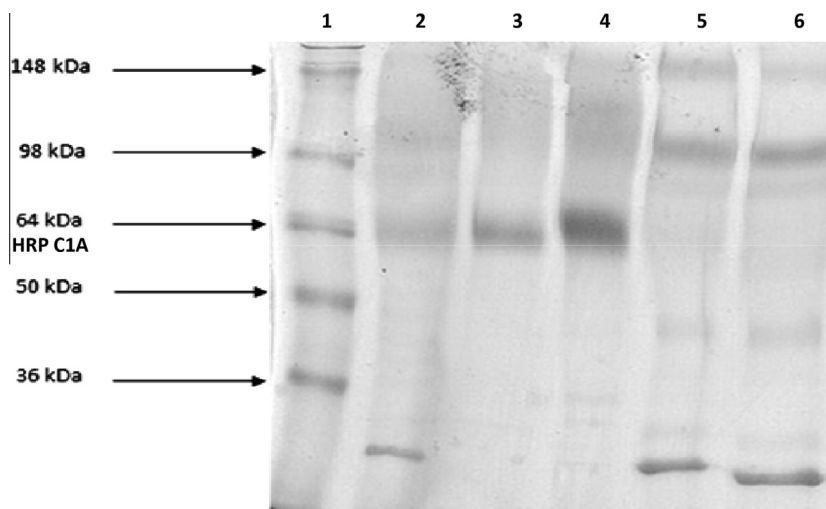


Fig. 3. SDS-PAGE of fractions from AEC with HRP C1A. Lane 1, molecular mass standard; lane 2, cell-free cultivation supernatant (5 µg); lane 3, flowthrough (5 µg); lane 4, flowthrough (10 µg); lanes 5 and 6, fractions eluted with buffer AEC-B (5 µg).

Table 3

Kinetic parameters of recombinant HRP isoenzyme preparations after 2-step flow-through purification. Kinetic data of the purified HRP isoenzyme preparations were recorded for the electron donors ABTS and TMB at a concentration of 1.0 mM H₂O₂. In some preparations, no peroxidase activity could be detected. In these cases, no values for V_{\max} or K_M are available (n/a).

HRP isoenzyme	ABTS		TMB	
	V_{\max} [U mg ⁻¹]	K_M [mM]	V_{\max} [U mg ⁻¹]	K_M [mM]
C1A	105.54	1.01	2031.50	0.11
25148.1 (C1C)	8.13	4.02	243.14	0.16
25148.2 (C1D)	9.94	3.55	139.77	0.13
04627 (C2)	5.52	4.49	82.34	0.15
C3	0.31	12.5	2.60	0.08
A2A	483.02	1.95	397.99	0.12
A2B	538.40	1.73	1049.11	0.18
E5	33.15	3.51	14.38	0.06
1805	2.95	2.36	39.02	0.11
22684.1	n/a	n/a	n/a	n/a
22684.2	1.08	3.36	11.02	0.07
1350	2.64	2.62	23.62	0.06
5508	42.40	0.46	9.89	0.10
6351	n/a	n/a	n/a	n/a
22489.1	0.17	3.03	n/a	n/a
22489.2	2.42	2.70	1.89	0.16
17517.2	0.11	0.39	0.24	0.32
08562.4	0.05	0.31	0.10	0.20
08562.1	0.10	0.18	0.06	0.11

considerable importance to choose the most suitable isoenzyme for a certain application in the future, e.g. to use a HRP A2B preparation for a diagnostic kit with ABTS as substrate, but a HRP C1A preparation for diagnostics with TMB as substrate, to achieve optimal assay sensitivity. On that note, the here described efficient purification strategy is a prerequisite for the application of specific HRP isoenzyme preparations. Also, the possibility for the recombi-

nant production of a certain HRP isoenzyme with favorable characteristics for a given application in *P. pastoris* is superior to the currently applied, but unpredictable and irreproducible isolation of a mixture of HRP isoenzymes from horseradish roots.

Table 4

Calculated half life times at 60 °C ($\tau_{1/2}$) of recombinant HRP isoenzyme preparations. Some isoenzymes did not show any detectable loss in HRP activity after 60 min. The thermal stability of recombinant HRP preparations with an initial V_{\max} lower than 0.5 U mg⁻¹ for ABTS were not determined (n.d.). Due to a limited amount of purified enzyme, HRP 04627 (C2) and HRP E5 were not included in this study (n.i.).

HRP isoenzyme	$\tau_{1/2}$ [min]
C1A	Stable for 60
25148.1 (C1C)	159
25148.2 (C1D)	21
04627 (C2)	n.i.
C3	n.d.
A2A	64
A2B	55
E5	n.i.
1805	Stable for 60
22684.1	n.d.
22684.2	46
1350	62
5508	17
6351	n.d.
22489.1	n.d.
22489.2	11
17517.2	n.d.
08562.4	n.d.
08562.1	n.d.

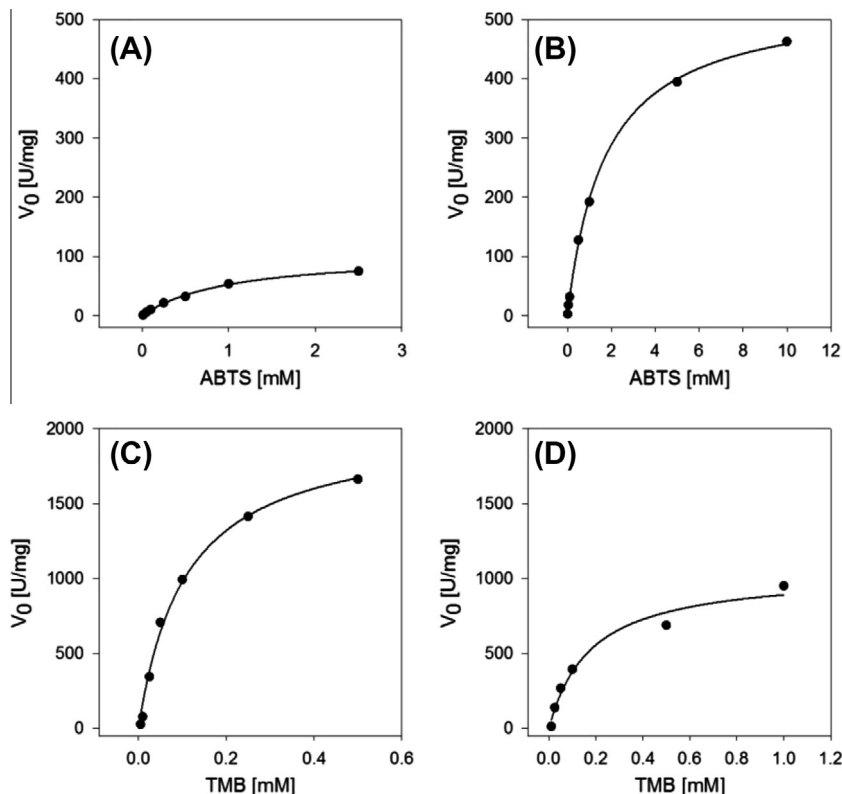


Fig. 4. Michaelis-Menten plots for preparations of recombinant HRP C1A and A2B. (A) HRP C1A with ABTS; (B) HRP A2B with ABTS; (C) HRP C1A with TMB; (D) HRP A2B with TMB. The Michaelis-Menten plots for all HRP isoenzyme preparations of this study are shown in [Supplementary Figs. 1–6](#).

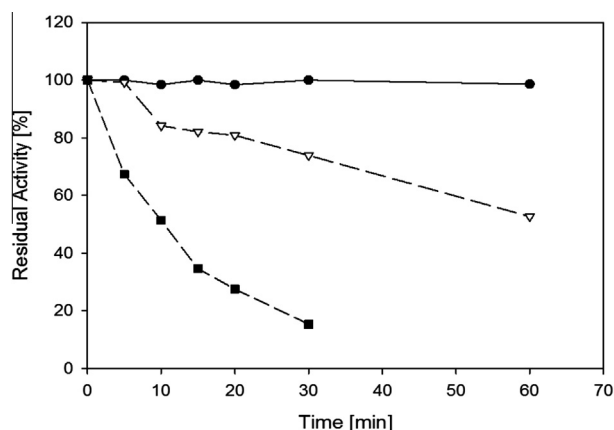


Fig. 5. Thermal stability profiles of selected recombinant HRP preparations. Filled circles, HRP C1A; open triangles, HRP A2A; filled squares, HRP 22489.2. Residual HRP activity was determined over 60 min of incubation at 60 °C.

Thermostability of HRP isoenzyme preparations

The HRP isoenzyme preparations did not only differ in terms of enzymatic activity and substrate specificity, but also in thermal stability (Table 4). The preparations of HRP C1A and HRP 1805 did not show a detectable decrease in catalytic activity after 60 min of incubation at 60 °C, whereas the activity of HRP 22489.2 was already below 20% of the initial activity after 30 min. A summary of all the calculated thermal half-life times ($\tau_{1/2}$) is given in Table 4. The thermal stability profiles of the stable HRP C1A preparation, the moderately stable HRP A2A and the quite unstable HRP 22489.2 at 60 °C over time are exemplarily shown in Fig. 5. As shown in Table 4, the most thermostable HRP preparations of this study were HRP C1A and HRP 1805, which both did not show any detectable loss in catalytic activity at 60 °C after 60 min. HRP A2A and A2B, which are highly interesting in terms of catalytic activity with ABTS and TMB (Table 3), showed a significantly lower thermal stability (Table 4, Fig. 5). However, for possible future applications of these isoenzymes in sensitive bioassays, their stability is supposedly sufficient. In addition, no significant loss of peroxidase activity of these two isoenzymes could be detected over weeks when stored at 4 °C.

Conclusions

In the present study, we recombinantly produced 19 single HRP isoenzymes in *P. pastoris* in shake flask cultivations. We optimized our recently reported 2-step purification approach for recombinant hyperglycosylated HRP replacing the tedious SEC step with an AEC step using a tube monolithic column. After purification, we biochemically characterized the individual HRP isoenzyme preparations with different substrates and evaluated their thermal stability. The main outcomes of this study can be summarized as:

- The novel 2-step flowthrough purification strategy gave a recovery yield of 55% and a PF of approximately 77 for the recombinant HRP isoenzyme C1A. Although the recovery yield was lower, the PF was more than 7-fold higher compared to our previous study, where we achieved a recovery yield of 93% but only a PF of 10. Despite the lower recovery, the here presented strategy is superior, since the second purification step can be run in flowthrough mode, thus allowing both high sample volumes and flow rates.

- Regarding the other isoenzymes especially HRP 04627 (C2), A2A and 5508 could be purified very efficiently with PFs of 62, 684 and 144, respectively. HRP 25148.1 (C1C), 25148.2 (C1D), 04627 (C2), A2B and 1805 were purified 15- to 38-fold.
- The correlation between the amount of potential N-glycosylation sites and the success in flowthrough purification can be used to design an efficient purification strategy for glycosylated proteins expressed in *P. pastoris* in general.
- Basic biochemical characterization using ABTS and TMB revealed significant differences of the individual isoenzyme preparations. The preparations of HRP A2A and HRP A2B turned out to be highly active with H₂O₂ and ABTS and hence are especially interesting for applications in diagnostic assays with high sensitivity.

The data provided in this study pave the way for cost-effective recombinant production of HRP isoenzymes in *P. pastoris*. Current efforts are made in our lab to provide detailed information on the identification of new HRP isoenzymes from a next generation sequencing of the horseradish transcriptome and to show classifying data on the new HRP isoenzyme sequences (Näätsaari et al., in preparation). Future in-depth studies will provide information on the molecular mechanisms underlying the differences in activity and stability of the various interesting HRP isoenzymes.

Acknowledgments

The authors are very grateful to the Austrian Science Fund FWF: project P24861-B19 and FWF: W901 DK Molecular Enzymology for financial support. We further thank the company BIA separations (Slovenia) for providing the monolithic columns and Ms. Astrid Weninger for excellent technical assistance in the lab.

Appendix A. Supplementary data

Supplementary data associated with this article can be found, in the online version, at <http://dx.doi.org/10.1016/j.jpep.2013.12.003>.

References

- [1] B. Chance, The kinetics and stoichiometry of the transition from the primary to the secondary peroxidase peroxide complexes, *Arch. Biochem. Biophys.* 41 (1952) 416–424.
- [2] P. George, Chemical nature of the secondary hydrogen peroxide compound formed by cytochrome-c peroxidase and horseradish peroxidase, *Nature* 169 (1952) 612–613.
- [3] P. George, The chemical nature of the second hydrogen peroxide compound formed by cytochrome c peroxidase and horseradish peroxidase. I. Titration with reducing agents, *Biochem. J.* 54 (1953) 267–276.
- [4] L.A. Planche, Note sur la sophistication de la résine de jalap et sur les moyens de la reconnaître, *Bull. Pharm.* 2 (1810) 578–580.
- [5] J.F. Kratochvil, R.H. Burris, M.K. Seikel, J.M. Harkin, Isolation and characterization of α -guaiaconic acid and the nature of guaiacum blue, *Phytochemistry* 10 (1971) 2529–2531.
- [6] A.J. Gross, I.W. Sizer, The oxidation of tyramine, tyrosine, and related compounds by peroxidase, *J. Biol. Chem.* 234 (1959) 1611–1614.
- [7] F. Passardi, C. Penel, C. Dunand, Performing the paradoxical: how plant peroxidases modify the cell wall, *Trends Plant Sci.* 9 (2004) 534–540.
- [8] F. Passardi, C. Cosio, C. Penel, C. Dunand, Peroxidases have more functions than a Swiss army knife, *Plant Cell Rep.* 24 (2005) 255–265.
- [9] M.C. Hoyle, High resolution of peroxidase-indoleacetic acid oxidase isoenzymes from horseradish by isoelectric focusing, *Plant Physiol.* 60 (1977) 787–793.
- [10] M.A. Jermyn, Horseradish peroxidase, *Nature* 169 (1952) 488–489.
- [11] M.A. Jermyn, R. Thomas, Multiple components in horseradish peroxidase, *Biochem. J.* 56 (1954) 631–639.
- [12] L.M. Shannon, E. Kay, J.Y. Lew, Peroxidase isozymes from horseradish roots. I. Isolation and physical properties, *J. Biol. Chem.* 241 (1966) 2166–2172.
- [13] E. Kay, L.M. Shannon, J.Y. Lew, Peroxidase isozymes from horseradish roots. II. Catalytic properties, *J. Biol. Chem.* 242 (1967) 2470–2473.

- [14] S. Marklund, P.I. Ohlsson, A. Opara, K.G. Paul, The substrate profiles of the acidic and slightly basic horseradish peroxidases, *Biochim. Biophys. Acta* 350 (1974) 304–313.
- [15] S. Aibara, T. Kobayashi, Y. Morita, Isolation and properties of basic isoenzymes of horseradish peroxidase, *J. Biochem.* 90 (1981) 489–496.
- [16] S. Aibara, H. Yamashita, E. Mori, M. Kato, Y. Morita, Isolation and characterization of five neutral isoenzymes of horseradish peroxidase, *J. Biochem.* 92 (1982) 531–539.
- [17] K. Fujiyama, H. Takemura, S. Shibayama, K. Kobayashi, J.K. Choi, A. Shinmyo, et al., Structure of the horseradish peroxidase isozyme C genes, *Eur. J. Biochem.* 173 (1988) 681–687.
- [18] M. Gajhede, D.J. Schuller, A. Henriksen, A.T. Smith, T.L. Poulos, Crystal structure of horseradish peroxidase C at 2.15 Å resolution, *Nat. Struct. Biol.* 4 (1997) 1032–1038.
- [19] K.G. Welinder, Amino acid sequence studies of horseradish peroxidase. Amino and carboxyl termini, cyanogen bromide and tryptic fragments, the complete sequence, and some structural characteristics of horseradish peroxidase C, *Eur. J. Biochem.* 96 (1979) 483–502.
- [20] B.Y. Yang, J.S. Gray, R. Montgomery, The glycans of horseradish peroxidase, *Carbohydr. Res.* 287 (1996) 203–212.
- [21] J.W. Tams, K.G. Welinder, Mild chemical deglycosylation of horseradish peroxidase yields a fully active, homogeneous enzyme, *Anal. Biochem.* 228 (1995) 48–55.
- [22] J.W. Tams, K.G. Welinder, Glycosylation and thermodynamic versus kinetic stability of horseradish peroxidase, *FEBS Lett.* 421 (1998) 234–236.
- [23] C.B. Lavery, M.C. Macinnis, M.J. Macdonald, J.B. Williams, C.A. Spencer, A.A. Burke, et al., Purification of peroxidase from Horseradish (*Armoracia rusticana*) roots, *J. Agric. Food Chem.* 58 (2010) 8471–8476.
- [24] A.T. Smith, N. Santama, S. Dacey, M. Edwards, R.C. Bray, R.N. Thorneley, et al., Expression of a synthetic gene for horseradish peroxidase C in *Escherichia coli* and folding and activation of the recombinant enzyme with Ca²⁺ and heme, *J. Biol. Chem.* 265 (1990) 13335–13343.
- [25] V. Grigorenko, T. Chubar, Y. Kapeliuch, T. Borchers, F. Spener, A. Egorov, New approaches for functional expression of recombinant horseradish peroxidase C in *Escherichia coli*, *Biocatalysis Biotransformation* 17 (1999) 359–379.
- [26] C. Hartmann, P.R. Ortiz de Montellano, Baculovirus expression and characterization of catalytically active horseradish peroxidase, *Arch. Biochem. Biophys.* 297 (1992) 61–72.
- [27] M. de las, M. Segura, G. Levin, M.V. Miranda, F.M. Mendive, H.M. Targovnik, O. Cascone, High-level expression and purification of recombinant horseradish peroxidase isozyme C in SF-9 insect cell culture, *Process Biochem.* 40 (2005) 795–800.
- [28] A. Vlamis-Gardikas, A.T. Smith, J.M. Clements, J.F. Burke, Expression of active horseradish peroxidase in *Saccharomyces cerevisiae*, *Biochem. Soc. Trans.* 20 (1992) 111S.
- [29] B. Morawski, Z. Lin, P. Cirino, H. Joo, G. Bandara, F.H. Arnold, Functional expression of horseradish peroxidase in *Saccharomyces cerevisiae* and *Pichia pastoris*, *Protein Eng.* 13 (2000) 377–384.
- [30] B. Morawski, S. Quan, F.H. Arnold, Functional expression and stabilization of horseradish peroxidase by directed evolution in *Saccharomyces cerevisiae*, *Biotechnol. Bioeng.* 76 (2001) 99–107.
- [31] F.W. Krainer, C. Dietzsch, T. Hajek, C. Herwig, O. Spadiut, A. Glieder, Recombinant protein expression in *Pichia pastoris* strains with an engineered methanol utilization pathway, *Microb. Cell Factor* 11 (2012) 22–35.
- [32] C. Dietzsch, O. Spadiut, C. Herwig, A dynamic method based on the specific substrate uptake rate to set up a feeding strategy for *Pichia pastoris*, *Microb. Cell Factor* 10 (2011) 14–22.
- [33] O. Spadiut, L. Rossetti, C. Dietzsch, C. Herwig, Purification of a recombinant plant peroxidase produced in *Pichia pastoris* by a simple 2-step strategy, *Protein Expr. Purif.* 86 (2012) 89–97.
- [34] M.G. Brattain, M.E. Marks, T.G. Pretlow, The purification of horseradish peroxidase by affinity chromatography on Sepharose-bound concanavalin A1,2, *Anal. Biochem.* 72 (1976) 346–352.
- [35] M.V. Miranda, H.M. Fernández-Lahore, J. Dobrecky, O. Cascone, The extractive purification of peroxidase from plant raw materials in aqueous two-phase systems, *Acta Biotechnol.* 18 (1998) 179–188.
- [36] W. Guo, E. Ruckenstein, Separation and purification of horseradish peroxidase by membrane affinity chromatography, *J. Membr. Sci.* 211 (2003) 101–111.
- [37] L.F. Fraguas, F. Batista-Viera, J. Carlsson, Preparation of high-density concanavalin A adsorbent and its use for rapid, high-yield purification of peroxidase from horseradish roots, *J. Chromatogr. B Analyt. Technol. Biomed. Life Sci.* 803 (2004) 237–241.
- [38] A. Glieder, F.W. Krainer, M. Kulterer, L. Näätsaari, V. Reichel, Horseradish peroxidase isoenzymes, EP2584035 A1, 2013.
- [39] S.K. Sharma, N. Sehgal, A. Kumar, A quick and simple biostrip technique for detection of lactose, *Biotechnol. Lett.* 24 (2002) 1737–1739.
- [40] C.C. Chiou, P.Y. Chang, E.C. Chan, T.L. Wu, K.C. Tsao, J.T. Wu, Urinary 8-hydroxydeoxyguanosine and its analogs as DNA marker of oxidative stress: development of an ELISA and measurement in both bladder and prostate cancers, *Clin. Chim. Acta* 334 (2003) 87–94.
- [41] A. Singh, D. Ma, D.L. Kaplan, Enzyme-mediated free radical polymerization of styrene, *Biomacromolecules* 1 (2000) 592–596.
- [42] N. Vasileva, T. Godjevargova, D. Ivanova, K. Gabrovska, Application of immobilized horseradish peroxidase onto modified acrylonitrile copolymer membrane in removing of phenol from water, *Int. J. Biol. Macromol.* 44 (2009) 190–194.
- [43] O. Greco, S. Rossiter, C. Kanthou, L.K. Folkes, P. Wardman, G.M. Tozer, et al., Horseradish peroxidase-mediated gene therapy: choice of prodrugs in oxic and anoxic tumor conditions, *Mol. Cancer Ther.* 1 (2001) 151–160.
- [44] L. Näätsaari, B. Mistlberger, C. Ruth, T. Hajek, F.S. Hartner, A. Glieder, Deletion of the *Pichia pastoris* KU70 homologue facilitates platform strain generation for gene expression and synthetic biology, *PLoS One* 7 (2012) e39720.
- [45] R. Weis, R. Luiten, W. Skranc, W. Schwab, M. Wubbolts, A. Glieder, Reliable high-throughput screening with *Pichia pastoris* by limiting yeast cell death phenomena, *FEMS Yeast Res.* 5 (2004) 179–189.
- [46] O. Spadiut, C. Leitner, C. Salaheddin, B. Varga, B.G. Vertessy, T.-C. Tan, et al., Improving thermostability and catalytic activity of pyranose 2-oxidase from *Trametes multicolor* by rational and semi-rational design, *FEBS J.* 276 (2009) 776–792.
- [47] D. Mattanovich, A. Graf, J. Stadlmann, M. Dragosits, A. Redl, M. Maurer, et al., Genome, secretome and glucose transport highlight unique features of the protein production host *Pichia pastoris*, *Microb. Cell Factor* 8 (2009) 29.
- [48] C.-J. Huang, L.M. Damasceno, K.A. Anderson, S. Zhang, L.J. Old, C.A. Batt, A proteomic analysis of the *Pichia pastoris* secretome in methanol-induced cultures, *Appl. Microbiol. Biotechnol.* 90 (2011) 235–247.
- [49] H. Podgornik, A. Podgornik, A. Perdih, A method of fast separation of lignin peroxidases using convective interaction media disks, *Anal. Biochem.* 272 (1999) 43–47.
- [50] H. Podgornik, A. Podgornik, P. Milavec, A. Perdih, The effect of agitation and nitrogen concentration on lignin peroxidase (LiP) isoform composition during fermentation of *Phanerochaete chrysosporium*, *J. Biotechnol.* 88 (2001) 173–176.
- [51] H. Podgornik, A. Podgornik, Separation of manganese peroxidase isoenzymes on strong anion-exchange monolithic column using pH-salt gradient, *J. Chromatogr. B Analyt. Technol. Biomed. Life Sci.* 799 (2004) 343–347.
- [52] M. Barut, A. Podgornik, P. Brne, A. Strancar, Convective interaction media short monolithic columns: enabling chromatographic supports for the separation and purification of large biomolecules, *J. Sep. Sci.* 28 (2005) 1876–1892.
- [53] A.N. Hiner, J. Hernández-Ruiz, M.B. Arnao, F. García-Cánovas, M. Acosta, A comparative study of the purity, enzyme activity, and inactivation by hydrogen peroxide of commercially available horseradish peroxidase isoenzymes A and C, *Biotechnol. Bioeng.* 50 (1996) 655–662.
- [54] D.J. Gilfoyle, J.N. Rodriguez-Lopez, A.T. Smith, Probing the aromatic-donor-binding site of horseradish peroxidase using site-directed mutagenesis and the suicide substrate phenylhydrazine, *Eur. J. Biochem.* 236 (1996) 714–722.
- [55] B. Bjellqvist, G.J. Hughes, C. Pasquali, N. Paquet, F. Ravier, J.C. Sanchez, et al., The focusing positions of polypeptides in immobilized pH gradients can be predicted from their amino acid sequences, *Electrophoresis* 14 (1993) 1023–1031.
- [56] B. Bjellqvist, B. Basse, E. Olsen, J.E. Celis, Reference points for comparisons of two-dimensional maps of proteins from different human cell types defined in a pH scale where isoelectric points correlate with polypeptide compositions, *Electrophoresis* 15 (1994) 529–539.
- [57] R. Gupta, E. Jung, S. Brunak, Prediction of N-glycosylation sites in human proteins, 2004 (in preparation).

- Chapter 3 -

Knockout of an endogenous mannosyltransferase increases the homogeneity of glycoproteins produced in *Pichia pastoris*

Florian W. Krainer¹, Christoph Gmeiner², Lukas Neutsch³, Robert Pletzenauer², Anton Glieder⁴ and Oliver Spadiut^{2*}

¹ Graz University of Technology, Institute of Molecular Biotechnology, Graz, Austria

² Vienna University of Technology, Institute of Chemical Engineering, Research Area Biochemical Engineering, Vienna, Austria

³ University of Vienna, Department of Pharmaceutical Technology and Biopharmaceutics, Vienna, Austria

⁴ Austrian Centre of Industrial Biotechnology (ACIB GmbH), Graz, Austria

* Corresponding Author: Oliver Spadiut, Vienna University of Technology, Institute of Chemical Engineering, Research Area Biochemical Engineering, Gumpendorfer Strasse 1a, A-1060 Vienna, Austria. Tel: +43 1 58801 166473, Fax: +43 1 58801 166980; e-mail: oliver.spadiut@tuwien.ac.at



OPEN

Knockout of an endogenous mannosyltransferase increases the homogeneity of glycoproteins produced in *Pichia pastoris*

SUBJECT AREAS:

ENZYMES

GLYCOPROTEINS

EXPRESSION SYSTEMS

PROTEIN DESIGN

Received
20 May 2013Accepted
4 November 2013Published
20 November 2013Correspondence and
requests for materials
should be addressed to
O.S. (oliver.spadiut@
tuwien.ac.at)Florian W. Krainer¹, Christoph Gmeiner², Lukas Neutsch³, Markus Windwarder⁴, Robert Pletzenauer², Christoph Herwig², Friedrich Altmann⁴, Anton Glieder⁵ & Oliver Spadiut²¹Graz University of Technology, Institute of Molecular Biotechnology, Graz, Austria, ²Vienna University of Technology, Institute of Chemical Engineering, Research Area Biochemical Engineering, Vienna, Austria, ³University of Vienna, Department of Pharmaceutical Technology and Biopharmaceutics, Vienna, Austria, ⁴Department of Chemistry, University of Natural Resources and Life Sciences, Vienna Austria, ⁵Austrian Centre of Industrial Biotechnology (ACIB GmbH), Graz, Austria.

The yeast *Pichia pastoris* is a common host for the recombinant production of biopharmaceuticals, capable of performing posttranslational modifications like glycosylation of secreted proteins. However, the activity of the *OCH1* encoded α -1,6-mannosyltransferase triggers hypermannosylation of secreted proteins at great heterogeneity, considerably hampering downstream processing and reproducibility. Horseradish peroxidases are versatile enzymes with applications in diagnostics, bioremediation and cancer treatment. Despite the importance of these enzymes, they are still isolated from plant at low yields with different biochemical properties. Here we show the production of homogeneous glycoprotein species of recombinant horseradish peroxidase by using a *P. pastoris* platform strain in which *OCH1* was deleted. This *och1* knockout strain showed a growth impaired phenotype and considerable rearrangements of cell wall components, but nevertheless secreted more homogeneously glycosylated protein carrying mainly Man₈ instead of Man₁₀ N-glycans as a dominant core glycan structure at a volumetric productivity of 70% of the wildtype strain.

The methylotrophic yeast *Pichia pastoris* has long been used for the production of recombinant proteins at high titers. Up to 22 g·L⁻¹ have been reported for intracellularly produced recombinant hydroxynitrile lyase¹ and approximately 15 g·L⁻¹ for secreted recombinant gelatin², demonstrating the high production capacity of this microbial host while being able to grow on comparatively simple and inexpensive media. Not only can *P. pastoris* be grown to cell densities as high as 160 g·L⁻¹ dry cell weight³, it is also capable of performing posttranslational modifications, including the formation of correct disulfide bridges and the glycosylation of secretory proteins, rendering *P. pastoris* specifically suitable for the production of complex eukaryotic proteins⁴.

Glycosylation has long been known to affect various protein properties such as solubility, stability and enzymatic activity (e.g.^{5,6}), which need to be evaluated on a case-by-case basis. Whereas only little is known about O-linked glycosylation, the biosynthesis of N-glycans is well understood. N-glycans are linked to the amido groups of asparagine residues that are recognized by glycotransferases in the sequence motif N-X-S/T, where X is any amino acid but proline. Initially, the biosynthesis steps of N-glycans in yeast and mammals are identical. Dolichol phosphate-linked N-acetylglucosamine (DolP-GlcNAc) is synthesized by the transfer of GlcNAc from uridine diphosphate (UDP) onto DolP on the cytoplasmic side of the ER. After extension to DolP-linked Man₅GlcNAc₂, this structure is enzymatically flipped to the ER lumen, where further glucose (Glc) and Man residues are added to form a core glycan, Glc₃Man₉GlcNAc₂, which is transferred to an asparagine within the N-X-S/T sequence motif of a nascent protein chain. Subsequently, the three terminal Glc residues and one Man residue are trimmed by glucosidases I and II and an ER-residing α -1,2-mannosidase to form Man₈GlcNAc₂. At this point, the newly formed glycoprotein is transported to the Golgi apparatus, which is where the yeast and mammalian N-glycosylation pathways diverge⁷⁻⁹. In the mammalian Golgi apparatus, α -1,2-mannosidases trim the core glycan further to form Man₅GlcNAc₂. Ultimately, addition of GlcNAc by a β -N-acetylglucosaminyltransferase I

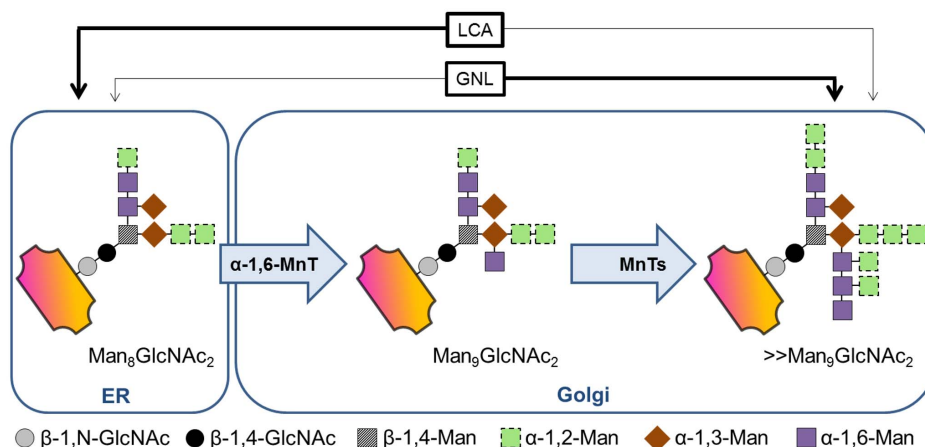


Figure 1 | Och1p in N-glycan biosynthesis. In the Golgi, the α -1,6-mannosyltransferase activity (α -1,6-MnT) of Och1p extends the N-linked $\text{Man}_8\text{GlcNAc}_2$ core glycan, which is then heterogeneously hyperglycosylated by several additional (phospho-) mannosyltransferases (MnTs). *Galanthus nivalis* lectin (GNL) and *Lens culinaris* lectin (LCA) bind to the different glycan structures either with high (thick arrow) or low (thin arrow) specificity.

(GnTI), trimming of two further Man residues by a mannosidase II and yet further addition of GlcNAc, galactose (Gal) and sialic acid (Sia) residues by the respective transferases result in the complex N-glycan structures of mammalian proteins¹⁰. In the yeast Golgi, on the other hand, the $\text{Man}_8\text{GlcNAc}_2$ glycan is not subjected to further trimming reactions but is substantially extended. In *Saccharomyces cerevisiae*, more than 100 Man residues may account for hypermannosyl N-glycans on secretory proteins. However, the extent of hypermannosylation varies considerably and seems to depend on so far unknown influences, causing vast heterogeneity in the N-glycan pattern of secreted glycoproteins. In *S. cerevisiae* as well as in *P. pastoris* and other yeasts, the first reaction in hypermannosylation is catalyzed by an α -1,6-mannosyltransferase (Och1p) that is encoded by the gene Outer CHain elongation 1 (*OCH1*), which was first discovered and characterized in *S. cerevisiae*^{11,12}. Och1p uses Man from guanosin diphosphate and links it to the core glycan by an α -1,6-glycosidic bond, forming a substrate that triggers additional mannosylation (Figure 1). Whereas *S. cerevisiae* holds a repertoire of Golgi-resident α -1,2-, α -1,3 and α -1,6-mannosyl and mannosylphosphate transferases, *P. pastoris* seems to lack the Golgi-resident α -1,3-mannosyltransferase, but to possess four additional β -mannosyltransferases instead^{7,13,14}.

Although not as extensive as those of *S. cerevisiae*, the N-glycans of *P. pastoris* are also of the high mannose type and the humanization of the N-glycosylation machinery of *P. pastoris* has been the subject of several studies (Table 1).

Here, we report the deletion of the *OCH1* gene from the *P. pastoris* genome in an irreversible and straight forward approach. Thereby, we generated a new *P. pastoris* platform strain that allows the production of recombinant proteins with shorter glycan structures of considerably increased homogeneity compared to proteins produced in a wildtype strain. In contrast to previous glycoengineering studies, which required several time- and labor-intensive steps of strain engineering, we achieved more homogeneously glycosylated protein with a single gene knockout step. Horseradish peroxidase (HRP) is a versatile enzyme with applications in diagnostics and histochemistry, bioremediation and cancer treatment. However, due to the lack of an appropriate recombinant production process, HRP preparations are still derived from horseradish roots as mixtures of different isoenzymes¹⁵. In the present study, we produced recombinant HRP in an *och1* knockout strain in the controlled environment of a bioreactor, purified and characterized the enzyme, thus demonstrating the general applicability of this new platform strain by the example of this industrially and medically relevant enzyme.

Results

Knockout of *OCH1* from *Ppku70-* and *PpMutS*. In yeast, the *OCH1* gene encodes an α -1,6-mannosyltransferase whose activity triggers the subsequent transfer of further mannose and phosphomannose residues onto the N-glycans of secreted proteins in the Golgi apparatus, resulting in heterogeneously hyperglycosylated protein species that appear as a smear on SDS gels, e.g.^{16,17}. This hyperglycosylation not only limits the use of yeast derived proteins as biopharmaceuticals but also greatly impedes traditional downstream processing. Hence, a *P. pastoris* strain that allows the production of less heterogeneously glycosylated proteins would considerably relieve protein production processes with *P. pastoris*.

A flipper cassette targeting to the *OCH1* locus was transformed to a *Ppku70-* strain to replace the *OCH1* open reading frame. This *Ppku70-* strain has to rely on homologous recombination for gene integration events, in contrast to a wildtype strain¹⁸. The cassette construct and the knockout workflow are schematically shown in Fig. 2.

Transformation of the flipper cassette to the *Ppku70-* strain resulted in only few Zeocin™ resistant clones. However, Sanger sequencing of

Table 1 | Humanization of N-glycans in *P. pastoris*. Selected studies focusing on the humanization of the N-glycans on *P. pastoris* derived glycoproteins. Bmt, β -mannosyltransferase; Mns, mannosidase; GnT, β -N-acetylglucosaminyltransferase; UDP-GlcNAc, uridine diphosphate-N-acetylglucosamine; *OCH1*, outer chain elongation gene 1

content	references
introduction of α -1,2-Mns, GnTI and an UDP-GlcNAc transporter via a combinatorial genetic library approach in a $\Delta och1::URA3$ strain	13,50
introduction of an UDP-GlcNAc transporter, α -1,2-MnslA, MnslI, GnTI, GnTII in a $\Delta och1::URA3$ strain	51
introduction of α -1,2-Mns and GnTI, <i>OCH1</i> inactivation via a knockin plasmid	10
GlycoSwitch plasmids for <i>OCH1</i> inactivation and introduction of glycosidase and glycosyltransferase activities to produce complex terminally galactosylated glycoproteins	52
introduction of sialic acid biosynthesis pathway and corresponding transporter and transferase activities to produce complex terminally sialylated glycoproteins	53
elimination of α -Mns resistant glycan structures by inactivation of the activities of Bmt1p, Bmt2p and Bmt3p	54



a PCR amplified fragment of the *OCH1* locus from genomic DNA showed that the majority of the tested transformants had correct integration of the transformed cassette. The transformants grew slowly and formed colonies of abnormal shape. This phenotype was preserved when the strains were grown on minimal methanol agar plates to induce the production of the FLP recombinase and subsequent excision of the inner part of the flipper cassette containing the expression cassettes for the FLP recombinase and the ZeocinTM resistance enzyme. Reconstituted sensitivity to ZeocinTM, PCR and Sanger sequencing of the former *OCH1* locus confirmed the successful excision of the inner part of the flipper cassette and the efficient replacement of the former *OCH1* ORF with a single *FRT* site of 34 bp.

Transformation of the same *OCH1* flipper cassette to *PpMutS* resulted in hundreds of clones resistant to ZeocinTM. Initial PCR based screenings of over 100 randomly chosen clones did not give any positive hits, analogously to what has been described by Verweken *et al.*¹⁰. However, after having identified the corresponding phenotype of positive transformants in the *Ppku70*-based *och1* knockout strain, designated *PpFWK1*, also *PpMutS* based transformants with correct integration of the flipper cassette could be spotted easily on the agar plates since they showed the same unusual colony phenotype as colonies of *PpFWK1* (Figure 3).

Increasing the incubation time of the transformed cells on the agar plates to at least four days allowed growth of the *och1* knockout colonies to a size at which their abnormal shape was an obvious hint to their genotype (Figure 3). Again, ZeocinTM sensitivity was reconstituted by induction of the FLP recombinase on minimal methanol agar plates and the replacement of the *OCH1* ORF by a single *FRT* site was shown by PCR and Sanger sequencing. The observed phenotype of the generated *och1* knockout strain *PpFWK3* included slow

growth, abnormal colony shape and temperature sensitivity at 37°C (data not shown). Upon transformation of the wildtype *OCH1* promoter and *OCH1* ORF to *PpFWK3*, the detrimental phenotype was found to be complemented. PCR analyses confirmed the unaltered replacement of the former *OCH1* ORF by a *FRT* site, but the presence of the complementing *OCH1* ORF somewhere else in the genome due to ectopic integration of the transformed plasmid *pPpT4*-*BamHI*_{*OCH1*}rescue.

Strain morphology. *Cell morphology and cell division of an och1 knockout strain.* Consistent with previous reports on *Och1p* deficient *S. cerevisiae* strains^{19,20}, we found the N-glycosylation mutant to be characterized by an altered phenotype and growth profile (Table 2). In contrast to the wildtype based strain *PpMutS*, the *och1* knockout strain *PpFWK3* grew in the form of large cell clusters with clumpy appearance and multibudded cells (Figure 4). Daughter cells within these clusters displayed clearly segregated vacuoles, but remained stably attached to the wall of mother cells (Supplementary Figure 1).

Knockout induced stress response is reflected by a spatial rearrangement of WGA/STL binding sites. The direct functional implication of the altered N-glycosylation in *PpFWK3* for cell morphology and cytokinesis was further illustrated by a striking difference in the chitin deposition after *OCH1* knockout (Supplementary Figure 1). In lectin based glycoprofiling studies, we observed substantially altered binding patterns for the GlcNAc-specific lectin WGA, with the reactive carbohydrate motifs being homogeneously distributed across the entire cell surface in the *och1* knockout strain, instead of remaining confined to the bud scars as in *PpMutS* (Figure 5 and Supplementary Figure 1).

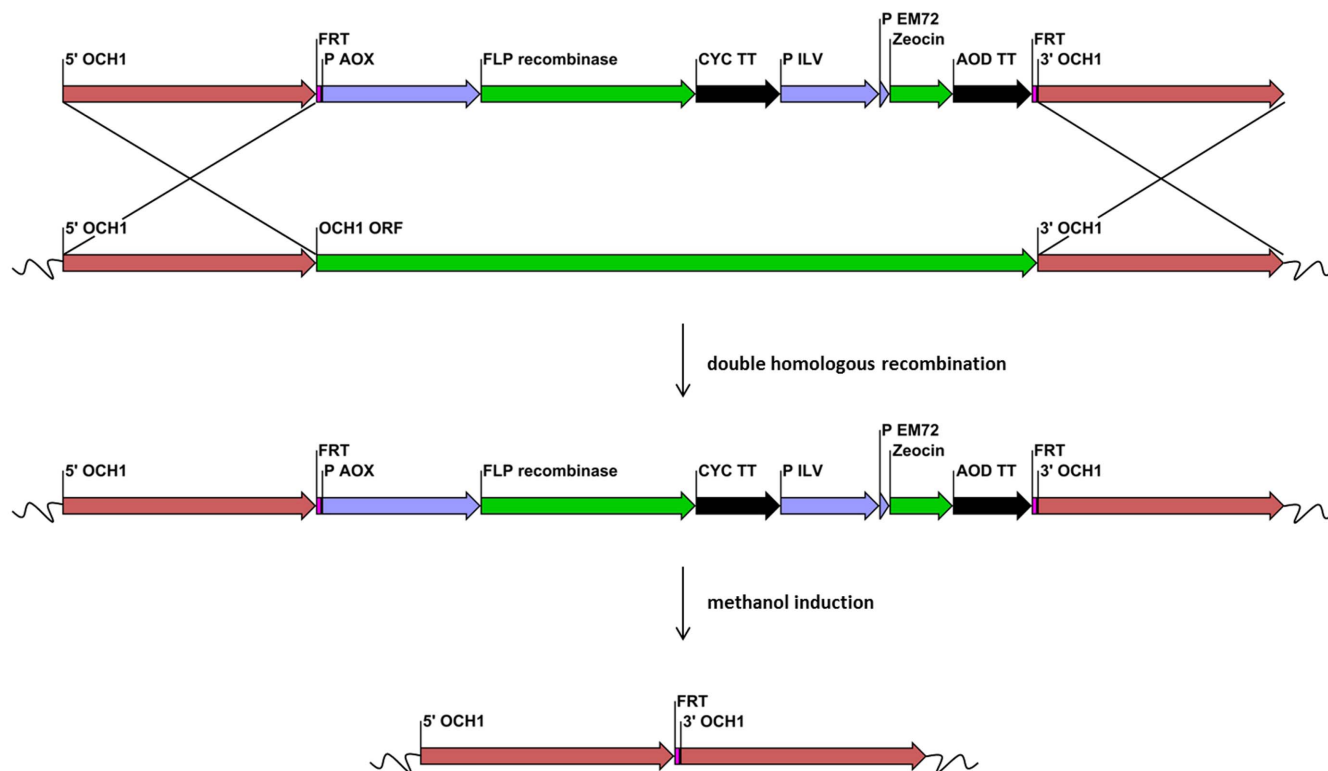


Figure 2 | Schematic workflow of the knockout of *OCH1* using a flipper cassette. The regions 5' *OCH1* and 3' *OCH1* represent sequences upstream and downstream of the *OCH1* ORF, respectively. The 34 bp flipper recombinase target (*FRT*) sequences flank the *AOX1* promoter (P *AOX1*), the FLP recombinase ORF, the *CYC1* transcription terminator (CYC TT), a constitutive eukaryotic and a prokaryotic promoter (P *ILV* and P *EM72*, respectively), a *ble* ORF mediating ZeocinTM resistance and an *AOD* transcription terminator (AOD TT). A double homologous recombination event replaced the *OCH1* ORF in the genome with the flipper cassette. Growth of recombinant cells on methanol induced the production of the FLP recombinase which recognized the two *FRT* sites and excised the inner sequence, leaving only one *FRT* site in the genome. Single fragments are not drawn to scale.

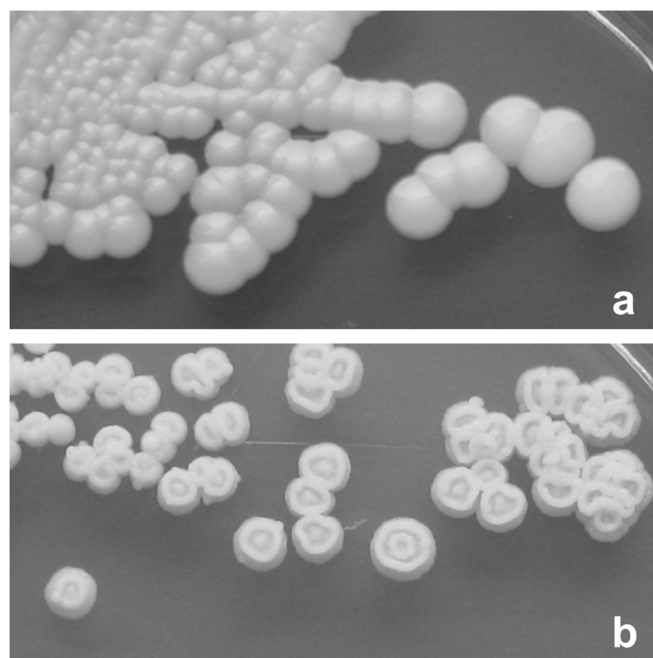


Figure 3 | Colony phenotypes. (a), *PpMutS*; (b), *PpFWK3*. Both strains were grown on YPD agar.

In order to assess whether a mere alteration in the steric accessibility of chitin chains in the lateral wall was responsible for the difference in the WGA staining behavior or whether chitin was actually specifically localized at bud scars, *PpMutS* cells were subjected to the same fluorescence microscopic analysis after treatment with concentrated methanol, leading to denaturation of mannoproteins and a substantial increase in cell wall permeability²¹. The efficiency of the cell wall permeabilization protocol was validated by concomitant incubation with a usually non-membrane penetrating DAPI dye, which could readily access the nuclear space after methanol treatment. Still, methanol permeabilized *PpMutS* cells displayed only the conventional, bud scar selective staining pattern, contrasting to the generalized binding of GNL, which served as a control (Supplementary Figure 2).

Quantitatively, comparative overall ratios of WGA/FM[®] 4–64 were found for *PpMutS* and the *och1* knockout strain *PpFWK3* (Figure 6), indicating that mainly a spatial redistribution of chitin

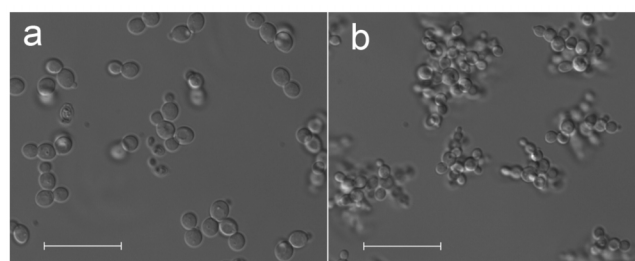


Figure 4 | Phenotypic change in *P. pastoris* upon *OCH1* knockout. Representative DIC micrographs of *PpMutS* and *PpFWK3*. (a), *PpMutS* cells in batch culture. (b), covalently linked clusters of multibudded cells in *PpFWK3* during the same cultivation phase. Scale bars represent 25 μm .

may be induced by altering the glycosylation machinery, but without general enhancement of the total cellular chitin level. In other words, the rather high chitin concentration at the bud scars in *PpMutS* seemed to be reduced in favor of an increased chitin deposition in the lateral cell walls of *PpFWK3*. These results were also confirmed via the chitin binding lectin STL, which has a similar carbohydrate specificity profile as WGA but only limited affinity to isolated GlcNAc residues (Figure 6).

Inactivation of the Och1p activity shifted the interaction capacity of mannose specific lectins. The *och1* knockout cells of the *PpFWK3* strain displayed a lower binding capacity for the lectin GNL than *PpMutS* cells (Figure 6). GNL interacts with high mannose N-glycans and preferably reacts with α -1,3-Man residues, but also binds to α -1,6 linked Man residues^{22,23}. In the current study, the GNL/FM[®] 4–64 ratio was reduced by 50% in *PpFWK3* as compared to *PpMutS*, but still remained the lectin with highest binding capacity for this strain (Figure 6). In striking contrast, the binding levels of the glycan core-binding lectin LCA were increased upon *OCH1* knockout (Figure 6). Both, GNL and LCA showed an equal distribution across the entire cell wall (Figure 5), corresponding to the established localization of their putative targets, high-mannose N-glycans and core glycans, respectively.

Production of HRP in the strains *PpMutS*^{HRP} and *PpFWK3*^{HRP}. To show the applicability of the generated *och1* knockout strain for the production of recombinant proteins, a vector harboring a gene coding for an acidic HRP isoenzyme was transformed into either *PpMutS* or *PpFWK3*. Transformation of the linearized constructs

Table 2 | Strain specific parameters of the different *P. pastoris* strains. Parameters are defined in the footnote^x

	<i>PpMutS</i>	<i>PpMutS</i> ^{HRP}	<i>PpFWK3</i>	<i>PpFWK3</i> ^{HRP}
max. μ_{Gly} (h^{-1})	0.30	0.31	0.20	0.20
q_{Gly} ($\text{mmol} \cdot \text{g}^{-1} \cdot \text{h}^{-1}$)	2.90	3.10	1.90	1.90
$Y_{\text{X/Gly}}$ ($\text{Cmol} \cdot \text{Cmol}^{-1}$)	0.63	0.41	0.61	0.54
$Y_{\text{CO}_2/\text{Gly}}$ ($\text{Cmol} \cdot \text{Cmol}^{-1}$)	0.33	0.64	0.37	0.44
$\Delta\text{time}_{\text{adapt}}$ (h)	15.7	19.9	6.60	8.90
q_{MeOH} ($\text{mmol} \cdot \text{g}^{-1} \cdot \text{h}^{-1}$)	0.62	0.70	0.52	0.43
max. q_{MeOH} ($\text{mmol} \cdot \text{g}^{-1} \cdot \text{h}^{-1}$)	0.67	0.78	0.69	0.53
$Y_{\text{X/MeOH}}$ ($\text{Cmol} \cdot \text{Cmol}^{-1}$)	0.39	0.07	0.05	0.04
$Y_{\text{CO}_2/\text{MeOH}}$ ($\text{Cmol} \cdot \text{Cmol}^{-1}$)	0.57	1.02	constantly decreasing	constantly decreasing
C-balance	0.97	1.04	constantly decreasing	constantly decreasing
q_{p} ($\text{U} \cdot \text{g}^{-1} \cdot \text{h}^{-1}$)	-	0.77	-	0.50
vol. productivity ($\text{U} \cdot \text{L}^{-1} \cdot \text{h}^{-1}$)	-	2.60	-	1.80
efficiency factor (η) ($\text{U} \cdot \text{mmol}^{-1}$)²⁶	-	1.10	-	1.20

^xmax. μ_{Gly} , maximum specific growth rate on glycerol; q_{Gly} , specific uptake rate of glycerol during the batch; $Y_{\text{X/Gly}}$, biomass yield on glycerol; $Y_{\text{CO}_2/\text{Gly}}$, CO_2 yield on glycerol; $\Delta\text{time}_{\text{adapt}}$, time from first addition of methanol to a maximum in offgas activity; q_{MeOH} , average specific uptake rate of methanol during consecutive methanol pulses; max. q_{MeOH} , maximum specific uptake rate of methanol during consecutive methanol pulses; $Y_{\text{X/MeOH}}$, biomass yield on methanol; $Y_{\text{CO}_2/\text{MeOH}}$, CO_2 yield on methanol; C-balance, sum of biomass and CO_2 yields; q_{p} , specific productivity of HRP; vol. productivity, volumetric productivity of HRP; efficiency factor; efficiency of the conversion of substrate methanol into product HRP.

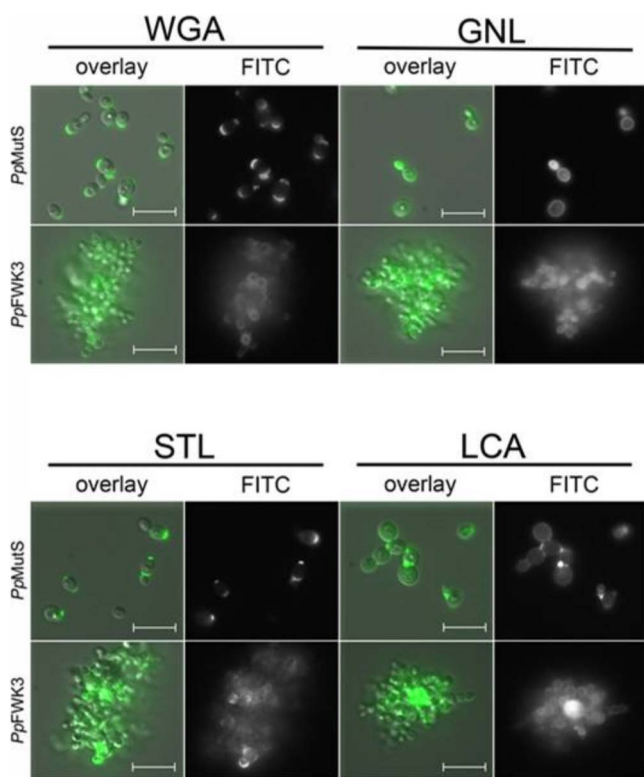


Figure 5 | Lectin based glycoprofiling of surface carbohydrate motifs in *PpMutS* and *PpFWK3*. Live cells harvested in the exponential growth phase of batch cultivation were incubated with fluorescein labeled lectins. Micrographs show the isolated channel for FITC detection and merged images with DIC (overlay). Scale bars represent 10 μm .

into *PpFWK3* resulted in fewer ZeocinTM resistant clones than for *PpMutS*, but sufficient to allow screening for HRP activity after cultivation in a 96-deep well plate in minimal media. Despite the apparent growth defect of *PpFWK3*, the volumetric yields in HRP activity in these micro-scale cultivations were comparable to those of *PpMutS* based transformants. Prior to cultivation of *PpMutS*^{HRP} or *PpFWK3*^{HRP} in the bioreactor, both strains were analyzed in terms of copy number of the transformed HRP gene to ensure comparability on this level. Both strains were found to have a single copy integration of the HRP encoding gene and were thus considered suitable for comparative bioreactor cultivations.

Strain characterization in bioreactors. We characterized four *P. pastoris* strains (Table 2) with a recently published method of conducting dynamic experiments during batch cultivations in the controlled environment of a bioreactor^{16,24,25}. After depletion of glucose, a first methanol adaption pulse with a final concentration of 0.5% (v/v) was applied. The adaptation times to the new substrate methanol ($\Delta\text{time}_{\text{adapt}}$), defined as the maximum in offgas activity, were determined for all four *P. pastoris* strains and are shown in Table 2.

The calculated carbon dioxide evolution rate (CER), illustrating the metabolic activity of the different strains, the specific substrate uptake rate (q_s) and, where appropriate, the specific productivity (q_p), during the methanol pulses are shown in Supplementary Fig. 3–6. As shown in Supplementary Fig. 3 and 4, the CER profiles for the strains *PpMutS* and *PpMutS*^{HRP} showed a similar pattern during the consecutive methanol pulses and q_s values stayed constant over time. In contrast, the CER profiles for the strains *PpFWK3* and *PpFWK3*^{HRP} substantially changed over time (Supplementary Figures 5 and 6). After each methanol pulse, less CO₂ was produced per time and volume, indicating that the *P. pastoris* cells became

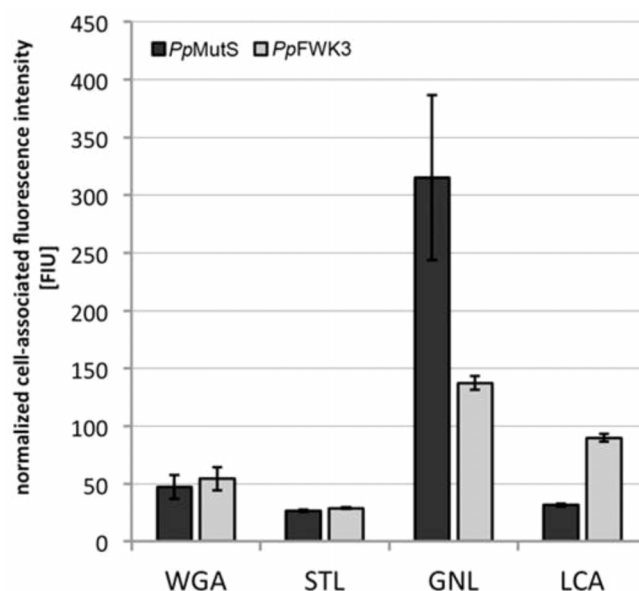


Figure 6 | Quantitative determination of lectin binding on *PpMutS* and *PpFWK3* cells. Cell suspensions adjusted to the same concentration level were incubated with FITC labeled lectins. After thorough washing, cells were lysed and the fluorescence intensity of the lysis buffer recorded. Binding data was normalized to the average cellular content of FM[®] 4–64, which was shown to be similar in both strains via FACS analysis. Values represent mean \pm SD of three independent experiments.

metabolically less active. Thus, the consumption of 1% (v/v) methanol took longer after each consecutive pulse (compare Supplementary Figures 3 and 4 with Supplementary Figures 5 and 6). The altered metabolic activity of the *och1* knockout strains was also depicted in the calculated yields ($Y_{X/S}$ and $Y_{CO_2/S}$), which are shown in Fig. 7.

For the strains *PpMutS* and *PpMutS*^{HRP} both the carbon dioxide yield ($Y_{CO_2/S}$) and the biomass yield ($Y_{X/S}$) stayed constant during the six conducted consecutive methanol pulses (Figure 7a and b). Evidently, the insertion of the HRP gene into strain *PpMutS* affected its physiology as $Y_{X/S}$ decreased, whereas $Y_{CO_2/S}$ increased (compare Figure 7a and b). Hence, *PpMutS*^{HRP} mainly used the substrate methanol for protein production and dissimilation than for biomass growth.

Interestingly, the calculated yields for *PpFWK3* and *PpFWK3*^{HRP} strains showed a very different behaviour. Although $Y_{X/S}$ was again rather constant, $Y_{CO_2/S}$ decreased dramatically in the course of the six to seven consecutive methanol pulses (Figure 7c and d), indicating that these two strains became more and more metabolically inactive. Since HPLC analysis revealed that no undesired metabolites were produced in substantial amounts during any of the four cultivations, the C-balances for strains *PpFWK3* and *PpFWK3*^{HRP} were determined close to 1.0 only at the beginning of the cultivation but rapidly decreased over time, whereas the C-balances for strains *PpMutS* and *PpMutS*^{HRP} were always determined to be close to 1.0 (Supplementary Figure 7). A summary of the determined strain specific parameters of the four different *P. pastoris* strains is given in Table 2.

As shown in Table 2, the maximum specific growth rates on glycerol (max. μ_{Gly}) for *PpFWK3* strains were approximately 1.5-fold lower than for *PpMutS* strains. The yields on glycerol showed a similar pattern for *PpMutS* and *PpFWK3* strains, as the yields were shifted towards production of carbon dioxide rather than biomass when the strains were hosting the gene for recombinant HRP. Both *PpFWK3* strains needed less than half of the adaptation time to methanol ($\Delta\text{time}_{\text{adapt}}$) compared to the *PpMutS* strains. The altered glycosylation machinery in the *PpFWK3* strains seems to allow a

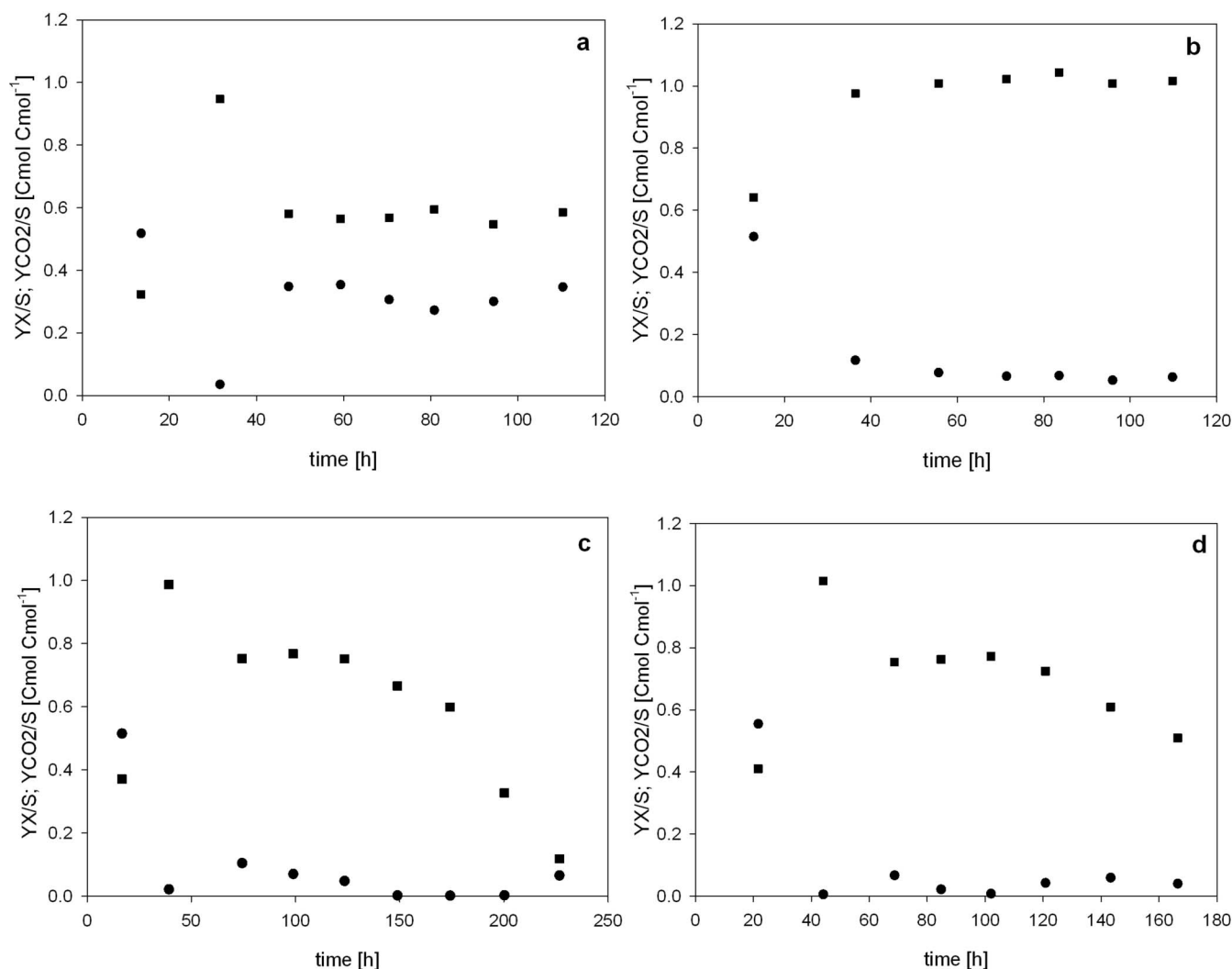


Figure 7 | Calculated yields for the different *P. pastoris* strains during batch cultivations with methanol pulses. (a), *PpMutS*; (b), *PpMutS^{HRP}*; (c), *PpFWK3*; (d), *PpFWK3^{HRP}*. Black square, carbon dioxide yield ($Y_{CO_2/S}$); black dot, biomass yield ($Y_{X/S}$).

faster adaptation to methanol, which could be of great significance for industrial applications where fast and efficient bioprocesses are required. As expected, the adaptation times of the strains hosting the recombinant enzyme were longer compared to the strains not carrying this additional gene. The average specific substrate uptake rates for both substrates (q_s) glycerol and methanol were lower for the *PpFWK3* strains than for *PpMutS* strains. In respect to the maximum specific uptake rate for methanol ($\max. q_{MeOH}$) the values for the different strains were quite similar. However, these values were determined during the 3rd and the 5th methanol pulse for *PpMutS* and *PpMutS^{HRP}*, respectively. The values during the other pulses were alike. For *PpFWK3* strains on the other hand, these maxima could only be determined during the 1st methanol pulse. After that, the values for q_s constantly decreased, indicating a progressional reduction of the metabolic activity of the *PpFWK3* strains during consecutive methanol pulses. This was also underlined by constantly decreasing $Y_{CO_2/S}$ and C-balances. However, despite this seemingly negative impact, *PpFWK3^{HRP}* produced the HRP isoenzyme at specific and volumetric productivities which were only reduced by 35% and 30%, respectively, compared to *PpMutS^{HRP}*. In a previous study, we introduced the efficiency factor η , which puts the productivity of the strains in direct relation to the consumed substrate²⁶. In this respect, the *och1* knockout strain *PpFWK3^{HRP}* even showed a higher ratio than *PpMutS^{HRP}* and thus proved to be of justifiable interest for the production of recombinant proteins.

Enzyme purification and characterization. In order to demonstrate the successful decrease of heterogeneity in the glycosylation of HRP when produced in an *och1* knockout strain, size exclusion chromatography (SEC) was performed with cell free cultivation broth (Figure 8). A SEC elution profile has higher specificity and sensitivity than an image of an SDS polyacrylamide gel and was therefore preferably used for this purpose. HRP produced in *PpMutS^{HRP}* eluted with higher heterogeneity than HRP produced in *PpFWK3^{HRP}*.

Judging by the size exclusion chromatogram (Figure 8), HRP produced in a *PpMutS^{HRP}* strain substantially differed in its surface glycosylation pattern compared to HRP produced in a *PpFWK3^{HRP}* strain, which showed higher homogeneity. To analyze this phenomenon in detail, we enzymatically released the glycans from the produced recombinant HRPs and analyzed them via liquid chromatography-mass spectrometry (LC-MS). Reducing glycans were observed mainly as doubly charged $[M + H + NH_4]^{2+}$ ions (Figure 9). Analysis of enzymatically released glycans from HRP produced in either *PpMutS^{HRP}* or *PpFWK3^{HRP}* confirmed the expected decrease in both N-glycan size and heterogeneity. The dominant core glycan structure shifted from Man10 to Man8 in strain *PpFWK3^{HRP}* (Table 3). As shown in Fig. 9, HRP produced in the strain *PpMutS^{HRP}* carried a greater variety of different glycan chains consisting of up to 17 mannoses and a higher amount of phosphorylated sugars than HRP produced in *PpFWK3^{HRP}*.



The evaluation of the relative peak areas underlined this observation (Table 3), as around 60% of the identified glycan structures cleaved off from HRP produced in the *och1* knockout strain *PpFWK3*^{HRP} were of the Man₈ type, whereas no structure of that type was identified for HRP from *PpMutS*^{HRP}. As shown in Table 3 there were also much more different glycan chains identified on HRP from *PpMutS*^{HRP} and interestingly no phosphorylated mannose structures were found on HRP from *PpFWK3*^{HRP}.

To check whether the kinetic constants or the stability of the enzyme were affected by the altered glycosylation pattern, we characterized purified preparations of HRP. HRP preparations produced by either *PpMutS*^{HRP} or *PpFWK3*^{HRP} in bioreactor cultivations were purified by using a recently described strategy for HRP isoenzyme C1A²⁷. Both HRP preparations did not bind to the mixed mode HCIC resin but were found in the flowthrough, *i.e.* 93% of HRP produced in *PpMutS*^{HRP} and 87% of HRP produced in *PpFWK3*^{HRP}. Contaminating proteins were retained on the resin, leading to a partial purification at a factor of approximately 2.5 for both enzyme solutions. A subsequent size exclusion step gave an additional purification factor of approximately 2.0. After purification, the fractions with the highest purification factor were pooled and ultrafiltered. The enzyme HRP produced in *PpMutS*^{HRP} was concentrated to around 3.0 mg·mL⁻¹, whereas HRP produced in *PpFWK3*^{HRP} could not be concentrated due to the immediate formation of precipitates during ultrafiltration and the resulting clogging of the membrane, indicating a reduced solubility of the extracellular proteins in this preparation. We determined the kinetic constants for both enzyme preparations with H₂O₂ as electron donor at saturating concentration and ABTS as electron acceptor in varying concentrations (Table 4; Supplementary Figure 8).

As shown in Table 4, the affinity of HRP towards the substrate ABTS was increased, as the K_M was found to be decreased by approximately 15% by the altered surface glycosylation. However, V_{max} was decreased by nearly 20%. Also, the thermal stability of the produced HRP glycovariants at 60°C was studied (Supplementary Figure 9) and the half life times ($\tau_{1/2}$) were determined²⁸. The $\tau_{1/2}$ of HRP produced in *PpMutS*^{HRP} was determined with 384 s, whereas HRP from *PpFWK3*^{HRP} showed a reduction in its thermal half life time of around 50% with 198 s.

Discussion

Despite the numerous advantages of using *P. pastoris* as a host organism for recombinant protein production, its inherent heterogeneous yeast type hyperglycosylation of secreted proteins has to be addressed by extensive and elaborated strain modifications. Here, we present a straight forward approach for the generation of a wildtype based *P.*

pastoris platform strain that allows the production of more homogeneously glycosylated recombinant proteins due to an irreversible deletion of the *OCH1* gene.

Yeast hypermannosylation largely depends on the initial activity of an α -1,6-mannosyltransferase in the Golgi apparatus. Elimination of this activity was achieved by replacement of the *OCH1* ORF with a single 34 bp *FRT* site by using a flipper cassette. However, this approach required double homologous recombination at the correct locus in the genome. Unfortunately, homologous integration events only play a minor part in *P. pastoris*, as recently demonstrated by Näätsaari *et al.*¹⁸ and which was found to be especially true for the *OCH1* locus by Vervecken *et al.*¹⁰. A new *P. pastoris* strain with inactivated non-homologous end joining pathway, designated *Ppku70-*, proved to be a particularly convenient tool to identify the phenotype of the specific knockout strain in this study. Since homologous integration was the sole possibility for recombination events in the *Ppku70-* strain, the total number of positive transformants was predominantly made up by transformants with homologous integration. The fact that particularly few colonies were obtained by targeting of the transformed flipper cassette to the *OCH1* locus when using the *Ppku70-* strain also supported the hypothesis of increased difficulty of homologous recombination in that locus.

An *och1* knockout strain of *S. cerevisiae* was described to show several defects such as impaired budding and increased temperature sensitivity¹¹. Choi *et al.* mentioned temperature sensitivity and increased flocculation for their *P. pastoris och1* knockout strain¹³, but neither they nor Vervecken *et al.*¹⁰ described any further severe growth defects. However, the *och1* knockout strain in the present study was found to show not only formation of cell clusters and temperature sensitivity, but also decreased growth which might be due to an impaired cell wall structure and thus complicated bud formation. Similarly, a recently generated *och1* knockout strain based on the *his4* mutant strain *P. pastoris* GS115 was described with slower growth and rough colony surface²⁹. Explanations for these divergent findings remain speculative, but might be due to single nucleotide polymorphisms and hence different strain backgrounds. Also, a secondary integration event of the transformed flipper cassette cannot be completely excluded. However, considering that as little as 100 ng of the cassette were transformed and that all clones that exposed the described phenotype had the correct integration of the cassette in the *OCH1* locus indicates that the observed phenotype can be ascribed rather to the knockout of *OCH1* than to any additional genomic rearrangement. Also, the similarity of the observed phenotype in the present *P. pastoris och1* knockout strain to the phenotype described for a *S. cerevisiae och1* knockout strain¹¹ very much suggests that the deletion of the *OCH1* gene is actually responsible for the phenotype observed in this study. Most strikingly, reintroduction of the wildtype *OCH1* gene to the *och1* knockout strain *PpFWK3* restored its phenotype, thus conclusively linking the observed phenotype of *PpFWK3* to the deletion of the *OCH1* gene. Transformation of the *och1* knockout strain with a linearized vector harboring an expression cassette for the production of an HRP isoenzyme via electroporation was found to result in lower transformation efficiency than electroporation of a *P. pastoris* wildtype strain. This increased sensitivity to electroporation might be another reflection of the altered cell wall composition that could be shown by lectin based glycoprofiling.

The highly specific interaction of the lectin WGA with the exposed chitin ring of bud scars³⁰ has previously been reported for other yeasts and can be used for the precise determination of the number of cell divisions performed^{31,32}. To the best of our knowledge, this is the first confirmation of this structure-related specificity for *P. pastoris*. However, in the *och1* knockout strain, we noticed an almost complete loss of bud scar selectivity. The reasons for the regionally diverse distribution of chitin in *PpFWK3* may either lie in an increased accessibility of previously cryptic chitin chains in the

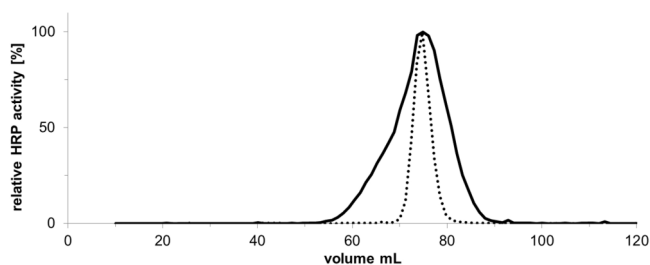


Figure 8 | Size exclusion chromatogram of HRP glycovariants. Solid line, HRP produced in *PpMutS*^{HRP}; dashed line, HRP produced in *PpFWK3*^{HRP}. The run was performed at a flow of 9 cm³·h⁻¹ and fractions of 1.2 mL were collected. The measured HRP activities per fraction are shown as relative activities with the respective maximum activities set to 100% for better comparability. The unnormalized maximum activities were 2.6 and 15.1 U·mL⁻¹ for HRP from *PpMutS*^{HRP} and from *PpFWK3*^{HRP}, respectively. The loaded volume was approximately 200 μ L for HRP from either *PpMutS*^{HRP} or *PpFWK3*^{HRP}.

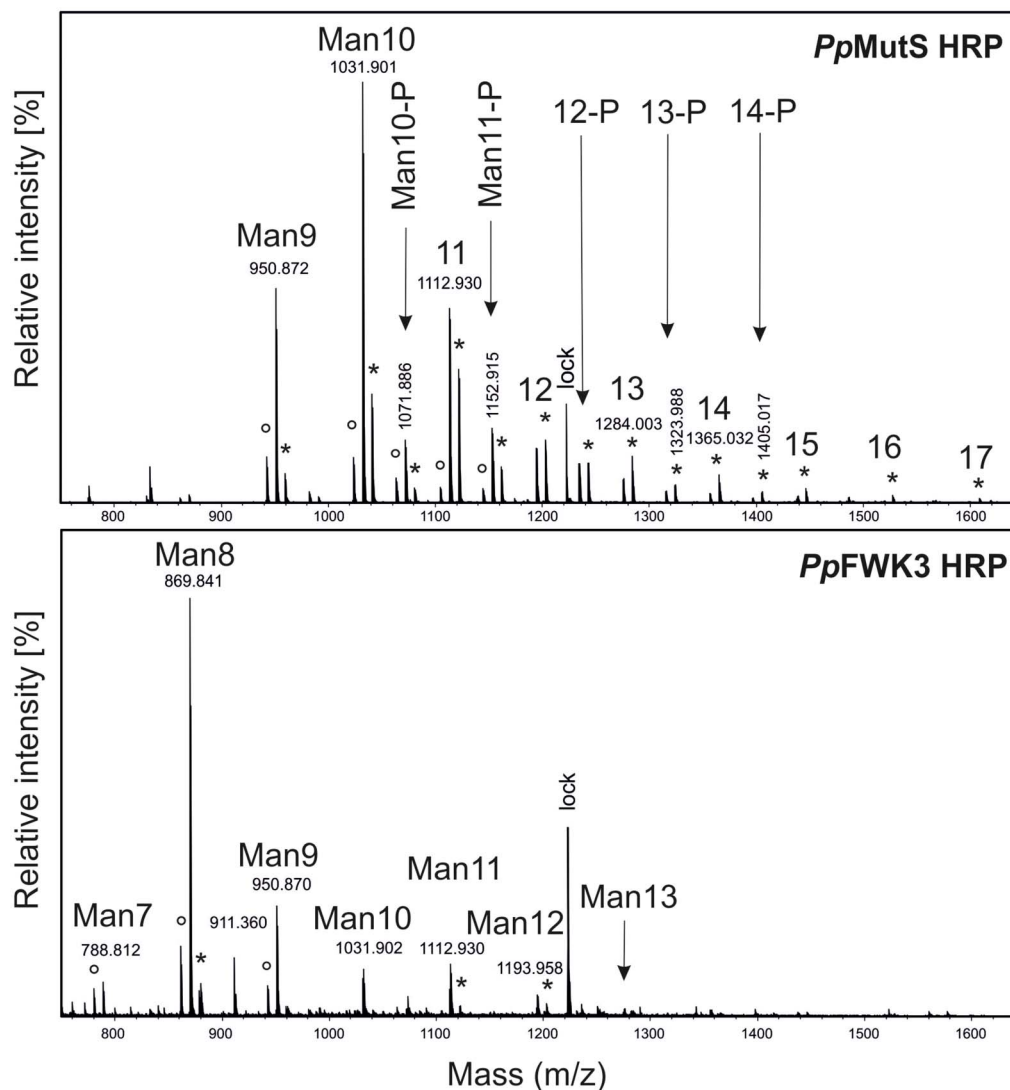


Figure 9 | Chromatogram of liquid chromatography-mass spectrometry of glycans released from HRP produced in either *PpMutS*^{HRP} or in *PpFWK3*^{HRP}. HRP $[M + 2H]^{2+}$ and $[M + 2NH_4]^{2+}$ ions are marked with ° and *, respectively. “Man10-P” or just “12-P” indicate phosphorylated glycans. lock, lock mass.

lateral cell wall (*i.e.* when the protective polymannan layer is missing), or in an actively increased chitin synthesis and deposition at the cell wall, *i.e.* as a compensatory response to the cell wall stress caused by the impaired barrier function. Such stimulation of counter-regulatory pathways upon impairment of cell wall integrity has been observed in several yeast species^{33,34} and involves diverse mechanisms and signaling cascades³⁵, which are believed to be directly or indirectly connected to the deletion of Och1p activity²⁰. Especially the osmotic stress exerted on the cell as a result of the impaired cell wall integrity is known to present an important factor for the induction of counter-regulatory pathways³⁶. Due to the persistence of bud scar specific binding of WGA in methanol treated *PpMutS* cells, we concluded that the strong affinity of WGA to the overall cell wall of *PpFWK3* cells traced back to a *de novo* deposition of carbohydrate epitopes (most probably chitin) in this *och1* knockout strain, and not an increased exposure of constitutive cell wall glycans that are invariably present but usually shielded by an outer chain hypermannan structure in the wildtype strain. The somewhat reduced STL/FM[®] 4–64 ratio compared to the WGA/FM[®] 4–64 ratio may be connected to the minor differences regarding the preferentially binding ligand. Based on the similarity between STL and WGA staining patterns, it is unlikely that any GlcNAc motifs other than chitin (*e.g.* in the core glycan of mannoproteins) were the primary binding epitopes

detected by either of the two lectins. As a side aspect of the current work, we were able to demonstrate the use of fluorescence labeled lectins as convenient and versatile probes for visualizing stress responses derived from impaired cell wall integrity in yeast. The decreased GNL/FM[®] 4–64 ratio of *PpFWK3* compared to *PpMutS* could be explained by the minimized amount of high mannose N-glycans and the therefore inherently lower amount of potential GNL target ligands (*i.e.* α -1,3- and α -1,6-Man residues) of *PpFWK3* compared to *PpMutS*. Nevertheless, the remaining core glycan provided sufficient GNL targets for a distinct signal. The increased LCA/FM[®] 4–64 ratio of *PpFWK3* on the other hand, may be explained by the preference of this lectin for short chain X- α -1,2-Man-Man motifs, with X representing either α -Man or β -GlcNAc³⁷. In mannoproteins, such short motifs may be found in the core glycans, the accessibility of which may be enhanced in absence of the usually highly branched polymannan structures of a *P. pastoris* wildtype strain^{33,34}.

The detailed characterization of the different *P. pastoris* strains in the controlled environment of a bioreactor revealed that the *och1* knockout strains were physiologically impaired compared to their wildtype equivalents. During the consecutive pulses, the carbon dioxide yield $Y_{CO_2/S}$ and the C-balances constantly decreased, indicating a loss in metabolic activity. This was also apparent in the CER signals during the single methanol pulses (Supplementary Figure 5



Table 3 | Relative peak areas of identified glycan structures cleaved off from HRP recombinantly produced in either *PpMutS^{HRP}* or in *PpFWK3^{HRP}*

glycan structure	<i>PpMutS^{HRP}</i>	<i>PpFWK3^{HRP}</i>
	relative peak area [%]	
Man7	0.0	7.9
Man8	0.0	57.3
Man9	15.7	16.8
Man10	31.4	6.1
Man10-P	5.6	0.0
Man11	18.7	6.8
Man11-P	6.7	0.0
Man12	6.7	3.2
Man12-P	4.4	0.0
Man13	3.7	1.8
Man13-P	1.8	0.0
Man14	2.1	0.0
Man14-P	1.1	0.0
Man15	1.2	0.0
Man16	0.5	0.0
Man17	0.4	0.0
total	100.0	100.0

and 6). At the beginning of the cultivation, methanol was metabolized much faster than during later methanol pulses. We followed the morphology of the *P. pastoris* cells during cultivations via microscopy and identified formation of cell clusters by the *och1* knockout strains. Obviously, the altered surface glycosylation of *och1* knockout cells also affected the budding process. Instead of budding off, the daughter cells stayed attached to the mother cell. The microscopically observed increased tendency for cluster formation may be regarded as an effect which is intrinsically linked to the loss of the polymannan layer upon Och1p inactivation. Cell disruption experiments showed that neither treatment with Triton X-100, 0.5% EDTA or 5 M urea, nor extensive mechanic shearing via sonication allowed breaking the clusters to single cells. Thus, we conclude that deficiencies in the constitutive cell division machinery upon Och1p inactivation led to a strong, covalent linkage between the cell walls, which remained intact even after the end of the normal budding process. The exact nature of this linkage remains speculative at the current point, but may be associated to aberrant glycosylation steps in the glycan backbone, occurring as a compensatory adaptation to the lack of Och1p activity^{20,38}. Due to these very dense and compact formations we hypothesize that the cells in the center of these clusters became limited in oxygen and nutrients and showed no more metabolic activity. Since these cell clusters increased in size over time, the overall metabolic activity of the total amount of cells in the bioreactor decreased, which we observed in decreasing $Y_{CO_2/S}$ and C-balances. However, these cell clusters were still able to produce recombinant protein. In fact, both the specific productivity and the volumetric productivity, the main focus of industrial bioprocesses, were only reduced by 35% and 30%, respectively, compared to the *P. pastoris* strain with an intact *OCH1* gene. However, due to the constant

Table 4 | Enzymatic characterization of homogeneously glycosylated HRP. Kinetic constants of HRP produced in either *PpMutS^{HRP}* or *PpFWK3^{HRP}* with H_2O_2 as electron donor at saturating concentration and ABTS as electron acceptor in varying concentrations were determined at 420 nm and 30°C

production strain	$K_{M, ABTS}$ [mM]	V_{max} [$\mu\text{mol}\cdot\text{s}^{-1}\cdot\mu\text{g}^{-1}$]
<i>PpMutS^{HRP}</i>	2.40	3.07
<i>PpFWK3^{HRP}</i>	2.03	2.46

decrease in metabolic activity over time, use of the *och1* knockout strain in industrial processes will require considerable modifications to current standard protocols to optimize recombinant protein production in this strain.

When we analyzed the HRP produced by either a *PpMutS^{HRP}* strain or the *och1* knockout strain *PpFWK3^{HRP}*, we found the enzyme preparation from *PpFWK3^{HRP}* to be considerably more homogeneously glycosylated. More detailed analyses of the surface glycan chains of HRP by mass spectrometry revealed striking differences in the glycosylation pattern between HRP produced in *PpMutS^{HRP}* and *PpFWK3^{HRP}*. HRP produced in *PpMutS^{HRP}* carried a more heterogeneous glycopattern with several high-mannose structures and a great amount of phosphorylated sugars. The most dominant glycan was found to be a Man10 structure. In contrast, the most dominant glycan of HRP produced in *PpFWK3^{HRP}* was a Man8 core glycan structure. This reduction is in agreement with our expectations since no Och1p could act on Man₈GlcNAc₂ core glycan structures in the Golgi of the *PpFWK3^{HRP}* strain as it could in *PpMutS^{HRP}*. Due to the missing Och1p activity, other glycosyltransferases, especially mannosylphosphate transferases, were reduced in their activity resulting in a more homogeneous glycopattern on the surface of recombinantly produced HRP from *PpFWK3^{HRP}* (Table 3).

Enzymatic characterizations of HRP revealed an increase in the affinity to the substrate ABTS, but a decrease of V_{max} for HRP with a more homogeneous glycopattern. Also, a decreased stability at 60°C for the homogeneously glycosylated HRP compared to the heterogeneously hyperglycosylated glycovariant was observed.

In conclusion, we irreversibly eliminated the *OCH1* encoded α -1,6-mannosyltransferase activity of *P. pastoris*. The phenotype of the generated *och1* knockout platform strain resembled the phenotype described for the same knockout in *S. cerevisiae*. Nevertheless, the strain was successfully employed for the production of recombinant HRP as a reporter enzyme. Strain specific parameters were determined in comparative bioreactor cultivations. Recombinant HRP from either an unaltered *P. pastoris* strain or the *och1* knockout strain was purified and characterized. The main findings of this study can be summarized as:

- The *och1* knockout strains were characterized by slow growth, increased temperature sensitivity and formation of cell clusters. The altered N-glycosylation pathway and resultant structural impacts in the *PpFWK3* strain appears to have triggered the dynamic reorganization of surface mannose residues and other glycan structures. The cellular response seemed to be more diverse than just a simple lack of an outer chain hypermannan structure, and may also involve secondary counter-regulatory mechanisms on the metabolic or structural level^{20,38}. Our results in this regard are in direct agreement with previous work on *och1* deletion strains of *S. cerevisiae*^{19,39}. Lectin based glycoprofiling represented a rapid and reliable method to provide functional proof for the successful deletion of Och1p activity in *P. pastoris*.
- In the course of consecutive methanol pulses, the *och1* knockout strains lost their metabolic activity due to the formation of cell clusters, thus making the adaption of current production processes necessary.
- As shown by detailed LC-MS data, the produced recombinant enzyme exhibited a more homogeneous surface glycosylation, which is beneficial for subsequent downstream processing and applications.
- V_{max} with ABTS as substrate and the thermal stability at 60°C were reduced for the homogeneously glycosylated HRP, whereas its affinity for ABTS was increased, rendering the enzyme suitable for most applications.

Here, we report the thorough biotechnological characterization of a *P. pastoris* platform strain that allows the production of recombinant proteins with considerably increased homogeneity in their



glycosylation pattern due to an irreversible knockout of the *OCH1* gene. Currently, efforts are driven forward to elucidate the potential benefits of the cell morphological changes in glycoengineered *P. pastoris* strains for the expression of recombinant proteins⁴⁰. Also, future studies will focus on rescuing the growth impaired phenotype to generate a strain that shares the favorable growth phenotype of a wildtype strain but still allows the production of homogeneously glycosylated secreted proteins.

Methods

Chemicals. Enzymes and deoxynucleotide triphosphates were obtained from Thermo Scientific (formerly Fermentas, Germany). Phusion™ High-Fidelity DNA-polymerase was from Finnzymes (Finland). 2,2'-azino-bis(3-ethylbenzothiazoline-6-sulfonic acid) diammonium salt (ABTS) was purchased from Sigma-Aldrich (Austria). Difco™ yeast nitrogen base w/o amino acids (YNB), Difco™ yeast nitrogen base w/o amino acids and ammonia sulfate (YNB2), Bacto™ tryptone and Bacto™ yeast extract were purchased from Becton Dickinson (Austria). Zeocin™ was purchased from InvivoGen (France) via Eubio (Austria). Fluorescein isothiocyanate (FITC) labeled lectins for microscopic analysis were obtained from Vector Laboratories (USA), comprising wheat germ agglutinin (WGA) from *Triticum vulgare*, *Lens culinaris* agglutinin (LCA), *Galanthus nivalis* lectin (GNL) and *Solanum tuberosum* lectin (STL). FM® 4-64 membrane stain and Hoechst 33342 or 4',6-diamidino-2-phenylindole (DAPI) nucleic acid stains were purchased from Life Technologies (USA). Other chemicals were obtained from Carl Roth (Germany).

Microorganisms. DNA manipulations were performed in accordance to standard protocols⁴¹ in *E. coli* Top10F⁺ (Life Technologies, formerly Invitrogen, Austria). All *P. pastoris* strains in this study were based on the wildtype strain CBS 7435 (identical to NRRL Y-11430 or ATCC 76273). Initial *OCH1* knockout studies were performed in a *ku70* deletion strain, previously described by Näätäsaari *et al.*¹⁸, hereafter called *Ppku70*-. Since *P. pastoris* strains with Mut^s phenotype have been repeatedly shown to be superior over strains with Mut⁺ phenotype for the production of recombinant proteins (e.g.²⁶), the ultimate *och1* knockout strain was based on a Mut^s strain described in¹⁸, hereafter called *PpMutS*.

Deletion of the *OCH1* gene. Based on the genome sequence of the *P. pastoris* wildtype strain CBS 7435⁴², the primers *OCH1*-5int-fw1 and *OCH1*-5int-rv1 were designed to amplify a DNA fragment upstream the *OCH1* open reading frame from genomic DNA isolated according to⁴³. Primers *OCH1*-3int-fw1b and *OCH1*-3int-rv1b were designed to amplify a fragment downstream of the *OCH1* ORF. *OCH1*-5int-rv1 and *OCH1*-3int-fw1b were designed to add sequences that overlap with the *FRT* flanked inner part of a flipper cassette. All primer sequences are listed in Table 5.

The two *OCH1* targeting fragments of approximately 1.5 kb each were used to assemble a flipper cassette via overlap extension PCR⁴⁴. Transformation of 100 ng of the assembled flipper cassette into either *Ppku70*- or *PpMutS* was performed as described by Lin-Cereghino *et al.*⁴⁴. Transformants were identified on yeast extract-peptone-dextrose (YPD) agar plates containing 100 mg·L⁻¹ Zeocin™. Double homologous recombination of the flipper cassette in the *OCH1* locus was verified by PCR using the primers *OCH1*check-fw1 and *OCH1*check-rv2 (Table 5) and Sanger sequencing, using isolated genomic DNA as template. Expression of the FLP recombinase gene was induced by growing positive transformants on minimal methanol agar plates. The FLP recombinase mediated excision of the *FRT* flanked inner part of the flipper cassette was shown by restored sensitivity of the cells towards Zeocin™ and again by PCR and Sanger sequencing. The resulting *Ppku70*- *och1* knockout strain was designated *PpFWK1*, the *PpMutS* *och1* knockout strain was designated *PpFWK3*.

Complementation of the observed phenotype of the *PpFWK3* strain was performed by transforming a plasmid that was constructed by assembly⁴⁵ of two fragments, which were generated by PCR using the primers *OCH1*rescue-fw1 and *OCH1*rescue-rv1 using genomic DNA from *PpMutS* as template, and *OCH1*rescue_T4fw and *OCH1*rescue_T4rv using the plasmid *pPpT4_S*¹⁸ as template (Table 5). The resulting plasmid contained the wildtype *OCH1* ORF plus 698 bp of upstream sequence, putatively harboring the natural *OCH1* promoter, and was designated *pPpT4_BamHI_OCH1*rescue. Approximately 500 ng of *BamHI* linearized plasmid were transformed to *PpFWK3*, aliquots were plated on YPD Zeocin™ agar plates and incubated at 28°C for two days. PCR with the primers *OCH1*check-fw1 and *OCH1*check-rv2 from isolated genomic DNA of transformant strains was performed to confirm the unaltered replacement of the former *OCH1* ORF by a single *FRT* site. A second PCR with the primers *OCH1*-ORF-fw and *OCH1*-ORF-rv from the same genomic DNA was performed to confirm the presence of a plasmid transmitted *OCH1* ORF somewhere else in the genome. A resulting strain with restored wildtype phenotype was designated *PpFWK3*^R.

Phenotypic strain characterization. *Lectin based glycoprofiling via fluorescence microscopy.* Qualitative analysis of lectin binding was performed by incubating 500 µL of *PpMutS* or *PpFWK3* cell suspensions in 20 mM HEPES buffer, pH 7.4, at an OD₆₀₀ of 0.3 with 500 µL of the respective lectin solution (250 pmol·mL⁻¹ in 20 mM HEPES, pH 7.4) for 30 min at 4°C. If appropriate, 5 µg·mL⁻¹ HOECHST 33342 nucleic acid stain or 0.5 µg·mL⁻¹ FM® 4-64 membrane stain were included in the incubation mix. After thorough washing by repeated centrifugation (1700 × g, 5 min) and resuspension, cells were diluted in 1.0 mL of particle free phosphate buffered saline (PBS; 50 mM, pH 7.4) and mounted in FlexiPERM® coverslip 12-well plates for microscopic analysis. Images were acquired on a Zeiss Epifluorescence Axio Observer.Z1 deconvolution microscopy system (Carl Zeiss, Germany) equipped with LD Plan-Neofluar objectives and the LED illumination system Colibri®. Exposure wavelengths and filter sets of the individual channels were chosen according to the respective fluorophore(s) (DAPI/Hoechst 33342: ex/em 365/450 nm; FITC: ex/em 485/525 nm; FM® 4-64 ex/em 485/>620 nm), and combined with differential interference contrast (DIC) images for ease of orientation. Exposure time and illumination parameters were adjusted individually for optimal visibility. For bud scar visualization, Z-stack image series of representative spots were recorded and processed via moderate iterative deconvolution. Lectin cytoadhesion was quantified by incubating the cells with the respective lectin solutions and FM® 4-64 as described above (4°C, 30 min), followed by extensive washing. Cells were then lysed by treatment with Triton X-100/SDS (1.0/1.0%) for 24 h under vivid agitation. The FITC fluorescence intensity in the lysis buffer was assessed in a microplate reader (TECAN, Austria) at ex/em 485/525 nm and normalized to the content of FM® 4-64 for direct comparison between the individual samples. Lectin solutions without cells were subjected to the same treatment and analyzed in order to exclude potential degradation of the fluorophore. Control experiments via fluorescence-activated cell sorting (FACS) were performed to verify similar uptake of the membrane stain in both strains.

Membrane permeabilization experiments. To gain information on the steric accessibility of cell wall-embedded chitin and other carbohydrates, cell permeability was enhanced by treatment with concentrated methanol at -20°C for 20 min, followed by lectin staining. The cells contained in 1.0 mL of precooled suspension (OD₆₀₀ of 0.3) were harvested by centrifugation, resuspended in 100 µL PBS buffer and added dropwise to 1.0 mL of icecold methanol under vivid agitation. After 20 min, cells were pelleted again and excessive solvent was removed via repeated washing and centrifugation with fresh PBS buffer. After rehydration in 1.0 mL of 20 mM HEPES buffer, pH 7.4, cells were subjected to the same lectin staining protocol as described above and analyzed via fluorescence microscopy. Efficient membrane permeabilization was verified via successful counterstaining of the nuclear DNA with a normally non-membrane permeable DAPI dye.

Table 5 | Oligonucleotide primer list. Primers used for the amplification of upstream and downstream sequences of the *OCH1* locus from genomic DNA, for amplification of the whole *OCH1* locus for Sanger sequencing, for amplification of fragments to assemble *pPpT4_BamHI_OCH1*rescue and to amplify the *OCH1* ORF

primer name	sequence (5' - 3')
<i>OCH1</i> -5int-fw1	GAACTGTGTAACCTTTTAAATGACGGGATCTAAATACGTCATG
<i>OCH1</i> -5int-rv1	CTATTCTAGAAAGTATAGGAAGTCTCGGCTGATGATTTGCTACGAACACTG
<i>OCH1</i> -3int-fw1b	GTTCTATACCTTCTAGAGAATAGGAAGTCTCGGAGATTAGAGAATGAACCTTCTTCTAAGCGATCG
<i>OCH1</i> -3int-rv1b	GAAGTATTAGGAGCTGAAGAAGCAGAGGCCAGAG
<i>OCH1</i> check-fw1	CACACATATAAAGGCAATCTACG
<i>OCH1</i> check-rv2	CAATAACTTCTGCAATAGACTGC
<i>OCH1</i> rescue-fw1	TTCATAGGCTTGGGGTAATAG
<i>OCH1</i> rescue-rv1	CTTGAGCGGCGCTAGTCTTCCAACCTTCTCTC
<i>OCH1</i> rescue_T4fw	GCATACATTTGAAGGAAGTTGGAAGGACTAAGCGGCCGCTCAAGAGGAT
<i>OCH1</i> rescue_T4rv	CTATTTCTGTCTATCTATTACCCCAAGCCTATGAAGGATCTGGGTACCGCAGG
<i>OCH1</i> -ORF-fw	ATGGCGAAGGCAGATGGC
<i>OCH1</i> -ORF-rv	TTAGTCTTCCAACCTTCTTCAAAATG



Production of the reporter enzyme horseradish peroxidase in shake flask experiments. Aliquots of approximately 2 μg of *Smil* linearized plasmid pPpT4_S¹⁸, harboring a HRP gene containing nine potential N-glycosylation sites were transformed into either *PpMutS* or *PpFWK3*. The transformed HRP gene encodes for a new acidic HRP isoenzyme. A detailed description on the identification of new HRP isoenzymes will be given elsewhere (Näätsaari *et al.*, manuscript in preparation). The HRP gene was codon optimized for expression in *P. pastoris* based on a codon table described in⁴⁶. Expression of the gene was regulated by the *AOX1* promoter. Efficient secretion of HRP to the supernatant was facilitated by fusion of the prepro signal sequence of the *S. cerevisiae* mating factor alpha to the N-terminus of the mature HRP. Transformations were performed according to⁴⁴ with the following modification: Whereas an overnight culture of *PpMutS* was diluted to an OD₆₀₀ of 0.2 to grow to an OD₆₀₀ of 0.8–1.0 in approximately 5 h prior to preparation of the cells for electroporation, an overnight culture of *PpFWK3* was diluted to a starting OD₆₀₀ of 0.7 to account for its decreased growth rate. Transformants were grown on YPD Zeocin™ agar plates and randomly chosen for screening in micro scale cultivations in 96-deep well plates, similarly to⁴⁷. The cells were cultivated in 250 μL iron-supplemented BMD1% (11 $\text{g}\cdot\text{L}^{-1}$ $\alpha\text{-D}(+)\text{-glucose}$ monohydrate, 13.4 $\text{g}\cdot\text{L}^{-1}$ YNB, 0.4 $\text{mg}\cdot\text{L}^{-1}$ D(+)-biotin, 278 $\text{mg}\cdot\text{L}^{-1}$ FeSO₄·7H₂O, 0.1 M potassium phosphate buffer, pH 6.0) for approximately 60 h, then induced once with 250 μL BMM2 (1% (v/v) methanol, 13.4 $\text{g}\cdot\text{L}^{-1}$ YNB, 0.4 $\text{mg}\cdot\text{L}^{-1}$ D(+)-biotin, 0.1 M potassium phosphate buffer, pH 6.0) and three times with 50 μL BMM10 (5% (v/v) methanol, 13.4 $\text{g}\cdot\text{L}^{-1}$ YNB, 0.4 $\text{mg}\cdot\text{L}^{-1}$ D(+)-biotin, 0.1 M potassium phosphate buffer, pH 6.0) per well 12 h, 24 h and 36 h after the first addition of BMM2. Induction with the methanol containing media BMM2 and BMM10 induced the production of HRP which was under control of the *AOX1* promoter. The respective HRP production strains were designated *PpMutS*^{HRP} and *PpFWK3*^{HRP}.

Small scale cultivations were performed in 0.5 L Ultra Yield Flasks (BioSilta, Finland) in 45 mL iron-supplemented BMD1%. After approximately 60 h, 5 mL BMM10 were added. Twelve hours and 36 h after the first induction pulse, 0.5 mL pure methanol were added. Twentyfour hours and 48 h after the first induction pulse, 0.25 mL pure methanol were added. HRP activity in the supernatant was determined by mixing 15 μL of culture supernatant with 140 μL of assay solution (1 mM ABTS, 0.8 mM H₂O₂, 50 mM NaOAc buffer, pH 4.5) and following the increase in absorbance at 405 nm in a Spectramax Plus 384 platerader (Molecular Devices, Germany) at room temperature for 3 min. Promising clones were streaked to single colonies and cultivated again in quadruplicates for rescreening. The copy number of the HRP gene in selected *PpMutS* and *PpFWK3* transformant strains was determined via quantitative real-time PCR according to a protocol of Abad *et al.*⁴⁸ and as described previously in²⁶.

Bioreactor cultivations. Four different *P. pastoris* strains (Table 6) were characterized in terms of physiology, biomass growth and productivity by a novel, dynamic strategy of conducting methanol pulses during batch cultivations in the controlled environment of a bioreactor, which we have described recently^{16,24,26}.

Culture media. Yeast nitrogen base medium (YNBM): 20 $\text{g}\cdot\text{L}^{-1}$ $\alpha\text{-D}(+)\text{-glucose}$ monohydrate, 3.4 $\text{g}\cdot\text{L}^{-1}$ YNB2, 10 $\text{g}\cdot\text{L}^{-1}$ (NH₄)₂SO₄, 0.4 $\text{g}\cdot\text{L}^{-1}$ D(+)-biotin, 0.1 M potassium phosphate buffer, pH 6.0.

Trace element solution (PTM1): 6 $\text{g}\cdot\text{L}^{-1}$ CuSO₄·5H₂O, 0.08 $\text{g}\cdot\text{L}^{-1}$ NaI, 3 $\text{g}\cdot\text{L}^{-1}$ MnSO₄·H₂O, 0.2 $\text{g}\cdot\text{L}^{-1}$ Na₂MoO₄·2H₂O, 0.02 $\text{g}\cdot\text{L}^{-1}$ H₃BO₃, 0.5 $\text{g}\cdot\text{L}^{-1}$ CoCl₂, 20 $\text{g}\cdot\text{L}^{-1}$ ZnCl₂, 65 $\text{g}\cdot\text{L}^{-1}$ FeSO₄·7H₂O, 0.2 $\text{g}\cdot\text{L}^{-1}$ D(+)-biotin, 5 mL·L⁻¹ 95–98% H₂SO₄.

Basal salt medium (BSM): 44 $\text{g}\cdot\text{L}^{-1}$ $\alpha\text{-D}(+)\text{-glucose}$ monohydrate, 1.17 $\text{g}\cdot\text{L}^{-1}$ CaSO₄·2H₂O, 18.2 $\text{g}\cdot\text{L}^{-1}$ K₂SO₄, 14.9 $\text{g}\cdot\text{L}^{-1}$ MgSO₄·7H₂O, 4.13 $\text{g}\cdot\text{L}^{-1}$ KOH, 26.7 mL·L⁻¹ 85% (v/v) o-phosphoric acid, 0.2 mL·L⁻¹ Antifoam Struktol J650, 4.35 mL·L⁻¹ PTM1, NH₄OH as N-source (see experimental procedure).

Base: NH₄OH, concentration was determined by titration with 0.25 M potassium hydrogen phthalate.

Pre-culture. Frozen stocks (−80°C) of either *PpMutS*^{HRP} and *PpFWK3*^{HRP} were pre-cultivated in 100 mL of YNBM in 1 L shake flasks at 30°C and 230 rpm for max. 24 h. The pre-culture was transferred aseptically to the respective culture vessel. The inoculation volume was 10% of the final starting volume.

Batch cultivation. Batch cultivations were carried out in a 3 L working volume Labfors glass bioreactor (Infors, Switzerland). BSM was sterilized in the bioreactor and pH was adjusted to pH 5.0 by using concentrated ammonia solution after autoclaving. Sterile filtered PTM1 was transferred to the reactor aseptically. Dissolved oxygen (dO₂) was measured with a sterilizable polarographic dissolved oxygen electrode (Mettler Toledo, Switzerland). The pH was measured with a sterilizable electrode (Mettler Toledo, Switzerland) and maintained constant with a step controller using 2.5 M ammonia solution. Base consumption was determined gravimetrically. Cultivation temperature was set to 30°C and agitation was fixed to 1495 rpm. The culture was aerated with 2.0 vvm dried air and offgas of the culture was measured by using an infrared cell for CO₂ and a paramagnetic cell for O₂ concentration (Servomax, Switzerland). Temperature, pH, dO₂, agitation as well as CO₂ and O₂ in the offgas were measured online and logged in a process information management system (PIMS Lucullus; Biospectra, Switzerland).

Table 6 | *P. pastoris* strains used for biotechnological characterisation during bioreactor cultivations

strain	name
<i>P. pastoris</i> Mut ^S	<i>PpMutS</i>
<i>P. pastoris</i> Mut ^S HRP	<i>PpMutS</i> ^{HRP}
<i>P. pastoris</i> Mut ^S och1	<i>PpFWK3</i>
<i>P. pastoris</i> Mut ^S och1 HRP	<i>PpFWK3</i> ^{HRP}

After the complete consumption of the substrate glucose, which was indicated by an increase of dO₂ and a drop in offgas activity, the first methanol pulse (adaptation pulse) of a final concentration of 0.5% (v/v) was conducted with methanol supplemented with PTM1 (12 mL PTM1 per 1 L of methanol). Subsequently, between five and seven pulses were performed with 1% or 2% (v/v) methanol for each strain. For each pulse, at least two samples were taken to determine the concentrations of the substrate methanol and product as well as dry cell weight (DCW) and OD₆₀₀ to calculate the strain specific parameters. The induction period for *PpMutS*^{HRP} and *PpFWK3*^{HRP} was carried out in the presence of 1 mM of the heme precursor δ -aminolevulinic acid.

Analysis of growth- and expression-parameters. DCW was determined by centrifugation of 5 mL culture broth (4,000 \times g, 10 min, 4°C), washing the pellet with 5 mL deionized water and subsequent drying at 105°C to a constant weight in an oven. OD₆₀₀ of the culture broth was measured using a spectrophotometer (Genesys 20; Thermo Scientific, Austria). The activity of HRP was determined using a CubiAn XC enzymatic robot (Innovatis, Germany). Cell free samples (10 μL) were added to 140 μL of 1 mM ABTS in 50 mM potassium phosphate buffer, pH 6.5. The reaction mixture was incubated at 37°C and was started by the addition of 20 μL of 0.075% H₂O₂. Changes of absorbance at 415 nm were measured for 80 s and rates were calculated. Calibration was done using commercially available horseradish peroxidase (Type VI-A, Sigma-Aldrich, Austria, P6782, Lot# 118K76734) as standard at six different concentrations (0.02; 0.05; 0.1; 0.25; 0.5 and 1.0 U·mL⁻¹). Protein concentrations were determined at 595 nm using the Bradford Protein Assay Kit (Bio-Rad Laboratories GmbH, Austria) with bovine serum albumin as standard.

Substrate concentrations. Concentration of methanol was determined in cell free samples by HPLC (Agilent Technologies, USA) equipped with a Supelcoguard column, a Supelcogel C-610H ion-exchange column (Sigma-Aldrich, Austria) and a refractive index detector (Agilent Technologies, USA). The mobile phase was 0.1% H₃PO₄ with a constant flow rate of 0.5 mL·min⁻¹ and the system was run isocratically. Calibration was done by measuring standard points in the range of 0.1 to 10 $\text{g}\cdot\text{L}^{-1}$ methanol.

Data analysis. Strain characteristic parameters were determined at a carbon dioxide evolution rate (CER) above 2.5 mmol·L⁻¹·h⁻¹ during each methanol pulse. Measurements of biomass, product and substrate concentration were executed in duplicates. Along the observed standard deviation for the single measurement, the error was propagated to the specific rates q_s and q_p as well as to the yield coefficients. The error of determination of the specific rates and the yields was therefore set to 10% and 5%, respectively^{16,24}.

Enzyme purification. Size exclusion chromatography. The supernatants from *PpMutS*^{HRP} and *PpFWK3*^{HRP} produced in small scale cultures in 0.5 L Ultra Yield Flasks were concentrated to approximately 500 μL each using Vivaspin 20 tubes (Sartorius Stedim Biotech, Germany) with 10 kDa MWCO and recovered from the tubes resulting in a volume of max. 1500 μL , prior to size exclusion chromatography (SEC) on a HiLoad™ 16/60 Superdex 200 prep grade column (GE Healthcare Europe, Austria). SEC was performed at a flow rate of approximately 9 cm·h⁻¹, fractions of 1.2 mL were collected and assayed for HRP activity using ABTS as substrate.

2-step purification protocol. To purify the secreted HRP produced in bioreactor cultivations, the fermentation broths were harvested and centrifuged (4,000 \times g, 20 min) and the cell free supernatants were subjected to diafiltration with buffer (500 mM NaCl, 20 mM NaOAc, pH 6.0) for a subsequent purification step via a mixed mode resin (hydrophobic charge induction chromatography, HCIC) followed by a size exclusion step (SEC). We have recently described this 2-step flowthrough based strategy for the HRP isoenzyme C1A²⁷. The catalytic activity and the protein content in all fractions were determined, active fractions were pooled and concentrated via ultrafiltration to approximately 3 mg·mL⁻¹ for HRP produced in *PpMutS*^{HRP} and 0.3 mg·mL⁻¹ for HRP produced in *PpFWK3*^{HRP} for subsequent enzyme characterization.

Enzyme characterization. The two HRP preparations produced in either *PpMutS*^{HRP} or in *PpFWK3*^{HRP} were characterized to determine differences between the hypermannosylated HRP from *PpMutS*^{HRP} and its glycovariant produced in *PpFWK3*^{HRP}.



Liquid chromatography-mass spectrometry (LC-MS) analysis. Protein N-glycosylation was analyzed by releasing the N-glycans with peptide:N-glycosidase F (Roche, Mannheim). The released N-glycans were desalted and analyzed using a porous graphitic carbon capillary column (ThermoScientific) coupled to a mass spectrometer (Maxis 4 G, Bruker, Bremen). Deviating from previous work⁴⁹, glycans were not reduced and a steep gradient was applied leading to the elution of all glycans within approximately 2 min.

Kinetic constants with ABTS. Protein concentrations of the HRP preparations were determined at 595 nm using the Bradford Protein Assay Kit (Bio-Rad Laboratories GmbH, Austria) with bovine serum albumin as standard. The kinetic constants for ABTS were determined for both HRP glycovariants. The reaction was started by adding 10 μ L enzyme solution (3 $\text{mg} \cdot \text{mL}^{-1}$ HRP from PpMutS^{HRP} and 0.3 $\text{mg} \cdot \text{mL}^{-1}$ HRP from PpFWK3^{HRP}) to 990 μ L reaction buffer containing ABTS in varying concentrations (0.01–10 mM), 1 mM H₂O₂ and 50 mM potassium phosphate, pH 6.5. The change in absorbance at 420 nm was recorded in a spectrophotometer UV-1601 (Shimadzu, Japan) at 30°C controlled with a temperature controller (CPS controller 240 A; Shimadzu, Japan). Absorption curves were recorded with a software program (UVPC Optional Kinetics; Shimadzu, Japan). Measurements were performed in triplicates.

Thermal stability. Both enzyme solutions were incubated at 60°C for 1 h. At different time points, aliquots were withdrawn, the solutions were immediately cooled and centrifuged (20,000 \times g, 15 min) to pellet precipitated proteins and the remaining catalytic activity in the supernatants was measured²⁸.

- Hasslacher, M. *et al.* High-level intracellular expression of hydroxynitrile lyase from the tropical rubber tree *Hevea brasiliensis* in microbial hosts. *Protein Expr. Purif.* **11**, 61–71 (1997).
- Werten, M. W., van den Bosch, T. J., Wind, R. D., Mooibroek, H. & de Wolf, F. A. High-yield secretion of recombinant gelatins by *Pichia pastoris*. *Yeast* **15**, 1087–1096 (1999).
- Jahic, M., Rotticci-Mulder, J. C., Martinelle, M., Hult, K. & Enfors, S.-O. Modeling of growth and energy metabolism of *Pichia pastoris* producing a fusion protein. *Bioprocess Biosyst. Eng.* **24**, 385–393 (2002).
- Lin-Cereghino, G. P., Lin-Cereghino, J., Ilgen, C. & Cregg, J. M. Production of recombinant proteins in fermenter cultures of the yeast *Pichia pastoris*. *Curr. Opin. Biotechnol.* **13**, 329–332 (2002).
- Parekh, R. B. Effects of glycosylation on protein function. *Curr. Opin. Struct. Biol.* **1**, 750–754 (1991).
- Ryckaert, S., Martens, V., De Vusser, K. & Contreras, R. Development of a *S. cerevisiae* whole cell biocatalyst for in vitro sialylation of oligosaccharides. *J. Biotechnol.* **119**, 379–388 (2005).
- Wildt, S. & Gerngross, T. U. The humanization of N-glycosylation pathways in yeast. *Nat. Rev. Microbiol.* **3**, 119–128 (2005).
- Hamilton, S. R. & Gerngross, T. U. Glycosylation engineering in yeast: the advent of fully humanized yeast. *Curr. Opin. Biotechnol.* **18**, 387–392 (2007).
- De Pourcq, K., De Schutter, K. & Callewaert, N. Engineering of glycosylation in yeast and other fungi: current state and perspectives. *Appl. Microbiol. Biotechnol.* **87**, 1617–1631 (2010).
- Vervecken, W. *et al.* In vivo synthesis of mammalian-like, hybrid-type N-glycans in *Pichia pastoris*. *Appl. Environ. Microbiol.* **70**, 2639–2646 (2004).
- Nagasu, T. *et al.* Isolation of new temperature-sensitive mutants of *Saccharomyces cerevisiae* deficient in mannose outer chain elongation. *Yeast* **8**, 535–547 (1992).
- Nakayama, K., Nagasu, T., Shimma, Y., Kuromitsu, J. & Jigami, Y. OCH1 encodes a novel membrane bound mannosyltransferase: outer chain elongation of asparagine-linked oligosaccharides. *EMBO J.* **11**, 2511–2519 (1992).
- Choi, B.-K. *et al.* Use of combinatorial genetic libraries to humanize N-linked glycosylation in the yeast *Pichia pastoris*. *Proc. Natl. Acad. Sci. U.S.A.* **100**, 5022–5027 (2003).
- Mille, C. *et al.* Identification of a new family of genes involved in beta-1,2-mannosylation of glycans in *Pichia pastoris* and *Candida albicans*. *J. Biol. Chem.* **283**, 9724–9736 (2008).
- Veitch, N. C. Horseradish peroxidase: a modern view of a classic enzyme. *Phytochemistry* **65**, 249–259 (2004).
- Dietzsch, C., Spadiut, O. & Herwig, C. A dynamic method based on the specific substrate uptake rate to set up a feeding strategy for *Pichia pastoris*. *Microb. Cell Fact.* **10**, 14–22 (2011).
- Morawski, B. *et al.* Functional expression of horseradish peroxidase in *Saccharomyces cerevisiae* and *Pichia pastoris*. *Protein Eng.* **13**, 377–384 (2000).
- Näätsaari, L. *et al.* Deletion of the *Pichia pastoris* KU70 homologue facilitates platform strain generation for gene expression and synthetic biology. *PLoS ONE* **7**, e39720 (2012).
- Zhou, J., Zhang, H., Liu, X., Wang, P. G. & Qi, Q. Influence of N-glycosylation on *Saccharomyces cerevisiae* morphology: a golgi glycosylation mutant shows cell division defects. *Curr. Microbiol.* **55**, 198–204 (2007).
- Lee, B. N. & Elion, E. A. The MAPKKK Ste11 regulates vegetative growth through a kinase cascade of shared signaling components. *Proc. Natl. Acad. Sci. U.S.A.* **96**, 12679–12684 (1999).
- Non-Conventional Yeasts In Genetics, Biochemistry And Biotechnology.* (Springer Berlin Heidelberg, 2003). doi:10.1007/978-3-642-55758-3.
- Shibuya, N., Goldstein, I. J., Van Damme, E. J. & Peumans, W. J. Binding properties of a mannose-specific lectin from the snowdrop (*Galanthus nivalis*) bulb. *J. Biol. Chem.* **263**, 728–734 (1988).
- Fouquaert, E. *et al.* Related lectins from snowdrop and maize differ in their carbohydrate-binding specificity. *Biochem. Biophys. Res. Commun.* **380**, 260–265 (2009).
- Dietzsch, C., Spadiut, O. & Herwig, C. A fast approach to determine a fed batch feeding profile for recombinant *Pichia pastoris* strains. *Microb. Cell Fact.* **10**, 85–94 (2011).
- Zalai, D., Dietzsch, C., Herwig, C. & Spadiut, O. A dynamic fed batch strategy for a *Pichia pastoris* mixed feed system to increase process understanding. *Biotechnol. Prog.* **28**, 878–886 (2012).
- Krainer, F. W. *et al.* Recombinant protein expression in *Pichia pastoris* strains with an engineered methanol utilization pathway. *Microb. Cell Fact.* **11**, 22–35 (2012).
- Spadiut, O., Rossetti, L., Dietzsch, C. & Herwig, C. Purification of a recombinant plant peroxidase produced in *Pichia pastoris* by a simple 2-step strategy. *Protein Expr. Purif.* **86**, 89–97 (2012).
- Spadiut, O. *et al.* Improving thermostability and catalytic activity of pyranose 2-oxidase from *Trametes multicolor* by rational and semi-rational design. *FEBS J.* **276**, 776–792 (2009).
- Chen, Z. *et al.* Enhancement of the gene targeting efficiency of non-conventional yeasts by increasing genetic redundancy. *PLoS ONE* **8**, e57952 (2013).
- Cabib, E. & Bowers, B. Chitin and yeast budding. Localization of chitin in yeast bud scars. *J. Biol. Chem.* **246**, 152–159 (1971).
- Chen, C. *et al.* A high-throughput screening system for genes extending life-span. *Exp. Gerontol.* **38**, 1051–1063 (2003).
- Chaudhari, R. D., Stenson, J. D., Overton, T. W. & Thomas, C. R. Effect of bud scars on the mechanical properties of *Saccharomyces cerevisiae* cell walls. *Chem. Eng. Sci.* **84**, 188–196 (2012).
- Lesage, G. & Bussey, H. Cell wall assembly in *Saccharomyces cerevisiae*. *Microbiol. Mol. Biol. Rev.* **70**, 317–343 (2006).
- De Groot, P. W. J., Ram, A. F. & Klis, F. M. Features and functions of covalently linked proteins in fungal cell walls. *Fungal Genet. Biol.* **42**, 657–675 (2005).
- Klis, F. M., Boorsma, A. & De Groot, P. W. J. Cell wall construction in *Saccharomyces cerevisiae*. *Yeast* **23**, 185–202 (2006).
- Kapteyn, J. C. *et al.* Altered extent of cross-linking of beta1,6-glucosylated mannoproteins to chitin in *Saccharomyces cerevisiae* mutants with reduced cell wall beta1,3-glucan content. *J. Bacteriol.* **179**, 6279–6284 (1997).
- Maupin, K. A., Liden, D. & Haab, B. B. The fine specificity of mannose-binding and galactose-binding lectins revealed using outlier motif analysis of glycan array data. *Glycobiology* **22**, 160–169 (2012).
- Hirayama, H. & Suzuki, T. Metabolism of free oligosaccharides is facilitated in the och1D mutant of *Saccharomyces cerevisiae*. *Glycobiology* **21**, 1341–1348 (2011).
- Nakanishi-Shindo, Y., Nakayama, K., Tanaka, A., Toda, Y. & Jigami, Y. Structure of the N-linked oligosaccharides that show the complete loss of alpha-1,6-polymannose outer chain from och1, och1 mnn1, and och1 mnn1 alg3 mutants of *Saccharomyces cerevisiae*. *J. Biol. Chem.* **268**, 26338–26345 (1993).
- Jacobs, P. P. *et al.* *Pichia* surface display: display of proteins on the surface of glycoengineered *Pichia pastoris* strains. *Biotechnol. Lett.* **30**, 2173–2181 (2008).
- Current Protocols In Molecular Biology.* (John Wiley & Sons, Inc., 2001). doi:10.1002/0471142727.
- Küberl, A. *et al.* High-quality genome sequence of *Pichia pastoris* CBS7435. *J. Biotechnol.* **154**, 312–320 (2011).
- Harju, S., Fedosyuk, H. & Peterson, K. R. Rapid isolation of yeast genomic DNA: Bust n' Grab. *BMC Biotechnol.* **4**, 8–13 (2004).
- Lin-Cereghino, J. *et al.* Condensed protocol for competent cell preparation and transformation of the methylotrophic yeast *Pichia pastoris*. *BioTechniques* **38**, 44–48 (2005).
- Gibson, D. G. *et al.* Enzymatic assembly of DNA molecules up to several hundred kilobases. *Nat. Methods* **6**, 343–345 (2009).
- Abad, S. *et al.* Stepwise engineering of a *Pichia pastoris* D-amino acid oxidase whole cell catalyst. *Microb. Cell Fact.* **9**, 24–35 (2010).
- Weis, R. *et al.* Reliable high-throughput screening with *Pichia pastoris* by limiting yeast cell death phenomena. *FEMS Yeast Res.* **5**, 179–89 (2004).
- Abad, S. *et al.* Real-time PCR-based determination of gene copy numbers in *Pichia pastoris*. *Biotechnol. J.* **5**, 413–420 (2010).
- Pabst, M. *et al.* Isomeric analysis of oligomannosidic N-glycans and their dolichol-linked precursors. *Glycobiology* **22**, 389–399 (2012).
- Nett, J. H. *et al.* A combinatorial genetic library approach to target heterologous glycosylation enzymes to the endoplasmic reticulum or the Golgi apparatus of *Pichia pastoris*. *Yeast* **28**, 237–252 (2011).
- Hamilton, S. R. *et al.* Production of complex human glycoproteins in yeast. *Science* **301**, 1244–1246 (2003).
- Jacobs, P. P., Geysens, S., Vervecken, W., Contreras, R. & Callewaert, N. Engineering complex-type N-glycosylation in *Pichia pastoris* using GlycoSwitch technology. *Nat. Protoc.* **4**, 58–70 (2009).
- Hamilton, S. R. *et al.* Humanization of yeast to produce complex terminally sialylated glycoproteins. *Science* **313**, 1441–1443 (2006).



54. Hopkins, D. *et al.* Elimination of β -mannose glycan structures in *Pichia pastoris*. *Glycobiology* **21**, 1616–1626 (2011).

Acknowledgments

The authors are very grateful to the Austrian Science Fund (FWF): project P24861-B19 and FWF W901 DK Molecular Enzymology for financial support. We would also like to thank Michaela Gerstmann, Astrid Weninger and Karl Metzger for excellent technical assistance in the lab and Daniel Maresch for excellent assistance with LC-MS.

Author contributions

F.W.K. and O.S. conceived of and planned the study. F.W.K., C.G., L.N., M.W., R.P. and O.S. conducted the different experiments. C.H., A.G. and F.A. supervised parts of the research. F.W.K. and O.S. wrote the paper.

Additional information

Supplementary information accompanies this paper at <http://www.nature.com/scientificreports>

Competing financial interests: The authors declare no competing financial interests.

How to cite this article: Krainer, F.W. *et al.* Knockout of an endogenous mannosyltransferase increases the homogeneity of glycoproteins produced in *Pichia pastoris*. *Sci. Rep.* **3**, 3279; DOI:10.1038/srep03279 (2013).



This work is licensed under a Creative Commons Attribution 3.0 Unported license. To view a copy of this license, visit <http://creativecommons.org/licenses/by/3.0>

- Chapter 4 -

Optimizing cofactor availability for the production of recombinant heme peroxidase in *Pichia pastoris*

Florian W. Krainer^{1*}, Simona Capone^{2*}, Martin Jäger², Thomas Vogl¹, Michaela Gerstmann¹, Anton Glieder¹, Christoph Herwig², Oliver Spadiut^{2§}

¹ Graz University of Technology, Institute of Molecular Biotechnology, Graz, Austria

² Vienna University of Technology, Institute of Chemical Engineering, Research Area Biochemical Engineering, Vienna, Austria

* these authors contributed equally

[§] Corresponding Author: Oliver Spadiut, Vienna University of Technology, Institute of Chemical Engineering, Research Area Biochemical Engineering, Gumpendorfer Strasse 1a, A-1060 Vienna, Austria. Tel: +43 1 58801 166473, Fax: +43 1 58801 166980; e-mail: oliver.spadiut@tuwien.ac.at

TECHNICAL NOTES

Open Access

Optimizing cofactor availability for the production of recombinant heme peroxidase in *Pichia pastoris*

Florian W Krainer^{1†}, Simona Capone^{2†}, Martin Jäger², Thomas Vogl¹, Michaela Gerstmann¹, Anton Glieder¹, Christoph Herwig² and Oliver Spadiut^{2*}

Abstract

Background: Insufficient incorporation of heme is considered a central impeding cause in the recombinant production of active heme proteins. Currently, two approaches are commonly taken to overcome this bottleneck; metabolic engineering of the heme biosynthesis pathway in the host organism to enhance intracellular heme production, and supplementation of the growth medium with the desired cofactor or precursors thereof to allow saturation of recombinantly produced apo-forms of the target protein. In this study, we investigated the effect of both, pathway engineering and medium supplementation, to optimize the recombinant production of the heme protein horseradish peroxidase in the yeast *Pichia pastoris*.

Results: In contrast to studies with other hosts, co-overexpression of genes of the endogenous heme biosynthesis pathway did not improve the recombinant production of active heme protein. However, medium supplementation with hemin proved to be an efficient strategy to increase the yield of active enzyme, whereas supplementation with the commonly used precursor 5-aminolevulinic acid did not affect target protein yield.

Conclusions: The yield of active recombinant heme peroxidase from *P. pastoris* can be easily enhanced by supplementation of the cultivation medium with hemin. Thereby, secreted apo-species of the target protein are effectively saturated with cofactor, maximizing the yield of target enzyme activity.

Keywords: *Pichia pastoris*, Recombinant protein production, Plant peroxidase, Horseradish peroxidase, Metabolic engineering, Cofactor, Heme, Heme biosynthesis, Apo-protein

Background

The methylotrophic yeast *Pichia pastoris* is a valuable host for the recombinant production of complex proteins. A considerable number of these proteins requires cofactors, amongst others heme, to form active biocatalysts. Heme biosynthesis (Figure 1) is tightly regulated and highly conserved throughout evolution [1-3].

To deepen our understanding on pathway regulation and improve cofactor availability for recombinant heme proteins, metabolic engineering of the heme biosynthesis pathway has been performed in *Aspergillus niger* [4,5], *Escherichia coli* [6] and *Saccharomyces cerevisiae* [7-9]. Despite the high conservation of the heme biosynthesis

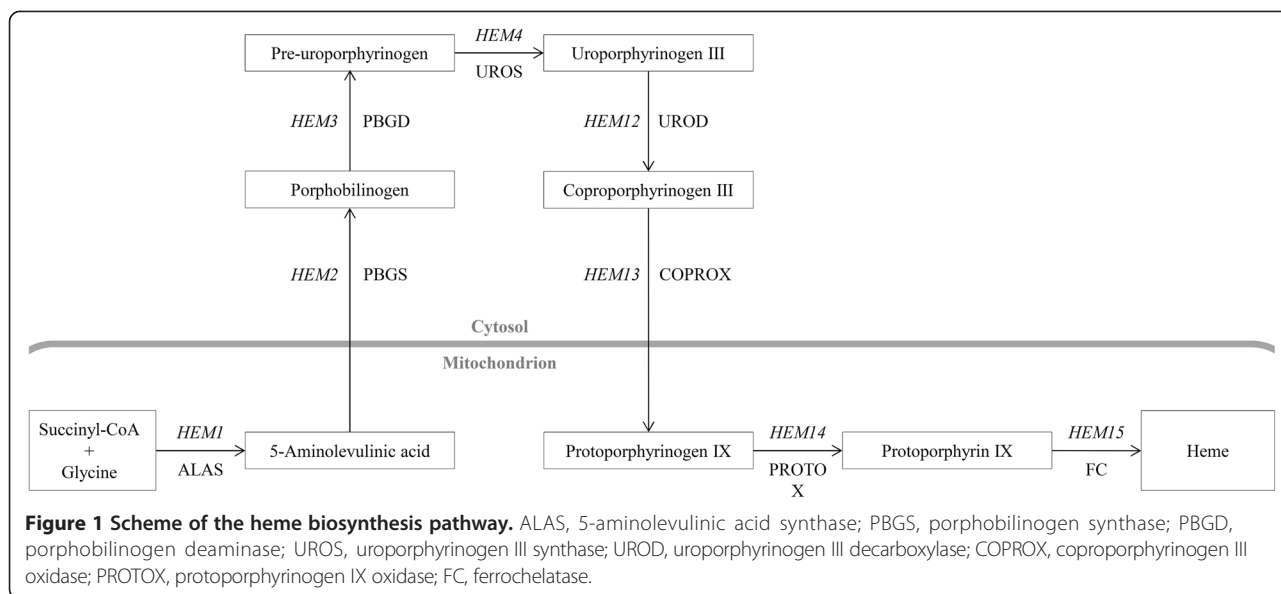
pathway, distinct differences were found among the different species. In *E. coli*, formation of 5-aminolevulinic acid (ALA) by the *HEM1*-encoded ALA synthase was described as rate-limiting step [10], whereas in *S. cerevisiae* the *HEM2*- and *HEM3*-encoded porphobilinogen synthase and deaminase, respectively, were described as rate-limiting [7]. Based thereon, overexpression of *HEM3* alone or in combination with *HEM2* and *HEM12* was described to be a valuable strategy to augment the production of recombinant heme proteins in *S. cerevisiae* [9,11]. Despite these promising results, there are some potential pitfalls connected to metabolic pathway engineering, such as the additional metabolic burden upon overexpression of multiple genes as well as an accumulation of free intracellular porphyrin intermediates which can lead to the formation of reactive oxygen species [12]. Thus, medium supplementation with iron, heme precursors or hemin (the ferric chloride species of heme) was assessed as alternative

* Correspondence: oliver.spadiut@tuwien.ac.at

†Equal contributors

²Vienna University of Technology, Institute of Chemical Engineering, Research Area Biochemical Engineering, Gumpendorfer Strasse 1a, 1060 Vienna, Austria

Full list of author information is available at the end of the article



strategy to effectively saturate recombinant apo-species of heme proteins [13-17].

In this study, we aimed at optimizing heme availability and thus boost the amount of recombinant active heme protein, namely horseradish peroxidase (HRP), in the yeast *P. pastoris* by evaluating pathway engineering and medium supplementation. In a systematic approach, we co-overexpressed HRP with genes of the endogenous heme biosynthesis pathway of *P. pastoris*, and assessed the effect of medium supplementation with iron, ALA and hemin on the yield of target enzyme activity.

Results and discussion

Heme biosynthesis pathway in *Pichia pastoris*

The heme biosynthesis pathway of several organisms has been described before and was found to be highly conserved [1-3]. Based on the *HEM* gene sequences from *S. cerevisiae*, we identified the corresponding homologs

in the partially annotated genome of *P. pastoris* [18] *in silico* (Table 1). Sanger sequencing confirmed the correct nucleotide sequences of *HEM1*, *HEM2*, *HEM3*, *HEM4*, *HEM12*, *HEM13* and *HEM14*. For *HEM15*, nucleotide 918 was G in the GenBank database entries of the published genomes of *P. pastoris* strains CBS 7435 and GS155, but T in the Sanger-sequenced CBS 7435 *P. pastoris* strain used in the present study (Additional file 1). However, this single nucleotide polymorphism only resulted in a silent mutation and did not alter the amino acid sequence of the encoded protoheme ferro-lyase.

Co-overexpression of *HEM* genes in microscale cultivations

In a recent study it was shown that metabolic engineering of the heme biosynthesis pathway allowed higher yields of active recombinant heme protein in *S. cerevisiae* [11]. Thus, we co-overexpressed either of the eight involved

Table 1 *In silico* identification of *HEM* homologs in *P. pastoris*

<i>S. cerevisiae</i>	<i>P. pastoris</i>			Sequence identity [%]
Gene annotation	Gene annotation	Chromosome	COG annotation	
<i>HEM1</i>	<i>HEM1</i>	II	5-aminolevulinate synthase	67.7
<i>HEM2</i>	<i>HEM2</i>	IV	delta-aminolevulinic acid dehydratase	75.3
<i>HEM3</i>	<i>HEM3</i>	I	porphobilinogen deaminase	54.0
<i>HEM4</i>	<i>HEM4</i>	II	uroporphyrinogen-III synthase	42.3
<i>HEM12</i>	n/a	III	uroporphyrinogen decarboxylase	73.2
<i>HEM13</i>	<i>HEM13</i>	III	coproporphyrinogen III oxidase	65.5
<i>HEM14</i>	n/a	IV	protoporphyrinogen oxidase	33.7
<i>HEM15</i>	n/a	III	protoheme ferro-lyase (ferrochelatase)	61.2

Genes *HEM12*, *HEM14* and *HEM15* were not annotated (n/a) for *P. pastoris* CBS 7435. Their chromosomal position in the genome, eukaryotic cluster of orthologous groups (COG; [19]) annotations and identities of the encoded amino acid sequences from *S. cerevisiae* and *P. pastoris* are shown.

HEM genes (Table 1) using the strong constitutive promoter *PGAP* [20] in a *P. pastoris* strain recombinantly producing the heme protein HRP. The screenings revealed trends of co-overexpressed *HEM1* and *HEM3* to be potentially beneficial for the production of active HRP (Figure 2). Surprisingly, there also seemed to be a negative trend upon co-overexpression of *HEM4*. We hypothesize, that *HEM4* co-overexpression might have led to the accumulation of a cytotoxic intermediate, which increased intracellular stress and ultimately caused a disadvantageous production environment for HRP under the tested conditions. At this point, we did not follow up on the effects of *HEM4* co-overexpression. Since co-overexpression of eGFP as negative control did not affect HRP productivity, the observed activity-enhancing trends seen for *HEM1* and *HEM3* were considered a consequence of the co-overexpressed *HEM* gene, although the standard deviation in these experiments was high. The high standard deviations in this screening (Figure 2) were caused by the transformant-to-transformant variation typically observed for *P. pastoris* [21]. Even the transformation of a single gene results in transformants showing different expression strengths. The majority of the transformants shaping the landscape behaved similar but a few transformants showed either no expression or elevated levels, leading to high standard deviations. Supplementation of the cultivation medium with 1 mM FeSO_4 to alleviate a potential iron limitation gave comparable results to non-supplemented medium

and did not affect the observed trends upon *HEM* gene co-overexpression (data not shown).

In addition to strong constitutive co-overexpression of either *HEM1* or *HEM3* from *PGAP*, we also tested co-overexpression of these two genes from either *PAOX1* or *PCAT1*. Both promoters are strongly methanol-inducible, however *PCAT1* is already active in the absence of glucose or glycerol and then even further induced by addition of methanol, thereby allowing *HEM* co-overexpression already prior to, but also during HRP production [Vogl et al., manuscript in preparation]. In order to indirectly assess the general functionality and applicability of the employed co-overexpression construct, we measured fluorescence of the eGFP co-overexpression control transformants and found this co-overexpression partner to be successfully produced (Additional file 2). Thus, we considered the endogenous *HEM* co-overexpression partners to be co-overexpressed in a comparable fashion. Ultimately, *PAOX1*-regulated co-overexpressions of *HEM1* and *HEM3* with HRP were found most promising (Additional file 3) and the best performing strains were used for further characterizations.

Since the data from microscale cultivations indicated merely trends for potential beneficial effects of co-overexpressed *HEM1* or *HEM3*, we aimed at obtaining more reliable data from controlled cultivations of the best performing strains in bioreactors. Prior to bioreactor cultivations, the strain producing HRP alone (hereafter called benchmark

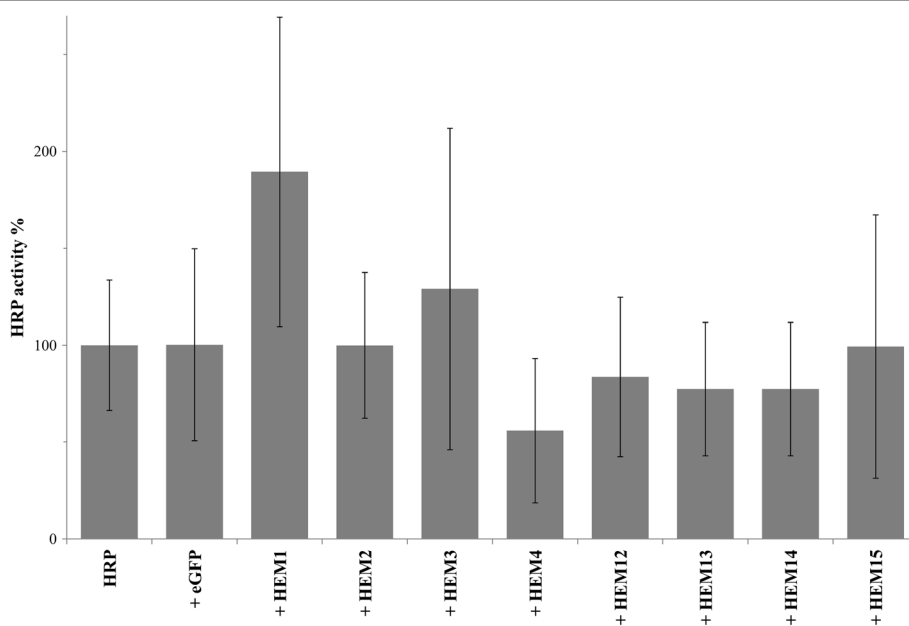


Figure 2 Co-overexpressions of *HEM* genes with HRP. HRP overexpression was regulated by *PAOX1*, co-overexpressions of eGFP and *HEM* were regulated by *PGAP*. Bars are average values of HRP production landscapes from microscale cultivations using 1 mM FeSO_4 -supplemented medium. Error bars are standard deviations from all measured clones of a landscape. Average activity from strains producing HRP alone was set to 100%.

strain) as well as the *HEM1* and *HEM3* co-overexpressing strains (hereafter called HEM1 and HEM3 strains) were characterized by quantitative real-time PCR as strains with single copy integration of the HRP gene. Since these strains contained the same HRP gene dosage, genomic rearrangement of HRP gene copy number upon transformation of a *HEM* co-overexpression construct was excluded and the strains were regarded comparable in terms of target gene dosage.

Co-overexpression of *HEM* genes in bioreactor cultivations

For physiological strain characterisation of the three yeast strains we employed a previously reported strategy of dynamic batch cultivations with methanol pulses [22-25]. The corresponding off-gas signals, specific uptake rates and yields are shown in Additional file 4. Physiological strain characteristic parameters of the three strains are summarized in Table 2. As shown in Table 2, C-balances for all cultivations closed to 1.0 indicating solid data quality. Apparently, the yeast strains were physiologically not impaired by co-overexpression of either *HEM1* or *HEM3* since adaptation time to methanol, yields and specific substrate uptake rates were comparable. However, co-overexpressing these genes did not boost the production of active HRP either. Whereas the benchmark and the HEM1 strain showed comparable production titres, the HEM3 strain even showed a 50% lower specific and volumetric productivity than the benchmark strain. Taken together, it turned out that the trends seen in microscale data could not be seen in the bioreactor. A possible explanation for these diverging findings could be found in the considerably different cultivation conditions. Microscale cultivations may challenge cell growth and productivity by phases of O₂ shortage or starvation, whereas a bioreactor provides optimal cultivation conditions.

Considering the complex and so far poorly understood regulation of heme biosynthesis, a multitude of single or combined factors may have either positive or negative effects on this pathway. Thus, additional studies will be required to unravel the regulation of heme biosynthesis, in order to allow non-speculative conclusions. Since our selection of *HEM* co-overexpression partners was based on trends from microscale cultivations, we cannot exclude,

that either of the remaining six *HEM* genes or combinations thereof might yield more beneficial results than co-overexpressed *HEM1* or *HEM3* in bioreactor cultivations. Ultimately, in contrast to analogous studies in *S. cerevisiae* [9,11], metabolic pathway engineering in *P. pastoris* did not prove to be a useful strategy to allow higher titres of recombinant active heme protein, suggesting distinct differences of this pathway between the two yeasts. However, co-overexpression of two or more *HEM* genes from a library of promoters of varying strengths might still enhance endogenous heme biosynthesis in *P. pastoris* and will be assessed in future studies.

Medium supplementation

Medium supplementation in microscale cultivations

We tested ALA, FeSO₄ and hemin as medium supplements in microscale cultivations of the benchmark strain. Supplementation with ALA at an excess concentration of 1 mM, as reported in literature [22,26,27], did not result in measurably more active product. However, addition of 1 mM FeSO₄ boosted the amount of active HRP up to 7-fold (Figure 3), hinting at a potential shortage of iron in heme biosynthesis. Upon supplementation of the minimal medium with different concentrations of hemin, we even measured 18-fold increased HRP activity compared to non-supplemented conditions. We also investigated the effect in case both, FeSO₄ and hemin, were supplemented concomitantly and observed that the beneficial effect of FeSO₄ became less pronounced with increasing concentrations of hemin (Figure 3). Apparently, as all apo-HRP was readily saturated with cofactor at a hemin concentration of 10 μM, additional excess of iron did not improve HRP activities any further and the cofactor bottleneck was opened up.

ALA supplementation in the bioreactor

We performed a comparative cultivation experiment in the bioreactor to confirm the results obtained in microscale cultivations that the commonly used supplement ALA [22,26,27] does not affect the production of a recombinant active heme protein in *P. pastoris*. We cultivated the benchmark strain in parallel dynamic batch cultivations with and without the presence of 1 mM ALA. Table 3 shows that both, strain physiology and productivity, were

Table 2 Strain characteristic physiological parameters determined for the benchmark, HEM1 and HEM3 strain

Strain	Δt_{adapt} [h]	$Y_{X/\text{MeOH}}$ [C-mol/C-mol]	$Y_{\text{CO}_2/\text{MeOH}}$ [C-mol/C-mol]	C-balance	q_{MeOH} [mmol/g/h]	q_p [U/g/h]	r_p [U/L/h]
Benchmark	8.2	0.02	1.00	1.02	0.75	1.11	37.5
HEM1	8.2	0.04	0.94	0.98	0.69	1.10	35.9
HEM3	7.9	0.03	0.93	0.96	0.70	0.49	17.1

Δt_{adapt} , time for adaptation of the culture to methanol; $Y_{X/\text{MeOH}}$, $Y_{\text{CO}_2/\text{MeOH}}$, yields of biomass or CO₂ per C-mol of substrate methanol; C-balance, sum of $Y_{X/\text{MeOH}}$ and $Y_{\text{CO}_2/\text{MeOH}}$ which ideally should result in 1.0; q_{MeOH} , average specific uptake rate of methanol during consecutive methanol pulses; q_p , specific HRP productivity; r_p , volumetric HRP productivity calculated from the point of induction until the end of cultivation.

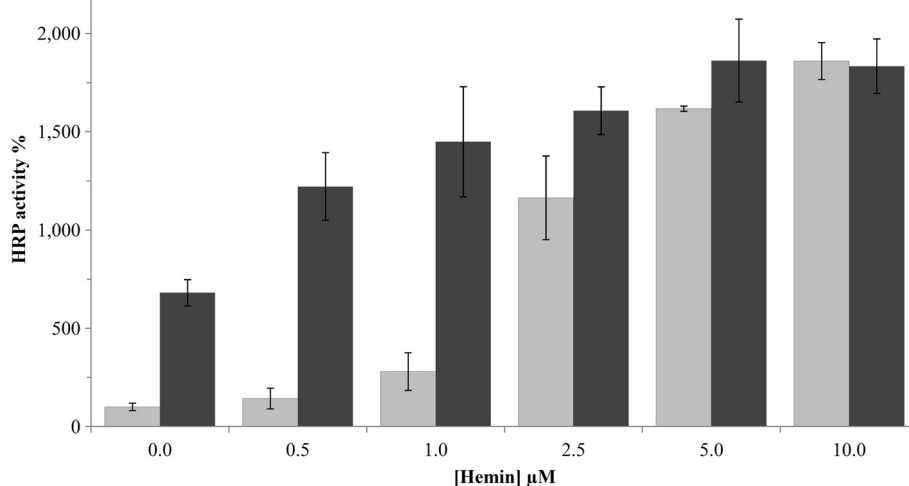


Figure 3 Effect of medium supplementation with FeSO₄ and hemin on HRP activity in microscale cultivations. Volumetric HRP activity from minimal medium without supplementation was set to 100%. Bars are average values \pm SD from independent triplicate cultivations. Light gray, no FeSO₄; dark gray, 1 mM FeSO₄.

not affected by the presence of ALA. Since the amount of active HRP was the same for both conditions, we concluded that ALA was not beneficial for the activation of the produced apo-HRP. This observation is different from what was described previously by Morawski *et al.*, where a 32% increase in HRP activity was measured in the culture supernatant after supplementation with ALA, trace elements and thiamine [17]. Thus, we speculate that the activation effect observed by Morawski *et al.* was rather caused by the addition of the iron-containing trace element solution than by ALA. Furthermore, our results conclusively showed that the intracellular production of ALA in the heme biosynthesis pathway of *P. pastoris* was not the rate limiting step in contrast to *E. coli* [10], which is also in agreement with the study of Arrese *et al.* [28].

Optimization of hemin supplementation in the bioreactor

Based on the results obtained in microscale cultivations, we supplemented the cultivation broth of three parallel dynamic batch cultivations of the benchmark strain with 0.1, 1.0 or 10.0 μ M hemin. As shown in Table 4, adaptation time, yields and uptake rates of the benchmark

strain were not affected by the presence of hemin. In terms of productivity, both the specific and the volumetric productivity were doubled at a concentration of 10.0 μ M hemin. Since the total extracellular protein content was comparable in all three cultivations, we concluded that not the productivity of the yeast was altered, but rather that the produced apo-protein was activated posttranslationally by hemin in the cultivation broth. Based on our previous experiences with this expression system [22,23,29,30], we estimated the amount of HRP in the cultivation broth to be $< 3 \mu$ M. Thus, we concluded that an excess hemin concentration is required to effectively saturate secreted apo-HRP (Table 4).

Activation studies with hemin

To prove our hypothesis of a posttranslational conversion of apo-HRP to holo-HRP by hemin, we incubated cell-free, sterile-filtered supernatant from a non-supplemented benchmark cultivation with different concentrations of hemin and analyzed activity over time. As shown in Table 5, already after 5 min of incubation a concentration dependent activation was observed and after 72 h of incubation the initial activity was even doubled. Based thereon,

Table 3 Strain specific physiological parameters of the benchmark strain with and without ALA supplementation

ALA [1 mM]	Δ time _{adapt} [h]	$Y_{X/MeOH}$ [C-mol/C-mol]	$Y_{CO_2/MeOH}$ [C-mol/C-mol]	C-balance	q_{MeOH} [mmol/g/h]	q_p [U/g/h]	r_p [U/L/h]
+	8.1	0.03	0.95	0.98	0.73	1.08	36.7
-	8.2	0.04	0.94	0.98	0.76	1.09	37.2

Δ time_{adapt}, time for adaptation of the culture to methanol; $Y_{X/MeOH}$, $Y_{CO_2/MeOH}$, yields of biomass or CO₂ per C-mol of substrate methanol; C-balance, sum of $Y_{X/MeOH}$ and $Y_{CO_2/MeOH}$ which ideally should result in 1.0; q_{MeOH} , average specific uptake rate of methanol during consecutive methanol pulses; q_p , specific HRP productivity; r_p , volumetric HRP productivity calculated from the point of induction until the end of cultivation.

Table 4 Strain characteristic physiological parameters determined for the benchmark strain cultivated in hemin-supplemented media

Hemin [μ M]	Δ time _{adapt} [h]	$Y_{X/MeOH}$ [C-mol/C-mol]	$Y_{CO_2/MeOH}$ [C-mol/C-mol]	C-balance	q_{MeOH} [mmol/g/h]	q_p [U/g/h]	r_p [U/L/h]
0.1	6.5	0.04	0.89	0.93	0.69	1.10	34.3
1.0	6.4	0.04	0.93	0.97	0.71	1.26	36.8
10.0	6.5	0.03	0.89	0.96	0.70	2.35	73.2

Δ time_{adapt}, time for adaptation of the culture to methanol; $Y_{X/MeOH}$, $Y_{CO_2/MeOH}$, yields of biomass or CO₂ per C-mol of substrate methanol; C-balance, sum of $Y_{X/MeOH}$ and $Y_{CO_2/MeOH}$ which ideally should result in 1.0; q_{MeOH} , average specific uptake rate of methanol during consecutive methanol pulses; q_p , specific HRP productivity; r_p , volumetric HRP productivity.

we concluded that hemin should be present in excess to allow effective apo-protein activation.

Conclusions

In this study we present a systematic approach to optimize heme availability and thus boost the amount of active heme protein produced in the yeast *P. pastoris* by evaluating metabolic pathway engineering and medium supplementation. The results can be summarized as:

- The heme biosynthesis pathway of *P. pastoris* was analyzed and corresponding genes were identified and annotated *in silico*.
- In contrast to previous studies, overexpression of single *HEM* genes did not result in enhanced activity or higher yield of the model heme protein HRP in bioreactor cultivations of recombinant *P. pastoris* strains. However, combinations of *HEM* genes co-overexpressed from a library of differently regulated promoters might still enhance endogenous heme biosynthesis of *P. pastoris*.
- Medium supplementation with the traditionally used and pricy heme precursor ALA did not increase the yield of active product and can be omitted in future cultivations. FeSO₄ and hemin on the other hand turned out to be useful medium supplements to increase the yield of active heme protein.
- Hemin was identified as the most effective supplement. It activated the secreted model heme protein posttranslationally in the cultivation broth and should be added in moderate excess to effectively saturate secreted apo-species of the target protein.

Table 5 Posttranslational activation of apo-HRP with hemin

Hemin [μ M]	Specific activity [U/mg] after 5 min of incubation	Specific activity [U/mg] after 72 h of incubation
-	34.8	35.3
1.0	42.4	67.0
5.0	46.8	75.4
10.0	51.8	77.8

Cell-free cultivation supernatant was incubated with the indicated concentrations of hemin and volumetric HRP activity was measured after 5 min and 72 h.

The results shown in this study present a guideline for the successful recombinant production of active heme protein in the yeast *P. pastoris* and offer an easy-to-do solution to maximize the ratio of holo- over apo-protein resulting in a considerable increase of active target protein.

Methods

Chemicals

2,2'-azino-bis(3-ethylbenzthiazoline-6-sulfonic acid) diammonium salt (ABTS), D(+)-biotin and hemin were purchased from Sigma-Aldrich (Austria). Difco™ yeast nitrogen base (YNB) w/o amino acids, Bacto™ tryptone and Bacto™ yeast extract were obtained from Becton Dickinson (Austria). Zeocin™ was obtained from InvivoGen (France). Other chemicals were obtained from Carl Roth (Germany).

Pichia pastoris strains

All strains in this study were based on the *P. pastoris* wildtype strain CBS 7435 (identical to NRRL Y-11430 and ATCC 76273). The Mut^S phenotype has been found previously to be superior over the Mut⁺ phenotype for recombinant HRP production in terms of volumetric productivity and production efficiency [24]. Hence, an *aox1* deletion strain (*PpMutS*) was used as starting strain [31]. Homologs of the *HEM* genes of *S. cerevisiae* were identified by BLAST searches [32] in the published genome sequence of *P. pastoris* CBS 7435 [18] and the sequences were verified by Sanger sequencing (Microsynth, Austria). Sequence identities of the *HEM* gene products from *S. cerevisiae* and *P. pastoris* were determined on the LALIGN server.

The HRP expression construct was based on the pPpT4_Alpha_S vector [31] where HRP C1A expression was under control of the promoter of the *AOX1* gene (*PAOX1*). Transformants were identified by Zeocin™ resistance. The *S. cerevisiae* MAT α prepro signal peptide facilitated HRP secretion. All *HEM* co-overexpression constructs were based on the plasmid pPpKan_S [32], harboring a kanamycin resistance gene for selection and the strongly methanol-inducible *PAOX1* for gene expression. Also, the promoters *PGAP* and *PCAT1* [Vogl *et al.*, manuscript in preparation] were tested for co-overexpression. Transformation of the HRP expression cassette to *PpMutS* and

of the co-overexpression constructs to the *PpMutS*-based HRP production strain (called benchmark strain) was performed as described previously [24]. All eight *HEM* genes of the heme biosynthesis pathway were co-overexpressed separately and their influence on HRP production was studied by cultivation of approximately 80 transformants per co-overexpression construct in 96-deep well plates (DWP). As negative co-overexpression control, eGFP was co-overexpressed with HRP. The copy number of the HRP gene in selected strains was determined by quantitative real-time PCR according to a previous protocol [33] and as described recently [24].

Microscale cultivations in 96-deep well plates

Microscale cultivations in 96-DWPs were performed similar to [34]: Strains were grown in 250 μ L BMD1% (11 g/L alpha-D(+)-glucose monohydrate, 13.4 g/L YNB, 0.4 mg/L D(+)-biotin, 0.1 M potassium phosphate buffer, pH 6.0) at 28°C, 320 rpm, 80% humidity. After approximately 60 h, an induction pulse of 250 μ L BMM2 (1% (v/v) methanol, 13.4 g/L YNB, 0.4 mg/L D(+)-biotin, 0.1 M potassium phosphate buffer, pH 6.0) was added, followed by three pulses of 50 μ L BMM10 (5% (v/v) methanol, 13.4 g/L YNB, 0.4 mg/L D(+)-biotin, 0.1 M potassium phosphate buffer, pH 6.0) per well 12, 24 and 36 h after the first pulse. HRP activity was determined by mixing 15 μ L supernatant with 140 μ L assay solution (1 mM ABTS, 0.9 mM H₂O₂, 50 mM sodium acetate, pH 4.5) in a microtiter plate and following the increase in absorbance at 405 nm on a Spectramax Plus 384 platereader (MolecularDevices, Germany) at room temperature. Medium supplementation studies were performed by additions of ALA, FeSO₄ and hemin to BMD1% from a 100 mM ALA stock, a 100 mM FeSO₄ stock and a 500 μ M hemin stock (in 10 mM KOH), respectively.

Bioreactor cultivations

Preculture

Precultures were grown in YNB medium (0.1 M potassium phosphate buffer, pH 6.0; 3.4 g/L YNB w/o amino acids and ammonium sulfate; 10 g/L (NH₄)₂SO₄; 400 mg/L biotin; 20 g/L glucose) in 1 L shake flasks at 30°C and 230 rpm for 24 h.

Dynamic batch cultivations

For dynamic batch cultivations, 1.8 L of double concentrated basal salt medium (BSM; 26.7 mL/L 85% phosphoric acid; 1.17 g/L CaSO₄·2H₂O; 18.2 g/L K₂SO₄; 14.9 g/L MgSO₄·7H₂O; 4.13 g/L KOH; 0.3 mL/L Antifoam Struktol J650; 60 g/L glycerol) were sterilized in 3 L bioreactor vessels (DR03F; DASGIP, Switzerland). After sterilization, 4.35 mL/L trace element solution (PTM1; 6.0 g/L CuSO₄·5H₂O; 0.08 g/L NaI; 3.0 g/L MnSO₄·H₂O; 0.2 g/L Na₂MoO₄·2H₂O; 0.02 g/L H₃BO₃; 0.5 g/L

CoCl₂; 20.0 g/L ZnCl₂; 65.0 g/L FeSO₄·7H₂O; 0.2 g/L biotin; 5 mL/L H₂SO₄) were added and pH was set to 5.0 with concentrated ammonia solution. The precultures were transferred aseptically to the respective vessel (the inoculation volume was 10%) and a batch phase on glycerol was carried out at 30°C with the stirrer fixed at 900 rpm. Aeration with compressed dry air was set to 1 vvm. Dissolved oxygen (dO₂) was measured with a sterilizable VisiFerm DO 225 probe (Hamilton, Switzerland) and controlled to be higher than 20%. The pH was measured with a sterilizable electrode (Mettler Toledo, Switzerland) and maintained constant at pH 5.0. Reactor weight was continuously recorded by a precision balance (Sartorius, Germany). Following complete glycerol consumption as indicated by an increase in the offgas signal, temperature was lowered to 25°C and an adaptation pulse of 0.5% (v/v) methanol (containing 4.35 mL/L PTM1) was added. After adaptation, 1.0% (v/v) methanol was pulsed repeatedly (for an example see Additional file 4). Before and after each pulse samples were taken and analyzed for OD₆₀₀, dry cell weight, HRP activity, extracellular protein content and methanol concentration.

Analysis of growth and expression parameters

Dry cell weight (DCW) was determined by centrifugation of 5 mL fermentation broth (4500 rpm, 10 min, 4°C), washing the pellet with 5 mL water and subsequent drying to a constant weight at 105°C. HRP activity in the cell-free supernatant was determined using a previously described assay [23] in a CuBiAn-XC enzymatic robot (OptoCell, Germany). Protein concentration was determined using a Bradford protein assay kit (Thermo Scientific, USA). All growth and protein expression parameters were determined in duplicates.

Analysis of substrate concentration

Methanol concentration in the cell-free supernatant was determined by HPLC as described previously [22]. Glycerol concentration was measured from cell-free samples in the CuBiAn-XC enzymatic robot. The device was calibrated with water-diluted glycerol standards ranging from 0 to 0.25 g/L. Samples with higher glycerol concentrations were automatically diluted by the system.

Calculation of strain physiological characteristics

Physiologically relevant parameters for characterization of the different yeast strains cultivated at different conditions and for quantification of the bioprocess were: Carbon dioxide evolution rate (CER; mmol/L/h), biomass yield ($Y_{X/MeOH}$; C-mol/C-mol), carbon dioxide yield ($Y_{CO_2/MeOH}$; C-mol/C-mol), C-balance, specific methanol uptake rate (q_{MeOH} ; mmol/g/h), specific productivity (q_p ; U/g/h), volumetric productivity (r_p ; U/L/h), specific activity (U/mg). All details on the calculation of these parameters have been published previously [34].

Additional files

Additional file 1: *Pichia pastoris* CBS 7435 HEM open reading frames. The single nucleotide polymorphism of *HEM15*, T918, is marked in grey.

Additional file 2: Co-overexpression of eGFP from PAOX1. The principal applicability of the employed co-overexpression construct is demonstrated indirectly by eGFP fluorescence of the strains co-overexpressing HRP and eGFP. The first two bars represent the starting strain, *PpMutS*, and the benchmark strain as controls. Fluorescence was determined at ex/em 488/507 nm, and normalized to the OD600 to account for potential growth differences.

Additional file 3: Co-overexpressions of HRP with either HEM1 or HEM3 from either PAOX1 or PCAT1. 1, co-overexpression of *HEM1* or *HEM3* from *PAOX1*; 2, co-overexpression of *HEM1* or *HEM3* from *PCAT1*. White bars, eGFP co-overexpression control; black bars, *HEM1* co-overexpression; gray bars, *HEM3* co-overexpression. The benchmark strain was included in all cultivations and set to 100% as reference (first bars).

Additional file 4: Batch cultivations of three recombinant *P. pastoris* strains. 1, benchmark strain; 2, *HEM1* strain; 3, *HEM3* strain; a/c/e, CER signal (solid line) and specific methanol uptake rate (open circles); b/d/f, carbon dioxide yields ($V_{CO_2/S}$; grey squares) and biomass yields ($X_{Y/S}$; black circles).

Abbreviations

ABTS: 2,2'-azino-bis(3-ethylbenzthiazoline-6-sulfonic acid) diammonium salt; ALA: 5-aminolevulinic acid; *AOX1*: Alcohol oxidase 1 gene; CER: Carbon evolution rate; 96-DWP: 96-deep well plate; eGFP: Enhanced green fluorescent protein; HRP: Horseradish peroxidase; YNB: Difco™ yeast nitrogen base.

Competing interests

The authors declare that they have no competing interests.

Authors' contributions

FWK, SC, TV and OS designed the experiments, analyzed and interpreted the data. FWK, SC, MJ, MGE and TV performed the experiments. FWK, SC and OS wrote the manuscript. FWK, AG, CH and OS conceived of the study. AG, CH and OS supervised the research. All authors read and approved the final manuscript.

Authors' information

FWK, TV, MGE, AG: Graz University of Technology, Institute of Molecular Biotechnology, NAWI Graz, Petersgasse 14, 8010 Graz, Austria. SC, MJ, CH, OS: Vienna University of Technology, Institute of Chemical Engineering, Research Area Biochemical Engineering, Gumpendorfer Strasse 1a, 1060 Vienna, Austria.

Acknowledgements

The authors would like to acknowledge support from NAWI Graz and the Austrian Science Fund FWF (projects: P24861-B19 and W901 DK Molecular Enzymology). This research was also funded by the European Union's Seventh Framework Programme (FP7/2007-2013) under grant agreement N°266025 (<http://bionexgen-fp7.eu>).

Author details

¹Graz University of Technology, NAWI Graz, Institute of Molecular Biotechnology, Graz, Austria. ²Vienna University of Technology, Institute of Chemical Engineering, Research Area Biochemical Engineering, Gumpendorfer Strasse 1a, 1060 Vienna, Austria.

Received: 29 October 2014 Accepted: 26 December 2014

Published online: 13 January 2015

References

1. Franken ACW, Lokman BC, Ram AFJ, Punt PJ, van den Hondel CAMJJ, De Weert S. Heme biosynthesis and its regulation: towards understanding and improvement of heme biosynthesis in filamentous fungi. *Appl Microbiol Biotechnol.* 2011;91:447–60.
2. Heinemann IU, Jahn M, Jahn D. The biochemistry of heme biosynthesis. *Arch Biochem Biophys.* 2008;474:238–51.
3. Layer G, Reichelt J, Jahn D, Heinz DW. Structure and function of enzymes in heme biosynthesis. *Prot Sci.* 2010;19:1137–61.
4. Franken ACW, Lokman BC, Ram AFJ, van den Hondel CAMJJ, de Weert S, Punt PJ. Analysis of the role of the *Aspergillus niger* aminolevulinic acid synthase (*hemA*) gene illustrates the difference between regulation of yeast and fungal haem- and sirohaem-dependent pathways. *Fems Microbiol Lett.* 2012;335:104–12.
5. Franken ACW, Werner ER, Haas H, Lokman BC, van den Hondel CAMJJ, Ram AFJ, et al. The role of coproporphyrinogen III oxidase and ferrochelatase genes in heme biosynthesis and regulation in *Aspergillus niger*. *Appl Microbiol Biotechnol.* 2013;97:9773–85.
6. Li FF, Wang Y, Gong K, Wang Q, Liang QF, Qi QS. Constitutive expression of *RyhB* regulates the heme biosynthesis pathway and increases the 5-aminolevulinic acid accumulation in *Escherichia coli*. *Fems Microbiol Lett.* 2014;350:209–15.
7. Hoffman M, Gora M, Rytka J. Identification of rate-limiting steps in yeast heme biosynthesis. *Biochem Biophys Res Comm.* 2003;310:1247–53.
8. Martinez JL, Liu L, Petranovic D, Nielsen J. Engineering the oxygen sensing regulation results in an enhanced recombinant human hemoglobin production by *Saccharomyces cerevisiae*. *Biotechnol Bioeng.* 2015;118:1–8.
9. Michener JK, Nielsen J, Smolke CD. Identification and treatment of heme depletion attributed to overexpression of a lineage of evolved P450 monooxygenases. *Proc Natl Acad Sci U S A.* 2012;109:19504–9.
10. Woodard SI, Dailey HA. Regulation of heme-biosynthesis in *Escherichia coli*. *Arch Biochem Biophys.* 1995;316:110–5.
11. Liu LF, Martinez JL, Liu ZH, Petranovic D, Nielsen J. Balanced globin protein expression and heme biosynthesis improve production of human hemoglobin in *Saccharomyces cerevisiae*. *Metab Eng.* 2014;21:9–16.
12. Krishnamurthy P, Xie T, Schuetz JD. The role of transporters in cellular heme and porphyrin homeostasis. *Pharmacol Ther.* 2007;114:345–58.
13. Nishimoto M, Clark JE, Masters BSS. Cytochrome-P450-4a4 - expression in *Escherichia coli*, purification, and characterization of catalytic properties. *Biochem.* 1993;32:8863–70.
14. Conesa A, van den Hondel CAMJJ, Punt PJ. Studies on the production of fungal peroxidases in *Aspergillus niger*. *Appl Environ Microbiol.* 2000;66:3016–23.
15. Varnado CL, Goodwin DC. System for the expression of recombinant hemoproteins in *Escherichia coli*. *Prot Expr Purif.* 2004;35:76–83.
16. Segura MD, Levin G, Miranda MV, Mendive FM, Targovnik HM, Cascone O. High-level expression and purification of recombinant horseradish peroxidase isozyme C in SF-9 insect cell culture. *Process Biochem.* 2005;40:795–800.
17. Morawski B, Lin ZL, Cirino PC, Joo H, Bandara G, Arnold FH. Functional expression of horseradish peroxidase in *Saccharomyces cerevisiae* and *Pichia pastoris*. *Protein Eng.* 2000;13:377–84.
18. Kueberl A, Schneider J, Thallinger GG, Anderl I, Wibberg D, Hajek T, et al. High-quality genome sequence of *Pichia pastoris* CBS7435. *J Biotechnol.* 2011;154:312–20.
19. Tatusov RL, Fedorova ND, Jackson JD, Jacobs AR, Kiryutin B, Koonin EV, et al. The COG database: an updated version includes eukaryotes. *BMC Bioinformatics.* 2003;4:41.
20. Vogl T, Glieder A. Regulation of *Pichia pastoris* promoters and its consequences for protein production. *N Biotechnol.* 2013;30:385–404.
21. Cregg JM, Tolstorukov I, Kusari A, Sunga J, Madden K, Chappell T. Expression in the yeast *Pichia pastoris*. *Methods Enzymol.* 2009;463:169–89.
22. Dietzsch C, Spadiut O, Herwig C. A fast approach to determine a fed batch feeding profile for recombinant *Pichia pastoris* strains. *Microb Cell Fact.* 2011;10:85.
23. Dietzsch C, Spadiut O, Herwig C. A dynamic method based on the specific substrate uptake rate to set up a feeding strategy for *Pichia pastoris*. *Microb Cell Fact.* 2011;10:14.
24. Kraimer FW, Dietzsch C, Hajek T, Herwig C, Spadiut O, Glieder A. Recombinant protein expression in *Pichia pastoris* strains with an engineered methanol utilization pathway. *Microb Cell Fact.* 2012;11:22.
25. Capone S, Pletzenauer R, Maresch D, Metzger K, Altmann F, Herwig C, et al. Glyco-variant library of the versatile enzyme horseradish peroxidase. *Glycobiol.* 2014;24:852–63.
26. Jiang H, Morgan JA. Optimization of an in vivo plant P450 monooxygenase system in *Saccharomyces cerevisiae*. *Biotechnol Bioeng.* 2004;85:130–7.
27. Morawski B, Quan S, Arnold FH. Functional expression and stabilization of horseradish peroxidase by directed evolution in *Saccharomyces cerevisiae*. *Biotechnol Bioeng.* 2001;76:99–107.

28. Arrese M, Carvajal E, Robison S, Sambunaris A, Panek A, Mattoon J. Cloning of the delta-aminolevulinic acid synthase structural gene in yeast. *Curr Genet.* 1983;7:175–83.
29. Spadiut O, Dietzsch C, Herwig C. Determination of a dynamic feeding strategy for recombinant *Pichia pastoris* strains. *Methods Mol Biol.* 2014;1152:185–94.
30. Spadiut O, Zalai D, Dietzsch C, Herwig C. Quantitative comparison of dynamic physiological feeding profiles for recombinant protein production with *Pichia pastoris*. *Bioprocess Biosyst Eng.* 2013. doi:10.1007/s00449-013-1087-z.
31. Näätäsaari L, Mistlberger B, Ruth C, Hajek T, Hartner FS, Glieder A. Deletion of the *Pichia pastoris* KU70 homologue facilitates platform strain generation for gene expression and synthetic biology. *PLoS One.* 2012;7:e39720.
32. Altschul SF, Gish W, Miller W, Myers EW, Lipman DJ. Basic local alignment search tool. *J Mol Biol.* 1990;215:403–10.
33. Abad S, Kitz K, Hormann A, Schreiner U, Hartner FS, Glieder A. Real-time PCR-based determination of gene copy numbers in *Pichia pastoris*. *Biotechnol J.* 2010;5:413–20.
34. Weis R, Luiten R, Skranc W, Schwab H, Wubbolts M, Glieder A. Reliable high-throughput screening with *Pichia pastoris* by limiting yeast cell death phenomena. *Fems Yeast Res.* 2004;5:179–89.

**Submit your next manuscript to BioMed Central
and take full advantage of:**

- Convenient online submission
- Thorough peer review
- No space constraints or color figure charges
- Immediate publication on acceptance
- Inclusion in PubMed, CAS, Scopus and Google Scholar
- Research which is freely available for redistribution

Submit your manuscript at
www.biomedcentral.com/submit



- Chapter 5 -

Systematic assessment of strategies for improved production of recombinant plant peroxidase in *Pichia pastoris*

Florian W. Krainer¹, Michaela A. Gerstmann¹, Barbara Darnhofer², Ruth Birner-Grünberger² and Anton Glieder^{1*}

¹ Graz University of Technology, Institute of Molecular Biotechnology, NAWI Graz, Petersgasse 14, 8010 Graz, Austria

² Functional Proteomics Core Facility, ACIB GmbH - Austrian Centre of Industrial Biotechnology, Medical University of Graz, Austria, office: Stiftingtalstraße 24, 8010 Graz, Austria

* Corresponding author: Anton Glieder, Graz University of Technology, Institute of Molecular Biotechnology, NAWI Graz, Petersgasse 14, 8010 Graz, Austria; a.glieder@tugraz.at; Tel: +43 664 608734074; Fax: +43 316 873 4071

Abstract

Horseradish peroxidase (HRP) is a high-demand enzyme for applications in diagnostics, bioremediation, biocatalysis and medicine. Current HRP preparations are isolated from horseradish roots as mixtures of biochemically diverse isoenzymes. Thus, there is a strong need for a recombinant production process enabling a steady supply with enzyme preparations of consistent high quality. However, most current recombinant production systems are limited at yields in the low mg/L range. In this study, we used the well-known yeast *Pichia pastoris* as host for recombinant HRP production. To enhance enzyme yields we evaluated engineering approaches on the secretion process with the *Saccharomyces cerevisiae* mating factor alpha prepro signal peptide, coproduction of Pdi1 and active Hac1 to avoid potential cellular stress due to accumulating unfolded protein, and compared expression from the strong methanol-inducible *PAOX1* promoter, the strong constitutive *PGAP* promoter, and a novel bidirectional promoter *PHTX1*. Ultimately, coproduction of HRP and active Hac1 from *PHTX1* allowed competitive recombinant HRP yields of 132 mg/L after 56 h of cultivation in a methanol-independent and easy-to-do bioreactor cultivation process.

Keywords

Pichia pastoris, recombinant protein production, plant peroxidase, horseradish peroxidase, mating factor alpha, unfolded protein response, constitutive expression

Background

Horseradish peroxidase (HRP; EC 1.11.1.7) is a secretory plant peroxidase that has been studied for more than two centuries. It is used in diverse applications worldwide. Most commonly, HRP is employed as a reporter enzyme in diagnostic kits and histochemical assays. More recent applications involve biocatalysis of polymerization reactions, biosensor and wastewater cleanup systems and enzyme-prodrug therapy for cancer treatment [1].

Despite a growing demand for a steady supply of considerable amounts of enzyme at consistent high quality, current HRP preparations are typically isolated from horseradish roots as isoenzyme mixtures. Up to 42 different isoenzymes have been detected by isoelectric focusing of commercial preparations [2]. Recently, we published the sequences of 28 isoenzymes and found them to show diverging substrate profiles [3, 4]. It has long been known that isoenzyme expression patterns vary and seem to depend on so far poorly understood environmental influences [5], negatively affecting the consistency of the quality of isolates. Therefore, recombinant production of a single HRP isoform of choice with defined biochemical characteristics by a suitable host organism presents an attractive alternative. However, current recombinant production systems could not compete with the natural source so far, mainly due to limited enzyme yields. Already back in 1988, production of recombinant HRP was reported in *Escherichia coli* [6]. Until now *E. coli* seems to be the preferred host for HRP production even though inactive enzyme requires inconvenient reactivation and refolding from inclusion bodies [7, 8] and yields are low at <10 mg/L [9]. Owing to the presence of four disulfide bridges in active HRP [10, 11] and glycosylation of the native enzyme [12], eukaryotic organisms might be more favorable production systems than bacterial ones. Apart from insect cell cultures [13] or horseradish hairy root cultures [14] most prominent eukaryotic production hosts are yeast systems. HRP yields from *Pichia pastoris* were reported to be higher than from *Saccharomyces cerevisiae* but still in the lower mg/L range [15, 16], albeit under non-optimized production conditions. The lesser-known basidiomycete yeast strain *Cryptococcus* sp. S-2 however was shown to produce 110 mg/L (based on a volumetric activity of 171000 U/L) after 120 h of bioreactor cultivation [17].

Major advantages of using *P. pastoris* as an expression platform are the well-established and fine-tuned handling and production protocols as well as its status of being generally

recognized as safe (GRAS)* by the U.S. Food and Drug Administration. High titers of more than 18 g/L of secreted *Trichoderma reesei* cellulase were recently achieved in *P. pastoris* [18] demonstrating the considerable production capacities of this host. In order to adequately exploit these capacities for maximum yields, the production system might require some tweaking. Regarding the nucleotide sequence of an expression target, codon optimization has been shown repeatedly to considerably affect production efficiency, e.g. [18, 19]. Transcript levels depend on the copy number of an integrated target gene, however the optimal gene dosage is strongly target dependent and requires evaluation on a case-by-case basis [20]. Also, the choice of a suitable transcription regulation system is mandatory for maximum output. The tightly regulated and strongly inducible promoter of the alcohol oxidase 1 gene, *PAOX1*, is most commonly used in *P. pastoris*. It is strongly repressed in the presence of carbon sources such as glucose or glycerol and greatly induced upon addition of methanol as the sole carbon source [21]. Strong constitutive production of a recombinant protein might overload the protein production machinery and impose a considerable metabolic burden on the cells causing cell death and lysis. This might be particularly true when additional recombinant target genes are constitutively coexpressed simultaneously. In contrast, inducible promoters allow protein production which is only initiated when cell growth is not mandatory any more, which is particularly advantageous for the production of demanding (e.g. cytotoxic) target proteins. On the downside, *PAOX1*-driven transcription requires an initial cell growth phase with glucose or glycerol and an induction phase with hazardous methanol. Similar to gene dosage, the choice of a promoter system, inducible or constitutive, needs to be assessed individually.

Most commonly, recombinant proteins from *P. pastoris* are efficiently secreted by fusing the *S. cerevisiae* mating factor alpha prepro signal peptide to the N-terminus. The pre peptide is processed in the endoplasmic reticulum, the pro peptide is further cleaved by the peptidases Kex2 and Ste13 at an Arg-Lys site and in Glu-Ala repeats, respectively [22, 23]. It has to be noted that processing by Ste13 is of limited specificity, resulting in heterogeneous N-termini [24]. Recently, a deletion mutant $\Delta N57-I70$ of the mating factor alpha prepro signal peptide was reported to increase volumetric HRP yields by almost 60% [25].

Proteins passing through the secretory pathway can be subjected to several modifications. Peptides forming disulfide bridges can interact with the protein disulfide isomerase, Pdi1,

* http://www.accessdata.fda.gov/scripts/fdcc/?set=GRASNotices&id=204&sort=GRN_No&order=DESC&startrow=1&type=basic&search=pichia%20pastoris (last accessed Apr 2015)

which acts as a chaperone and promotes formation of correct disulfide bridges. Hence, coexpression of *PDI1* is a rather common approach to enhance the yields of functional secretory proteins and has been performed repeatedly, *e.g.* [26, 27]. Alternatively, upregulation of the unfolded protein response (UPR) can be achieved by overexpression of an active form of the transcription factor Hac1 [28]. Under non-stress conditions, no active Hac1 is translated from unspliced *HAC1* mRNA due to attenuation. Initiation of an unconventional splicing event is necessary to allow translation of active Hac1 and was described in detail for *Saccharomyces cerevisiae* [29–31]: Upon accumulation of unfolded proteins in the ER, the chaperone Kar2 (BiP) dissociates from the kinase/endonuclease Ire1. Ire1 forms clusters and catalyzes the splicing of *HAC1* mRNA. Inducible coexpression of the homologous spliced *HAC1* gene of *P. pastoris* has been shown previously to augment the production of some recombinant proteins [32, 33].

Another aspect to be considered when producing secreted proteins in yeast is peptide glycosylation. Yeast-type glycosylation is typically characterized by heterogeneous hypermannosylation which causes proteins to appear as smear in SDS-PAGE (*e.g.* [15, 34]) and impedes downstream processing. We recently dealt with this issue by generating a *P. pastoris* strain with an inactivated key mannosyltransferase allowing for considerably more homogeneously glycosylated HRP [35].

The aim of this study was to systematically evaluate a set of strategies to increase the yields of HRP from *P. pastoris*. Based on initial data from high-throughput screenings we performed bioreactor cultivations of the most promising strains and achieved competitive HRP yields.

Results and discussion

Horseradish peroxidase gene dosage

The optimal gene dosage of a target gene is a thin line between providing sufficiently high levels of transcript and overloading a cell's translation/secretion machinery. Initially, we conducted a bottom-up approach in which we first performed high-throughput screenings in 96-deep well-plates (DWPs) to identify a production strain which produces most HRP. Just then was the copy number of HRP genes that were integrated into this strain's genome determined. The best production strain was found to carry two copies of the HRP expression cassette. Apparently, HRP production works best in *P. pastoris* at low gene dosage. In order

to perform a top-down approach as well, we attempted to enforce a high gene dosage by transforming the large amount of 17 μg of the HRP expression vector. However, due to the nature of the used pPpT4_S vector backbone [36], no striking difference was observable between the HRP expression landscape of this approach and the landscape from transformation of lower amounts ($\sim 3 \mu\text{g}$) of vector. On pPpT4_S, transcription of the zeocinTM resistance gene is regulated by the strong *ILV5* promoter resulting in a high level of zeocinTM resistance transcripts already from a single copy of integrated vector, hereby rendering the need for high copy integrations unnecessary for efficient cell growth on antibiotic media. When using another vector backbone, pPpB1 [19], on the other hand, zeocinTM resistance gene transcription is regulated by the weaker *ADH1* promoter and multi copy integrations are required for growth on zeocinTM. Consequently, pPpB1-based HRP expression landscapes showed lower HRP activities than pPpT4_S-based landscapes, most probably due to cells that were overburdened by high copy integrations. A pPpB1-based strain harboring seven copies yielded 60% reduced volumetric HRP activity compared to the pPpT4_S-based production strain with two copies. Interestingly, also a pPpB1-based double copy strain produced approximately 40% less HRP activity than the pPpT4_S-based production strain (also double copy), indicating that not only pPpB1-enforced high copy gene integration but this vector construct itself might not be as suitable for HRP production as the pPpT4_S construct in general. This effect was not only observed for the HRP isoenzyme C1A but also for other HRP isoenzymes (not shown).

Horseradish peroxidase secretion

The *S. cerevisiae* mating factor alpha prepro signal peptide is most commonly used to facilitate efficient secretion of recombinant proteins by *P. pastoris*. Ste13 mediates cleavage between the C-terminus of the signal peptide and the N-terminus of the target protein in Glu-Ala repeats, albeit in a heterogeneous fashion [23], resulting in HRP species with N-terminal Ala-Glu-Ala or Glu-Ala-Glu-Ala residues as seen by mass spectrometry. In order to test whether this heterogeneity might indicate a bottleneck in HRP secretion we followed two independent approaches. We removed the Glu-Ala repeat-encoding nucleotide sequence from the 3' end of the signal peptide CDS. However, HRP expression landscapes were reduced by at least 50% compared to the production strain with full length signal peptide indicating dramatically reduced secretion efficiency (Figure 1.A, white bars). Thus,

we attempted to go the other direction and tried to enhance Ste13 activity by strong *PAOX1*-driven coexpression of *STE13*. In addition, we tested whether processing of the signal peptide by Kex2 was limiting HRP secretion and coexpressed *KEX2* from *PAOX1*. To get a default coexpression landscape as control we recorded activity data from HRP strains coproducing eGFP from *PAOX1* which we assumed not to interfere with HRP production. Neither coexpression of *STE13* nor of *KEX2* proved to be beneficial for HRP secretion as HRP expression landscapes were generally reduced compared to the control landscape in both cases (Figure 1.B).

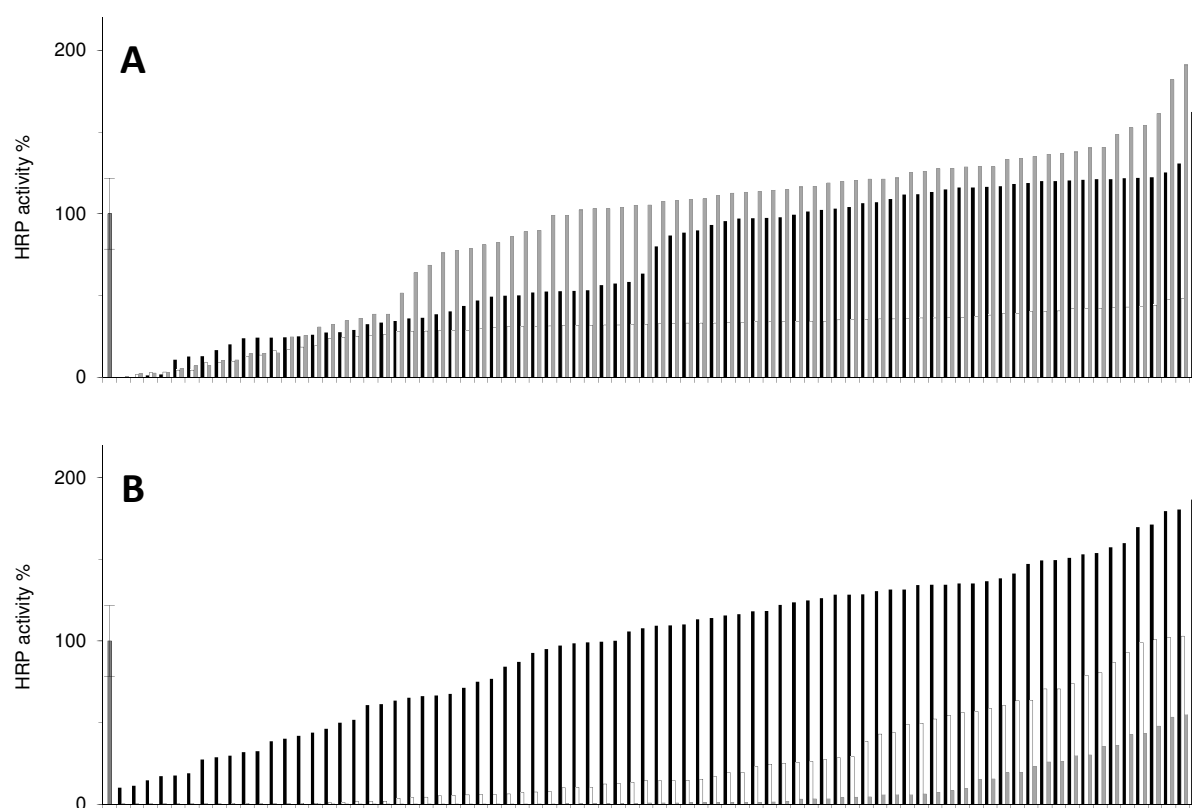


Figure 1. HRP expression landscapes from secretion studies. A, landscapes of strains secreting HRP with an unaltered mating factor alpha prepro signal peptide (black), a signal peptide lacking C-terminal Glu-Ala repeats (white) or a $\Delta N57-I70$ mutant of the signal peptide (gray). B, landscapes of strains coproducing HRP with eGFP as control (black), Ste13 (white) or Kex2 (gray) from *PAOX1*. The first bar is an average value of the unaltered HRP production strain as reference; error bars are standard deviations from at least triplicates.

Based on a recent study on enhanced HRP secretion due to the use of a deletion mutant ($\Delta N57-170$) of the mating factor alpha prepro signal peptide [25], we tried to reproduce the beneficial effect of this particular mutant. Judging from the HRP expression landscape (Figure 1.A, gray bars), there seemed to be a tendency for augmented secretion (approximately 30%) when compared to the landscape of strains secreting HRP with an unmutated full-length signal peptide (Figure 1.A, black bars).

Cellular stress upon peroxidase production

Despite the relatively small mass of HRP of approximately 35 kDa [4], its recombinant production seems to be somewhat complex and troublesome for *P. pastoris* as reflected by typical yields in the lower mg/L range [15]. To some extent, the need for formation of four disulfide bridges [10, 11] to yield active enzyme might be hold accountable. Thus, we evaluated a potentially alleviating effect of coexpressed *PDI1* on HRP folding. However, a HRP expression landscape of strains coexpressing *PDI1* from *PAOX1* did not show a beneficial effect of this strategy on HRP activity yields (Figure 2, white bars). Comparable results were found when *PDI1* coexpression was regulated by either the strong constitutive promoter *PGAP* or the promoter *PCAT* which is active in the absence of glucose or glycerol and further induced on methanol [Vogl *et al.*, manuscript in preparation]. Similarly, *PDI1* coexpression did not show an effect on HRP production in a HRP multicopy strain either.

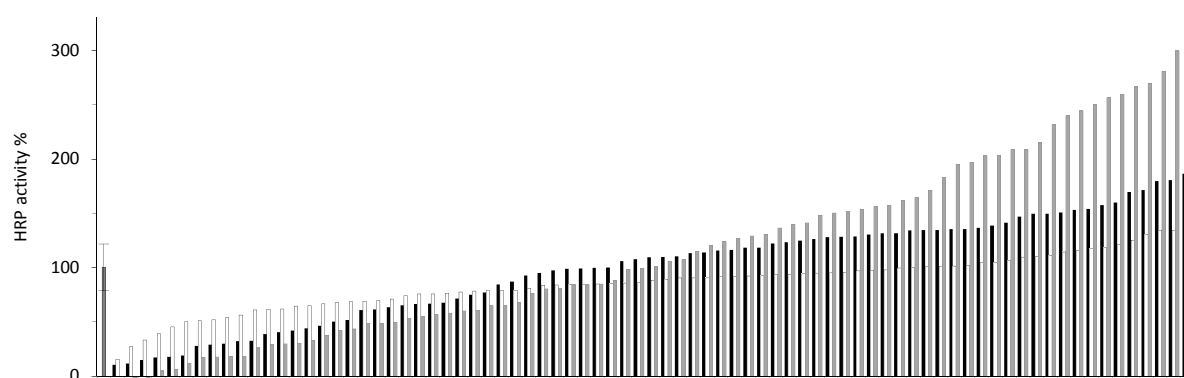


Figure 2. HRP expression landscapes from coexpression of Pdi1 and active Hac1. Landscapes of strains coproducing HRP with eGFP as control (black), Pdi1 (white) or active Hac1 (gray) from *PAOX1*. Reference activity as described in Figure 1.

Therefore, we focused on a more systemic approach to deal with potential cellular stress. By coexpressing active *HAC1* from *PAOX1*, we aimed to activate the UPR [28, 32] and hereby eliminate or at least reduce any stress-related bottleneck effects on HRP productivity. Intriguingly, this strategy resulted in an expression landscape that rose over the control landscape (Figure 2, gray bars). Active Hac1 triggers the expression of several UPR genes [37, 38], apparently altering the cells' physiological state to conditions that are more suitable for HRP production.

Methanol-independent production of horseradish peroxidase

Inducible expression from the promoter *PAOX1* is most commonly performed for recombinant protein production in *P. pastoris*. However, target protein production from the strong constitutive promoter *PGAP* offers an attractive alternative for expression independent from methanol [21]. When we performed microscale cultivations in DWPs using *PGAP* to drive HRP expression, we found HRP activities slightly reduced compared to the expression landscape of *PAOX1*-driven HRP strains (Figure 3). It has to be kept in mind however, that cultivations in DWPs only provide suboptimal conditions (*i.e.* limited O₂ supply, non-constant feeding) which limit cell growth and consequently the potential of *PGAP*-driven expression. In order to combine methanol-independent HRP production with the beneficial coproduction of active Hac1 (Figure 2), four distinct approaches were assessed: Transformations of vectors for coexpression of active *HAC1* by either of the constitutive promoters *PGAP*, *PADH2* or *PPG11* [Vogl *et al.*, manuscript in preparation] to the strain producing HRP under *PGAP*-regulation did not result in positive transformants, indicative of metabolically overburdened cells. Thus, coexpression of active *HAC1* by these promoters to enhance HRP production was not followed up at this point. Intriguingly however, we obtained promising results when we employed a novel bidirectional promoter, *PHTX1*. *In vivo*, the bidirectional activity of the *PHTX1* promoter regulates the expression of core histone genes [Vogl *et al.*, manuscript in preparation]. In analogy to *PAOX1*-regulated coexpression of active *HAC1*, the HRP expression landscape of the methanol-independent approach using *PHTX1* generally surpassed the controls (Figure 3, gray bars). Further comparative strain characterizations were performed in bioreactor cultivations, allowing cell growth to high cell densities under controlled conditions.

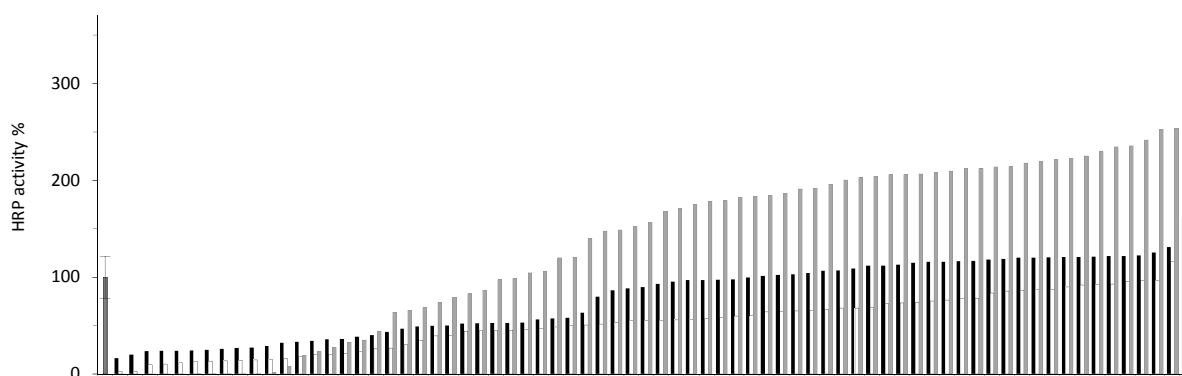


Figure 3. Landscapes from PAOX1-, PGAP- or PHTX1-driven HRP expression. Landscapes of strains producing HRP from PAOX1 (black) or PGAP (white) or PHTX1-regulated coproduction of HRP and active Hac1 (gray). Reference activity as described in Figure 1.

Production of recombinant horseradish peroxidase in bioreactor cultivations

In order to comparatively assess the performance of four HRP producing *P. pastoris* strains under controlled conditions, we performed bioreactor cultivations. We cultivated a strain secreting HRP with a full-length signal peptide from PAOX1 as reference, a strain secreting HRP with the mutant signal peptide [25] and coexpressing active HAC1 (both under PAOX1 control), a strain producing HRP (secreted with the mutant signal peptide) under PGAP control, and a strain coproducing active Hac1 and HRP (secreted with the mutant signal peptide) under control of the bidirectional PHTX1 promoter. For each strategy, the best strain was selected from screenings of microscale cultivations in DWPs to ensure that the obtained data represented the maximum production performance of the respective strategy. When HRP production was PAOX1-regulated, cells were first cultivated as glycerol batch cultures, then grown in glycerol fed-batch cultivations, and finally fed methanol to induce target protein production. When HRP production was PGAP-regulated, cells were also first cultivated in a glycerol batch culture but then fed growth-limiting amounts of glucose [39]. The PHTX1-regulated strain was fed growth-limiting amounts of glycerol after the initial batch phase. The OCH1-encoded mannosyltransferase activity was inactivated in all strains [35]. In contrast to a recent study on a fed-batch process with the same $\Delta och1$ strain [40], we did not experience foam formation under any conditions.

Striking differences were observed among the studied strains in terms of both, volumetric and specific HRP activities (Table 1, Figure 4). In terms of volumetric HRP activity, the two strains producing HRP under PAOX1 control produced similar amounts of HRP. However, the

strain coexpressing active *HAC1* reached this level of volumetric HRP activity already after 80 h, *i.e.* half the time of the reference strain. Also, the specific HRP activity from the coexpression strain was almost two orders of magnitude higher than from the reference strain, indicating substantially reduced cell lysis and hence reduced contamination with non-HRP proteins when active *HAC1* was coexpressed. Concerning HRP production under *PGAP* control, overall process handling required less hands-on time due to the independence from a methanol induction phase. Moreover, HRP production from *PGAP* resulted in up to 4-fold higher volumetric HRP activity (Table 1, Figure 4.C) compared to production from *PAOX1*. *PGAP*-driven HRP production yielded higher specific HRP activity than the reference strain, most probably due to the generally higher volumetric activity. Owing to the high cell density produced by the constant feed of glucose however, increased cell lysis towards the end of the cultivation caused higher total protein concentrations and thus still lower specific HRP activity than the *PAOX1*-regulated *HAC1* coexpression strain. *PHTX1*-regulated coproduction of active *Hac1* and HRP even yielded more than 5-fold higher volumetric activity than the *PAOX1*-regulated strains (Table 1, Figure 4.D). Similar to the *PAOX1*-regulated *HAC1* coproduction strain, *PHTX1*-driven coproduction of active *Hac1* allowed higher specific HRP activity than *PGAP*-driven HRP production and shorter production time at even higher volumetric activity yield (Table 1).

Table 1. HRP activity yields from bioreactor cultivations of different HRP producing strains.

Volumetric and specific HRP activities, as well as calculated HRP yields are shown at the indicated cultivation time for the three described strains. Shown errors are 20% by default.

strain description	volumetric activity U/mL	specific activity U/mg	yield mg/L	cultivation time h
<i>PAOX1</i> -HRP	50 ± 10	9 ± 2	25 ± 5	167
<i>PAOX1</i> -HRP, <i>PAOX1</i> - <i>Hac1</i>	52 ± 10	684 ± 137	26 ± 5	80
<i>PGAP</i> -HRP	205 ± 41	157 ± 31	102 ± 20	81
HRP- <i>PHTX1</i> - <i>Hac1</i>	266 ± 53	505 ± 101	132 ± 26	56

By applying an easy-to-do two-step purification protocol consisting of Ni^{2+} affinity chromatography and size exclusion chromatography we purified our recombinantly produced HRP to a specific activity of 2008 ± 97 U/mg, which is slightly higher than the recently published activity for recombinant HRP from *Cryptococcus* sp. S-2 of 1569 U/mg

[17]. By use of the *P. pastoris* strain *PpFWK3* the produced HRP was homogeneously glycosylated and eluted as a uniform peak from the size exclusion column as described previously [35]. Based on the determined specific activity and a volumetric activity of 266 U/mL, we calculated a HRP concentration of approximately 133 mg of HRP per liter of supernatant from *PHTX1*-driven coproduction of HRP with active Hac1 after 55.6 h.

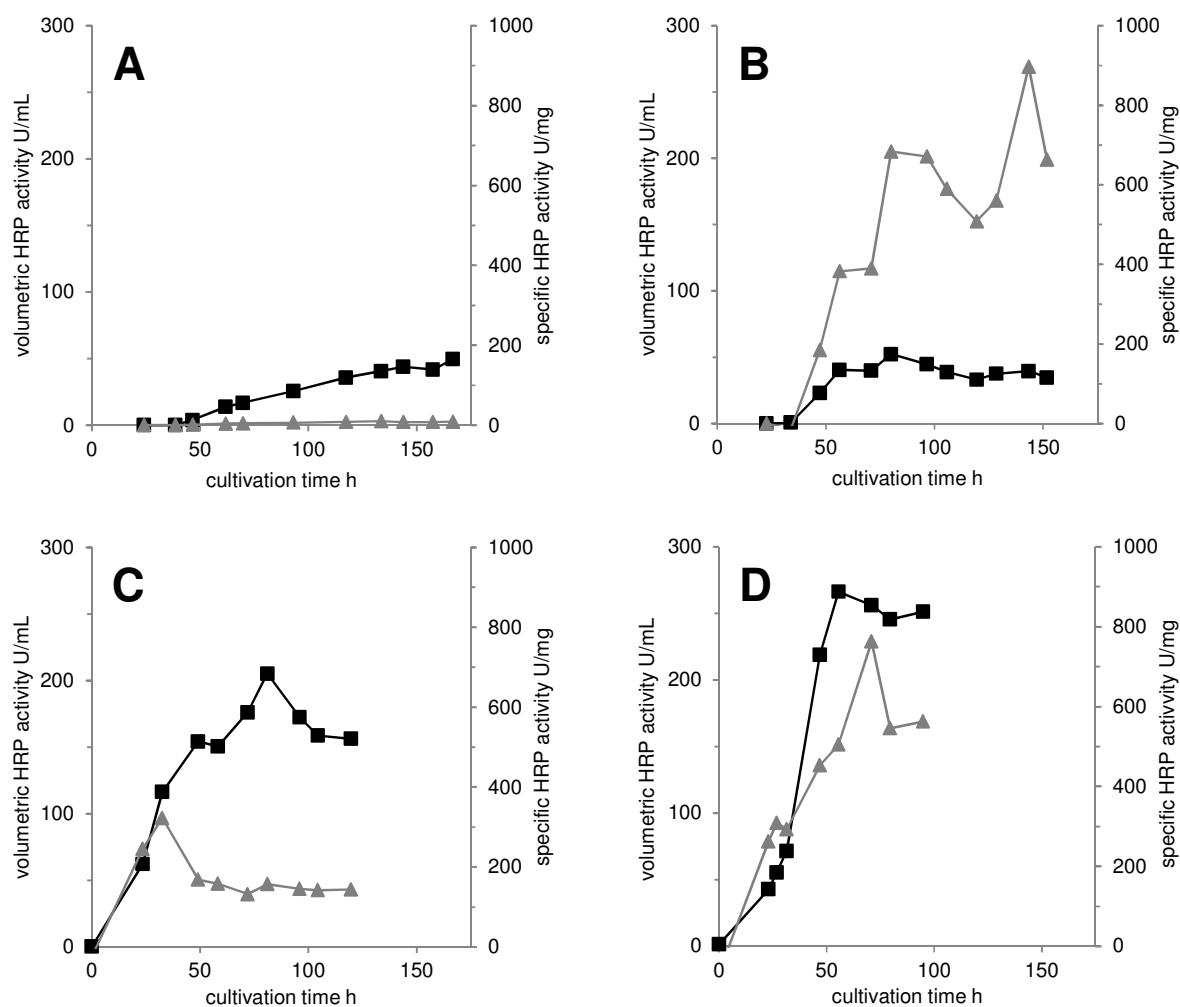


Figure 4. Bioreactor cultivations of HRP producing strains. A, PAOX1-regulated HRP reference strain, HRP secretion with full-length *S. cerevisiae* mating factor alpha prepro signal peptide; B, PAOX1-regulated coexpression strain, HRP secretion with $\Delta N57-I70$ mutant of the signal peptide, coexpression of active *HAC1*; C, PGAP-regulated constitutive expression strain, HRP secretion with $\Delta N57-I70$ mutant of the signal peptide; D, *PHTX1*-regulated bidirectional coexpression strain, HRP secretion with $\Delta N57-I70$ mutant of the signal peptide, coexpression of active *HAC1*. Black squares, volumetric HRP activity; gray triangles, specific HRP activity.

Conclusions

Currently, commercially available HRP preparations are isolated from the roots of the horseradish plant as mixtures of different isoenzymes with different biochemical properties. Due to the increasing number of applications for HRP in diagnostics, wastewater cleanup systems or medicine, and a growing demand for large amounts of HRP preparations at consistent high quality, recombinant HRP production offers an appealing alternative to the current isolation procedure [1]. So far however, most recombinant production hosts were limited at the lower mg/L range.

In this study, we systematically evaluated a broad range of strategies to enhance HRP production in *P. pastoris*. We found a low gene dosage to be most beneficial for HRP production. Interestingly enough, we also observed a dependence of HRP productivity on the employed vector backbone. Whereas the pPpT4_S vector resulted in decent HRP activities, the pPpB1 vector seemed unsuitable for HRP production, the dilemma being either impaired growth due to insufficient zeocin™ resistance transcript levels in low copy strains, or impaired HRP production due to overburdened cells in high copy strains.

In terms of secretion efficiency, we confirmed a potentially beneficial effect of a Δ N57-I70 mutant of the mating factor alpha prepro signal peptide as suggested by [25], although to a lesser extent. Strategies on improving the processing of the signal peptide by either Kex2 or Ste13 were found disadvantageous.

In order to alleviate intracellular stress due to putatively accumulating unfolded protein we tested coproduction of the chaperone and protein disulfide isomerase Pdi1, and of active Hac1, an UPR-regulating transcription factor. We did not observe any beneficial effect on HRP production when *PDI1* was coexpressed. However, by taking the more systemic approach of coexpressing active *HAC1* we observed increased levels of HRP activity in microscale screenings. The advantages of this coexpression strategy were further reflected by the obtained bioreactor data that showed a particularly high specific HRP activity and a volumetric activity that was at least as high as a reference strain but in considerably shorter cultivation time.

Microscale screenings of methanol-independent HRP production in DWPs already indicated HRP yields that were competitive to *PAOX1*-regulated production. By cultivating a strain constitutively producing HRP from *PGAP* in a bioreactor we observed very high volumetric HRP activity of up to 200000 U/L after approximately 80 h of cultivation time. Even higher

yields (266300 U/L after 55.6 h of cultivation time) were achieved by using the novel bidirectional *PHTX1* promoter for methanol-independent coproduction of active Hac1 and HRP.

In conclusion, we recommend using *P. pastoris* as host organism for HRP production due to the ease of its use, the well-established handling protocols, its GRAS status and the high competitive yields of recombinant HRP.

Outlook

In this study, we demonstrated that *P. pastoris* is capable of producing HRP in the range of 130 mg/L within 56 h of cultivation. However, we are far from reaching the end of the line and additional studies are likely to increase these yields even further. Alternative strategies that emerged just recently, such as the coexpression of *AFT1* [41] or engineering of the sorting receptor Vps10 of the Golgi [42] remain yet to be assessed for their potential to enhance HRP secretion. Moreover, assessment of additional differently regulated promoters and promoter combinations for bidirectional HRP expression or coexpressions are a matter of ongoing studies.

Material and methods

Chemicals

2,2'-azino-bis(3-ethylbenzthiazoline-6-sulfonic acid) diammonium salt (ABTS), D(+)-biotin and hemin were obtained from Sigma-Aldrich (Austria). Difco™ yeast nitrogen base w/o amino acids (YNB), Bacto™ tryptone and Bacto™ yeast extract (YE) were purchased from Becton Dickinson (Austria). Glanapon DG 160 defoamer was from Bussetti & Co, (Austria). Zeocin™ was obtained from InvivoGen (France). Other chemicals were purchased from Carl Roth (Germany).

Strains and vectors

P. pastoris strains were based on the wildtype strain CBS 7435 (identical to NRRL Y-11430 and ATCC 76273). We previously found a strain with Mut^S phenotype to be superior over the Mut⁺ phenotype for HRP production [43]. Therefore, all HRP production strains were based on a strain with $\Delta aox1::FRT$ mutation (*PpMutS*) [36]. In order to obtain homogeneously

glycosylated HRP we used a strain with an additional $\Delta och1::FRT$ mutation (*PpFWK3*) as described recently [35].

For *PAOX1*-regulated HRP production, a pPpT4_alpha_S-based vector [36] was transformed [44], resulting in zeocin™ resistant transformants and HRP secretion with the full length *S. cerevisiae* mating factor alpha prepro signal peptide. The HRP C1A gene has been codon optimized for production in *P. pastoris* [19] and has been ordered as synthetic polynucleotide as described in [3]. To facilitate purification, a hexahistidine tag was N-terminally fused to mature HRP. A gene encoding the $\Delta N57-170$ mutant signal peptide was PCR amplified using the primers shown in Supplementary table 1 and pPpT4_alpha_S as template. The deletion mutant replaced the full length signal peptide in that vector by double digest with *SacI* and *XhoI*, forming a new vector derivative pPpT4_Dalpha_S. Coexpression constructs were based on a pPpKan_S vector backbone [36], resulting in kanamycin and geneticin resistant transformants of *E. coli* and *P. pastoris*, respectively. A codon-optimized synthetic gene encoding Pdi1 preexisted in our lab (Abad, unpublished data). Other gene sequences of coexpression partners were identified from *P. pastoris* CBS 7435 genome sequences [45], PCR amplified from isolated genomic DNA [46] using the primers shown in Supplementary table 1, and cloned to the pPpKan_S vector by double digest with *EcoRI* and *NotI*. As a negative control for coproductions, eGFP [47, 48] was used. PGAP-driven HRP production was performed using a pPpT4GAP_S vector backbone [36]. A pPpT4_S-based vector backbone [36] was used for coproduction of HRP and active Hac1 by the bidirectional *PHTX1* promoter [Vogl *et al.*, manuscript in preparation]. The individual vector parts were assembled using the primers shown in Supplementary table 1, the vector map is shown in Supplementary figure 1.

Screening and strain characterization

Microscale cultivations were performed in DWPs similar to [49]. *P. pastoris* strains were grown initially in 250 μ L BMD1% minimal growth medium (11 g/L alpha-D(+)-glucose monohydrate, 13.4 g/L YNB, 0.4 mg/L D(+)-biotin, 0.1 M potassium phosphate buffer, pH 6.0) supplemented with 25 μ M hemin [50] at 28 °C, 320 rpm, 80% humidity. *PAOX1*-driven expression was induced by additions of 250 μ L BMM2 (1% v/v methanol, 13.4 g/L YNB, 0.4 mg/L, D(+)-biotin, 0.1 M potassium phosphate buffer, pH 6.0) after 60 h of growth in BMD1%, followed by three additions of 50 μ L BMM10 each (5% v/v methanol, 13.4 g/L YNB,

0.4 mg/L, D(+)-biotin, 0.1 M potassium phosphate buffer, pH 6.0) 10, 24 and 48 h after the addition of BMM2. In case of *PGAP*-regulated HRP production, additions of BMM2 and BMM10 were substituted by further additions of the initial minimal growth medium. In case of *PHTX1*-regulated expression, 25 μ M hemin-supplemented BMG1% medium (1% w/v glycerol, 13.4 g/L YNB, 0.4 mg/L D(+)-biotin, 0.1 M potassium phosphate buffer, pH 6.0) was used. HRP activities were quantified approximately 132 h after inoculation by following an increase in absorbance at 405 nm upon mixing of 15 μ L culture supernatant with 140 μ L assay solution (1 mM ABTS, 0.9 mM H₂O₂, 50 mM sodium acetate, pH 4.5) in a microtiter plate. HRP gene dosage was determined based on a previously published protocol [51].

Bioreactor cultivations

Media: Buffered minimal glycerol yeast medium (BMGY): 10 g/L YE, 13.4 g/L YNB, 20 g/L Bacto™ tryptone, 12.6 g/L glycerol, 0.4 mg/L D(+)-biotin, 100 mM potassium phosphate, pH 6. Trace element solution (PTM1): 5.99 g/L CuSO₄·5H₂O, 0.08 g/L KI, 3 g/L MnSO₄·H₂O, 0.2 g/L Na₂MoO₄·2H₂O, 0.02 g/L H₃BO₃, 0.92 g/L CoCl₂·6H₂O, 42.18 g/L ZnSO₄·7H₂O, 65 g/L FeSO₄·7H₂O, 5 mL/L 95-98% H₂SO₄. Basal salts medium (BSM): 40 g/L \geq 98% glycerol, 4.25 mL/L 85% phosphoric acid, 0.17 g/L CaSO₄·2H₂O, 0.22 g/L NaCl, 0.64 g/L KOH, 2.86 g/L K₂SO₄, 14 g/L MgSO₄·7H₂O, 4.36 mL/L PTM1, 0.87 mg/L D(+)-biotin, 0.2 mL/L Glanapon DG 160.

Cultivation procedure: Bioreactor cultivations were performed either in 6.9 L BIOSTAT® Cplus or 1.2 L BIOSTAT® B bioreactor systems (Sartorius, Germany). NH₄OH was used as nitrogen source and to set and maintain pH 6. A minimum dO₂ of 30% was set under cascade control settings. Two 50 mL precultures were grown for two days at 28 °C, 90 rpm, 80% humidity, then centrifuged at 500 x g, 22 °C, 5 min, and resuspended in a final volume of 50 mL. Batch cultivations were started by aseptic addition of the inoculum to BSM (4.8 mL/L sterile PTM1 and 4.8 mL/L sterile D(+)-biotin were added after autoclaving) and grown until glycerol was depleted as indicated by an increase in dO₂. In case of *PAOX1*-driven expressions, 67 g of glycerol per L of initial batch volume were fed over 7 h. For induction, 2.5 g/h of methanol per L of initial batch volume were fed for at least 130 h. In case of *PGAP*-driven HRP expression, 537 g of alpha-D(+)-glucose monohydrate per L of initial batch volume were fed over a total cultivation time of 96 h, based on a previous publication describing a combination of glycerol batch and glucose fed-batch phases as most beneficial for recombinant expression from *PGAP* [39]. In case of *PHTX1*-driven expression, 398 g of

glycerol per L of initial batch volume were fed over 68 h after glycerol batch cultivation. In order to effectively saturate secreted apospecies of HRP, an excess of 40 μM hemin was added [50] prior to starting the methanol feed for PAOX1 strains. In case of PGAP- or PHTX1-regulated expression, 40 μM hemin was already added to the initial batch phase. After cultivation, cells were harvested ($17700 \times g$, 4 °C, 40 min) and the supernatant was 0.2 μm filtered.

Sample handling: Samples were taken regularly throughout bioreactor cultivations to determine HRP activity and total protein concentration. HRP activity was determined from the supernatant with ABTS as reducing substrate as described above. Protein concentrations were determined using the Bradford-based Bio-Rad protein assay (Bio-Rad, Austria) with different concentrations of bovine serum albumin as standard.

Purification of recombinant horseradish peroxidase

Buffer changes and concentrations were performed using Vivaflow® 50 cassettes (30 kDa MWCO) and Vivaspin® 20 tubes (3 kDa MWCO) (both Sartorius, Germany). Cultivation supernatant was concentrated and changed to calcium-supplemented tris-buffered saline (Ca-TBS; 1 mM CaCl_2 , 150 mM NaCl, 50 mM Tris, pH 7.5 set with HCl) prior to loading on a 5 mL HisTrap FF column (GE Healthcare, Austria) on an ÄKTA pure system (GE Healthcare). After washing with at least five column volumes, bound protein was eluted with 200 mM imidazole in Ca-TBS. Unbound HRP from loading and washing fractions was reloaded on the column for reduced enzyme loss. Pooled elution fractions were concentrated to <1 mL and loaded on a HiLoad™ 16/60 Superdex™ 200 prep grade column (GE Healthcare) for polishing. Isocratic elution was performed with Ca-TBS buffer at a flowrate of 0.3 mL/min. HRP containing fractions were pooled, concentrated and the specific activity of the preparation was calculated.

Mass spectrometry

Liquid chromatography-tandem mass spectrometry: Protein identification and internal sequence information was received from liquid chromatography-tandem mass spectrometry (LC-MS/MS). The gel band was reduced, alkylated and digested with Promega modified trypsin according to the method of [52] or chymotrypsin according to the manufacturers protocol. Peptide extracts were dissolved in 0.1% formic acid, 5% acetonitrile and were

separated by nano-HPLC (Agilent 1200 system, Austria) equipped with a Zorbax 300SB-C18 enrichment column (5 μm , 5 x 0.3 mm) and a Zorbax 300SB-C18 nanocolumn (3.5 μm , 150 x 0.075 mm). Forty μL of sample were injected and concentrated on the enrichment column for 6 min using 0.1% formic acid as isocratic solvent at a flow rate of 20 $\mu\text{L}/\text{min}$. The column was then switched in the nanoflow circuit, and the sample was loaded on the nanocolumn at a flow rate of 300 nL/min. Separation was carried out using the following gradient, where solvent A was 0.3% formic acid in water and solvent B was a mixture of acetonitrile and water (4:1 v/v) containing 0.3% formic acid: 0-6min: 13% B; 6-35 min: 13-28% B; 35-47 min: 28-50% B, 47-48 min: 50-100% B; 48-58 min: 100% B; 58-59 min: 100-13% B; 59-70 min: re-equilibration at 13% B. The sample was ionized in the nanospray source equipped with nanospray tips (PicoTipTM Stock# FS360-75-15-D-20, Coating: 1P-4P, 15 \pm 1 μm Emitter, New Objective, Woburn, MA, USA). It was analysed in a Thermo LTQ-FT mass spectrometer (Thermo Fisher Scientific, Waltham, MA, USA) operated in positive ion mode, applying alternating full scan MS (m/z range from 400 to 2000) in the ion cyclotron and MS/MS by collision-induced dissociation of the five most intense peaks in the ion trap with dynamic exclusion enabled. The LC-MS/MS data was analyzed by searching an in-house database containing known contaminants (keratins) and proteases used for digests as well as HRP with Mascot 2.2 (MatrixScience, London, UK). A maximum false discovery rate of 5% using decoy database search, an ion score cutoff of 20 and a minimum of two identified peptides were chosen as identification criteria.

Intact mass determination: For matrix-assisted laser desorption/ionization-time of flight (MALDI-TOF) mass spectrometry on a Bruker Ultraflex extreme instrument, protein solution (6 $\mu\text{g}/100 \mu\text{L}$) was desalted using 10 kDa cutoff filters (Amicon, Merck Millipore, Austria). The sample was diluted 1:5 (v/v) in 50% acetonitrile and 0.1% trifluoroacetic acid and mixed 1:2 (v/v) with a suspension of 5 mg super-DHB matrix (Sigma-Aldrich; 9:1 mixture of 2,5-dihydroxybenzoic acid and 2-hydroxy-5-methoxybenzoic acid) in 50 μL acetonitrile and 50 μL 0.1% trifluoroacetic acid. One μL was spotted onto an 800 μm Bruker MTP Anchorchip and left to dry. Full MS spectra were obtained in positive linear mode after external calibration using an appropriate protein standard (10-70 kDa) in the m/z range from 550 to 73000 by summarizing 9000 laser shots.

Top-down sequencing of intact proteins: For top-down sequencing, the protein solution was mixed with a saturated solution of 1,5-diaminonaphthalene in 0.1% trifluoroacetic acid

containing 50% acetonitrile in a 1:2 (v/v) ratio. One μL was spotted onto an 800 μm Bruker MTP Anchorchip and left to dry. Full MS spectra were obtained in reflectron positive mode after external calibration using an appropriate peptide standard in a mass range from 400 to 3000.

Acknowledgements

The authors would like to acknowledge support from NAWI Graz and the Austrian Science Fund FWF project W901 "DK Molecular Enzymology". The authors declare that they have no conflict of interest.

References

1. Krainer FW, Glieder A: **An updated view on horseradish peroxidases: recombinant production and biotechnological applications.** *Appl. Microbiol. Biotechnol.* 2015.
2. Hoyle MC: **High resolution of peroxidase-indoleacetic acid oxidase isoenzymes from horseradish by isoelectric focusing.** *Plant Physiol.* 1977, **60**:787–93.
3. Näätäsaari L, Krainer FW, Schubert M, Glieder A, Thallinger GG: **Peroxidase gene discovery from the horseradish transcriptome.** *BMC Genomics* 2014, **15**:227.
4. Krainer FW, Pletzenauer R, Rossetti L, Herwig C, Glieder A, Spadiut O: **Purification and basic biochemical characterization of 19 recombinant plant peroxidase isoenzymes produced in *Pichia pastoris*.** *Protein Expr. Purif.* 2013, **95C**:104–112.
5. Jermyn MA, Thomas R: **Multiple components in horseradish peroxidase.** *Biochem. J.* 1954, **56**:631–9.
6. Chiswell DJ, Ortlepp SA: **DNA sequence coding for HRP enzyme.** *EP0299682A1* 1988.
7. Smith AT, Santama N, Dacey S, Edwards M, Bray RC, Thorneley RN, Burke JF: **Expression of a synthetic gene for horseradish peroxidase C in *Escherichia coli* and folding and activation of the recombinant enzyme with Ca^{2+} and heme.** *J. Biol. Chem.* 1990, **265**:13335–43.
8. Asad S, Dabirmanesh B, Ghaemi N, Etehad SM, Khajeh K: **Studies on the refolding process of recombinant horseradish peroxidase.** *Mol. Biotechnol.* 2013, **54**:484–92.
9. Grigorenko V, Chubar T, Kapeliuch Y, Borchers T, Spener F, Egorov A: **New approaches for functional expression of recombinant horseradish peroxidase C in *Escherichia coli*.** *Biocatal. Biotransformation* 1999, **17**:359–379.
10. Welinder KG: **Covalent structure of the glycoprotein horseradish peroxidase (EC 1.11.1.7).** *FEBS Lett.* 1976, **72**:19–23.
11. Gajhede M, Schuller DJ, Henriksen A, Smith AT, Poulos TL: **Crystal structure of horseradish peroxidase C at 2.15 Å resolution.** *Nat. Struct. Biol.* 1997, **4**:1032–8.
12. Welinder KG: **Amino acid sequence studies of horseradish peroxidase. Amino and carboxyl termini, cyanogen bromide and tryptic fragments, the complete sequence, and some structural characteristics of horseradish peroxidase C.** *Eur. J. Biochem.* 1979, **96**:483–502.
13. Segura M de las M, Levin G, Miranda M V, Mendive FM, Targovnik HM, Cascone O: **High-level expression and purification of recombinant horseradish peroxidase isozyme C in SF-9 insect cell culture.** *Process Biochem.* 2005, **40**:795–800.

14. Flocco CG, Alvarez MA, Giulietti AM: **Peroxidase production in vitro by *Armoracia lapathifolia* (horseradish)-transformed root cultures: effect of elicitation on level and profile of isoenzymes.** *Biotechnol. Appl. Biochem.* 1998, **28**:33–8.
15. Morawski B, Lin Z, Cirino P, Joo H, Bandara G, Arnold FH: **Functional expression of horseradish peroxidase in *Saccharomyces cerevisiae* and *Pichia pastoris*.** *Protein Eng.* 2000, **13**:377–84.
16. Morawski B, Quan S, Arnold FH: **Functional expression and stabilization of horseradish peroxidase by directed evolution in *Saccharomyces cerevisiae*.** *Biotechnol. Bioeng.* 2001, **76**:99–107.
17. Utashima Y, Matsumoto H, Masaki K, Iefuji H: **Heterologous production of horseradish peroxidase C1a by the basidiomycete yeast *Cryptococcus* sp. S-2 using codon and signal optimizations.** *Appl. Microbiol. Biotechnol.* 2014, **98**:7893–900.
18. Mellitzer A, Ruth C, Gustafsson C, Welch M, Birner-Grünberger R, Weis R, Purkarthofer T, Glieder A: **Synergistic modular promoter and gene optimization to push cellulase secretion by *Pichia pastoris* beyond existing benchmarks.** *J. Biotechnol.* 2014:1–9.
19. Abad S, Nahalka J, Bergler G, Arnold SA, Speight R, Fotheringham I, Nidetzky B, Glieder A: **Stepwise engineering of a *Pichia pastoris* D-amino acid oxidase whole cell catalyst.** *Microb. Cell Fact.* 2010, **9**:24.
20. Mattanovich D, Gasser B, Hohenblum H, Sauer M: **Stress in recombinant protein producing yeasts.** *J. Biotechnol.* 2004, **113**:121–35.
21. Vogl T, Glieder A: **Regulation of *Pichia pastoris* promoters and its consequences for protein production.** *N. Biotechnol.* 2013, **30**:385–404.
22. Brake AJ, Merryweather JP, Coit DG, Heberlein UA, Masiarz FR, Mullenbach GT, Urdea MS, Valenzuela P, Barr PJ: **Alpha-factor-directed synthesis and secretion of mature foreign proteins in *Saccharomyces cerevisiae*.** *Proc. Natl. Acad. Sci. U. S. A.* 1984, **81**:4642–6.
23. Bourbonnais Y, Bolin D, Shields D: **Secretion of somatostatin by *Saccharomyces cerevisiae*. Correct proteolytic processing of pro-alpha-factor-somatostatin hybrids requires the products of the KEX2 and STE13 genes.** *J. Biol. Chem.* 1988, **263**:15342–7.
24. Bitter GA, Chen KK, Banks AR, Lai PH: **Secretion of foreign proteins from *Saccharomyces cerevisiae* directed by alpha-factor gene fusions.** *Proc. Natl. Acad. Sci. U. S. A.* 1984, **81**:5330–4.
25. Lin-Cereghino GP, Stark CM, Kim D, Chang J, Shaheen N, Poerwanto H, Agari K, Moua P, Low LK, Tran N, Huang AD, Nattestad M, Oshiro KT, Chang JW, Chavan A, Tsai JW, Lin-Cereghino J: **The effect of α -mating factor secretion signal mutations on recombinant protein expression in *Pichia pastoris*.** *Gene* 2013, **519**:311–7.
26. Inan M, Aryasomayajula D, Sinha J, Meagher MM: **Enhancement of protein secretion in *Pichia pastoris* by overexpression of protein disulfide isomerase.** *Biotechnol. Bioeng.* 2006, **93**:771–8.
27. Gasser B, Maurer M, Gach J, Kunert R, Mattanovich D: **Engineering of *Pichia pastoris* for improved production of antibody fragments.** *Biotechnol. Bioeng.* 2006, **94**:353–61.
28. Valkonen M, Penttilä M, Saloheimo M: **Effects of inactivation and constitutive expression of the unfolded-protein response pathway on protein production in the yeast *Saccharomyces cerevisiae*.** *Appl. Environ. Microbiol.* 2003, **69**:2065–72.
29. Kawahara T, Yanagi H, Yura T, Mori K: **Endoplasmic reticulum stress-induced mRNA splicing permits synthesis of transcription factor Hac1p/Ern4p that activates the unfolded protein response.** *Mol. Biol. Cell* 1997, **8**:1845–62.
30. Chapman RE, Walter P: **Translational attenuation mediated by an mRNA intron.** *Curr. Biol.* 1997, **7**:850–9.
31. Kimata Y, Ishiwata-Kimata Y, Ito T, Hirata A, Suzuki T, Oikawa D, Takeuchi M, Kohno K: **Two regulatory steps of ER-stress sensor Ire1 involving its cluster formation and interaction with unfolded proteins.** *J. Cell Biol.* 2007, **179**:75–86.
32. Guerfal M, Ryckaert S, Jacobs PP, Ameloot P, Van Craenenbroeck K, Derycke R, Callewaert N: **The HAC1 gene from *Pichia pastoris*: characterization and effect of its overexpression on the production of secreted, surface displayed and membrane proteins.** *Microb. Cell Fact.* 2010, **9**:49.

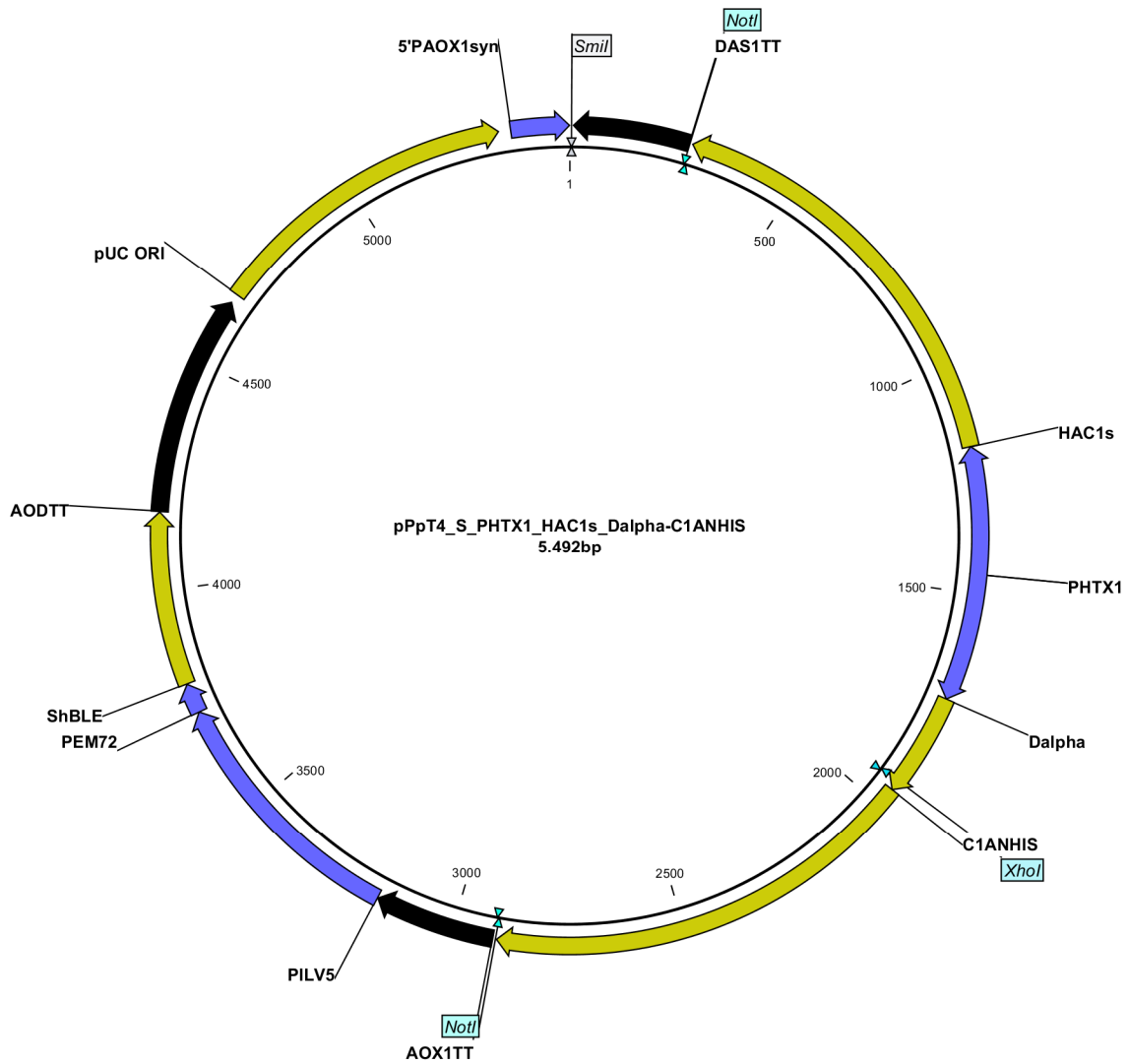
33. Vogl T, Thallinger GG, Zellnig G, Drew D, Cregg JM, Glieder A, Freigassner M: **Towards improved membrane protein production in *Pichia pastoris*: General and specific transcriptional response to membrane protein overexpression.** *N. Biotechnol.* 2014, **31**:538–52.
34. Dietzsch C, Spadiut O, Herwig C: **A dynamic method based on the specific substrate uptake rate to set up a feeding strategy for *Pichia pastoris*.** *Microb. Cell Fact.* 2011, **10**:14–22.
35. Krainer FW, Gmeiner C, Neutsch L, Windwarder M, Pletzenauer R, Herwig C, Altmann F, Glieder A, Spadiut O: **Knockout of an endogenous mannosyltransferase increases the homogeneity of glycoproteins produced in *Pichia pastoris*.** *Sci. Rep.* 2013, **3**:3279–91.
36. Näätäsaari L, Mistlberger B, Ruth C, Hajek T, Hartner FS, Glieder A: **Deletion of the *Pichia pastoris* KU70 Homologue Facilitates Platform Strain Generation for Gene Expression and Synthetic Biology.** *PLoS One* 2012, **7**:e39720.
37. Kaufman RJ: **Stress signaling from the lumen of the endoplasmic reticulum: coordination of gene transcriptional and translational controls.** *Genes Dev.* 1999, **13**:1211–33.
38. Travers KJ, Patil CK, Wodicka L, Lockhart DJ, Weissman JS, Walter P: **Functional and genomic analyses reveal an essential coordination between the unfolded protein response and ER-associated degradation.** *Cell* 2000, **101**:249–58.
39. Garcia-Ortega X, Ferrer P, Montesinos JL, Valero F: **Fed-batch operational strategies for recombinant Fab production with *Pichia pastoris* using the constitutive GAP promoter.** *Biochem. Eng. J.* 2013, **79**:172–181.
40. Gmeiner C, Saadati A, Maresch D, Krasteva S, Frank M, Altmann F, Herwig C, Spadiut O: **Development of a fed-batch process for a recombinant *Pichia pastoris* Δ och1 strain expressing a plant peroxidase.** *Microb. Cell Fact.* 2015, **14**.
41. Ruth C, Buchetics M, Vidimce V, Kotz D, Naschberger S, Mattanovich D, Pichler H, Gasser B: ***Pichia pastoris* Aft1 - a novel transcription factor, enhancing recombinant protein secretion.** *Microb. Cell Fact.* 2014, **13**:120.
42. Fitzgerald I, Glick BS: **Secretion of a foreign protein from budding yeasts is enhanced by cotranslational translocation and by suppression of vacuolar targeting.** *Microb. Cell Fact.* 2014, **13**:125.
43. Krainer FW, Dietzsch C, Hajek T, Herwig C, Spadiut O, Glieder A: **Recombinant protein expression in *Pichia pastoris* strains with an engineered methanol utilization pathway.** *Microb. Cell Fact.* 2012, **11**:22–35.
44. Lin-Cereghino J, Wong WW, Xiong S, Giang W, Luong LT, Vu J, Johnson SD, Lin-Cereghino GP: **Condensed protocol for competent cell preparation and transformation of the methylotrophic yeast *Pichia pastoris*.** *Biotechniques* 2005, **38**:44–48.
45. Küberl A, Schneider J, Thallinger GG, Anderl I, Wibberg D, Hajek T, Jaenicke S, Brinkrolf K, Goesmann A, Szczepanowski R, Pühler A, Schwab H, Glieder A, Pichler H: **High-quality genome sequence of *Pichia pastoris* CBS7435.** *J. Biotechnol.* 2011, **154**:312–320.
46. Harju S, Fedosyuk H, Peterson KR: **Rapid isolation of yeast genomic DNA: Bust n' Grab.** *BMC Biotechnol.* 2004, **4**:8–13.
47. Waldo GS, Standish BM, Berendzen J, Terwilliger TC: **Rapid protein-folding assay using green fluorescent protein.** *Nat. Biotechnol.* 1999, **17**:691–5.
48. Vogl T, Ruth C, Pitzer J, Kickenweiz T, Glieder A: **Synthetic Core Promoters for *Pichia pastoris*.** *ACS Synth. Biol.* 2013:0–3.
49. Weis R, Luiten R, Skranc W, Schwab H, Wubbolts M, Glieder A: **Reliable high-throughput screening with *Pichia pastoris* by limiting yeast cell death phenomena.** *FEMS Yeast Res.* 2004, **5**:179–89.
50. Krainer FW, Capone S, Jäger M, Vogl T, Gerstmann M, Glieder A, Herwig C, Spadiut O: **Optimizing cofactor availability for the production of recombinant heme peroxidase in *Pichia pastoris*.** *Microb. Cell Fact.* 2015, **14**.
51. Abad S, Kitz K, Hörmann A, Schreiner U, Hartner FS, Glieder A: **Real-time PCR-based determination of gene copy numbers in *Pichia pastoris*.** *Biotechnol. J.* 2010, **5**:413–20.
52. Shevchenko A, Wilm M, Vorm O, Mann M: **Mass spectrometric sequencing of proteins silver-stained polyacrylamide gels.** *Anal. Chem.* 1996, **68**:850–8.

Supplementary information

Supplementary table 1. Primer sequences. Oligonucleotides in 5'-3' orientation for PCR amplification of the indicated targets.

PCR product	forward primer	reverse primer
<i>DALPHA</i>	ATATGAGCTCGCTCATTCCAAT	ATATCTCGAGAGAGACACCCTTTCCT TAGCAGCAATGGAAGCAGAGAAAGGCA AAACAGCG
<i>KEX2</i>	ATATGAATTCCGAAACGATGTATTTGC CAGCACTTCG	ATATGCGGCCGCATTACAATGCCGCAC GTTTG
<i>STE13</i>	ATATGAATTCCGAAACGATGACATCTC GGACAGCTGAG	ATATGCGGCCGCATTACAAAAATCTAT CGTAAAATGCCCC
active <i>HAC1</i>	ATATGAATTCCGAAACGATGCCCGTAGA TTCTTCTCA	ATATGCGGCCGCATTATTCCTGGAAGA ATACAAAGTCATTCAAATCAAATGCAT TAGCGGTAAATGGTGCTGCTGGATGAT GCAACCGAT
PHTX1 with <i>HAC1</i> - and $\Delta\alpha$ -C1ANHIS overlaps	TAGCTGTCTTATGAGAAGAATCTACGG GCATTGTTGTAGTTTTAATATAGTTTTG AGTATG	AACAAGACAGCGGTGAAAATAGATGGG AATCTCATTITGATTTGTTTAGGTAAC TTGAAC
$\Delta\alpha$ -C1ANHIS	ATGAGATTCCCATCTATTTTCA	ATATGCGGCCGCATTATGAGTTAGAG
pPpT4_TT backbone with <i>HAC1</i> - and $\Delta\alpha$ - C1ANHIS overlaps	TTGAACTGCCGTGTTGTCAACTCTAAC TCATAATGCGGCCGCTCAAGAGGATGT CAG	GAATGACTTTGTATTCTTCCAGGAATA ATGCGGCCGCACGGGAAGTCTTTACAG TTTTAG

Supplementary figure 1. Vector map of pPpT4_SmiI_PHTX1_HAC1_Dalpha-C1ANHIS. AOX1TT, *AOX1* transcription terminator; PILV5, *ILV5* promoter; PEM72, synthetic *EM72* promoter; ShBLE, *BLE* gene for zeocin™ resistance; AODTT, *AOD* transcription terminator; pUC ORI, pUC origin of replication; 5'PAOX1syn, synthetic sequence upstream of *PAOX1*; DAS1TT, *DAS1* transcription terminator; HAC1s, active *HAC1* gene; PHTX1, bidirectional *HTX1* promoter; DALPHA, Δ N57-I70 mutant gene of the *S. cerevisiae* mating factor alpha prepro signal peptide; C1ANHIS, mature C1A gene with N-terminal hexahistidine tag.



- Chapter 6 -

**Characterization of recombinant horseradish peroxidase isoenzymes from
*Pichia pastoris***

Florian W. Krainer¹, Kirsty McLean², Joseph Hosford², Lu Shin Wong², Barbara Darnhofer³,
Ruth Birner-Grünberger³, Anton Glieder¹ and Andrew W. Munro^{2*}

¹ Graz University of Technology, Institute of Molecular Biotechnology, Graz, Austria

² University of Manchester, Manchester Institute of Biotechnology, Manchester,
United Kingdom

³ Functional Proteomics Core Facility, ACIB GmbH - Austrian Centre of Industrial
Biotechnology, Medical University of Graz, Austria, office: Stiftingtalstraße 24, 8010
Graz, Austria

* Corresponding author: Andrew W. Munro, University of Manchester, Manchester
Institute of Biotechnology, Faculty of Life Sciences, 3.026 John Garside Building, 131
Princess Street, Manchester, M1 7DN, United Kingdom;
andrew.munro@manchester.ac.uk; Tel: +44161 306 5151

Abstract

Horseradish peroxidase is a versatile enzyme with applications in diagnostics and histochemistry, biocatalysis, bioremediation and medicine. Despite the considerable demand for enzyme preparations at consistent high quality, current preparations are still isolated from horseradish roots as mixtures of isoenzymes with different biochemical properties. Most research on horseradish peroxidase focused on a single isoenzyme C1A, neglecting the distinct characteristics and potential of the other natural isoenzymes. Recombinant production in microbial hosts was hampered by low yields and challenging downstream processing. We recombinantly produced the well-studied isoenzyme C1A, an acidic isoenzyme A2A and a basic isoenzyme E5 in *Pichia pastoris* and performed comprehensive comparative characterizations thereof including the determination of biophysical properties as well as application-oriented kinetic studies on colorimetric substrates for diagnostic assays and on indole acetic acid which has been suggested as substrate in an enzyme-prodrug system for cancer treatment. The characterization of natural horseradish peroxidase isoenzymes broadens our understanding of this industrially relevant enzyme and will facilitate rational protein design studies towards improved biocatalysts.

Keywords

Horseradish peroxidase, plant peroxidase, isoenzymes, *Pichia pastoris*, protein purification, enzyme characterization, indole-3-acetic acid

Abbreviations

ABTS, 2,2'-azino-bis(3-ethylbenzothiazoline-6-sulfonic acid); BHA, benzhydroxamic acid; BMD, buffered minimal dextrose; BMGY, buffered minimal glycerol-complex medium; BMM, buffered minimal methanol; BSM, basal salts medium; Ca-TBS, calcium-supplemented Tris-buffered saline; DCFH-DA, 2',7'-dichlorodihydrofluorescein diacetate; DSC, differential scanning calorimetry; DWP, 96-deep well plate; EPR, electron paramagnetic resonance; HS, high-spin; IAA, indole-3-acetic acid; IMAC, immobilized metal affinity chromatography; IS, intermediate-spin; LS, low-spin; MALLS, multiangle laser light scattering; MS, mass spectrometry; Mut^S, methanol utilization slow; NHA, 2-naphthohydroxamic acid; PTM1, trace element solution; rHRP, recombinant horseradish peroxidase; QS, quantum-

mechanically mixed-spin; SEC, size exclusion chromatography; TMB, 3,3',5,5'-tetramethylbenzidine; YE, yeast extract; YNB, Difco™ yeast nitrogen base w/o amino acids.

Introduction

Peroxidase from horseradish (*Armoracia rusticana*) is a class III peroxidase, EC 1.11.1.7. The first appearance of horseradish peroxidase (HRP) activity in literature dates back to 1810 (1). Since then, multiple protein components from horseradish with peroxidase activity were found and described, *e.g.* (2–6). These isoenzymes were not only characterized by distinct reactivities towards different substrates but were also found to vary in their relative amounts in response to environmental factors such as soil, weather or season (3). Up to 42 different HRP isoenzymes were detected in commercial preparations by isoelectric focusing (7). So far, most studies focused on the isoenzyme C1A. Until recently, only eight amino acid sequences of HRP isoenzymes were available from public databases. In 2013, this number was greatly increased by a next-generation sequencing of the horseradish transcriptome (8, 9).

HRP contains a prosthetic heme group, which is bound to the Nε2 atom of the H170 residue at the fifth coordination site of the heme iron (10). Resting state HRP heme has been described previously by a quantum-mechanically mixed-spin (QS) state due to an admixture of high-spin (HS) and intermediate-spin (IS) states (11, 12), which was found to be common in class III peroxidases (13). Different HRP isoenzymes were described to vary in the extent of the admixed intermediate-spin states (11). Further typical structural features of active plant-derived HRP are the presence of N-glycans, four disulfide bridges and two calcium ions (10). A peroxidative cycle is the main route of HRP catalysis. Peroxide species, most commonly H₂O₂, oxidize HRP from its ferric resting state to compound I, an oxoferryl species with a porphyrin-based π cation radical. The latter can be eliminated by a reducing substrate, leaving the oxoferryl species, compound II. Oxidation of another molecule of a reducing substrate restores the resting state (14–17). In the absence of a reducing substrate, excess H₂O₂ forms a complex with compound I that can lead to irreversible inactivation of the enzyme. Inactivation can be avoided by restoring the ferric state either by formation of a dioxygen-bound ferrous species, compound III, or a pseudocatalase activity (18, 19).

Applications for HRP are diverse and numerous (20). Most commonly, HRP is used as a reporter enzyme in diagnostics. The oxidation of chromogenic substrates such as 2,2'-azino-bis(3-ethylbenzothiazoline-6-sulfonic acid) (ABTS) or 3,3',5,5'-tetramethylbenzidine (TMB) by HRP facilitates a rapid and easily quantifiable detection. Since 1999 (21, 22), the reaction of HRP with the plant hormone indole-3-acetic acid (IAA) has been studied extensively for its

use in cancer treatment. The reaction with IAA does not require the external addition of peroxide and follows a complex mechanism distinct from the peroxidative cycle that leads to the formation of several enzyme intermediates, IAA derivatives and radical species (23–25). A concomitant production of H₂O₂ by the IAA/HRP system was reported to induce apoptosis in cancer cells (26–29), explaining the cytotoxic effect of the IAA/HRP system that facilitates its application in targeted cancer treatment.

Owing to the large number of applications (20), there is a considerable demand for pure HRP. Whereas current commercial preparations are typically isolated from horseradish roots as isoenzyme mixtures, recombinant enzyme production offers an attractive alternative for an independent production process of single HRP isoenzymes at consistent quality and independent from environmental factors. Recombinant HRP (rHRP) has been produced in several host systems such as *Escherichia coli* (30–32), insect cell culture (33, 34) or *Saccharomyces cerevisiae* (35, 36). Also, the yeast *Pichia pastoris* has been successfully used for the production of active rHRPs (8, 9, 36–40). However, rHRP production is challenged by low yields and laborious downstream processing. We previously described a protocol for several rHRP isoenzyme preparations from *P. pastoris* that were partially purified by double negative chromatography (40). Here, we present the first enzymological characterization of rHRP isoenzymes from *P. pastoris*. Also, this is the first enzymological study on recombinantly produced HRP isoenzymes other than C1A.

Experimental procedures

Chemicals

Difco™ yeast nitrogen base w/o amino acids (YNB), Bacto™ tryptone and Bacto™ yeast extract (YE) were purchased from Becton Dickinson (Austria). ACEPOL 83 E was from Lubrizol Additives (Ohio, USA). Peroxidase from horseradish, Type VI-A, Lot # SLBH 1737 V, (VI-A) was purchased from Sigma-Aldrich, Austria. Other chemicals were from Carl Roth, Austria.

***Pichia pastoris* strains**

All *P. pastoris* strains in this study were based on the wildtype strain CBS 7435 (identical to NRRL Y-11430 and ATCC 76273). The Mut^S (methanol utilization slow) phenotype of *P. pastoris* was shown to be superior over the Mut⁺ phenotype in terms of volumetric productivity and production efficiency of rHRP (37). We recently described the strain

PpFWK3, a *P. pastoris* strain with Mut^S phenotype that allows a more homogeneous glycan pattern on secreted proteins than a wildtype based strain due to the inactivation of a key mannosyltransferase (38). This strain was used for the production of the recombinant HRP isoenzymes in this study. For the enzymological characterizations, we focused on the "classical" HRP isoenzyme C1A, a new acidic isoenzyme A2A, and the basic isoenzyme E5 (8, 9). To facilitate initial purification, a hexahistidine tag (6xHis) was N-terminally fused to the mature HRP peptide. Plasmids for transformation of HRP isoenzyme genes to *PpFWK3* were based on the pPpT4_Alpha_S vector (41), facilitating efficient secretion to the supernatant by the prepro peptide of the *S. cerevisiae* mating factor alpha. HRP expression was under control of the strong methanol inducible promoter of the *P. pastoris* *AOX1* gene. Transformation of HRP expression plasmids to *PpFWK3* was performed as described in (38). Screenings and rescreenings were performed in microscale cultivations in 96-deep well plates (DWP), similar to (42): Transformant strains were grown in 250 μL 3.26 $\text{mg}\cdot\text{L}^{-1}$ hemin-supplemented BMD1% (43) (11 $\text{g}\cdot\text{L}^{-1}$ alpha-D(+)-glucose monohydrate, 13.4 $\text{g}\cdot\text{L}^{-1}$ YNB, 0.4 $\text{mg}\cdot\text{L}^{-1}$ D(+)-biotin, 0.1 M potassium phosphate, pH 6.0) at 28 °C, 320 rpm, 80% humidity. After approximately 60 h, an induction pulse of 250 μL BMM2 (1% (v/v) methanol, 13.4 $\text{g}\cdot\text{L}^{-1}$ YNB, 0.4 $\text{mg}\cdot\text{L}^{-1}$ D(+)-biotin, 0.1 M potassium phosphate, pH 6.0) was added, followed by three pulses of 50 μL BMM10 (5% (v/v) methanol, 13.4 $\text{g}\cdot\text{L}^{-1}$ YNB, 0.4 $\text{mg}\cdot\text{L}^{-1}$ D(+)-biotin, 0.1 M potassium phosphate, pH 6.0) per well 12, 24 and 36 h after the first pulse. The relative amount of produced HRP activity per strain was quantified by mixing 15 μL supernatant with 140 μL assay solution (1 mM ABTS, 0.9 mM H_2O_2 , 50 mM sodium acetate, pH 4.5) in a microtiter plate and following the increase in absorbance at 405 nm on a Spectramax Plus 384 platereader (MolecularDevices, Germany) at room temperature.

Recombinant production of horseradish peroxidase isoenzymes in *Pichia pastoris*

Production of rHRPs was performed either in 5 L BIOSTAT[®]CT or BIOSTAT[®]Cplus fermentor systems (Sartorius Stedim Biotech, Germany). All bioreactor cultivations were performed at 28 °C at pH 5 and a minimal dO_2 of 30%, using the following media: Trace element solution (PTM1): 5.99 $\text{g}\cdot\text{L}^{-1}$ $\text{CuSO}_4\cdot 5\text{H}_2\text{O}$, 0.08 $\text{g}\cdot\text{L}^{-1}$ KI, 3 $\text{g}\cdot\text{L}^{-1}$ $\text{MnSO}_4\cdot\text{H}_2\text{O}$, 0.2 $\text{g}\cdot\text{L}^{-1}$ $\text{Na}_2\text{MoO}_4\cdot 2\text{H}_2\text{O}$, 0.02 $\text{g}\cdot\text{L}^{-1}$ H_3BO_3 , 0.92 $\text{g}\cdot\text{L}^{-1}$ $\text{CoCl}_2\cdot 6\text{H}_2\text{O}$, 42.18 $\text{g}\cdot\text{L}^{-1}$ $\text{ZnSO}_4\cdot 7\text{H}_2\text{O}$, 65 $\text{g}\cdot\text{L}^{-1}$ $\text{FeSO}_4\cdot 7\text{H}_2\text{O}$, 5 $\text{mL}\cdot\text{L}^{-1}$ 95-98% H_2SO_4 . Basal salts medium (BSM): 40 $\text{g}\cdot\text{L}^{-1}$ $\geq 98\%$ glycerol, 4.25 $\text{mL}\cdot\text{L}^{-1}$ 85% phosphoric acid, 0.17 $\text{g}\cdot\text{L}^{-1}$ $\text{CaSO}_4\cdot 2\text{H}_2\text{O}$, 0.22 $\text{g}\cdot\text{L}^{-1}$ NaCl, 0.64 $\text{g}\cdot\text{L}^{-1}$ KOH, 2.86 $\text{g}\cdot\text{L}^{-1}$ K_2SO_4 , 14 $\text{g}\cdot\text{L}^{-1}$

MgSO₄·7H₂O, 4.36 mL·L⁻¹ PTM1, 0.87 mg·L⁻¹ D(+)-biotin, 1 mL·L⁻¹ ACEPOL 83 E. NH₄OH was used as nitrogen source and to set and maintain pH 5. Batch cultivations were started by inoculation of 3 L BSM with two 50 mL precultures that were grown in BMGY (10 g·L⁻¹ YE, 13.4 g·L⁻¹ YNB, 20 g·L⁻¹ Bacto™ tryptone, 12.6 g·L⁻¹ glycerol, 0.4 mg·L⁻¹ D(+)-biotin, 100 mM potassium phosphate, pH 6). Upon glycerol depletion, as indicated by an increase in dO₂, a fedbatch cultivation was started by feeding glycerol at 27.2 g·h⁻¹ for 6 h. The feed media contained 50% (w/w) glycerol, 4.36 mL·L⁻¹ PTM1, 0.87 mg·L⁻¹ D(+)-biotin. HRP gene expression was induced by feeding pure methanol by using the following protocol: An initial methanol feed flow of 2.4 g·h⁻¹ was increased to 4 g·h⁻¹ over 6 h, then to 4.7 g·h⁻¹ over 2 h, to 5.5 g·h⁻¹ over 2 h, to 6.4 g·h⁻¹ over 2 h and to 7.1 g·h⁻¹ over 2 h, which was the final methanol feed rate that was maintained until the end of the cultivation. Prior to induction, hemin was added to a concentration of 19.56 mg·L⁻¹ (43). Methanol induction was performed for up to 142 h. Samples were taken regularly to determine wet cell weight, HRP activity and protein concentration. After the cultivation, the culture broth was centrifuged twice at 17,700 x *g*, 45 min, 10 °C. The supernatant was filtered through a 0.2 μm cellulose acetate filter to remove remaining cells.

Fast protein liquid chromatography

The cultivation supernatant was adjusted to pH 7.8 with sodium hydroxide and 0.2 μm filtered prior to immobilized metal affinity chromatography (IMAC) on a 5 mL HisTrap FF column (GE Healthcare, Austria) on an ÄKTA pure system (GE Healthcare). The sample was loaded onto the column at a flowrate of 10 mL·min⁻¹, the column was washed with phosphate buffered saline, pH 7.8. Bound protein was eluted with 100 mM imidazole.

Making use of the tight binding of HRP to the ligand 2-naphthohydroxamic acid (NHA), 6-amino-2-naphthoic acid was immobilized onto Affi-Gel 10 Gel agarose beads (Bio-Rad, UK) and transformed to yield agarose-bound NHA, cf. (44). Approximately 10 mL of this matrix were packed in a XK 16/20 column (GE Healthcare) for affinity chromatography. Up to 1.5 mL concentrated sample were loaded onto the column at a flowrate of 0.8 mL·min⁻¹. The column was washed with 50 mM potassium phosphate, pH 7.0. Elution was performed with 500 mM boric acid, 100 mM NaCl, pH 9.0 set with NaOH. Peroxidase-containing elution fractions were pooled, concentrated with VivaSpin 20 ultrafiltration units (5,000 Da MWCO;

Sartorius Stedim Biotech) and the buffer was changed to calcium-supplemented Tris-buffered saline (Ca-TBS; 1 mM CaCl₂, 150 mM NaCl, 50 mM Tris, pH 7.5 set with HCl).

As an alternative purification approach, approximately 14 mL of the mixed-mode chromatography resin CHT™ ceramic hydroxyapatite type I (Bio-Rad) was packed in a XK 16/20 column. Up to 1.5 mL sample in 10 mM potassium phosphate, pH 6.8, were loaded onto the column at a flowrate of 2 mL.min⁻¹. The column was washed with 10 mM potassium phosphate, pH 6.8. Elution was performed by a linear gradient to 100% 500 mM potassium phosphate, pH 6.8, over 10 column volumes.

Further size exclusion chromatography (SEC) on Superdex™ 200 columns (Superdex™ 200 10/300 GL or HiLoad™ 16/60 Superdex™ 200 prep grade; GE Healthcare) was performed with max. 1 mL sample at a flowrate of 0.3 mL.min⁻¹. Isocratic elution was performed with Ca-TBS, rHRP fractions were pooled and concentrated with VivaSpin 20 ultrafiltration units.

The relative heme content of HRP preparations was determined as the ratio of the absorbance at 403 nm over 280 nm. This ratio is referred to as *Rz* value (45). Molar concentrations of purified HRP preparations were determined by the pyridine hemochromogen method (46).

Size exclusion chromatography-multiangle laser light scattering (SEC-MALLS)

In order to evaluate the homogeneity and dispersity of purified rC1A, 200 μL of 1 mg.mL⁻¹ rC1A in Ca-TBS buffer was used for a SEC run at a flow rate of 0.75 mL.min⁻¹ on a Superdex™ 200 column connected to a Dawn® Heleos® system (Wyatt Technology, UK). The refractive index was measured with an Optilab® rEX, the data was analyzed with the Astra® 6 software (both Wyatt Technology).

Mass spectrometry

For tryptic digest, 20 μg of protein was solubilized in 50 μL of 100 mM NH₄HCO₃, reduced with 34 μL of 10 mM dithiothreitol for 20 min by shaking at 550 rpm at 56 °C and alkylated with 8 μL of 55 mM iodoacetamide by shaking at 550 rpm at room temperature for 15 min. Protein was digested by adding 0.5 μg of Promega modified trypsin or 0.5 μg chymotrypsin and shaking over night at 550 rpm, 37 °C. The resulting peptide solution was acidified by adding 1.6 μL of 5% formic acid and separated by nano-HPLC (Dionex Ultimate 3000) equipped with a C18 enrichment column (5 μm, 100 Å, 5 x 0.3 mm) and an Acclaim PepMap

RSLC nanocolumn (C18, 2 μm , 100 \AA , 500 x 0.075 mm) (all Thermo Fisher Scientific, Austria). Samples were concentrated on the enrichment column for 2 min at a flow rate of 20 $\mu\text{L}\cdot\text{min}^{-1}$ with 0.5% trifluoroacetic acid as isocratic solvent. Separation was carried out on the nanocolumn at a flow rate of 200 $\text{nL}\cdot\text{min}^{-1}$ using the following gradients, where solvent A is 0.3% formic acid in water and solvent B is a mixture of 80% acetonitrile in water containing 0.3% formic acid: 0-2 min 4% B, 2-35 min 4-28% B, 35-47 min 28-50% B, 47-48 min 50-95% B, 48-58 min 95% B, 58-58,1 min 95-4% B, 58,1-70 min 4% B. The sample was ionized in the nanospray source equipped with nanospray tips (PicoTipTM Stock# FS360-75-15-D-20, Coating: 1P-4P, 15 \pm 1 μm Emitter, New Objective) and analyzed in a Thermo LTQ-FT mass spectrometer in positive ion mode by alternating full scan mass spectrometry (MS) (m/z 200 to 2000) in the ICR cell and MS/MS by CID of the five most intense peaks in the ion trap. Proteome Discoverer 1.4 (Thermo Electron) and Mascot 2.4 (Matrix Science) were used for MS/MS data analysis by searching the NCBI nr database (downloaded on 02.02.2013, 7847231743 residues, 22826945 sequences) and the SwissProt database (downloaded on 04.12.2013, 541762 sequences). Detailed search criteria; enzyme: trypsin, maximum missed cleavage sides: 2, N-terminus: hydrogen, C-terminus: free acid, Cys modification: carbamidomethylation, search mode: homology search, possible multiple oxidized methionine, maximum precursor charge 3; precursor mass tolerance ± 0.05 Da, product mass tolerance ± 0.7 Da., 5% false discovery rate. We filtered according to stringent peptide acceptance criteria, including mass deviations of ± 10 ppm, Mascot ion score of at least 17 and a position rank 1 in Mascot search.

Electron paramagnetic resonance spectroscopy

Continuous wave X-band electron paramagnetic resonance (EPR) spectroscopy was performed on an ELEXSYS E500 EPR spectrometer with an ER 4122SHQ Super High Q cavity, an ESR900 cryostat connected to an ITC503 temperature controller (Oxford Instruments, UK). One hundred μM HRP solutions in Ca-TBS buffer were frozen in liquid N_2 . EPR spectra were recorded at 10 K at 0.5 mW microwave power, a modulation frequency of 100 kHz and a modulation amplitude of 10 Gs.

Redox potentiometry

Midpoint potentials of $\text{Fe}^{3+}/\text{Fe}^{2+}$ redox couples were determined in an anaerobic glove box (Belle Technology, UK) at 25 °C in N_2 atmosphere ($\text{O}_2 < 5$ ppm). Spectroelectrochemical titration was performed in 100 mM potassium phosphate, pH 7.0, 10% (w/w) glycerol, which was deoxygenated by sparging with N_2 gas for >1 h. Five to ten μM HRP samples were deoxygenated by passing through a Econo-Pac[®] 10DG gravity flow column (Bio-Rad) in the glove box. Reductive titration was done with sodium dithionite, reoxidation with potassium ferricyanide. Approximately 2 μM phenazine methosulfate, 7 μM 2-hydroxy-1,4-naphthoquinone, 0.3 μM methyl viologen, 1 μM benzyl viologen were used as mediators from -480 to 100 mV. Spectra were recorded from 800 to 250 nm throughout the titrations with a fiber optic absorption probe connected to a Cary 50 Bio UV-Vis spectrophotometer (both Varian, UK). Potentials were measured with an InLab[®] Redox Micro electrode connected to a SevenEasy[™] pH meter (both Mettler-Toledo, UK). Absorbance changes at A403, A437 and A490 as well as the triple absorbance change $A440 - (A430 + A450)/2$ (47) were used for comparative analysis. Data fitting and analysis were done as described previously (48, 49).

pH stability

The influence of pH on HRP stability was evaluated by diluting the enzyme to a final storage concentration of 0.1 μM in either 50 mM sodium citrate, pH 4, pH 5, pH 6, or in 50 mM potassium phosphate, pH 6, pH 7, pH 8, or in 50 mM Tris-HCl, pH 8, pH 9. The solutions were stored at 4 °C for two weeks. Residual HRP activity was determined regularly by further diluting aliquots in Ca-TBS buffer and subsequent ABTS assay: Sixty μL of these dilutions was mixed with 740 μL assay solution containing ABTS and H_2O_2 with final concentrations of 5 mM and 3 mM respectively.

Kinetic stability towards H_2O_2 inactivation

The kinetic stability towards inactivation by H_2O_2 was studied by incubation of 0.1 μM HRP with varying molar ratios of $[\text{H}_2\text{O}_2]/[\text{HRP}]$ from 250 to 150,000 for 3 h at room temperature. Residual HRP activity was measured regularly throughout the incubation and k_{in} values were calculated. By plotting k_{in} over $[\text{H}_2\text{O}_2]/[\text{HRP}]$, the maximal k_{in} , the half life $\tau_{1/2}$, and the molar

$[H_2O_2]/[HRP]$ ratio at which inactivation occurred at halfmaximal rate, K_i , were calculated by non-linear curve fitting using Origin 9.0 (Origin Lab Corp., Massachusetts, USA).

Kinetic stability towards temperature

The kinetic stability towards temperature was determined at 25, 37, 50, 60, 70 °C at a HRP concentration of 0.1 μ M. Due to evaporation, unbiased data could not be guaranteed at temperatures higher than 70 °C. The residual HRP activity was measured in regular intervals throughout the incubation with the ABTS assay as described above. In case of a continuous decrease in residual activity, k_{in} and the half life $\tau_{1/2}$, were determined as described in (50).

Differential scanning calorimetry

Thermal unfolding of HRP was studied by differential scanning calorimetry (DSC) in a VP-DSC Micro Calorimeter (MicroCal Inc., Massachusetts, USA) controlled by the VPViewer 2000 1.4.23 software (MicroCal) with 50 μ M HRP from 20 to 100 °C at a scan rate of 90 °C.h⁻¹ and a 10 min pre-scan thermostat period. Prior to DSC scans, samples were dialyzed against degassed Ca-TBS. The same buffer was used for background scans. The data was analyzed with the Microcal™ Origin™ 5.0 software.

Ligand binding titrations

Spectral titrations were performed at 25 °C on a Cary 50 Bio UV-Vis spectrophotometer. An initial ligand-free spectrum of 3 μ M HRP was recorded prior to ligand titration. Ligand-bound spectra were recorded after stepwise additions of benzhydroxamic acid (BHA; in Ca-TBS buffer). Difference spectra were calculated by subtracting ligand-bound spectra from the initial ligand-free spectrum. Absorbance values were corrected for dilution. K_d values were calculated by fitting a quadratic function (51) to the double absorbance change A408-A403 as a function of BHA concentration.

Steady-state kinetics with ABTS, TMB and H₂O₂

A 20 mM ABTS stock solution (in 50 mM sodium acetate, pH 4.5) was diluted to final ABTS concentrations ranging from 0.1 to 10 mM in the reaction mixture with a constant H₂O₂ concentration of 3 mM. A 0.5 mM TMB stock solution was prepared by dissolving 4.7 mg TMB dihydrochloride hydrate in 3 mL dimethyl sulfoxide and addition of 27 mL 50 mM

sodium citrate, pH 5.5. The TMB stock was further diluted with 50 mM sodium citrate, pH 5.5, to final TMB concentrations ranging from 0.02 to 0.4 mM in the reaction mixture with a constant H₂O₂ concentration of 3 mM. A 50 mM H₂O₂ stock solution was diluted to final concentrations from 0.1 to 3 mM in the reaction mixture with constant concentrations of either 10 mM ABTS or 0.4 mM TMB. Sixty μ L of 1 - 5 nM HRP was mixed with 640 μ L of a solution with the reducing substrate. The reaction was started by adding 100 μ L of H₂O₂ solution and mixing by inversion. The increase in absorbance at 405 nm or at 652 nm was followed on a Cary 50 Bio UV-Vis spectrophotometer at 25 °C with either ABTS ($\epsilon_{405} = 34.700 \text{ M}^{-1} \cdot \text{cm}^{-1}$, (36)) or TMB ($\epsilon_{652} = 39,000 \text{ M}^{-1} \cdot \text{cm}^{-1}$, (52)) as reducing substrate. Non-linear curve fitting with the Michaelis-Menten function of the Origin 9.0 software was used to calculate rate constants.

Steady-state kinetics with indole acetic acid

The reaction of HRP with IAA was studied by following the formation of reactive oxygen species (ROS), similar to (27). 2',7'-dichlorodihydrofluorescein diacetate (DCFH-DA) is oxidized by ROS, yielding a fluorescent product. A 12.5 mM DCFH-DA stock solution was prepared in absolute ethanol. The DCFH-DA stock solution was activated by 1:6 dilution in 10 mM sodium hydroxide and incubation for 30 min at room temperature. The reaction was started by mixing 400 μ L of HRP with 400 μ L of assay solution, containing 0.02 mM DCFH-DA and varying concentrations of IAA. Final IAA concentrations ranged from 5 to 500 μ M in the reaction mixture. The increase in fluorescence (ex/em 485/527 nm) was followed on a Cary Eclipse Fluorescence spectrophotometer from Varian at 25 °C to allow a relative comparison of the ROS productivities of the different HRP preparations reacting with IAA.

Stopped-flow studies with indole acetic acid

Stopped-flow studies were performed on a SX18 MR stopped-flow spectrophotometer (Applied Photophysics, UK) equipped with a xenon lamp, a 360 nm filter to eliminate UV-induced photolysis (24) and a photodiode array detector. Experiments were performed in 50 mM potassium phosphate, pH 7.2. All solutions were prepared with water of Type 1 grade (18 M Ω .cm). Four μ M HRP solutions were shot against 5 mM IAA, the reaction was followed for 30 s. Data analysis was performed with the Pro-Kineticist 1.0.12 software (Applied Photophysics).

Results

Production of recombinant horseradish peroxidase isoenzymes

Recombinant production of HRP in microorganisms such as *P. pastoris* allows consistent yields of individual target HRP isoenzymes in controllable production processes. Basic protein parameters of the rHRPs of this study are shown in Table 1, an alignment of the mature amino acid sequences is shown in Figure 1. The three isoenzymes are rather different from one another (Table 1) and much more similar (*i.e.* approximately 90% identity) to homologous peroxidases from mouse-ear cress (*Arabidopsis thaliana*) (9). Conserved regions involve residues of the distal and proximal heme cavity, R38-V46 and D162-H170 respectively.

C1A	QLTPTFYDNSCPNVSNIIVRDTIVNELRSDPRIAASILRLHFHDCFVNGCD	50
A2A	QLNATFYSGTCCPNASAIIVRSTIQQAFQSDTRIGASLIRLHFHDCFVNGCD	50
E5	QLRPDFYSRTCPSVFNIIKNVIVDELQTDPRIAASILRLHFHDCFVNGCD	50
	** ** . : ** . . * : : . . * : : : * ** . * : : * * * * * * * * * * * * * * * *	
C1A	ASILLDNTTSFRTEKDAFGNANSARGFPVIDRMKAAVESACPRTVSCADL	100
A2A	ASILLDDSGSIQSEKNAGPNANSARGFNVDNIKTALENTCPGVVSCSDI	100
E5	ASILLDTSKSFRTKDAAPNVNSARGFNVIDRMKTALERACPRTVSCADI	100
	* * * * * : * : : : * * * * * * . * * * * * * * : * . : * : * * * * * * * * * * * * * * * *	
C1A	LTIAAQQSVTLGGPSWRVPLGRRDSLQAFDLANANLPAPFFFTLPQLKD	150
A2A	LALASEASVSLTGGPSWTVLLGRRDSLANTLAGANSAIPSPFEGLSNITS	150
E5	LTIASQISVLLSGGPSWAVPLGRRDSVEAFFDLANTALPSFFFTLAQLKK	150
	* : * : : * * * * * * * * * * * * * * * * * * : * * * : * : * * * * * * * * * * * * * * * *	
C1A	SFRNVGLNRSSDLVALSGGHTFGKNQCRFIMDRLYNFSNTGLPDPPTLNNT	200
A2A	KFSAVGLNT-NDLVALSGAHTFGRARCGVFNRRLFNFSGTGNPDPTLNST	199
E5	AFADVGLNRPSDLVALSGGHTFGRARCLFVTARLYNFNGTNRPDPTLNPS	200
	* * * * * . * * * * * * * * * * * : * * . . * * : * * . * * * * * * * * * * * * * * * *	
C1A	YLQTLRGLCPLNGNLSALVDFDLRTPTIFDNKYVNLLEEQKGLIQSDQEL	250
A2A	LLSSLQQLCPQNGSASTITNLDLSTPDAFDNNYFANLQSNNGLLQSDQEL	249
E5	YLADLRRRCPRNGNGTVLVNFDVMTPTFDNQFYTNLRNGKGLIQSDQEL	250
	* * : * * * * * . : : : : * * * * * : : * * . . * * : * * * * * * * * * * * * * * * *	
C1A	FSSPNATDIPLVRSFANSTQTFNFAFVEAMDRMGNITPLTGTQGQIRLN	300
A2A	FSTTG-SATIAVVTSFASNQTLFFQAFASMINMGNISPLTGSNGEIRLD	298
E5	FSTPG-ADTIPLVNLYSNTLSFFGAFADAMIRMGNLRPLTGTQGEIRQN	299
	* * : * * * * * : *	
C1A	CRVVNSN	307
A2A	CKKVNGS	305
E5	CRVVNSR	306
	* : * * .	

Figure 1. Alignment of the amino acid sequences of mature C1A, A2A, E5.

Production strains for rHRPs were selected based on high-throughput screens from microscale cultivations in 96-DWPs. Recombinant HRP were produced in bioreactor cultivations. Volumetric activity yields of up to 50 U.mL⁻¹ were achieved for rC1A in bioreactor cultivations. Volumetric yields of rA2A and rE5 were lower with max. 20 U.mL⁻¹ and 4 U.mL⁻¹ respectively. Although the volumetric HRP activity was still increasing over

cultivation time, the specific activity flattened at the end of the cultivation indicating beginning cell lysis and thus leakage of intracellular proteins to the culture broth. In contrast to a recent bioprocessing study using the same strain *PpFWK3* for HRP production (53), we did not observe foam formation.

Table 1. Protein parameters of recombinant horseradish peroxidase isoenzymes. Sequence identities were calculated with mature HRP peptide sequences (LALIGN). Calculations of molecular weight (MW), isoelectric point (pI) (Compute pI/MW, (54, 55)), the amount of potential N-glycosylation (N-X-S/T) sites (NetNGlyc 1.0) and disulfide bonds (9) were based on sequences assuming cleavage of the prepro mating factor alpha between A87 and E88, upstream the 6xHis tag and the mature HRP peptide.

HRP	% identity rC1A	% identity rA2A	% identity rE5	MW kDa	pI	N-X-S/T sites	disulfide bonds
rC1A	100.0	56.4	69.6	34.85	6.54	9	19-99, 52-57, 105-309, 185-217
rA2A	56.4	100.0	57.6	32.91	5.64	9	19-99, 52-57, 105-307, 184-216
rE5	69.6	57.6	100.0	34.75	8.99	3	19-99, 52-57, 105-308, 185-217

The commercial preparation VI-A was analyzed by MS. The lot tested in this study (Lot # SLBH 1737 V) was found to contain at least the isoenzymes C1A (9) and A2 (56). Also, the copresence of similar isoenzymes such as 1805, C1D or C2 (9) in this preparation can not be excluded.

Purification of recombinant horseradish peroxidase isoenzymes

Purification of yeast-derived rHRP has been known to be challenging (36, 40) and previous purification of rC1A from *P. pastoris* was reported to be limited at *Rz* values of 1.2 - 1.9 (36). Initial crude purification for all rHRPs was achieved by IMAC. Additional NHA affinity chromatography yielded a rC1A preparation of *Rz* 2.2 with >95% recovery. However, NHA affinity chromatography was not successful for rA2A and rE5 due to low enzyme recovery from the elution fractions (<10%). By performing mixed-mode chromatography with CHT™ ceramic hydroxyapatite type I, rA2A could be purified to *Rz* 0.9 at >75% recovery by negative

purification. Unfortunately, rE5 could not be purified efficiently any further after IMAC. Additional SEC gave ultimate R_z values of at least 2.6, 1.6 and 0.6 for rC1A, rA2A and rE5 respectively. In repeated production batches, R_z values of up to 3.0 and 3.3 could be reached for rC1A and rA2A respectively. Whereas rC1A and rA2A eluted as distinct narrow peaks, rE5 eluted in several overlapping peaks (Supplementary Figure 1). By performing SEC-MALLS with purified rC1A, a protein species of an apparent average molar mass of 62.62 ± 0.22 kDa at a dispersity (M_w/M_n) of 1.00 ± 0.07 was determined (Supplementary Figure 2), complementing the homogeneous SEC elution behavior of this isoenzyme.

Electron paramagnetic resonance spectroscopy

Ferric class III peroxidases have been characterized by relatively complex EPR spectra arising from heme configurations in QS states consisting of mixtures of HS ($S = 5/2$) and IS ($S = 3/2$) states (12, 57).

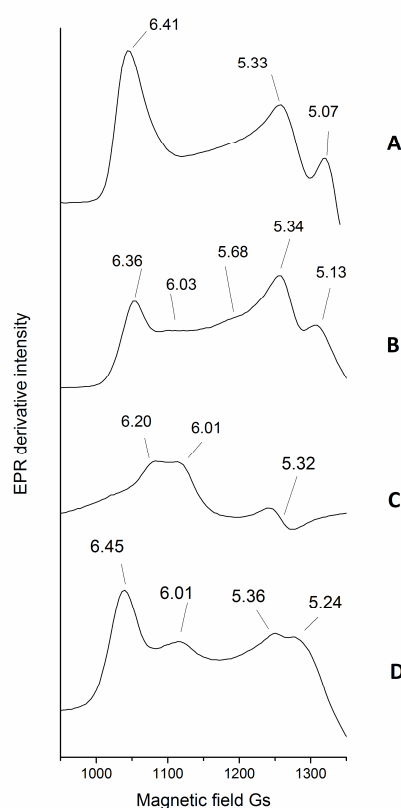


Figure 2. Mixed-spin signals of horseradish peroxidase preparations in continuous wave X-band electron paramagnetic resonance spectra. The prominent $g \sim 6$ and $g \sim 5$ signals defining the HS/QS states of the HRP preparations are indicated. HRP concentration was $100 \mu\text{M}$ in Ca-TBS buffer. EPR spectra were collected as described in the Experimental procedures section. A, VI-A; B, rC1A; C, rA2A; D, rE5.

In order to comparatively characterize the magnetic properties of the commercial preparation VI-A and the recombinant preparations rC1A, rA2A and rE5, EPR spectroscopy was performed. Similar to previous magnetic descriptions of the isoenzymes C2 and A2 (57), we observed various signals in the $g \sim 6$ and $g \sim 5$ regions, representing the HS/QS states of the studied HRP preparations (Figure 2). VI-A and rC1A shared similar HS/QS signals with g -values of 6.41 and 6.36, 5.33 and 5.34, and 5.07 and 5.13 respectively (Figure 2.A and .B), albeit at different ratios. Only a small contribution of LS ($S = 1/2$) signals with g -values of 3.13 and 3.01 for VI-A, 3.19 and 3.00 for rC1A, 3.18 and 2.93 for rA2A and 3.18 and 2.99 for rE5 were identified, which might be attributed to 6-coordinated water (not shown). In case of rHRPs from *P. pastoris*, also signals of adventitious iron were observed ($g \sim 4.26$).

Redox potentiometry

The $\text{Fe}^{3+}/\text{Fe}^{2+}$ redox couples of heme peroxidases typically have negative reduction potentials, stabilizing the ferric over the ferrous state of the resting enzyme. A stable ferric state is of particular importance *in vivo* to allow rapid oxidation of the resting enzyme by H_2O_2 to form the first catalytic intermediate species, compound I (58).

Table 2. Midpoint potentials of heme $\text{Fe}^{3+}/\text{Fe}^{2+}$ redox couples. Midpoint potentials (vs. NHE) were calculated by non-linear fitting of the redox titration data to the Nernst equation for one-electron transfers using the absorbance changes at three different wavelengths and the triple absorbance change $A_{440}-(A_{430}+A_{450})/2$.

Δ Absorbance	E^0 mV			
	VI-A	rC1A	rA2A	rE5
ΔA_{403}	-173 \pm 4	-95 \pm 2	-141 \pm 2	-112 \pm 5
ΔA_{437}	-182 \pm 5	-98 \pm 3	-144 \pm 2	-128 \pm 5
ΔA_{490}	-185 \pm 4	-91 \pm 2	-132 \pm 4	-103 \pm 5
$\Delta(A_{440}-(A_{430}+A_{450})/2)$	-186 \pm 5	-97 \pm 3	-144 \pm 3	-129 \pm 6

Spectroelectrochemical titrations were performed to determine midpoint potentials of the heme $\text{Fe}^{3+}/\text{Fe}^{2+}$ redox couples. Most notable changes were bleaching of the resting state

Soret band at 403 nm and concomitant red-shifting upon reduction of the ferric enzyme to its ferrous species. The ferrous Soret band was at 437 nm for VI-A, at 436 nm for rC1A and rA2A, and at 420 nm for rE5 (Figure 3). Isosbestic points were found at 347, 416, 466 and 533 nm for VI-A, at 350, 416, 465 and 532 nm for rC1A, at 343, 416, 463 and 533 nm for rA2A, and at 415 and 456 nm for rE5. For rE5, peak formation in the area from 530 to 600 nm was less pronounced compared to the other preparations and was only obvious in the late stages of reduction. The determined midpoint potentials (vs. NHE) of the heme $\text{Fe}^{3+}/\text{Fe}^{2+}$ redox couples of VI-A, rC1A, rA2A and rE5 are summarized in Table 2.

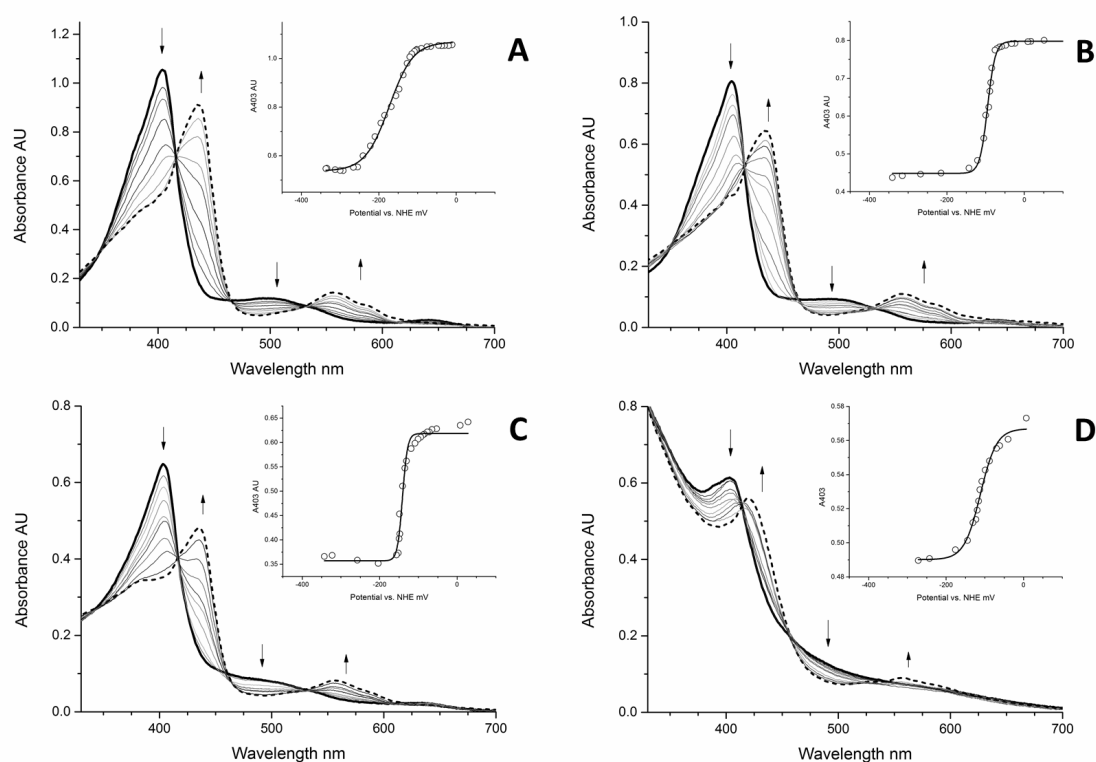


Figure 3. Redox potentiometry spectra from spectroelectrochemical titrations. Ferric and ferrous HRP spectra are shown as thick solid and dashed lines respectively. Arrows indicate absorbance changes throughout the titrations. Insets show plots of the absorbance change at 403 nm over the applied potential (vs. NHE) with a curve fitted to the one-electron Nernst equation. A, VI-A; B, rC1A; C, rA2A; D, rE5.

pH stability

We assessed the stability of the commercial preparation VI-A and the three rHRP preparations from *P. pastoris* in response to pH, temperature and H_2O_2 . The influence of pH on the kinetic stability of the enzyme was tested over a storage period of two weeks at 4 °C.

At pH 6 or higher, all HRPs retained their activities over the tested time. At pH 5, only rE5 retained its full activity, whereas VI-A, rC1A and rA2A were reduced by approximately 50% (Figure 4). After two weeks at pH 4, VI-A, rC1A and rA2A had lost more than 90% of their initial activities. Although also reduced, rE5 still showed 60% of its initial activity after two weeks at pH 4.

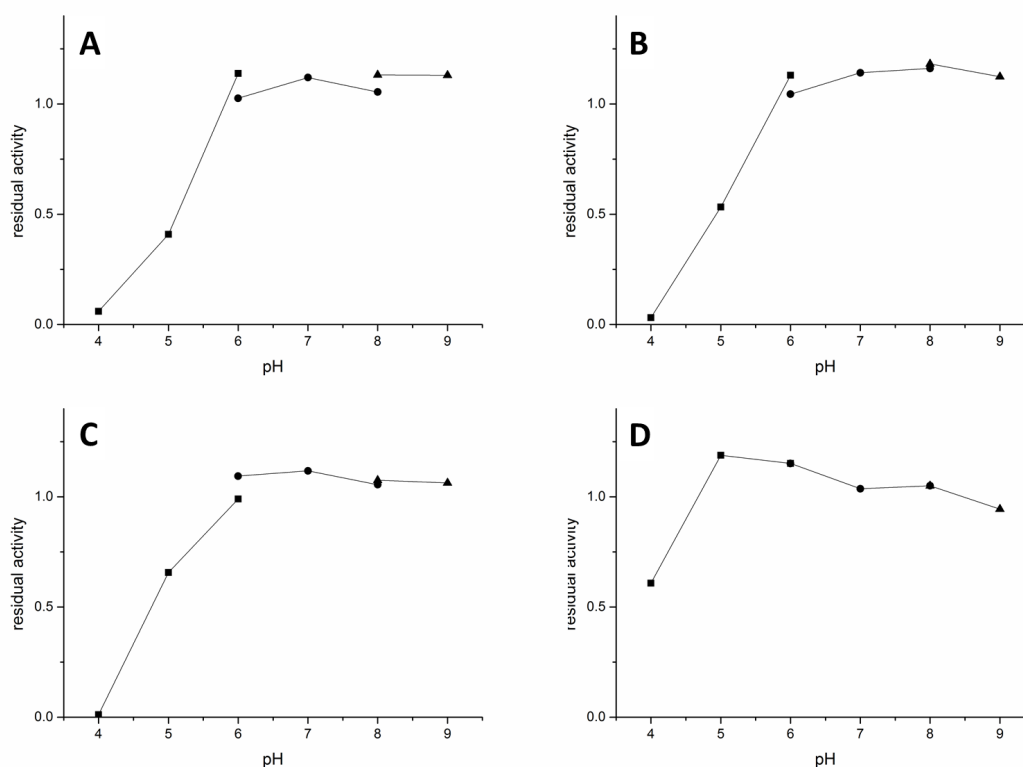


Figure 4. Residual activity after two weeks at different pH. One hundred nM HRP was incubated in buffers of different pH at 4 °C. Residual activities were measured with ABTS as reducing substrate. Square, sodium citrate buffer, pH 4, pH 5, pH 6; circle, potassium phosphate buffer, pH 6, pH 7, pH 8; triangle, Tris-HCl buffer, pH 8, pH 9. A, VI-A; B, rC1A; C, rA2A; D, rE5.

Kinetic stability towards inactivation by H₂O₂

In the absence of a reducing substrate, H₂O₂ has been described to act as a suicide substrate on peroxidases (18, 19). Rates of HRP inactivation, k_{in} , followed saturation kinetics in response to [H₂O₂]/[HRP] ratios (Figure 5). The [H₂O₂]/[HRP] ratios to yield halfmaximal k_{in} , were approximately in the same range for all four HRP preparations (Table 3) and as previously reported (59). However, the max. k_{in} varied greatly among the different isoenzymes. In contrast to the kinetic stabilities towards temperature (see below), rA2A and

rE5 were approximately four times less susceptible to inactivation by H_2O_2 than VI-A and rC1A. Even at max. k_{in} at a 150,000-fold molar excess of H_2O_2 , rA2A had a $\tau_{1/2}$ of almost three hours (Table 3).

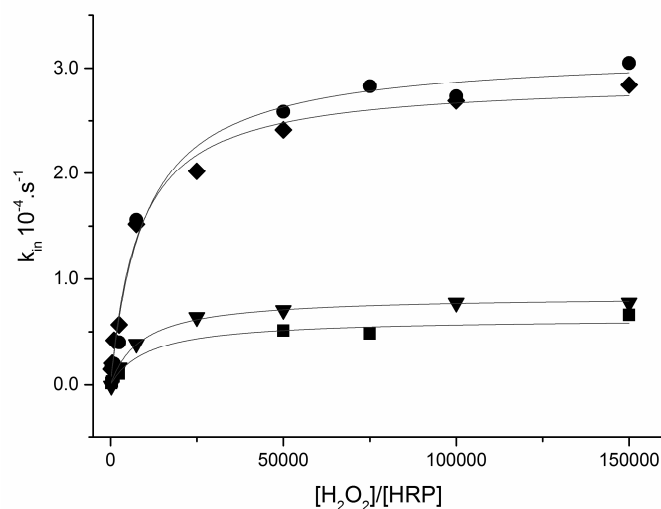


Figure 5. Kinetics of horseradish peroxidase inactivation by H_2O_2 . One hundred nM HRP was incubated with H_2O_2 at different $[\text{H}_2\text{O}_2]/[\text{HRP}]$ ratios. Residual activities were measured regularly. Diamond, VI-A; circle, rC1A; square, rA2A; triangle, rE5.

Table 3. Constants describing the inactivation of horseradish peroxidases by H_2O_2 . Max. k_{in} , maximal rate of inactivation; $\tau_{1/2}$, half life at max. k_{in} ; K_i , molar $[\text{H}_2\text{O}_2]/[\text{HRP}]$ ratio to yield half max. k_{in} .

	VI-A	rC1A	rA2A	rE5
max. k_{in} $10^{-4} \cdot \text{s}^{-1}$	2.9 ± 0.1	3.1 ± 0.2	0.7 ± 0.1	0.8 ± 0.1
$\tau_{1/2}$ min	40 ± 1	37 ± 2	174 ± 17	142 ± 4
K_i	$8,246 \pm 1,126$	$11,060 \pm 2,281$	$17,332 \pm 4,498$	$8,621 \pm 1,083$

Kinetic stability towards temperature

The process of heat-induced irreversible denaturation was followed by incubation at different temperatures. In case of VI-A and rC1A, no loss of HRP activity was observed upon incubation at temperatures as high as 70 °C. rA2A on the other hand showed a slight decrease in activity over time at 50 °C and a more pronounced decrease at 60 °C (Figure 6.A).

At 70 °C, a biphasic inactivation behavior of rA2A was observed. rA2A activity was reduced by 60% within the initial 5 min of incubation at 70 °C. Then the activity kept decreasing more slowly, comparable to k_{in} at 60 °C. rE5 only showed signs of irreversible inactivation by temperature when incubated at 70 °C (Figure 6.B). The results of the temperature-dependent inactivation of rA2A and rE5 are summarized in Table 4.

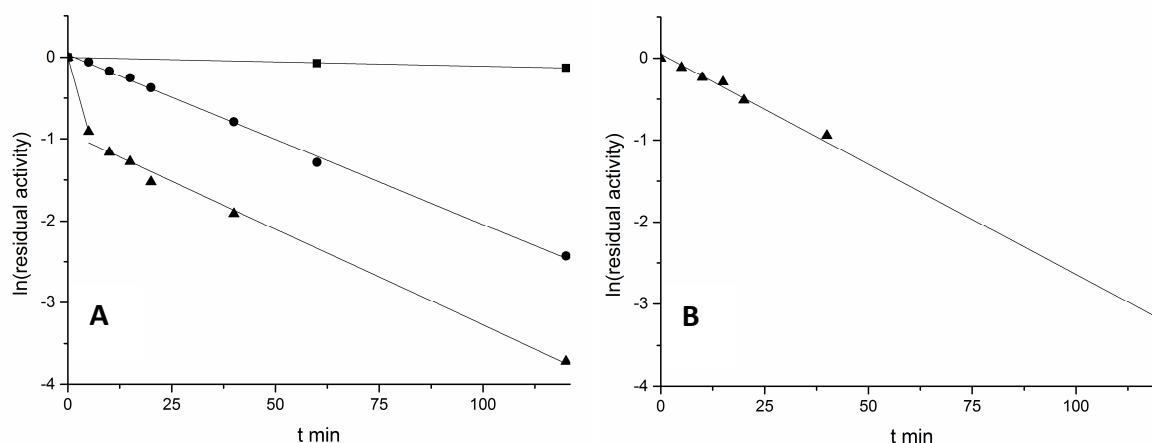


Figure 6. Kinetic stability of rA2A and rE5 at different temperatures. One hundred nM HRP was incubated at different temperatures. Residual activities were measured regularly. A, rA2A; B, rE5. Square, 50 °C; circle, 60 °C; triangle, 70 °C. rC1A and VI-A were stable at all tested temperatures.

Table 4. Kinetic stability of rA2A and rE5 at different temperatures. k_{in} , rate of inactivation; $\tau_{1/2}$, half life. In case no continuous decrease in HRP activity could be observed, the preparation was considered stable, the tested incubation time is indicated in parentheses, $\tau_{1/2}$ could not be calculated (n/a). *At 70 °C, rA2A activity decayed in two distinct steps and $\tau_{1/2}$ could not be calculated. rC1A and VI-A were stable at all tested temperatures.

		rA2A	rE5
50 °C	$k_{in} \text{ s}^{-1}$	0.06±0.01	stable (120 min)
	$\tau_{1/2} \text{ min}$	655.8±53.2	n/a
60 °C	$k_{in} \text{ s}^{-1}$	1.2±0.1	stable (120 min)
	$\tau_{1/2} \text{ min}$	33.4±0.6	n/a
70 °C	$k_{in} \text{ s}^{-1}$	10.9±1.6 / 1.4±0.1	1.4±0.1
	$\tau_{1/2} \text{ min}$	n/a *	25.8±1.3

Differential scanning calorimetry

In addition to studies on the kinetic stability towards temperature, the process of thermal unfolding of HRP was followed in DSC upscans from 20 - 100 °C. Enzyme denaturation was typically characterized by two overlapping peaks, most probably the almost simultaneous unfolding of the proximal and the distal domains of HRP. Deconvolution of the combined peak resulted in two T_m values to describe the unfolding behavior. VI-A unfolded at 81.9 ± 0.3 and 86.2 ± 0.1 °C, rC1A at 81.7 ± 0.3 and 85.7 ± 0.1 °C, rA2A at 67.0 ± 0.3 and 70.4 ± 0.1 °C (Figure 7). Due to the lower purity of rE5, its DSC data was more ambiguous than of the other preparations. However, most dominant features were approximately at 79 - 85 °C.

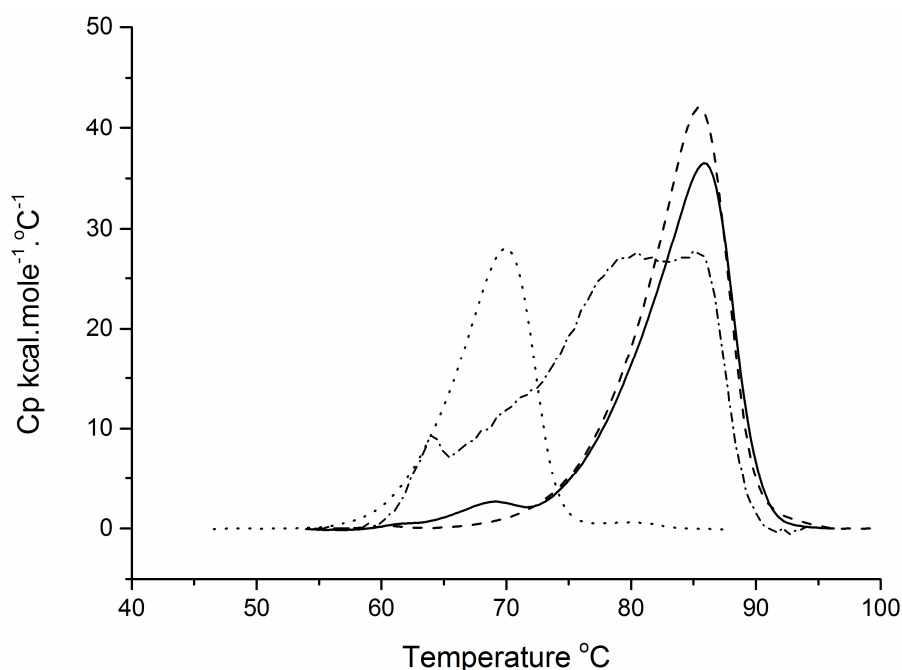


Figure 7. Thermal unfolding of horseradish peroxidases studied by differential scanning calorimetry. DSC upscan data from 20 to 100 °C, 90 °C.h^{-1} . Solid line, VI-A; dashed line, rC1A; dotted line, rA2A; dash-dotted line, rE5.

Benzhydroxamic acid binding

Aromatic hydroxamic acids such as BHA or NHA have long been known for their tight binding to HRP C1A with dissociation constants in the lower μM range (60, 61). As determined by ligand titration, the K_d values of the different HRP isoenzymes for BHA binding were found to differ by several orders of magnitude. Titration with BHA caused a narrowing of the Soret peak accompanied by a slight red-shift, indicative of a direct involvement of the heme

environment in ligand binding. Difference spectra are shown in Figure 8 exemplarily for BHA binding to rC1A. The BHA titration curves of all HRPs are shown in Supplementary Figure 3. The determined K_d values were 3.8 ± 0.2 , 3.3 ± 0.1 , $1,371.4 \pm 213.2$ and 701.2 ± 285.5 μM for BHA binding by VI-A, rC1A, rA2A and rE5 respectively. Formation of the red-shifted Soret peak upon BHA binding was considerably more pronounced in case of VI-A and rC1A than rA2A and rE5, resulting in lowered accuracy of the K_d values for the latter two.

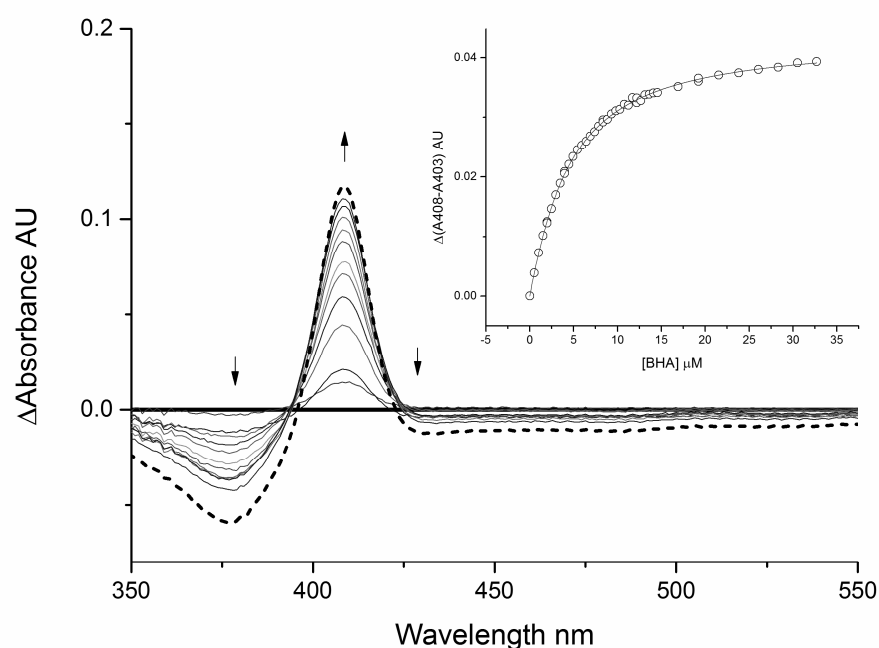


Figure 8. Difference spectra of rC1A upon titration with benzhydroxamic acid. Ligand-free and ligand-saturated difference spectra of 3 μM rC1A are shown as thick solid and dashed lines respectively. Arrows indicate absorbance changes throughout the titration. The inset shows a plot of the double absorbance change $A_{408}-A_{403}$ as a function of BHA concentration.

Steady-state kinetics with ELISA substrates

The use of HRP as a reporter enzyme is one of its most common applications. ABTS and TMB are popular chromogenic peroxidase substrates that are routinely used in diagnostic assays such as ELISA. The kinetic constants of the four tested HRP preparations with either ABTS or TMB as reducing substrate and H_2O_2 as oxidizing cosubstrate are summarized in Table 5. For VI-A, rC1A and rE5, TMB turnover was approximately equal to or faster than ABTS turnover. In contrast, rA2A-catalyzed TMB turnover was approximately 2-fold slower than ABTS

turnover (Figure 9.A and B). Also, rA2A seemed to have comparatively low affinity for ABTS as reducing substrate (Figure 9.C). In general, all four HRP preparations showed higher affinity for TMB than for ABTS (Figure 9.C). rA2A and rE5 showed considerably lower affinities for H₂O₂ than VI-A and rC1A (Figure 9.D).

Table 5. Kinetic constants for the reactions of horseradish peroxidases with colorimetric substrates. Steady-state kinetic constants were determined either with varying concentrations of ABTS or TMB as reducing substrates and H₂O₂ as initiating oxidant at constant concentration (k_{cat} , $K_M(\text{ABTS/TMB})$, k_{cat}/K_M), or with constant concentrations of ABTS or TMB and varying concentrations of H₂O₂ ($k_{cat(\text{H}_2\text{O}_2)}$, $K_M(\text{H}_2\text{O}_2)$, $k_{cat}/K_M(\text{H}_2\text{O}_2)$). Experiments were performed in triplicates, average values \pm standard deviations are shown.

Reducing substrate: ABTS						
HRP	k_{cat} s ⁻¹	$K_M(\text{ABTS})$ mM	k_{cat}/K_M mM ⁻¹ .s ⁻¹	$k_{cat(\text{H}_2\text{O}_2)}$ s ⁻¹	$K_M(\text{H}_2\text{O}_2)$ mM	$k_{cat}/K_M(\text{H}_2\text{O}_2)$ mM ⁻¹ .s ⁻¹
VI-A	2,192.2±78.0	0.606±0.031	3,618.7±185.8	2,875.9±224.0	0.943±0.155	3,050.1±500.6
rC1A	2,264.4±52.7	0.770±0.065	2,940.0±247.0	3,245.3±69.0	0.721±0.026	4,501.1±163.6
rA2A	972.8±74.5	2.184±0.215	445.5±43.9	1,656.8±274.3	2.206±0.499	751.1±169.8
rE5	2,628.4±97.6	0.607±0.064	4,328.0±455.4	4,060.9±151.9	1.698±0.131	2,391.7±184.8
Reducing substrate: TMB						
HRP	k_{cat} s ⁻¹	$K_M(\text{TMB})$ mM	k_{cat}/K_M mM ⁻¹ .s ⁻¹	$k_{cat(\text{H}_2\text{O}_2)}$ s ⁻¹	$K_M(\text{H}_2\text{O}_2)$ mM	$k_{cat}/K_M(\text{H}_2\text{O}_2)$ mM ⁻¹ .s ⁻¹
VI-A	2,798.9±233.8	0.238±0.036	11,754.3±1,792.9	2,809.7±151.6	0.596±0.077	4,712.7±608.4
rC1A	3,355.1±384.2	0.429±0.074	6,724.4±899.1	3,132.8±212.0	0.469±0.104	6,675.1±1,473.1
rA2A	539.9±37.4	0.151±0.022	3,576.0±510.4	759.4±54.5	2.396±0.386	316.9±51.1
rE5	3,124.3±192.9	0.062±0.018	50,198.1±14,485.2	4,761.8±367.7	2.463±0.255	1,933.6±200.2

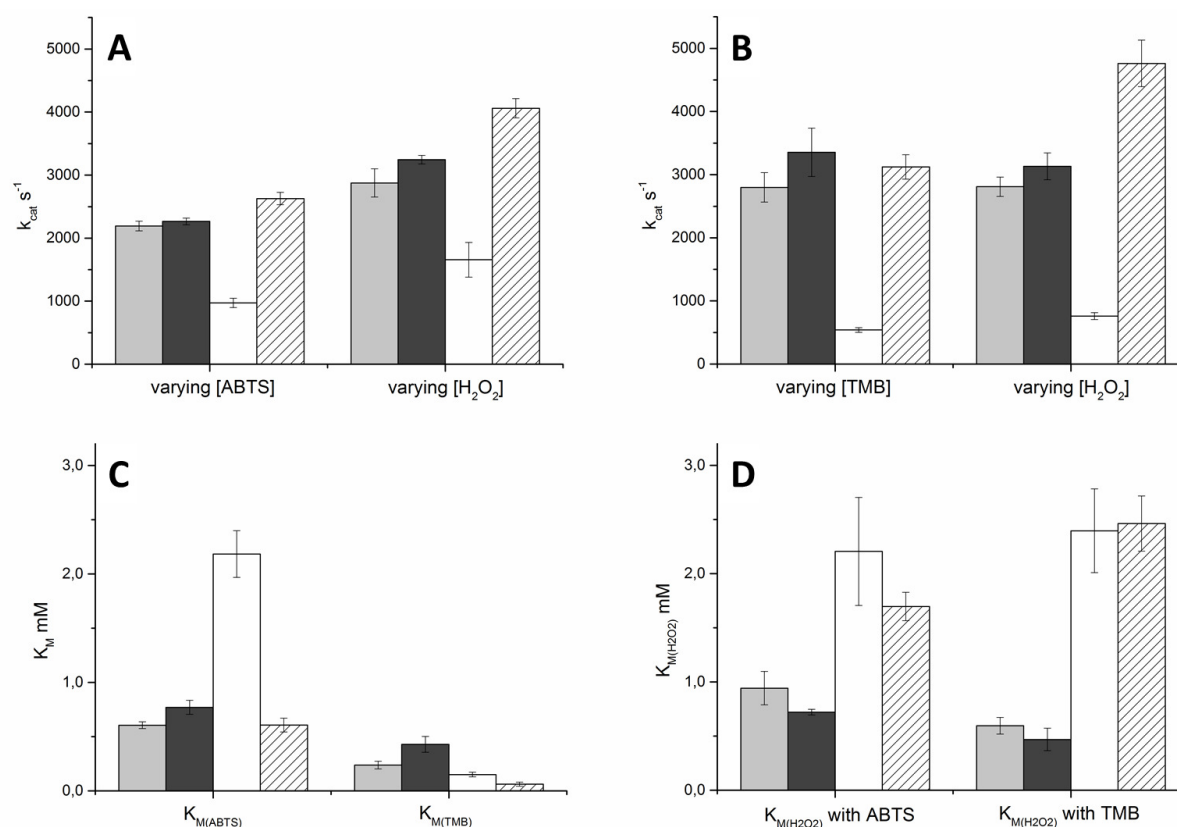


Figure 9. Kinetic constants of horseradish peroxidases with colorimetric substrates. A, k_{cat} values for ABTS oxidation from varying [ABTS] or [H₂O₂]; B, k_{cat} values for TMB oxidation from varying [TMB] or [H₂O₂]; C, K_M values for ABTS or TMB; D, K_M values for H₂O₂ with either ABTS or TMB as reducing substrate. Light gray, VI-A; dark gray, rC1A; white, rA2A; striped, rE5. Bars are average values \pm standard deviations from triplicate measurements.

Kinetic studies with indole acetic acid

In contrast to the oxidation of ABTS or TMB, oxidation of the plant hormone IAA does not require any initiating addition of peroxide. The IAA/HRP system produces ROS which are believed to induce apoptosis in targeted tumor cells in enzyme-prodrug therapy (27). The fluorogenic molecule DCFH-DA was used to follow the production of ROS upon incubation of IAA with either of the four HRP preparations. rC1A yielded fluorescence signals that were similar to those of VI-A (Figure 10.A). rA2A only gave signals of approximately 20% of VI-A and rC1A. rE5 showed a higher dependence on substrate concentration within the tested range than the other HRPs. At 500 μ M IAA, rE5 activity was approximately as high as rC1A and VI-A. However, at lower IAA concentrations rE5 activity dropped (Figure 10.A). Previous stopped-flow studies of the C1A/IAA system at neutral pH were characterized by formation

of compound II as predominant enzyme species (24) with a red-shifted Soret peak at 419 nm. We observed full conversion of ferric enzyme to compound II after an initial lag phase for the commercial preparation VI-A and rC1A (Figure 10.B) at saturating IAA concentration. We determined rates from global fits to compare compound II formation of the HRP preparations. VI-A and rC1A formed compound II with similar rate constants of 0.120 and 0.127 s^{-1} respectively. In agreement with the steady-state data, this process was approximately 80% slower for rA2A with a rate constant of 0.027 s^{-1} . rE5 was approximately 25% slower than VI-A and rC1A with a rate constant of 0.090 s^{-1} . Also, peak formation at 419 nm was less pronounced with rA2A and rE5 than with VI-A and rC1A.

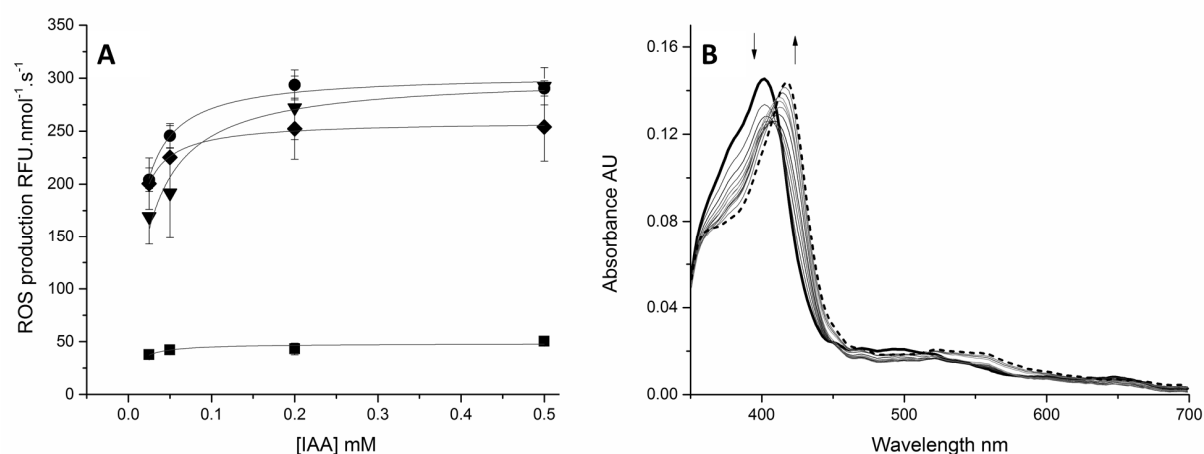


Figure 10. Oxidation of indole acetic acid by horseradish peroxidases. A, ROS production was followed by monitoring the fluorogenic oxidation of DCFH-DA (ex/em 485/527 nm). Diamond, VI-A; circle, rC1A; square, rA2A; triangle, rE5. B, Selected spectra from stopped-flow spectrophotometry. Compound II formation of 2 μ M rC1A upon mixing with 2.5 mM IAA. Solid line, resting enzyme; dashed line, compound II. Error bars are standard deviations from triplicate measurements.

Discussion

Production and purification of rHRPs

There is an undeniable demand for HRP at consistent high quality. Owing to the large number of natural isoenzymes, their different biochemical properties and uncontrollable expression patterns, the isolation procedure of HRP from the plant as the current source can not offer the same level of consistency as a recombinant production process. The *P. pastoris*

expression system for rHRP production outcompetes other microbial systems such as *E. coli* or *S. cerevisiae* due to its capability of producing comparatively high yields of active enzyme. Optimizations of the production process and strain tweaking are likely to further improve both, yield and product quality by minimizing cell lysis and maximizing rHRP secretion.

The purification of rHRPs from *P. pastoris* has been described as challenging before due to the limited feasibility of classical purification approaches, e.g. ion exchangers, hydrophobic interaction chromatography (39, 40). The heterogeneous extensive N- and O-linked yeast-type glycans on secretory proteins from *P. pastoris* are believed to mask physicochemical properties, thereby hampering the downstream processing. We have recently assessed an alternative approach based on negative chromatography with a mixed-mode hydrophobic charge induction resin and a monolithic anion exchange column and found considerable differences in the purification outcome among the tested rHRP isoenzymes (40). In 1978, the use of immobilized BHA for affinity chromatography has been reported for efficient purification of C1A due to tight binding of the ligand to this isoenzyme. An isoenzyme A was reported to have considerably weaker BHA binding, rendering the ligand unsuitable for affinity chromatography with this isoenzyme (44). However, the binding to another aromatic hydroxamic acid, NHA, was reported to be very tight (K_d 0.2 μ M) for isoenzyme C1A and at least moderately tight for isoenzyme A (K_d 10.5 μ M) (44). Hence, we tested immobilized NHA for its applicability in ligand affinity chromatography. The purification of rC1A allowed full recovery of the loaded activity and could even render the preceding IMAC step and thus the 6xHis tag unnecessary. However, neither rA2A nor rE5 showed the desirable binding behavior of rC1A to immobilized NHA. The NHA affinity matrix could thus be used to enrich C1A from a mixture of HRP isoenzymes. The identification of tightly binding ligands of rA2A and rE5 could allow analogous affinity purification approaches and considerably facilitate their purification. Since NHA affinity chromatography could not be successfully performed for rA2A and rE5 as a second purification step after IMAC, a hydroxyapatite resin was tested. The majority of rA2A activity did not bind to this resin and eluted with the loading and washing fractions whereas contaminating proteins were retained on the resin and hereby separated efficiently from rA2A. In contrast to rA2A, rE5 did bind to the hydroxyapatite resin and eluted broadly with contaminating proteins, indicating considerable physicochemical differences between these two isoenzymes, probably due to different degrees of glycosylation (Table 1). Unfortunately, further purification of rE5 with this resin was thus

unfeasible and consistent with the persistent resistance of this isoenzyme towards purification as in our previous attempts (40). We found that rHRPs from *P. pastoris* tend to elute as broad peaks from SEC columns when large amounts of contaminating proteins are present, as observed for rE5, which might indicate the formation of intermolecular aggregates. Since rC1A and rA2A could be efficiently prepurified by NHA affinity and mixed-mode chromatography respectively, they did not show this unfavorable SEC elution behavior any more. Also, use of the engineered *PpFWK3* strain for rHRP production resulted in more homogeneous N-glycosylation (38), considerably improving SEC elution. The ultimately achievable *Rz* values of 3.0 and 3.3 for rC1A and rA2A respectively indicated high purity of these HRP isoenzyme preparations (Supplementary Figure 1). The suggested molecular weight of 63 kDa for rC1A from the MALLS data is almost twice the calculated molecular weight of 35 kDa (cf. Table 1 and Supplementary Figure 2). This considerable increase in molecular weight can be ascribed to the glycan structures of rC1A from *P. pastoris* and is in agreement with previous findings, *e.g.* (43).

Biophysical characterization of rHRPs

Due to the high number of natural HRP isoenzymes, their unknown expression regulations and the considerable variation in similarity in terms of peptide sequence and biochemical properties (7, 9), a reliable separation of allelic isoenzyme variants from one another might prove to be rather laborious. Also, the yields of single isoenzymes from plant were found to be extremely low, *e.g.* 10 mg of isoenzyme E1 from 200 kg of horseradish roots (62). Recombinant production of HRP in *P. pastoris* allowed the production of individual isoenzymes without adventitious peroxidase contaminations and thus a comparative biochemical characterization of individual HRP isoenzymes.

The characterization of the magnetic properties of the different HRP preparations by EPR confirmed a QS state of the heme iron which has been described as typical for class III peroxidases (13). Also, variations in the amount of admixed HS and IS species among the isoenzymes could be observed. In this regard, the commercial preparation VI-A was most similar to rC1A, however not identical. Differences between these two samples might originate from contributions of further alike isoenzymes (*e.g.* C1B, C1C, C1D, C2, A2, 1805, (8, 9)) in the commercial preparation.

Further biophysical characterizations involved the determination of the reduction potentials (vs. NHE) of the heme $\text{Fe}^{3+}/\text{Fe}^{2+}$ redox couples. The commercial preparation VI-A showed the most negative potential of approximately -180 mV, followed by rA2A with -140 mV and rC1A and rE5 with approximately -100 mV. The lower reduction potential of VI-A compared to rHRPs might originate from so far unknown influences of its plant origin (*e.g.* peculiarities of plant-type glycans). The conserved proximal H170 residue binds the heme iron and stabilizes its ferric state due to its anionic imidazolate character which is maintained by proximal residues. In C1A, the proximal F221 is stacked against the H170 imidazole ring and a F221M mutant was found to show a lower $\text{Fe}^{3+}/\text{Fe}^{2+}$ reduction potential than the wildtype (63), probably due to removal of π - π interactions and ultimately an altered intramolecular hydrogen bonding network resulting in a stronger bond between the H170 imidazolate and the heme iron and thus a lower $\text{Fe}^{3+}/\text{Fe}^{2+}$ potential (58). Whereas F221 is conserved in C1A and E5, it is replaced in A2A by L220 (Figure 11) which might contribute to the observed lower $\text{Fe}^{3+}/\text{Fe}^{2+}$ reduction potential of rA2A compared to rC1A and rE5.

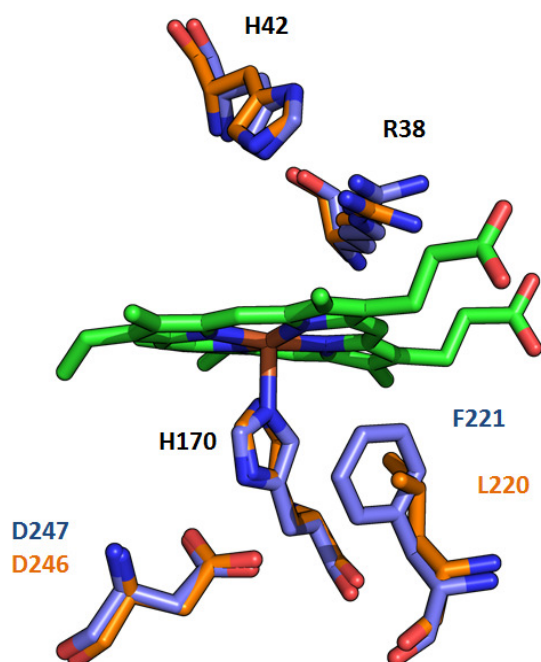


Figure 11. Heme pocket residues of C1A and A2A. Structural alignment of HRP C1A (PDB ID 1H5A; (64)) with a Phyre2 model (65) of A2A. The catalytically important distal residues H42 and R38 are shown above the heme plane (green) for orientation. Below the heme plane, the heme-coordinated H170, the proximal residues D247 and F221 of C1A (blue), and D246 and L220 of A2A (orange) are shown.

However, additional characteristics of the protein matrix are also involved in stabilizing the ferric heme state and are likely to further contribute to the determined reduction potentials. The ferrous Soret peak of rE5 (420 nm) was found closer to the ferric one compared to the other isoenzymes (436 nm), which might indicate differences among the ferrous species of the isoenzymes. However, an influence from contaminating proteins can not be excluded due to the lower purity of the rE5 preparation compared to the other isoenzymes.

Interestingly, previous reduction potentials of C1A were generally lower than the ones determined in this study (58). This deviation might reflect differences among the isoenzyme content of the used HRP preparations as well as differences dependent on the production host. However, we would like to point out that a considerable influence of the employed method and the experimental conditions on the determined potentials has been mentioned before (58) and might have contributed to the observed deviation from the previous data as well.

Characterizations of rHRP stabilities

Characterizations of HRP stability towards external stimuli revealed striking differences among the studied preparations. The basic isoenzyme rE5 was found to be more stable at lower pH than the other isoenzymes which might be attributed to its high pI of 8.99 (Table 1). In terms of stability towards H₂O₂ inactivation, rA2A and rE5 were more resistant than VI-A and rC1A. The apparent higher resistance of rA2A and rE5 might be connected to the generally lower affinities for H₂O₂ of the former two HRPs as reflected in their higher $K_{M(H_2O_2)}$ values. In a previous study, T110V and K232N mutants of rC1A produced in *E. coli* showed 25- and 18-fold improved H₂O₂ resistance respectively (66). In rA2A and rE5, K232 of rC1A is replaced by N231 and Q232 respectively. Increased H₂O₂ resistance upon loss of K232 in rC1A was suggested to be due to an altered charge distribution and hence increased pseudocatalase activity (66). T110 of rC1A is replaced by S110 and L110 in rA2A and rE5 respectively. Oxidation of the hydroxygroup of T110 of rC1A during H₂O₂ catalysis was suggested to cause lower H₂O₂ resistance to explain the higher resistance of the T110V mutant of rC1A (66). However, considering the conservation of a hydroxygroup in this position in S110 of rA2A, other structural features seem to play more important roles in terms of H₂O₂ resistance. As found for the acidic isoenzyme A2A in the present study, also the acidic isoenzymes A1 and A2 have been described before to be less sensitive to H₂O₂

inactivation than an isoenzyme C preparation (67). The apparent rate constants for max. k_{in} determined in the present study were lower than previously reported values (*e.g.* (68)). The determined higher resistance to H_2O_2 inactivation might correlate with the elevated pH of the buffer solutions used here, as reported in a previous study (59). The inactivation experiments in this study were performed at pH 7.5 whereas the previous experiments were done at pH 6.5, which could have led to the observed decreased susceptibility towards H_2O_2 inactivation.

In terms of thermal stability, VI-A and rC1A showed rather similar behavior and were found most stable, as determined by their kinetic stabilities upon incubation at different temperatures and by their unfolding behavior in DSC studies. In contrast to rC1A however, the VI-A preparation also showed a small leading peak at approximately 69 °C, more similar to rA2A than to rC1A, fitting well to the MS-verified presence of isoenzyme A2 (which is 98% identical to A2A) in the VI-A preparation. Due to the high R_z value of approximately 3 of the VI-A preparation, this peak is more likely to originate from an additional HRP isoenzyme than from other protein contaminants. The downshifted T_m of rA2A in comparison to VI-A and rC1A is in good agreement with the observed lower kinetic thermal stability, confirming a more pronounced thermal susceptibility of rA2A as opposed to the other HRP preparations. Regarding the thermal unfolding data of rE5, albeit indistinctive, it was at least indicative of a T_m between rA2A and rC1A, as in its observed kinetic thermal stability.

Binding of rHRPs to the ligand BHA

BHA has been used repeatedly in ligand binding studies with HRP, *e.g.* (69, 70). Similar to other aromatic molecules with hydroxamate function, BHA has been described to bind tightly to HRP C1A (44). The BHA dissociation constants determined in this present study were in good agreement with previous data, *e.g.* (61, 71). Whereas the tight binding of BHA to VI-A and C1A could be confirmed, rA2A and rE5 bound BHA less tightly by two to three orders of magnitude. This low affinity of rA2A and rE5 for BHA as a model aromatic hydroxamic acid agrees well with the inapplicability of immobilized NHA in affinity chromatography for these two isoenzymes. In a previous structure of a BHA-C1A complex (69), several residues were found to provide hydrophobic interactions for BHA (in addition to hydrogen bonds with the conserved active site residues R38 and H42). F68 of C1A is replaced by G68 and A68 in A2A and E5 respectively, which might weaken hydrophobic interaction

with BHA from this position. Also, A140 of C1A is replaced by S140 in both A2A and E5. And a F179 residue which is conserved in C1A and E5 is replaced by V178 at this structural position in rA2A (Figure 12). Accordingly, a F179A mutant of C1A showed a 34-fold decreased affinity for BHA (72). In conclusion, F179 seems to play an important role in the binding of aromatic molecules, however other residues are also involved as illustrated by E5 which retained F179 but still bound BHA rather weakly. Single or double mutants of rE5 (A68F, S140A) might strengthen its binding of aromatic hydroxamic acids and thus render purification of rE5 via NHA affinity chromatography feasible.

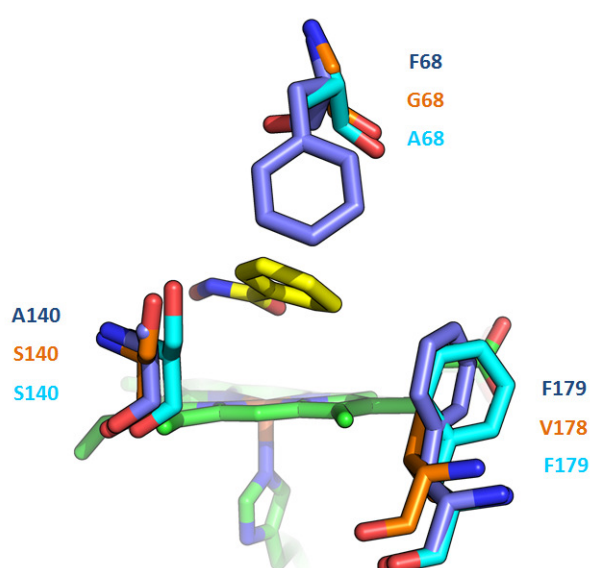


Figure 12. Selected residues of the benzhydroxamic acid binding site. Structural alignment of HRP C1A (PDB ID 2ATJ; (69)) with Phyre2 models (65) of A2A and E5. BHA (yellow) is shown above the H170-coordinated heme plane (green). Blue, C1A; orange, A2A; cyan, E5.

Enzymatic activities of rHRPs with ELISA substrates and IAA

With regards to the activity towards the ELISA substrates ABTS and TMB, rE5 outcompeted the other isoenzymes at saturating H_2O_2 concentration, with rC1A as a close second. Both rC1A and rE5 gave higher turnover rates than the commercial VI-A and could be considered for diagnostic assays with increased sensitivity. Owing to the high TMB turnover and the low K_M of rE5 for TMB, its catalytic efficiency was by far the highest of all HRP preparations. rA2A showed a much higher affinity for TMB than for ABTS but considerably slower turnover of the former than of the latter. Despite the long-lasting research on HRP no definitive

substrate binding site could be identified. The three surface phenylalanines F143, F179 and F221 are conserved in C1A and E5 but not in A2A (see Figure 1). They are close to the exposed heme methyl C18H₃ where the oxidation of aromatic substrate molecules is thought to occur (73), and might be responsible for the different behavior of rA2A towards ABTS and TMB. The importance of a peripheral hydrophobic region as binding pocket for aromatic reducing substrates has been mentioned previously (10). Further comparative studies on additional natural HRP isoenzymes are expected to contribute considerably to a better understanding of substrate binding and will allow rational protein engineering studies to design reporter rHRPs with improved substrate affinity and better catalytic efficiency.

The reaction of IAA with HRP is fairly complex, owing to large numbers of intermediates, products and enzyme states. Observations of the HRP/IAA reaction were reported to strongly depend on the experimental setup, *i.e.* pH, enzyme/substrate ratio, UV-induced photolysis (24, 74). As mentioned previously (24), ferric enzyme was found in stopped-flow studies to be transformed to compound II as the main species upon reaction with IAA (and O₂) after an initial lag phase. The global analysis performed in the present study simplified the reaction and allowed a comparison of the reactions of IAA with the different HRP preparations which was found in good agreement with the data from steady-state studies. Formation of the compound II Soret peak at 419 nm was less pronounced with rA2A and rE5 than with VI-A and rC1A and more similar to the reaction of IAA with tobacco peroxidase at neutral pH (24) and might indicate yet additional routes for IAA oxidation among HRP isoenzymes. As found in steady-state studies the affinity of the tested HRP preparations for the natural substrate IAA seemed to be higher than for the non-natural substrates ABTS and TMB. The lower activity of acidic HRP isoenzymes towards IAA has been mentioned before (75) and could be confirmed in this study. It seems likely that IAA is not a physiological substrate of acidic isoenzymes such as A2A. With regards to an application of rHRPs in cancer treatment, rC1A would be the isoenzyme of choice due to the possibility for high purity preparation and its consistently high reactivity towards IAA also at lower concentrations. However, the glycan structures on the enzyme surface are likely to interfere with the human immune system and the use of engineered yeast strains that allow the production of human-type glycans could be considered.

In conclusion, rE5 was found more similar to rC1A than rA2A (kinetic activities, Fe³⁺/Fe²⁺ reduction potential). These similarities are accompanied by a low RMS value of 0.120 of

aligned Phyre2 models (65) of rE5 and rC1A, as opposed to RMS values of 0.639 and 0.667 of structural alignments of rA2A with rC1A, and rE5 with rA2A respectively (not shown). On the other hand, rE5 shared a decreased kinetic stability towards temperature, an increased kinetic stability towards H₂O₂ and a high K_{M(H₂O₂)} with rA2A, distinguishing it from rC1A. In turn, rC1A was the isoenzyme most similar to the commercial preparation VI-A confirming a high content of this isoenzyme or similar isoenzymes therein.

In this study we presented a protocol for the recombinant production and purification of the HRP isoenzyme C1A which is a high-demand enzyme for numerous applications in life sciences. Moreover, we performed a comprehensive enzymological characterization of three different rHRP isoenzymes from *P. pastoris*. The shown data provides a profound starting point for further in-depth characterizations of these rHRPs as well as for studies on additional natural HRP isoenzymes and applications thereof.

Acknowledgements

The authors would like to gratefully acknowledge the Austrian Science Fund FWF project W901 DK Molecular Enzymology for financial support and support from NAWI Graz.

References

1. Planche, L. A. (1810) Note sur la sophistication de la résine de jalap et sur les moyens de la reconnaître. *Bull. Pharm.* **2**, 578–580.
2. Jermyn, M. A. (1952) Horseradish peroxidase. *Nature* **169**, 488–9.
3. Jermyn, M. A., and Thomas, R. (1954) Multiple components in horseradish peroxidase. *Biochem. J.* **56**, 631–9.
4. Paul, K. G. (1958) Die Isolierung von Meerrettichperoxydase. *Acta Chem. Scand.* **12**, 1312–1318
5. Shannon, L. M., Kay, E., and Lew, J. Y. (1966) Peroxidase isozymes from horseradish roots. I. Isolation and physical properties. *J. Biol. Chem.* **241**, 2166–72.
6. Kay, E., Shannon, L. M., and Lew, J. Y. (1967) Peroxidase isozymes from horseradish roots. II. Catalytic properties. *J. Biol. Chem.* **242**, 2470–3.
7. Hoyle, M. C. (1977) High resolution of peroxidase-indoleacetic acid oxidase isoenzymes from horseradish by isoelectric focusing. *Plant Physiol.* **60**, 787–93.
8. Glieder, A., Krainer, F. W., Kulterer, M., Näätäsaari, L., and Reichel, V. (2013) Horseradish peroxidase isoenzymes. *EP2584035A1*
9. Näätäsaari, L., Krainer, F. W., Schubert, M., Glieder, A., and Thallinger, G. G. (2014) Peroxidase gene discovery from the horseradish transcriptome. *BMC Genomics* **15**, 227.
10. Gajhede, M., Schuller, D. J., Henriksen, A., Smith, A. T., and Poulos, T. L. (1997) Crystal structure of horseradish peroxidase C at 2.15 Å resolution. *Nat. Struct. Biol.* **4**, 1032–8.

11. De Ropp, J. S., Mandal, P., Brauer, S. L., and La Mar, G. N. (1997) Solution NMR Study of the Electronic and Molecular Structure of the Heme Cavity in High-Spin, Resting State Horseradish Peroxidase. *J. Am. Chem. Soc.* **119**, 4732–4739.
12. Feis, A., Howes, B. D., Indiani, C., and Smulevich, G. (1998) Resonance Raman and electronic absorption spectra of horseradish peroxidase isozyme A2: evidence for a quantum-mixed spin species. *J. Raman Spectrosc.* **29**, 933–938.
13. Howes, B. D., Schiodt, C. B., Welinder, K. G., Marzocchi, M. P., Ma, J. G., Zhang, J., Shelnutz, J. A., and Smulevich, G. (1999) The quantum mixed-spin heme state of barley peroxidase: A paradigm for class III peroxidases. *Biophys. J.* **77**, 478–92.
14. Chance, B. (1952) The kinetics and stoichiometry of the transition from the primary to the secondary peroxidase peroxide complexes. *Arch. Biochem. Biophys.* **41**, 416–24.
15. George, P. (1952) Chemical nature of the secondary hydrogen peroxide compound formed by cytochrome c peroxidase and horseradish peroxidase. *Nature* **169**, 612–3.
16. George, P. (1953) The chemical nature of the second hydrogen peroxide compound formed by cytochrome c peroxidase and horseradish peroxidase. I. Titration with reducing agents. *Biochem. J.* **54**, 267–76.
17. Dolphin, D., Forman, A., Borg, D. C., Fajer, J., and Felton, R. H. (1971) Compounds I of catalase and horse radish peroxidase: pi-cation radicals. *Proc. Natl. Acad. Sci. U. S. A.* **68**, 614–8.
18. Arnao, M. B., Acosta, M., del Río, J. A., and García-Cánovas, F. (1990) Inactivation of peroxidase by hydrogen peroxide and its protection by a reductant agent. *Biochim. Biophys. Acta* **1038**, 85–9.
19. Arnao, M. B., Acosta, M., del Río, J. A., Varón, R., and García-Cánovas, F. (1990) A kinetic study on the suicide inactivation of peroxidase by hydrogen peroxide. *Biochim. Biophys. Acta* **1041**, 43–7.
20. Krainer, F. W., and Glieder, A. (2015) An updated view on horseradish peroxidases: recombinant production and biotechnological applications. *Appl. Microbiol. Biotechnol.* **99**, 1611–1625.
21. Folkes, L. K., Dennis, M. F., Stratford, M. R., Candeias, L. P., and Wardman, P. (1999) Peroxidase-catalyzed effects of indole-3-acetic acid and analogues on lipid membranes, DNA, and mammalian cells in vitro. *Biochem. Pharmacol.* **57**, 375–82.
22. Folkes, L. K., and Wardman, P. (2001) Oxidative activation of indole-3-acetic acids to cytotoxic species- a potential new role for plant auxins in cancer therapy. *Biochem. Pharmacol.* **61**, 129–36.
23. Ricard, J., and Job, D. (1974) Reaction mechanisms of indole-3-acetate degradation by peroxidases. A stopped-flow and low-temperature spectroscopic study. *Eur. J. Biochem.* **44**, 359–74.
24. Gazaryan, I. G., Lagrimini, L. M., Ashby, G. A., and Thorneley, R. N. (1996) Mechanism of indole-3-acetic acid oxidation by plant peroxidases: anaerobic stopped-flow spectrophotometric studies on horseradish and tobacco peroxidases. *Biochem. J.* **313**, 841–7.
25. Gazarian, I. G., Lagrimini, L. M., Mellon, F. A., Naldrett, M. J., Ashby, G. A., and Thorneley, R. N. (1998) Identification of skatolyl hydroperoxide and its role in the peroxidase-catalysed oxidation of indol-3-yl acetic acid. *Biochem. J.* **333**, 223–32.
26. Kim, D.-S., Jeon, S.-E., and Park, K.-C. (2004) Oxidation of indole-3-acetic acid by horseradish peroxidase induces apoptosis in G361 human melanoma cells. *Cell. Signal.* **16**, 81–8.
27. Kim, D.-S., Jeon, S.-E., Jeong, Y.-M., Kim, S.-Y., Kwon, S.-B., and Park, K.-C. (2006) Hydrogen peroxide is a mediator of indole-3-acetic acid/horseradish peroxidase-induced apoptosis. *FEBS Lett.* **580**, 1439–46.
28. Kim, D.-S., Kim, S.-Y., Jeong, Y.-M., Jeon, S.-E., Kim, M.-K., Kwon, S.-B., and Park, K.-C. (2006) Indole-3-acetic acid/horseradish peroxidase-induced apoptosis involves cell surface CD95 (Fas/APO-1) expression. *Biol. Pharm. Bull.* **29**, 1625–9.
29. Jeong, Y.-M., Oh, M. H., Kim, S. Y., Li, H., Yun, H.-Y., Baek, K. J., Kwon, N. S., Kim, W. Y., and Kim, D.-S. (2010) Indole-3-acetic acid/horseradish peroxidase induces apoptosis in TCCSUP human urinary bladder carcinoma cells. *Pharmazie* **65**, 122–6.
30. Burke, J. F., Smith, A., Santama, N., Bray, R. C., Thorneley, R. N., Dacey, S., Griffiths, J., Catlin, G., and Edwards, M. (1989) Expression of recombinant horseradish peroxidase C in *Escherichia coli*. *Biochem. Soc. Trans.* **17**, 1077–8.

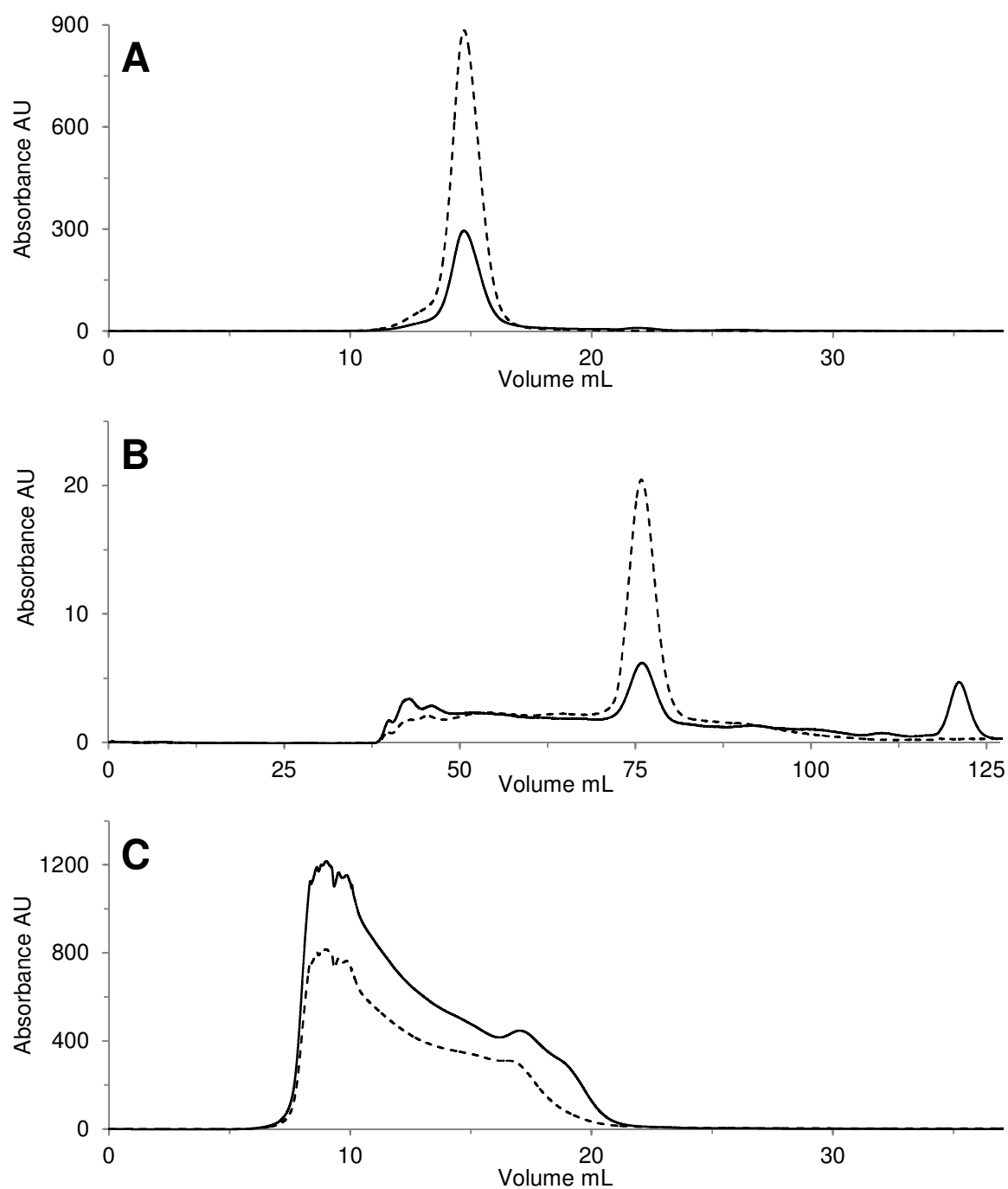
-
31. Smith, A. T., Santama, N., Dacey, S., Edwards, M., Bray, R. C., Thorneley, R. N., and Burke, J. F. (1990) Expression of a synthetic gene for horseradish peroxidase C in *Escherichia coli* and folding and activation of the recombinant enzyme with Ca²⁺ and heme. *J. Biol. Chem.* **265**, 13335–43.
32. Grigorenko, V., Chubar, T., Kapeliuch, Y., Börchers, T., Spener, F., and Egorov, A. (1999) New approaches for functional expression of recombinant horseradish peroxidase C in *Escherichia coli*. *Biocatal. Biotransformation* **17**, 359–379.
33. Hartmann, C., and Ortiz de Montellano, P. R. (1992) Baculovirus expression and characterization of catalytically active horseradish peroxidase. *Arch. Biochem. Biophys.* **297**, 61–72.
34. Segura, M. de las M., Levin, G., Miranda, M. V, Mendive, F. M., Targovnik, H. M., and Cascone, O. (2005) High-level expression and purification of recombinant horseradish peroxidase isozyme C in SF-9 insect cell culture. *Process Biochem.* **40**, 795–800.
35. Vlamis-Gardikas, A., Smith, A. T., Clements, J. M., and Burke, J. F. (1992) Expression of active horseradish peroxidase in *Saccharomyces cerevisiae*. *Biochem. Soc. Trans.* **20**, 111S.
36. Morawski, B., Lin, Z., Cirino, P., Joo, H., Bandara, G., and Arnold, F. H. (2000) Functional expression of horseradish peroxidase in *Saccharomyces cerevisiae* and *Pichia pastoris*. *Protein Eng.* **13**, 377–84.
37. Krainer, F. W., Dietzsch, C., Hajek, T., Herwig, C., Spadiut, O., and Glieder, A. (2012) Recombinant protein expression in *Pichia pastoris* strains with an engineered methanol utilization pathway. *Microb. Cell Fact.* **11**, 22–35.
38. Krainer, F. W., Gmeiner, C., Neutsch, L., Windwarder, M., Pletzenauer, R., Herwig, C., Altmann, F., Glieder, A., and Spadiut, O. (2013) Knockout of an endogenous mannosyltransferase increases the homogeneity of glycoproteins produced in *Pichia pastoris*. *Sci. Rep.* **3**, 3279–91.
39. Spadiut, O., Rossetti, L., Dietzsch, C., and Herwig, C. (2012) Purification of a recombinant plant peroxidase produced in *Pichia pastoris* by a simple 2-step strategy. *Protein Expr. Purif.* **86**, 89–97.
40. Krainer, F. W., Pletzenauer, R., Rossetti, L., Herwig, C., Glieder, A., and Spadiut, O. (2013) Purification and basic biochemical characterization of 19 recombinant plant peroxidase isoenzymes produced in *Pichia pastoris*. *Protein Expr. Purif.* **95C**, 104–112.
41. Näätäsaari, L., Mistlberger, B., Ruth, C., Hajek, T., Hartner, F. S., and Glieder, A. (2012) Deletion of the *Pichia pastoris* KU70 Homologue Facilitates Platform Strain Generation for Gene Expression and Synthetic Biology. *PLoS One* **7**, e39720.
42. Weis, R., Luiten, R., Skranc, W., Schwab, H., Wubbolts, M., and Glieder, A. (2004) Reliable high-throughput screening with *Pichia pastoris* by limiting yeast cell death phenomena. *FEMS Yeast Res.* **5**, 179–89.
43. Krainer, F. W., Capone, S., Jäger, M., Vogl, T., Gerstmann, M., Glieder, A., Herwig, C., and Spadiut, O. (2015) Optimizing cofactor availability for the production of recombinant heme peroxidase in *Pichia pastoris*. *Microb. Cell Fact.* **14**.
44. Reimann, L., and Schonbaum, G. R. (1978) Purification of plant peroxidases by affinity chromatography. *Methods Enzymol.* **52**, 514–21.
45. Paul, K.-G., Stigbrand, T., Nimmich, W., Rönquist, O., and Werner, P.-E. (1970) Four Isoperoxidases from Horse Radish Root. *Acta Chem. Scand.* **24**, 3607–3617.
46. Berry, E. A., and Trumpower, B. L. (1987) Simultaneous determination of hemes a, b, and c from pyridine hemochrome spectra. *Anal. Biochem.* **161**, 1–15.
47. Meunier, B., Rodriguez-Lopez, J. N., Smith, A. T., Thorneley, R. N., and Rich, P. R. (1998) Redox- and anion-linked protonation sites in horseradish peroxidase: analysis of distal haem pocket mutants. *Biochem. J.* **330**, 303–9.
48. Dutton, P. L. (1978) Redox potentiometry: determination of midpoint potentials of oxidation-reduction components of biological electron-transfer systems. *Methods Enzymol.* **54**, 411–435.
49. Girvan, H. M., Marshall, K. R., Lawson, R. J., Leys, D., Joyce, M. G., Clarkson, J., Smith, W. E., Cheesman, M. R., and Munro, A. W. (2004) Flavocytochrome P450 BM3 mutant A264E undergoes substrate-dependent formation of a novel heme iron ligand set. *J. Biol. Chem.* **279**, 23274–86.
-

50. Polizzi, K. M., Bommarius, A. S., Broering, J. M., and Chaparro-Riggers, J. F. (2007) Stability of biocatalysts. *Curr. Opin. Chem. Biol.* **11**, 220–225.
51. Bui, S. H., McLean, K. J., Cheesman, M. R., Bradley, J. M., Rigby, S. E. J., Levy, C. W., Leys, D., and Munro, A. W. (2012) Unusual spectroscopic and ligand binding properties of the cytochrome P450-flavodoxin fusion enzyme XpIA. *J. Biol. Chem.* **287**, 19699–714.
52. Josephy, P. D., Eling, T., and Mason, R. P. (1982) The horseradish peroxidase-catalyzed oxidation of 3,5,3',5'-tetramethylbenzidine. Free radical and charge-transfer complex intermediates. *J. Biol. Chem.* **257**, 3669–75.
53. Gmeiner, C., Saadati, A., Maresch, D., Krasteva, S., Frank, M., Altmann, F., Herwig, C., and Spadiut, O. (2015) Development of a fed-batch process for a recombinant *Pichia pastoris* Δ och1 strain expressing a plant peroxidase. *Microb. Cell Fact.* **14**.
54. Bjellqvist, B., Hughes, G. J., Pasquali, C., Paquet, N., Ravier, F., Sanchez, J. C., Frutiger, S., and Hochstrasser, D. (1993) The focusing positions of polypeptides in immobilized pH gradients can be predicted from their amino acid sequences. *Electrophoresis* **14**, 1023–31.
55. Bjellqvist, B., Basse, B., Olsen, E., and Celis, J. E. (1994) Reference points for comparisons of two-dimensional maps of proteins from different human cell types defined in a pH scale where isoelectric points correlate with polypeptide compositions. *Electrophoresis* **15**, 529–39.
56. Nielsen, K. L., Indiani, C., Henriksen, A., Feis, A., Becucci, M., Gajhede, M., Smulevich, G., and Welinder, K. G. (2001) Differential activity and structure of highly similar peroxidases. Spectroscopic, crystallographic, and enzymatic analyses of lignifying *Arabidopsis thaliana* peroxidase A2 and horseradish peroxidase A2. *Biochemistry* **40**, 11013–21.
57. Maltempo, M. M., Ohlsson, P. I., Paul, K. G., Petersson, L., and Ehrenberg, A. (1979) Electron paramagnetic resonance analyses of horseradish peroxidase in situ and after purification. *Biochemistry* **18**, 2935–41.
58. Battistuzzi, G., Bellei, M., Bortolotti, C. A., and Sola, M. (2010) Redox properties of heme peroxidases. *Arch. Biochem. Biophys.* **500**, 21–36.
59. Hiner, A. N. P., Hernández-Ruiz, J., Rodríguez-López, J. N., Arnao, M. B., Varón, R., García-Cánovas, F., and Acosta, M. (2001) The inactivation of horseradish peroxidase isoenzyme A2 by hydrogen peroxide: an example of partial resistance due to the formation of a stable enzyme intermediate. *J. Biol. Inorg. Chem.* **6**, 504–16.
60. Veitch, N. C., and Smith, A. T. (2001) Horseradish peroxidase. *Adv. Inorg. Chem. Vol. 51* **51**, 107–162.
61. Aitken, S. M., Turnbull, J. L., Percival, M. D., and English, A. M. (2001) Thermodynamic analysis of the binding of aromatic hydroxamic acid analogues to ferric horseradish peroxidase. *Biochemistry* **40**, 13980–9.
62. Aibara, S., Kobayashi, T., and Morita, Y. (1981) Isolation and properties of basic isoenzymes of horseradish peroxidase. *J. Biochem.* **90**, 489–96.
63. Howes, B. D., Veitch, N. C., Smith, A. T., White, C. G., and Smulevich, G. (2001) Haem-linked interactions in horseradish peroxidase revealed by spectroscopic analysis of the Phe-221-->Met mutant. *Biochem. J.* **353**, 181–91.
64. Berglund, G. I., Carlsson, G. H., Smith, A. T., Szöke, H., Henriksen, A., and Hajdu, J. (2002) The catalytic pathway of horseradish peroxidase at high resolution. *Nature* **417**, 463–8.
65. Kelley, L. A., and Sternberg, M. J. E. (2009) Protein structure prediction on the Web: a case study using the Phyre server. *Nat. Protoc.* **4**, 363–71.
66. Ryan, B. J., and O'Fágáin, C. (2007) Effects of single mutations on the stability of horseradish peroxidase to hydrogen peroxide. *Biochimie* **89**, 1029–32.
67. Hiner, A. N., Hernández-Ruiz, J., Arnao, M. B., García-Cánovas, F., and Acosta, M. (1996) A comparative study of the purity, enzyme activity, and inactivation by hydrogen peroxide of commercially available horseradish peroxidase isoenzymes A and C. *Biotechnol. Bioeng.* **50**, 655–62.
68. Hiner, A. N., Hernández-Ruiz, J., García-Cánovas, F., Smith, A. T., Arnao, M. B., and Acosta, M. (1995) A comparative study of the inactivation of wild-type, recombinant and two mutant horseradish peroxidase isoenzymes C by hydrogen peroxide and m-chloroperoxybenzoic acid. *Eur. J. Biochem.* **234**, 506–12.

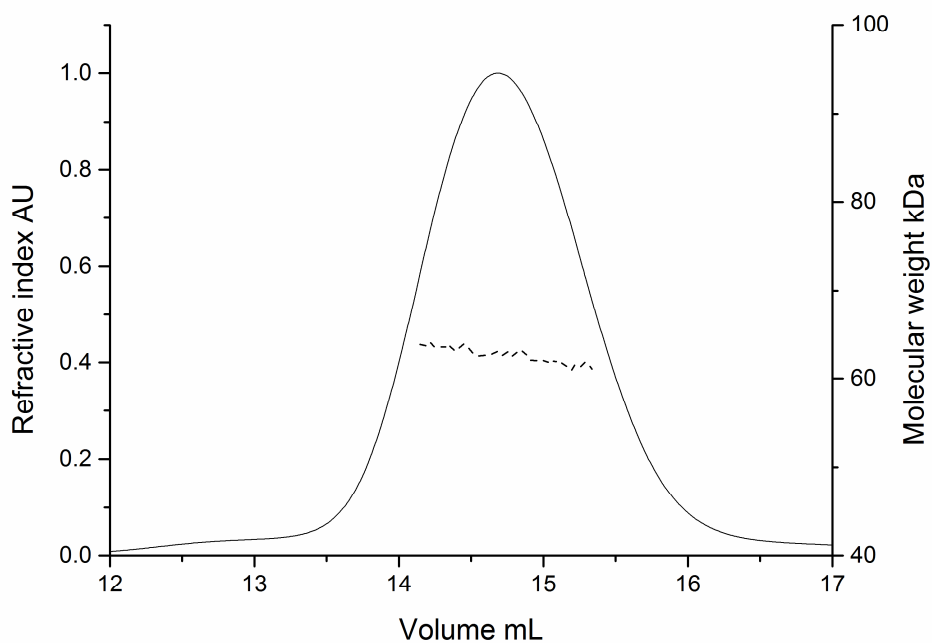
69. Henriksen, A., Schuller, D. J., Meno, K., Welinder, K. G., Smith, A. T., and Gajhede, M. (1998) Structural interactions between horseradish peroxidase C and the substrate benzhydroxamic acid determined by X-ray crystallography. *Biochemistry* **37**, 8054–60.
70. Howes, B. D., Rodriguez-Lopez, J. N., Smith, A. T., and Smulevich, G. (1997) Mutation of distal residues of horseradish peroxidase: influence on substrate binding and cavity properties. *Biochemistry* **36**, 1532–43.
71. Tanaka, M., Nagano, S., Ishimori, K., and Morishima, I. (1997) Hydrogen bond network in the distal site of peroxidases: spectroscopic properties of Asn70 --> Asp horseradish peroxidase mutant. *Biochemistry* **36**, 9791–8.
72. Veitch, N. C., Gao, Y., Smith, A. T., and White, C. G. (1997) Identification of a critical phenylalanine residue in horseradish peroxidase, Phe179, by site-directed mutagenesis and ¹H-NMR: implications for complex formation with aromatic donor molecules. *Biochemistry* **36**, 14751–61.
73. Ator, M. A., and Ortiz de Montellano, P. R. (1987) Protein control of prosthetic heme reactivity. Reaction of substrates with the heme edge of horseradish peroxidase. *J. Biol. Chem.* **262**, 1542–51.
74. Krylov, S. N., and Brian Dunford, H. (1996) Evidence for a free radical chain mechanism in the reaction between peroxidase and indole-3-acetic acid at neutral pH. *Biophys. Chem.* **58**, 325–34.
75. Nakajima, R., and Yamazaki, I. (1979) The mechanism of indole-3-acetic acid oxidation by horseradish peroxidases. *J. Biol. Chem.* **254**, 872–8.

Supplementary data

Supplementary Figure 1. Size exclusion chromatograms of recombinant horseradish peroxidases. Size exclusion chromatography of rC1A (A), rA2A (B) and rE5 (C) was performed on a Superdex™ 200 10/300 GL column or a HiLoad™ 16/60 Superdex™ 200 prep grade column. Solid line, A280; dashed line, A403.

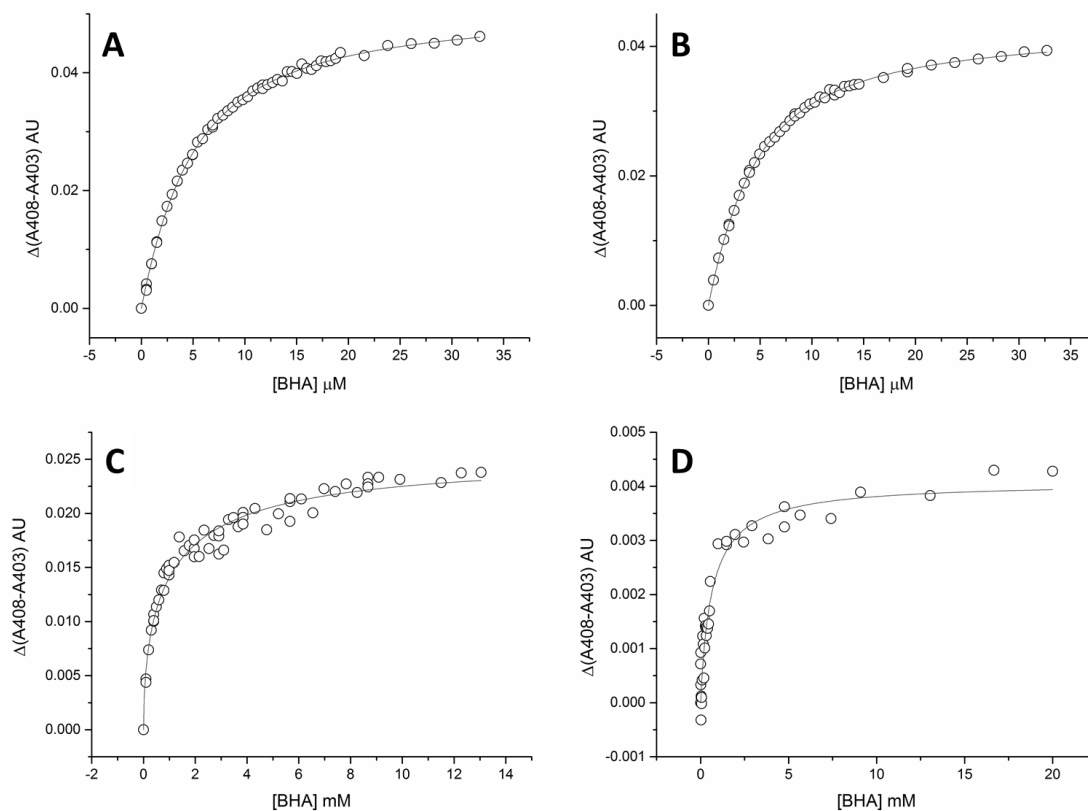


Supplementary Figure 2. Size exclusion chromatography of rC1A with multiangle laser light scattering detection. Size exclusion chromatography of rC1A was performed with a Superdex™ 200 10/300 GL column and a Dawn® Heleos® system. The elution of rC1A and the corresponding molar mass are shown. Solid line, refractive index; dashed line, molecular weight.



Supplementary Figure 3. Titration of horseradish peroxidases with benzhydroxamic acid.

Three μM solutions of HRP were titrated with BHA (all in Ca-TBS buffer). HRP binding to BHA led to a red-shift of the Soret peak. The double absorbance change A408-A403 was plotted as a function of [BHA] and a quadratic function (51) was fitted to the data. Please note the different axes scales. A, VI-A; B, rC1A; C, rA2A; D, rE5.



- Chapter 7 -

Recombinant protein expression in *Pichia pastoris* strains with an engineered methanol utilization pathway

Florian W. Krainer^{1*}, Christian Dietzsch^{2*}, Tanja Hajek¹, Christoph Herwig², Oliver Spadiut^{2†}, Anton Glieder³

¹ Graz University of Technology, Institute of Molecular Biotechnology, Graz, Austria

² Vienna University of Technology, Institute of Chemical Engineering, Research Area Biochemical Engineering, Vienna, Austria

³ Austrian Centre of Industrial Biotechnology (ACIB GmbH), Graz, Austria

* these authors contributed equally

[†] Corresponding author: Oliver Spadiut, Vienna University of Technology, Institute of Chemical Engineering, Research Area Biochemical Engineering, Gumpendorfer Strasse 1a, A-1060 Vienna, Austria; oliver.spadiut@tuwien.ac.at; Tel: +43 (0)1 58801 166473

RESEARCH

Open Access

Recombinant protein expression in *Pichia pastoris* strains with an engineered methanol utilization pathway

Florian W Krainer^{1†}, Christian Dietzsch^{2†}, Tanja Hajek¹, Christoph Herwig², Oliver Spadiut^{2*} and Anton Glieder³

Abstract

Background: The methylotrophic yeast *Pichia pastoris* has become an important host organism for recombinant protein production and is able to use methanol as a sole carbon source. The methanol utilization pathway describes all the catalytic reactions, which happen during methanol metabolism. Despite the importance of certain key enzymes in this pathway, so far very little is known about possible effects of overexpressing either of these key enzymes on the overall energetic behavior, the productivity and the substrate uptake rate in *P. pastoris* strains.

Results: A fast and easy-to-do approach based on batch cultivations with methanol pulses was used to characterize different *P. pastoris* strains. A strain with Mut^S phenotype was found to be superior over a strain with Mut⁺ phenotype in both the volumetric productivity and the efficiency in expressing recombinant horseradish peroxidase C1A. Consequently, either of the enzymes dihydroxyacetone synthase, transketolase or formaldehyde dehydrogenase, which play key roles in the methanol utilization pathway, was co-overexpressed in Mut^S strains harboring either of the reporter enzymes horseradish peroxidase or *Candida antarctica* lipase B. Although the co-overexpression of these enzymes did not change the stoichiometric yields of the recombinant Mut^S strains, significant changes in the specific growth rate, the specific substrate uptake rate and the specific productivity were observed. Co-overexpression of dihydroxyacetone synthase yielded a 2- to 3-fold more efficient conversion of the substrate methanol into product, but also resulted in a reduced volumetric productivity. Co-overexpression of formaldehyde dehydrogenase resulted in a 2-fold more efficient conversion of the substrate into product and at least similar volumetric productivities compared to strains without an engineered methanol utilization pathway, and thus turned out to be a valuable strategy to improve recombinant protein production.

Conclusions: Co-overexpressing enzymes of the methanol utilization pathway significantly affected the specific growth rate, the methanol uptake and the specific productivity of recombinant *P. pastoris* Mut^S strains. A recently developed methodology to determine strain specific parameters based on dynamic batch cultivations proved to be a valuable tool for fast strain characterization and thus early process development.

Keywords: *Pichia pastoris*, methanol utilization pathway, Mut⁺, Mut^S, recombinant protein expression, dihydroxyacetone synthase, formaldehyde dehydrogenase, transketolase, horseradish peroxidase, *Candida antarctica* lipase B

* Correspondence: oliver.spadiut@tuwien.ac.at

† Contributed equally

²Oliver Spadiut, Vienna University of Technology, Institute of Chemical Engineering, Research Area Biochemical Engineering, Gumpendorfer Strasse 1a, A-1060 Vienna, Austria

Full list of author information is available at the end of the article

Background

The methylotrophic yeast *Pichia pastoris* has become an important host organism for the high level production of recombinant proteins (e.g. [1-3]). It can be grown to high cell densities, is characterized by an efficient secretory system and many tools for molecular manipulation are available. Thus, *P. pastoris* has become an interesting and important alternative to bacterial expression systems such as *E. coli*, especially when it comes to the production of complex proteins which require typical eukaryotic post-translational modifications or contain disulfide bridges [4].

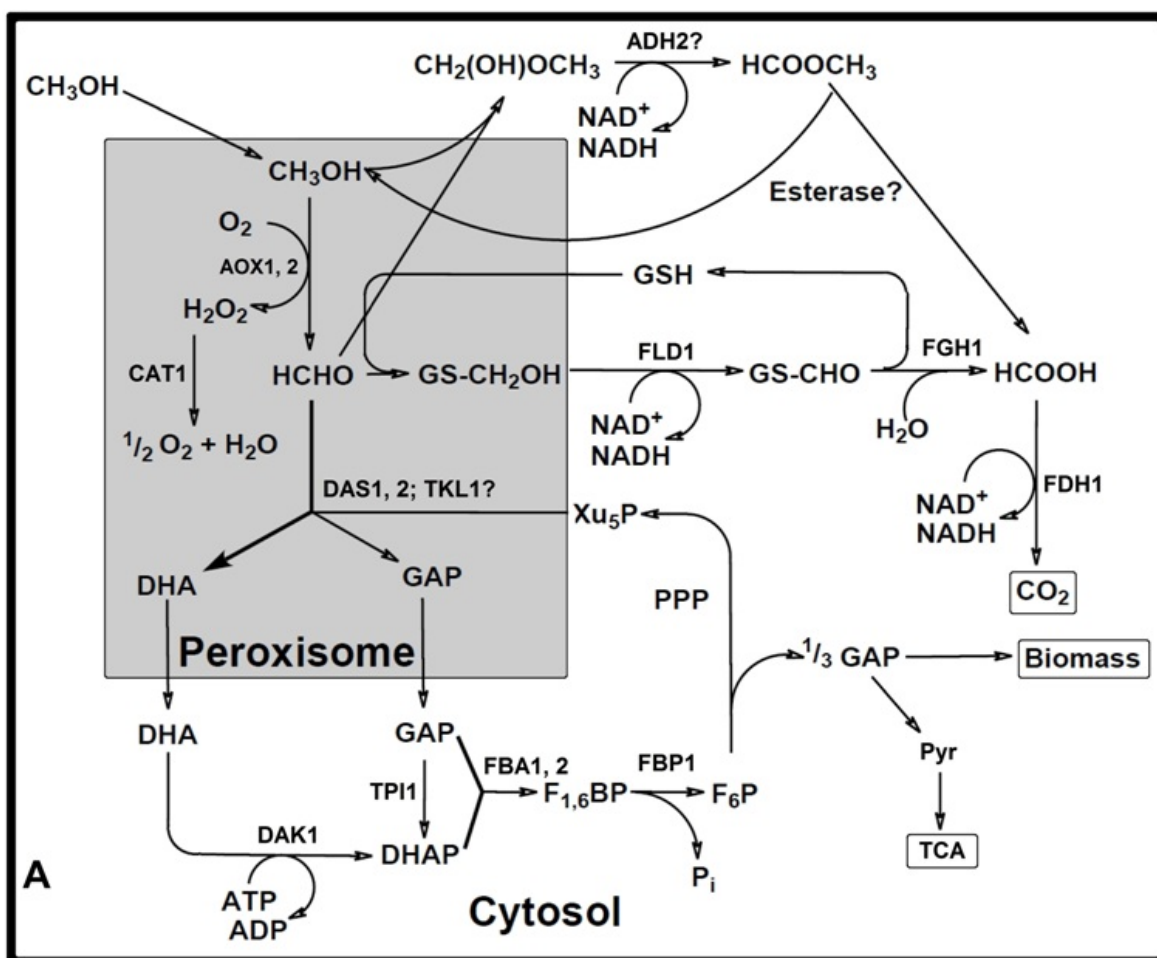
The ability of *P. pastoris* to utilize methanol as the sole carbon source is a crucial aspect of its metabolism. The enzyme alcohol oxidase (AOX, EC 1.1.3.13) catalyzes the first step in the recently described methanol utilization pathway (MUT pathway) [5]. The genome of *P. pastoris* contains two genes, *AOX1* and *AOX2*, encoding two enzymes with AOX activity [2]. *AOX1* can comprise up to 30% of the total soluble protein in extracts of *P. pastoris* grown solely on methanol [5-7], showing the outstanding strength of the *AOX1* promoter (*pAOX1*). On the contrary, the second alcohol oxidase *AOX2* is controlled by a much weaker promoter (*pAOX2*) and thus accounts for just 15% of the overall AOX activity in the cell [8]. The tight regulation of these promoters [9], the strong inducibility of *pAOX1* and differently regulated *pAOX1* promoter variants [10] as well as the alternative weaker *AOX2*-mediated methanol oxidation allow the design of different expression strains with specific properties. Three phenotypes of *P. pastoris* with regard to methanol utilization are currently available: I, Mut⁺ (methanol utilization plus), where both *AOX* genes are intact and active; II, Mut^S (methanol utilization slow), where *AOX1* is knocked out; and III, Mut⁻ (methanol utilization minus), which is unable to grow on methanol as the sole carbon source due to a knock-out of both *AOX* genes [2]. In Mut⁺ and Mut^S strains the transcription of MUT pathway genes is repressed when grown in the presence of sufficiently high concentrations of glucose or glycerol. Employing either of the two natural AOX promoters, protein expression at high levels can be induced by methanol in media lacking such fermentable carbon sources [11]. De-repression at low concentrations of glucose or glycerol can be used for strong induction, if *AOX1* promoter variants are used [10].

In general, Mut⁺ strains are characterized by a higher growth rate than Mut^S strains and have also been reported to show higher productivities [12-15]. In addition, if antibiotics are used for selection of transformants, there is no direct need to employ Mut^S strains, but wildtype strains such as *P. pastoris* CBS7435 (which

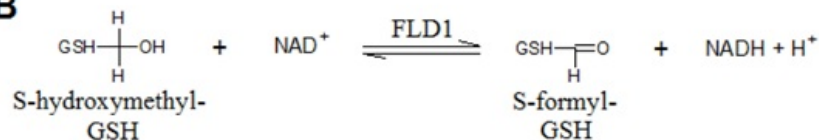
is identical to *P. pastoris* NRRL Y-11430 [16]) or *P. pastoris* X-33 can be used as hosts. This is why the majority of research so far has been performed with this phenotype. However, Mut⁺ strains are very sensitive to transient high methanol concentrations, rendering the scale up of bioprocesses more difficult [15,17,18]. Methanol oxidation is also linked to hydrogen peroxide formation as a by-product which is known to cause cellular stress and to induce cell death [19]. The combustion of methanol (-727 kJ·C·mol⁻¹) results in the production of heat, which might also constitute a problem in large scale processes. Another important issue is the high demand for oxygen in high cell density cultures of *P. pastoris* with Mut⁺ phenotype [20,21]. By using *P. pastoris* strains with Mut^S phenotype these problems can be bypassed due to the lower methanol consumption rate. However, the Mut^S phenotype also leads to long induction times and reduced growth rates. Mixed feed strategies (e.g. glycerol and methanol) are commonly employed for the fermentation induction phase when using Mut^S strains. Hereby the cells are not dependent on the slow metabolization of methanol, which then primarily functions as an inducer, and can use the alternative C-source for growth [20,22]. Moreover, the strong production of *AOX1* in Mut⁺ strains during growth on methanol may compete with the production of recombinant proteins [15]. Other advantages and disadvantages of using the *AOX1* promoter system in *P. pastoris* Mut⁺ strains have been summarized by Macauley-Patrick et al. recently [7]. Interestingly, Mut^S strains have been reported to be advantageous over Mut⁺ strains for the production of some recombinant proteins [23-25], which currently drives the ongoing discussion in the scientific community about the most favorable *P. pastoris* phenotype for recombinant protein production.

Regardless of which phenotype is used, AOX catalyzes the first reaction in the MUT pathway, oxidizing methanol to formaldehyde while reducing O₂ to H₂O₂ (Figure 1A). Formaldehyde is then either oxidized to CO₂ in the dissimilative branch of the MUT pathway giving 2 NADH molecules per molecule formaldehyde, or is condensed with xylulose-5-phosphate and subsequently converted to dihydroxyacetone and glyceraldehyde-3-phosphate in the assimilative branch of the MUT pathway (Figure 1A; see also [5]).

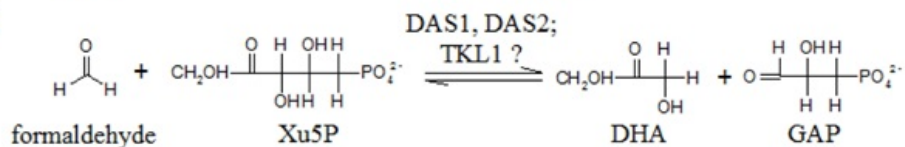
Knock-out studies of the genes encoding formaldehyde dehydrogenase (FLD, EC 1.2.1.1) and formate dehydrogenase (FDH; EC 1.2.1.2) revealed FLD, hereafter called FLD1, to be the key enzyme in the dissimilative branch of the MUT pathway [26,27]. FLD1 is encoded by the *FLD1* gene and catalyzes the NAD⁺-dependent oxidation of S-hydroxymethylglutathione to S-formylglutathione (Figure 1B). Consequently, FLD1 has



B



C



D

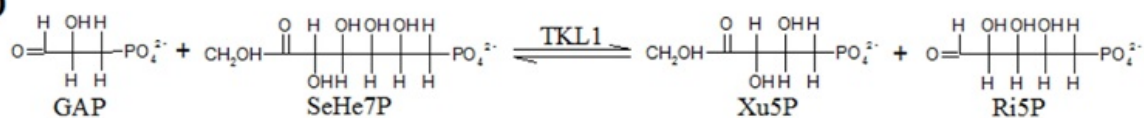


Figure 1 Methanol utilization (MUT) pathway in *P. pastoris*. **A**, MUT pathway overview (adapted from [5] and [16]); **B**, catalytic reaction of DAS1, DAS2 and hypothetically TKL1; **C**, catalytic reaction of FLD1; **D**, catalytic reaction of TKL1 in the pentose phosphate pathway. ADH: methylformate synthase. AOX: alcohol oxidase. CAT: catalase. DAK: dihydroxyacetone kinase. DHA: dihydroxyacetone. DHAP: dihydroxyacetone phosphate. F_{1,6}BP: fructose-1,6-bisphosphate. F₆P: fructose-6-phosphate. FBA: fructose-1,6-bisphosphate aldolase. FBP: fructose-1,6-bisphosphatase. FLD: formaldehyde dehydrogenase. FDH: formate dehydrogenase. FGH: S-formylglutathione hydrolase. GAP: glyceraldehyde-3-phosphate. GSH: glutathione. Pyr: pyruvate. PPP: pentose phosphate pathway. Ri5P: ribose-5-phosphate. SeHe7P: sedoheptulose-7-phosphate. TCA: tricarboxylic acid cycle. Xu₅P: xylulose-5-phosphate.

been studied in more detail in terms of being a promising enzyme for improved cofactor regeneration recently [28].

The key enzyme in the assimilative branch of the MUT pathway is dihydroxyacetone synthase (DAS; EC 2.2.1.3). In *P. pastoris*, two isoforms of DAS are encoded by the two genes *DAS1* and *DAS2* which are 91% identical [5,16]. Due to the high sequence identity, wrong sequences for these two genes were described before, which were artefacts from wrong assemblies during sequencing. Both *DAS1* and *DAS2* catalyze the conversion of xylulose-5-phosphate and formaldehyde to dihydroxyacetone and glyceraldehyde-3-phosphate (Figure 1C; [5,16]). Despite the importance of this enzyme, no analysis has been reported so far, describing whether the transcription of the two genes *DAS1* and *DAS2* is equally high induced upon methanol induction or if differences in transcription, such as for *AOX1* and *AOX2*, occur.

Another important enzyme in the assimilative branch is the transketolase (TKL; EC 2.2.1.1) [16], hereafter called TKL1, which catalyzes the reaction between xylulose-5-phosphate and ribose-5-phosphate to form glyceraldehydes-3-phosphate and sedoheptulose-7-phosphate and vice versa (Figure 1D). In *Saccharomyces cerevisiae* transketolase activity has been shown to constitute the rate-limiting factor in the non-oxidative part of the pentose phosphate pathway [29], demonstrating the importance of this enzyme in yeast metabolism. In *P. pastoris* TKL1 has recently been assigned a hypothetical dihydroxyacetone synthase activity (Figure 1C; [16]). A highly conserved domain structure of the enzymes *DAS1*, *DAS2* and TKL1 and the fact that a double knock-out strain of *DAS1* and *DAS2* is still able to grow on the substrate methanol (personal communication with Prof. Anton Glieder) actually underline this hypothesis (Additional file 1: Figure S1).

In this study, we determined and compared the specific substrate uptake rate (q_s) and the specific productivity (q_p) of a recombinant *P. pastoris* CBS7435 Mut^+ strain with a Mut^S strain, both overexpressing the reporter enzyme horseradish peroxidase (HRP), to determine the more efficient phenotype for recombinant protein expression. Based on our findings, we co-overexpressed either of the enzymes *DAS1*, TKL1 or *FLD1*, which all play key roles in the MUT pathway, in recombinant *P. pastoris* Mut^S strains harboring either of the reporter enzymes horseradish peroxidase (HRP) or *Candida antarctica* lipase B (CalB), to check for possible influences on stoichiometric yields, the growth rate, the methanol uptake and the production of the respective reporter enzyme. We used a novel and fast approach based on batch cultivations with repeated methanol pulses, which has proven to be a valuable alternative to the

traditionally more often used strategies of either employing continuous cultures or repetitive fed-batch cultivations at different parameter sets [30,31], to determine these strain specific parameters.

Results and discussion

Mut^+ vs. Mut^S for recombinant protein production

To date, the majority of research has been performed with *P. pastoris* Mut^+ strains, since they have been reported to grow faster on methanol and thus to produce more recombinant protein (e.g. [14]). However, several other studies have shown Mut^S strains to be superior over Mut^+ strains in terms of recombinant protein production (e.g. [23]). To shed more light on this controversial topic, we designed *P. pastoris* strains overexpressing the reporter enzyme HRP in both phenotypes Mut^+ and Mut^S , and compared these two strains in terms of specific substrate uptake rate, specific productivity and volumetric productivity. This strain characterization was performed using a recently reported strategy employing fast and easy-to-do batch cultivations with methanol pulses [30,31] and is shown for the Mut^S and for the Mut^+ phenotype in Additional file 2: Figure S2 and Additional file 3: Figure S3, respectively.

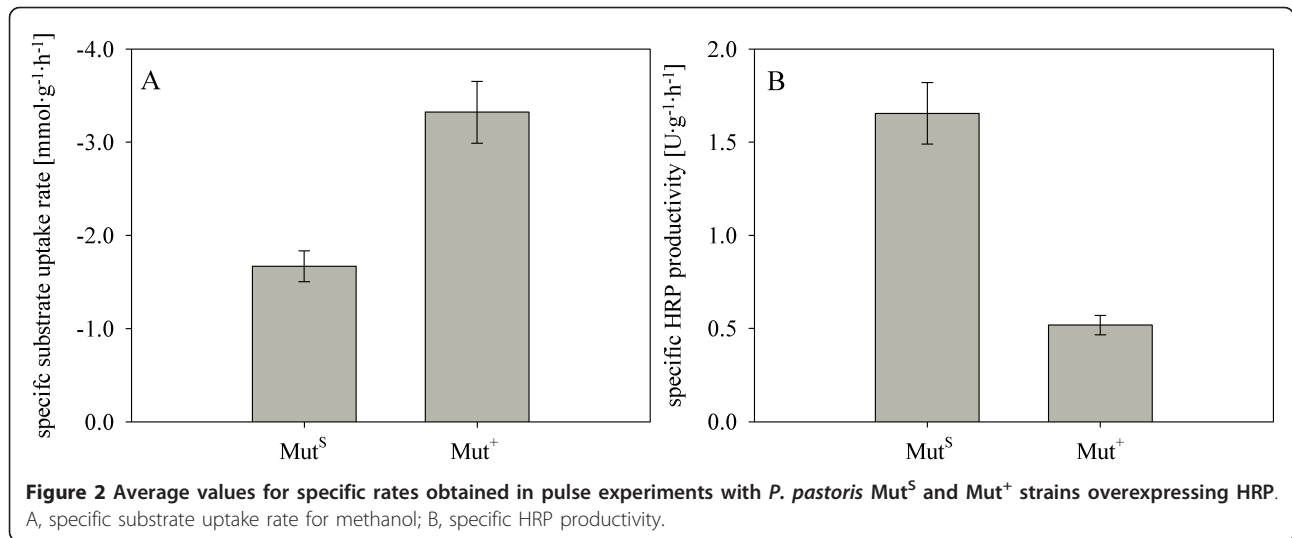
The frequent determination of biomass, methanol and product concentration allowed specific rate calculations during methanol pulses. Average values for the specific rates were calculated out of several pulses to be able to compare the two strains on the basis of a reliable set of data. The specific growth rate of the Mut^+ strain was calculated to be approximately 1.5-fold higher than for the Mut^S strain (data not shown). As shown in Figure 2, the Mut^+ strain was also characterized by a nearly 2-fold higher specific uptake rate for methanol (q_s), whereas the specific productivity (q_p) was 3-fold lower compared to the Mut^S strain.

To combine the observed effect on q_s and q_p in just one parameter and thus put the productivity of the strains in direct relation to the consumed substrate, we introduced the efficiency factor η (Eq. 1), which is in fact the product yield respective to the substrate methanol.

$$\eta = \left| \frac{q_p}{q_s} \right| \quad [\text{U/mmol}] \quad (1)$$

In Figure 3A, the benefit of using a Mut^S strain for the recombinant production of HRP is highlighted, as the substrate methanol was converted 7-fold more efficient into product compared to the Mut^+ strain.

Additionally, the volumetric productivity was calculated to compare the two Mut phenotypes in terms of product formation per volume and time. As shown in Figure 3B, the volumetric productivity of the Mut^S



strain was more than 3-fold higher than for the Mut⁺ strain, underlining the usefulness of this phenotype for the production of recombinant proteins. Interestingly, Morawski *et al.* reported up to 3-fold higher HRP activity levels using the *P. pastoris* wildtype strain X-33 with Mut⁺ phenotype compared to the strain KM71 with Mut^S phenotype (*his4, aox1::ARG4*) [32]. An explanation for this contradictory result might be a difference in the gene copy number of HRP in the Mut⁺ and Mut^S strains studied by Morawski *et al.* and/or differences in the operational conditions. Since the strains used in the present study both were found to have a single copy integration of the HRP encoding gene, and since the batch cultivations were performed in the same way in the same bioreactors, we can exclude such influences. Consequently, the *P. pastoris* Mut^S strain was chosen as the basis for subsequent overexpression studies.

Transcription of the genes DAS1 and DAS2 upon methanol induction

In order to study a possible difference between *DAS1* and *DAS2* transcription upon methanol induction, as known for the *AOX1* and *AOX2* genes [33], we determined the respective transcript levels in a *P. pastoris* Mut^S strain and calculated the increase in transcription after 5 h upon induction. The transcription of *DAS1* and *DAS2* was found to be equally high induced upon methanol induction, as *DAS1* transcription was 98.1-fold and *DAS2* was 99.1-fold induced. Methanol induction of the *DAS1* and *DAS2* genes was also much stronger than for *AOX2* (about 30-fold). Considering the high sequence similarity of *DAS1* and *DAS2* and the equivalent increase in transcript levels upon methanol induction, we focused on the co-overexpression of *DAS1* to subsequently study the influence of emphasized



dihydroxyacetone synthase activity on recombinant protein expression.

Co-overexpression of the MUT pathway enzymes DAS1/FLD1/TKL1

We co-overexpressed three key enzymes of the MUT pathway, *i.e.* dihydroxyacetone synthase 1 (DAS1), formaldehyde dehydrogenase 1 (FLD1) and transketolase 1 (TKL1), to analyze possible effects on stoichiometric yields and on the strain specific parameters q_s and q_p . We used a Mut^S strain for this study, since it had been shown to be superior to the Mut⁺ phenotype in terms of recombinant protein production (*vide supra*). To be able to draw more general valid conclusions from these experiments, we used two recombinant *P. pastoris* Mut^S strains overexpressing either the reporter enzyme HRP or CalB, hereafter called benchmark strains, as a platform for co-overexpression studies with the above mentioned MUT pathway enzymes. We characterized all strains in terms of gene copy numbers of the respective reporter enzyme to exclude variations in the measured enzyme activity levels due to copy number rearrangements, such as duplications or deletions. All the generated strains had a single copy integration of the gene encoding the respective reporter enzyme. Thus, all observed variations in enzymatic activity were considered to be due to the respective co-overexpressed MUT pathway enzyme. In order to verify the successful co-overexpression of the MUT pathway enzymes, the mRNA levels of *DAS1*, *FLD1* and *TKL1* were quantified relatively to the transcript levels of the constitutively transcribed *ARG4* gene via qPCR analysis (Figure 4).

In all strains the transcript level of *AOX2* increased upon methanol addition, indicating successful induction with methanol. We also observed elevated transcript levels of the respective mRNAs of *DAS1*, *FLD1* and *TKL1* upon methanol induction in all co-overexpression strains compared to the benchmark strains (Figure 4), proving the successful co-overexpression of the MUT pathway enzymes in these strains. However, transcript levels varied between HRP and CalB strains: the transcript level of *FLD1* in the CalB FLD1 strain was 2.5-fold higher than in the HRP FLD1 strain, whereas *DAS1* and *TKL1* were 1.5-fold and 2.5-fold higher transcribed in HRP DAS1/TKL1 strains, respectively. This could be due to two reasons: despite the fact that the same amount of DNA was used for each transformation, different copy numbers of the respective genes might have integrated. Also, the genes might have integrated at different loci in the chromosome, which might influence the accessibility of the transcription machinery to the transformed gene and thus the extent of transcription. Regardless of these variations, all MUT pathway enzymes were successfully co-overexpressed, which is

why observed effects on stoichiometric yields, the specific substrate uptake rate and the specific productivity of the recombinant *P. pastoris* Mut^S strains were ascribed to these enzymes.

Characterization of *P. Pastoris* strains in the bioreactor

We characterized the *P. pastoris* Mut^S strains HRP FLD1/TKL1/DAS1 and CalB FLD1/TKL1/DAS1 using a fast and dynamic approach based on batch cultivations with repeated methanol pulses, as described in detail before [30,31].

Growth rate and stoichiometric yields of the different *P. Pastoris* strains

Due to the very low biomass growth rate of all *P. pastoris* strains in the pulsed batch experiments, the error of the dry cell weight duplicate measurements yielded standard deviations close to the determined biomass increase within one pulse (for an example see Additional files 2 and 3: Figures S2 and S3). Thus, the biomass growth rate had to be calculated using the carbon balance and the degree of reduction balance to get more accurate values. All the calculated h-values for a χ^2 test were lower than 3.84, implying that all determined values were within error margins. Furthermore, the respiratory quotients (RQ) of the strains were calculated using the online measured off-gas data and were compared with the theoretical values for RQ, which had been estimated based on the reconciled biomass yields. In general, calculated and theoretical RQ were very similar (data not shown), signifying that the reconciled biomass rates were accurate.

The specific growth rate was reduced 2- to 3-fold for strains which co-overexpressed either of the MUT pathway enzymes, compared to the benchmark strains. Apparently, the overexpression of yet another enzyme described an additional metabolic burden for the host cells and/or down-regulated the transcription of *AOX2*, as indicated by the transcription analysis (Figure 4), thus reducing the specific growth rate.

In analogy to the determination of the specific growth rates, we studied the influence of the co-overexpressed MUT pathway enzymes on the stoichiometric yields of the recombinant *P. pastoris* Mut^S strains. The yields of biomass on substrate ($Y_{X/\text{methanol}}$), CO₂ on substrate ($Y_{\text{CO}_2/\text{methanol}}$) and O₂ on substrate ($Y_{\text{O}_2/\text{methanol}}$) were calculated in a way to close both the carbon balance and the degree of reduction balance to 100% [34]. No significant differences between the Mut^S strains could be observed as equal yields were detected for all the strains (*i.e.* $Y_{X/\text{Methanol}} = 0.42 \text{ C-mol-C-mol}^{-1}$, $Y_{\text{CO}_2/\text{Methanol}} = 0.57 \text{ C-mol-C-mol}^{-1}$ and $Y_{\text{O}_2/\text{Methanol}} = 1.06 \text{ C-mol-C-mol}^{-1}$). Apparently, the energetic behavior of the recombinant strains was not affected by co-overexpressing either of the three MUT pathway enzymes. This

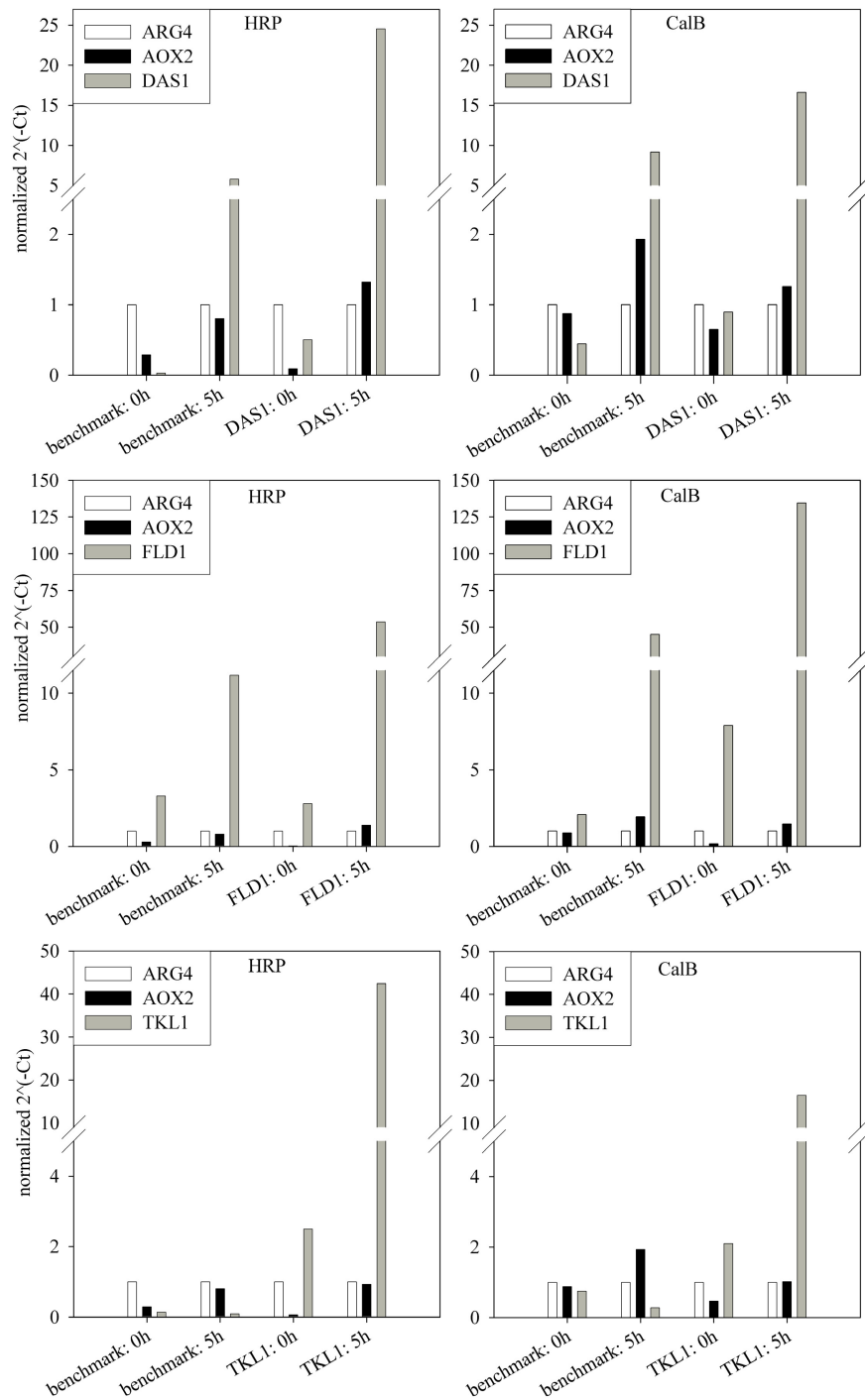


Figure 4 Transcription analysis of the co-overexpressed MUT pathway genes *DAS1/FLD1/TKL1* in HRP/CalB overexpressing strains. The transcript levels were normalized to the corresponding transcript levels of *ARG4*. The increase in *AOX2* transcript levels indicated successful induction with methanol. All co-overexpression strains showed elevated transcript levels of the respective target mRNAs compared to the benchmark strains.

fact was further underlined by the analysis of the respiratory quotient (RQ), since no significant differences in RQ between the different strains were detected (Table 1).

We believe that the fact that Mut^S strains metabolize methanol at a lower rate, and thus produce less of the intermediate formaldehyde, compared to Mut⁺ strains, describes the metabolic bottleneck responsible for this outcome. The situation might be different for the Mut⁺ phenotype, which has been found to be faster in methanol oxidation (*vide supra*). Thus, possible effects of overexpressing either of the MUT pathway enzymes, e.g. an increased formation of CO₂ by overexpression of FLD1, have to be determined independently for Mut⁺ strains.

Specific substrate uptake rate and specific productivity

The specific substrate uptake rate (q_s) and the specific productivity (q_p) of all the strains were calculated as average values from all the conducted pulses after data reconciliation and are summarized in Table 1.

Regarding q_s , all strains co-overexpressing either of the MUT pathway enzymes consumed less methanol per biomass and time than the benchmark strains (Table 1). Co-overexpression of DAS1 decreased q_s even up to 3-fold compared to the benchmark strains. Although the total numbers differ slightly the same trend for HRP strains and CalB strains can be seen (Table 1). The lowered q_s might be explained by a general deceleration of the metabolism of the cells which have to deal with the overexpression of recombinant proteins (*i.e.* either of the reporter enzymes HRP or CalB and additionally either of the MUT pathway enzymes).

Interestingly, co-overexpression of FLD1 increased q_p of both the HRP FLD1 strain and the CalB FLD1 strain compared to the benchmark strains, whereas co-overexpression of DAS1 decreased q_p (Table 1).

Co-overexpression of TKL1 led to controversial results with regard to q_p , as a slightly higher q_p for HRP could be observed, whereas q_p for CalB was even lower than for the benchmark strain. Since the strains were checked for the copy number of the integrated reporter enzyme and for the successful overexpression of the MUT pathway enzymes on transcript level (*vide supra*), and since the bioreactor cultivations of the TKL1 co-overexpressing strains were conducted repeatedly, giving the same results, we currently have no evident explanation for this outcome. We hypothesize that product specific effects might be the reason for the observed difference in q_p for TKL1 co-overexpressing strains.

Due to the unaltered stoichiometric yields of the co-overexpression strains compared to the respective benchmark strains, we can currently not explain on which metabolic level the co-overexpressed MUT pathway enzymes affected the production of the recombinant reporter enzymes. However, this outcome underlines the importance and necessity of having a fast and easy-to-do methodology to characterize recombinant *P. pastoris* strains, as certain changes in the metabolism apparently might not have the same effect on different Mut^S strains harboring different target enzymes.

Efficiency factor η

Co-overexpression of DAS1 resulted in the most efficient conversion of the substrate methanol into product, regardless of which reporter enzyme was produced; for HRP 3-fold more product was obtained per substrate, and for CalB a more than 2-fold increase could be observed (Table 1). Also co-overexpression of FLD1 led to an approximately 2-fold increased efficiency for both reporter enzymes (Table 1). Interestingly, we found that the calculated efficiency factors correlated with the observed transcription levels of the co-overexpressed MUT pathway genes (Figure 4): *DAS1* transcript levels were higher in the

Table 1 Summary Table.

reporter enzyme	MUT enzyme	RQ	q_s [mmol·g ⁻¹ ·h ⁻¹]	q_p [U·g ⁻¹ ·h ⁻¹]	η [U·mmol ⁻¹]	vol. productivity [U·l ⁻¹ ·h ⁻¹]
HRP	benchmark	0.54	- 1.67	1.66	0.99	38.79
	DAS1	0.56	- 0.51	1.56	3.06	28.35
	FLD1	0.57	- 1.22	2.01	1.65	49.11
	TKL1	0.57	- 0.88	1.96	2.22	39.87
CalB	benchmark	0.57	- 1.32	1.39	1.05	30.27
	DAS1	0.57	- 0.36	0.78	2.15	15.23
	FLD1	0.57	- 0.70	1.49	2.13	31.27
	TKL1	0.57	- 0.35	0.12	0.34	2.07

The respiratory quotient (RQ), the specific substrate uptake rate (q_s), the specific productivity (q_p), the efficiency factor (η) and the volumetric productivity of the benchmark strains (overexpressing either HRP or CalB) and the respective benchmark strains co-overexpressing either of the MUT pathway enzymes DAS1, FLD1 or TKL1 were determined

HRP strain than in the CalB strain, whereas *FLD1* transcript levels were higher in the CalB strain than in the HRP strain. This trend can also be seen in the respective efficiency factors (Table 1). Thus, increasing the copy number of the respective MUT pathway gene in the genome of *P. pastoris* might intensify the beneficial effects on recombinant protein production and could be an interesting target for future studies.

For the recombinant strains co-overexpressing TKL1 different results for HRP strains and CalB strains were observed. While the co-overexpression of TKL1 resulted in a 2-fold more efficient conversion of methanol into the product HRP, a lower η than for the benchmark strain was detected for the production of CalB due to the very low q_p (Table 1).

Summarizing, all strains which co-overexpressed enzymes of the MUT pathway, excluding the CalB TKL1 strain, showed a more efficient conversion of the substrate methanol into the respective product. In particular, an expression platform, where the MUT pathway enzyme DAS1 is overexpressed, could be interesting for industrial large-scale protein production processes due to significantly lower substrate consumption and consequently a reduced risk management compared to strains without an engineered MUT pathway.

Volumetric productivity

Besides the importance of reducing the required amount of methanol and the associated reduction in cost and risk management, the volumetric productivity, *i.e.* the amount of product per volume and time, is an important factor in industrial production processes. The determined average volumetric productivities of the different recombinant *P. pastoris* strains are summarized in Table 1.

In terms of volumetric productivity only FLD1 co-overexpressing strains showed slightly higher or similar volumetric productivities compared to the benchmark strains, whereas the DAS1/TKL1 co-overexpressing strains produced less product per volume and time. The beneficial effect of co-overexpressing the MUT pathway enzyme DAS1, which resulted in a much better conversion of substrate to product (Table 1), obviously came at cost of process time.

Taking into account all the different strain specific parameters, an expression platform where the MUT pathway enzyme FLD1 is overexpressed turned out to be a very interesting tool for the industrial production of proteins, since not only methanol can be converted into product 2-fold more efficiently, but also the volumetric productivity is at least equally high compared to benchmark strains.

In summary, several aspects have to be considered when designing and choosing a production strain, *i.e.* if the main goal is a significant reduction in cost and risk management due to a more efficient conversion of

substrate into product or a fast production process due to a high volumetric productivity. With the methodology described here, these strain characteristics can be determined in a fast and easy way, which significantly speeds up bioprocess development.

Conclusions

In this study a fast and easy-to-do method based on batch cultivations with methanol pulses was used to characterize different recombinant *P. pastoris* strains. The results can be summarized as follows:

- a direct comparison of a Mut^S and a Mut⁺ strain, both overexpressing the recombinant enzyme HRP, revealed the Mut^S strain to be 7-fold more efficient in the conversion of substrate into product and to have a 3-fold higher volumetric productivity.
- the transcription of the genes *DAS1* and *DAS2*, which encode the key enzymes of the assimilative branch of the MUT pathway, was equally high induced upon MeOH addition.
- co-overexpression of either of the MUT pathway enzymes DAS1, TKL1 or FLD1 in *P. pastoris* Mut^S strains overexpressing either HRP or CalB did not cause any changes in the energetic behavior of the strains, as calculated yields and observed respiratory quotients were equal, but significantly reduced the growth rate.
- co-overexpressing MUT pathway enzymes affected the specific substrate uptake rate as well as the specific productivity of recombinant Mut^S strains. The co-overexpression of DAS1 resulted in a 2- to 3-fold more efficient conversion of methanol into product, but came at cost of process time.
- co-overexpression of FLD1 resulted in an approximately 2-fold increased efficiency in the conversion of methanol into product and showed at least equally high volumetric productivities compared to benchmark strains, making this expression platform highly interesting for industrial production processes.
- since product specific effects might influence certain strain specific parameters, as shown for TKL1 overexpressing strains in this study, the necessity of having a fast methodology to characterize recombinant strains before going into industrial production processes was highlighted. The methodology described here provides such a tool and has great potential for the use in early process development in an industrial environment.

Outlook

The present study shows the effect of co-overexpressing MUT pathway enzymes on strain specific parameters of

different recombinant *P. pastoris* Mut^S strains and revealed interesting targets for strain engineering. However, this study was performed using only a Mut^S strain as expression platform since, it showed significantly better properties compared to the Mut⁺ strain (without co-overexpression of MUT pathway genes). Thus, effects on some strain specific parameters might be more pronounced in Mut⁺ strains and have to be evaluated independently. Moreover, the molecular mechanisms that cause the beneficial influence of the studied MUT pathway enzymes on the efficiency in recombinant protein production remain to be elucidated in more detail. Increasing the copy number of the respective MUT pathway genes in the chromosome might further intensify their effects and should be considered when designing a specific *P. pastoris* expression host in future studies. We further recommend to analyze interesting co-overexpressing strains in fed-batch cultivations, which can be easily set up with the parameters extracted out of the described batch method with methanol pulses (see also [30,31]), to test their long term stability in production processes.

Material and methods

Chemicals

Enzymes were purchased from Fermentas GmbH, Germany. 2,2'-azino-bis(3-ethylbenzthiazoline-6-sulphonic acid) diammonium salt (ABTS) was obtained from Sigma-Aldrich Handels GmbH, Austria. Difco™ yeast nitrogen base w/o amino acids (YNB), Bacto™ tryptone and Bacto™ yeast extract were obtained from Becton Dickinson and Company, Austria. Zeocin™ was obtained from InvivoGen-Eubio, Austria. D-Biotin and p-nitrophenyl butyrate (p-NPB) were obtained from Fluka Chemia AG, Switzerland. All other chemicals were purchased from Carl Roth GmbH & Co. KG, Germany.

Strains and vectors

The strain *P. pastoris* Mut^S ($\Delta aox1::FRT$) was engineered by Näätsaari et al. (manuscript in preparation) at Graz University of Technology, Institute of Molecular Biotechnology, based on the *P. pastoris* wildtype strain CBS7435. These two strains were used as starting strains for the corresponding overexpression studies. The shuttle vectors pPpT4_S and pPpKan_S, derivatives of pPpT2 [35] with two point mutations in the EM72 promoter and a *SmiI* restriction site instead of *BglII*, were used for cloning. pPpKan_S contains a kanamycin/geneticin resistance gene instead of a zeocin resistance gene [36,37]. pPpT4_S was used for harboring either the HRP isoenzyme C1A or CalB, which both were codon-optimized for high-level expression in *P. pastoris*. The codon table described in [35] was applied for codon

optimization. Overexpression of *DAS1*, *FLD1*, *TKL1* and the genes encoding HRP and CalB was under the control of *pAOX1*. Secretion of HRP and CalB to the cultivation supernatant was facilitated by a N-terminally fused prepro-signal sequence of the *S. cerevisiae* alpha-factor. pPpKan_S was used as shuttle vector harboring *DAS1*, *FLD1* or *TKL1*, which were amplified from chromosomal DNA of *P. pastoris* CBS7435 using the cloning primers depicted in Table 2A with Phusion™ high fidelity DNA-polymerase (Finnzymes Oy, Finland) and GC buffer according to the manufacturer's protocol.

Strain construction and screening procedure

Transformation of approximately 2 μ g *SmiI*-linearized pPpT4_S or pPpKan_S plasmid DNA harboring the respective gene of interest into *P. pastoris* was done as described by Lin-Cereghino et al. [38]. Selection of successfully transformed clones was performed on YPD agar plates containing 25 mg·l⁻¹ zeocin (for HRP/CalB strains) or 25 mg·l⁻¹ zeocin plus 300 mg·l⁻¹ geneticin (for HRP/CalB *DAS1*/*FLD1*/*TKL1* strains). Screening of randomly chosen transformants and rescreening of promising clones (in quadruplicates) were done as micro-scale cultivations in 96-deep well plates similar to the protocol described by Weis et al. [39]: cells were cultivated in 250 μ l BMD1% (1% α -D(+)-glucose monohydrate, 6.0 g·l⁻¹ K₂HPO₄, 23.6 g·l⁻¹ KH₂PO₄, 13.4 g·l⁻¹ YNB, 0.4 mg/l D-biotin) for approximately 60 h, followed by addition of 250 μ l BMM2 (1% methanol, 6.0 g·l⁻¹ K₂HPO₄, 23.6 g·l⁻¹ KH₂PO₄, 13.4 g·l⁻¹ YNB, 0.4 mg·l⁻¹ D-biotin) and 50 μ l BMM10 (5% methanol, 6.0 g·l⁻¹ K₂HPO₄, 23.6 g·l⁻¹ KH₂PO₄, 13.4 g·l⁻¹ YNB, 0.4 mg·l⁻¹ D-biotin) per well 12 h, 24 h and 36 h after the first addition of BMM2.

HRP activity was verified by using an ABTS assay: after centrifugation of the induced transformants (3000 g, 10 min), 15 μ l of the cultivation supernatant were mixed with 140 μ l assay solution (0.5 mM ABTS in 50 mM NaOAc, pH 4.5, 2.9 mM H₂O₂) in a 96-well PS-microplate [32]. The increase in absorbance at 405 nm was followed in a Spectramax Plus 384 platereader (Molecular Devices, Germany) at room temperature for 5 min. CalB activity was evaluated by an esterase activity assay similar to the assay described by Zhang et al. [40]: 20 μ l cultivation supernatant were mixed with 180 μ l fresh assay solution (4 mM p-NPB in 300 mM Tris-HCl, pH 7.4, 1% dimethyl sulfoxid). The increase in absorbance at 405 nm was followed in a Spectramax Plus 384 platereader at room temperature for 5 min.

Evaluation of the transcription of *DAS1* and *DAS2* upon methanol induction was performed by quantitative real-time PCR (qPCR). For this purpose, RNA was isolated from the corresponding strains before and 5 h after methanol induction using the ZR Fungal/Bacterial

Table 2 Oligonucleotide-primers used for A, amplification of *DAS1/FLD1/TKL1* from chromosomal DNA; B, evaluation of *DAS1/DAS2* transcription induction; C, the analysis of *DAS1/FLD1/TKL1* overexpression; D, copy number determination of the reporter genes (via verification of the *Zeo^R* copy number)

A.	target	orientation	sequence 5'-3'
	DAS1	forward	AAAAGCGCGCCGAAACGATGGCTAGAATCCCAAAGCAG
		reverse	TTTGCGGCCGCTTACAACCTGTGTCATGCTTTGGTTTTTC
	FLD1	forward	AACACTAGTATGTCTACCGAAGGTCAA
		reverse	AACGCGGCCGCTTAGTGCATAGTAATCAC
	TKL1	forward	AGAGAATTCGAAACGATGTCTGATCTCTTAGCTATCAACAC
		reverse	AGAGCGGCCGCTACGCATGAACAGACTCAAAAG
B.	target	orientation	sequence 5'-3'
	ARG4	forward	TGCTGGCTACAGATCTTGCCGACT
		reverse	CTCGGCTTGTCTGACACATTCACCAG
	AOX2	forward	ATACTCATCCGAGGCCAGAGCTTACG
		reverse	ACCGTGAGCAAGACCAGCAGTCAA
	DAS1	forward	CTGAGAAACCAGCTAAAGGTGACGAGT
		reverse	TCTTGTCCCTCACGAGGGTACTCT
	DAS2	forward	CTGAAAAACCAGCCGAGGGTGATC
		reverse	TTCCTCACCTTCTTGAGGATAGTTCTTAACG
C.	target	orientation	sequence 5'-3'
	ARG4	forward	TGCTGGCTACAGATCTTGCCGACT
		reverse	CTCGGCTTGTCTGACACATTCACCAG
	AOX2	forward	ATACTCATCCGAGGCCAGAGCTTAC
		reverse	ACCGTGAGCAAGACCAGCAGTCAA
	DAS1	forward	CTGAGAAACCAGCTAAAGGTGACGAGT
		reverse	TCTTGTCCCTCACGAGGGTACTCT
	FLD1	forward	TGGATTATCTGTCATCCAAGGTGCAGTTTC
		reverse	GTCCGCCCATGCCTTCTTTGAATC
	TKL1	forward	GTCGCTACACATGACTCGATTGGTC
		reverse	CATGAGGTTTGGGAAGAGCTCTCAAGTG
D.	target	orientation	sequence 5'-3'
	<i>Zeo^R</i>	forward	GACTCGGTTTCTCCCGTACT
		reverse	CTGCGGAGATGAACAGGGTAA
	ARG4	forward	TCCTCCGGTGGCAGTTCTT
		reverse	TCCATTGACTCCCGTTTTGAG

RNA MicroPrep™ kit from Zymo Research Corporation (Irvine, CA, USA). In-column DNase digestion was performed according to the manufacturer's recommendations using RNase-free DNase I from Zymo Research. RNA was eluted in 20 µl DNase/RNase-free water (plus 1 µl RNaseOUT™ Recombinant Ribonuclease Inhibitor from Invitrogen Corporation, CA, USA) and used directly for qPCR using the SuperScript® III Platinum® SYBR® Green One-Step qRT-PCR Kit (Invitrogen). The qPCR was performed in the ABI PRISM 7500 Real Time PCR System (Applied Biosystems, CA, USA) according to the manufacturer's recommendations employing the primers listed in Table 2B. For visualization of the magnitude of transcription induction, the

determined cycle threshold (Ct) signals were transformed to 2^{-Ct} and normalized to the corresponding *ARG4* signals (which is supposed to be constitutively transcribed). The extent of induction of a target transcript was calculated as the ratio of the normalized 2^{-Ct} signal of the target transcript at 5 h over the normalized signal at 0 h (*i.e.* before induction). The time point 0 h represented the de-repression state of the *P. pastoris* culture, since the C-source glucose was depleted before the addition of methanol. Analogically, the overexpression of genes encoding MUT pathway enzymes was verified via qPCR with the primers listed in Table 2C. The transcript levels were shown as 2^{-Ct} signals, normalized to the corresponding *ARG4* signals.

To determine the copy number of the transformed genes, a qPCR based method was used as described by Abad *et al.* [41] using the Power SYBR[®] Green Master Mix (Applied Biosystems) with the ABI PRISM 7500 Real Time PCR System. Hereto, genomic DNA was isolated from *P. pastoris* according to the protocol by Hoffman *et al.* [42]. The primers (Table 2D) were used at concentrations of 200 nM per primer with 0.66 ng of genomic DNA as template. The copy number of the genes encoding the target enzymes was determined indirectly via verification of the copy number of the Zeocin[™] resistance-mediating gene *Zeo^R*. Conditions were 10 min at 95 C, 40 cycles of 15 s at 95 C and 60 s at 60 C followed by a final dissociation step.

Strain characterization in bioreactors

Culture media

Precultures were done in yeast nitrogen base medium (YNBM; 0.1 M potassium phosphate buffer pH 6.0, 3.4 g·l⁻¹ YNB w/o amino acids and ammonia sulfate, 10 g·l⁻¹ (NH₄)₂SO₄, 400 mg·l⁻¹ biotin, 20 g·l⁻¹ glucose). Batch cultivations were performed in basal salt medium (26.7 ml·l⁻¹ 85% phosphoric acid, 1.17 g·l⁻¹ CaSO₄·2H₂O, 18.2 g·l⁻¹ K₂SO₄, 14.9 g·l⁻¹ MgSO₄·7H₂O, 4.13 g·l⁻¹ KOH, 44 g·l⁻¹ C₆H₁₂O₆·H₂O, 0.2 ml·l⁻¹ Antifoam Struktol J650, 4.35 ml·l⁻¹ PTM1, NH₄OH as N-source). Trace element solution (PTM1) was made of 6.0 g·l⁻¹ CuSO₄·5H₂O, 0.08 g·l⁻¹ NaI, 3.0 g·l⁻¹ MnSO₄·H₂O, 0.2 g·l⁻¹ Na₂MoO₄·2H₂O, 0.02 g·l⁻¹ H₃BO₃, 0.5 g·l⁻¹ CoCl₂, 20.0 g·l⁻¹ ZnCl₂, 65.0 g·l⁻¹ FeSO₄·7H₂O, 0.2 g·l⁻¹ biotin, 5 ml·l⁻¹ H₂SO₄. Induction was carried out in presence of 1 mM δ-aminolevulinic acid for HRP overexpressing strains. The concentration of the base NH₄OH was determined by titration with 0.25 M potassium hydrogen phthalate.

Experimental procedure

Preculture Frozen stocks (-80 C) were pre-cultivated in 100 ml YNBM in 1000 ml shake flasks at 28 C and 230 rpm for max. 24 h. The grown preculture was transferred aseptically to the respective culture vessel. The inoculation volume was approximately 10% of the final starting volume.

Batch cultivation Batch cultivations were carried out in either a 3 l or a 5 l working volume glass bioreactor (Infors, Switzerland). Basal salt medium was sterilized in the bioreactor and pH was adjusted to pH 5.0 by using concentrated NH₄OH solution after autoclaving. Sterile filtered trace elements were transferred to the reactor aseptically. Dissolved oxygen (dO₂) was measured with a sterilizable dO₂ electrode (Visiform[™], Hamilton, Switzerland). The pH was measured with a sterilizable electrode (Easyferm[™], Hamilton, Switzerland) and maintained constant with a PID controller using NH₄OH solution (1 to 3 M). Base consumption was

determined gravimetrically. Cultivation temperature was set to 28 C and agitation was fixed to 1200 rpm. The culture was aerated with 1.0 vvm dried air and off-gas of the culture was measured by using an infrared cell for CO₂ and a paramagnetic cell for O₂ concentration (Servomax, Switzerland). Temperature, pH, dO₂, agitation as well as CO₂ and O₂ in the off-gas were measured online and logged in a process information management system (PIMS; Lucullus, Biospectra, Switzerland).

After the complete consumption of the substrate glucose, indicated by an increase of dO₂ and a drop in off-gas activity, the first methanol pulse of a final concentration of 0.5% (v/v) was conducted with methanol (supplemented with 12 ml·l⁻¹ PTM1). Following pulses were performed with 1% methanol (v/v). All pulses were conducted directly after exhaustion of the substrate without lack phases. For each pulse, at least two samples were taken to determine the concentrations of substrate and product, as well as dry cell weight to calculate specific rates and yields.

Analysis of growth- and expression-parameters

Dry cell weight was determined by centrifugation of 5 ml culture broth (5000 rpm, 4 C, 10 min) in a laboratory centrifuge (Sigma 4 K15, rotor 11156), washing the pellet with 5 ml deionized water and subsequent drying at 105 C to a constant weight in an oven.

The enzymatic activity of HRP was measured using an ABTS assay in a CuBiAn XC enzymatic robot (Innovatis, Germany). Ten µl of sample were mixed with 140 µl 1 mM ABTS solution (50 mM KH₂PO₄, pH 6.5). The reaction mixture was incubated at 37 C for 5 min before the reaction was started by the addition of 20 µl 0.078% H₂O₂ (v/v). Changes in absorbance at 415 nm were measured for 80 s and rates were calculated. The standard curve was prepared using a commercially available HRP preparation (Type VI-A, Sigma-Aldrich, USA) in the range from 0.02 to 2.0 U·ml⁻¹.

The enzymatic activity of CalB was measured by determining the esterase activity of CalB. A stock solution was generated by mixing 42 µl p-NPB with 458 µl DMSO and stored at -20 C. The assay reagent was prepared freshly by addition of 100 µl stock solution to 10 ml TrisHCl (300 mM, pH 7.5). Color development at 405 nm was followed in a UV-1601 spectrophotometer (Shimadzu GmbH; Austria) at 30 C for 5 min. One Unit of CalB was defined as the formation of 1 µmol p-nitrophenol·min⁻¹.

Substrate concentrations

Concentrations of methanol were determined in cell free samples by HPLC (Agilent Technologies, USA) equipped with an ion-exclusion column (Supelcogel C-610H Sigma-Aldrich, USA) and a refractive index detector (Agilent Technologies, USA). The mobile phase was 0.1% H₃PO₄ with a constant flow rate of 0.5 ml·min⁻¹

and the system was run isocratically. Calibration was done by measuring standard points in the range from 0.1 to 10 g·l⁻¹ methanol.

Data analysis

Measurements of biomass concentration, product concentration and substrate concentration were executed in duplicates. Along the observed standard deviation for the single measurements, the error was propagated to the specific rates q_s and q_p as well as to the yield coefficients. The error for the volumetric rate of product formation was set to 5%.

Data reconciliation

The Mut^S phenotype caused a slow biomass growth during conducted methanol pulses. Thus, the determined increase of biomass during one pulse was close to the standard deviation observed for one duplicate measurement and could therefore not be regarded as accurate. Hence, the biomass rate was calculated using the MATLAB software (MathWorks, USA), using the carbon balance and the degree of reduction balance, made of the determined volumetric rates for the substrate uptake, the oxygen consumption and the carbon dioxide evolution. As the system of equations consisted of two elemental balances and only one rate to be calculated, the degree of freedom was 1. Consequently, the statistical test value h had to be lower than 3.84 not to reject the null hypothesis, that there were no errors in the measurements at a 95% confidence level for each data point. Including error margins of 5% for off-gas measurements and substrate determinations, a χ^2 (chi-square distribution) test was conducted for each data point and gave the corresponding h -values. This method was described in detail elsewhere [34].

Additional material

Additional file 1: Figure S1. Domain structure of DAS1, DAS2 and TKL1 (conserved domain prediction via CD-search tool [43-45]). All three enzymes belong to I, a thiamine pyrophosphate (TPP)-enzyme superfamily [NCBI CDD:c101629]; II, a superfamily of TPP-depending enzymes containing a pyrimidine binding domain [NCBI CDD:c111410]; and III, a superfamily of enzymes with a transketolase C-terminal domain [NCBI CDD:c108363]. Amino acid sequences of *P. pastoris* strain CBS7435 from [16].

Additional file 2: Figure S2. Experimental strategy for the fast determination of strain specific parameters of the *P. pastoris* Mut^S HRP strain using a batch experiment with methanol pulses of 0.5% and 1% (v/v). A, (continuous line), oxygen uptake rate OUR; (diamond) biomass dry cell weight concentration; B, (continuous line), carbon dioxide emission rate CER; (circle), calculated specific substrate uptake rate q_s ; (triangle up), calculated specific HRP productivity q_p .

Additional file 3: Figure S3. Experimental strategy for the fast determination of strain specific parameters of the *P. pastoris* Mut⁺ HRP strain using a batch experiment with methanol pulses of 0.5% and 1% (v/v). A, (continuous line), oxygen uptake rate OUR; (diamond) biomass dry cell weight concentration; B, (continuous line), carbon dioxide

emission rate CER; (circle), calculated specific substrate uptake rate q_s ; (triangle up), calculated specific HRP productivity q_p .

Abbreviations

ADH: methylformate synthase; AOX: alcohol oxidase; CalB: *Candida antarctica* lipase B; CAT: catalase; CER: carbon dioxide emission rate; C-mol: molarity of component based on one carbon atom; DAK: dihydroxyacetone kinase; DAS1: dehydroxyacetone synthase 1; DHA: dihydroxyacetone; DHAP: dihydroxyacetone phosphate; F_{1,6}BP: fructose-1,6-bisphosphate; F₆P: fructose-6-phosphate; FBA: fructose-1,6-bisphosphate aldolase; FBP: fructose-1,6-bisphosphatase; FDH: formate dehydrogenase; FGH: S-formylglutathione hydrolase; FLD1: formaldehyde dehydrogenase; GAP: glyceraldehyde 3-phosphate; GSH: glutathione; HRP: horseradish peroxidase; MUT: methanol utilization pathway; Mut⁺: methanol utilization positive (AOX1 intact); Mut⁻: methanol utilization minus (knock-out of AOX1 and AOX2); Mut^S: methanol utilization slow (knock-out of AOX1); OUR: oxygen uptake rate; PPP: pentose phosphate pathway; Pyr: pyruvate; q_p : specific productivity [U·g⁻¹·h⁻¹]; q_s : specific substrate uptake rate [mmol·g⁻¹·h⁻¹]; Ri5P: ribose-5-phosphate; SeHe7P: sedoheptulose-7-phosphate; TCA: tricarboxylic acid cycle; TKL1: transketolase; Xu5P: xylulose-5-phosphate; η : efficiency factor.

Acknowledgements

The authors would like to thank Anna Hatzl for technical assistance in the lab. Financial support by ACIB GmbH is gratefully acknowledged.

Author details

¹Graz University of Technology, Institute of Molecular Biotechnology, Graz, Austria. ²Oliver Spadiut, Vienna University of Technology, Institute of Chemical Engineering, Research Area Biochemical Engineering, Gumpendorfer Strasse 1a, A-1060 Vienna, Austria. ³Austrian Centre of Industrial Biotechnology (ACIB GmbH), Graz, Austria.

Authors' contributions

FK, CD, TH and OS designed and performed the experiments, analyzed and interpreted the data. FK, CD and OS wrote the manuscript. AG, CH and OS conceived the study and supervised the research. All authors read and approved the final manuscript.

Competing interests

The authors declare that they have no competing interests.

Received: 6 December 2011 Accepted: 13 February 2012

Published: 13 February 2012

References

1. Abad S, Nahalka J, Winkler M, Bergler G, Speight R, Glieder A, Nidetzky B: High-level expression of Rhodotorula gracilis d-amino acid oxidase in Pichia pastoris. *Biotechnol Lett* 2011, **33**:557-563.
2. Cereghino JL, Cregg JM: Heterologous protein expression in the methylotrophic yeast Pichia pastoris. *Fems Microbiol Rev* 2000, **24**:45-66.
3. Cregg JM, Cereghino JL, Shi JY, Higgins DR: Recombinant protein expression in Pichia pastoris. *Mol Biotechnol* 2000, **16**:23-52.
4. Cereghino GPL, Cereghino JL, Ilgen C, Cregg JM: Production of recombinant proteins in fermenter cultures of the yeast Pichia pastoris. *Curr Opin Biotechnol* 2002, **13**:329-332.
5. Hartner FS, Glieder A: Regulation of methanol utilisation pathway genes in yeasts. *Microbial Cell Factories* 2006, **5**:39.
6. Couderc R, Baratti J: Oxidation of Methanol by the Yeast, Pichia-Pastoris - Purification and Properties of the Alcohol Oxidase. *Agric Biol Chem* 1980, **44**:2279-2289.
7. Macauley-Patrick S, Fazenda ML, McNeil B, Harvey LM: Heterologous protein production using the Pichia pastoris expression system. *Yeast* 2005, **22**:249-270.
8. Cregg JM, Madden KR, Barringer KJ, Thill GP, Stillman CA: Functional-Characterization of the 2 Alcohol Oxidase Genes from the Yeast Pichia-Pastoris. *Mol Cel Biol* 1989, **9**:1316-1323.
9. Brierley RA, Bussineau C, Kosson R, Melton A, Siegel RS: Fermentation Development of Recombinant Pichia-Pastoris Expressing the

- Heterologous Gene - Bovine Lysozyme. *Ann N Y Acad Sci* 1990, **589**:350-362.
10. Hartner FS, Ruth C, Langenegger D, Johnson SN, Hyka P, Lin-Cereghino GP, Lin-Cereghino J, Kovar K, Cregg JM, Glieder A: **Promoter library designed for fine-tuned gene expression in *Pichia pastoris***. *Nucleic Acids Res* 2008, **36**:e76.
 11. Cregg JM, Tschopp JF, Stillman C, Siegel R, Akong M, Craig WS, Buckholz RG, Madden KR, Kellaris PA, Davis GR, *et al*: **High-Level Expression and Efficient Assembly of Hepatitis-B Surface-Antigen in the Methylophilic Yeast, *Pichia-Pastoris***. *Bio-Technology* 1987, **5**:479-485.
 12. Romanos MA, Scorer CA, Clare JJ: **Foreign Gene-Expression in Yeast - a Review**. *Yeast* 1992, **8**:423-488.
 13. van den Burg HA, de Wit PJGM, Vervoort J: **Efficient C-13/N-15 double labeling of the avirulence protein AVR4 in a methanol-utilizing strain (Mut(+)) of *Pichia pastoris***. *J Biomol Nmr* 2001, **20**:251-261.
 14. Kim SJ, Lee JA, Kim YH, Song BK: **Optimization of the Functional Expression of Coprinus cinereus Peroxidase in *Pichia pastoris* by Varying the Host and Promoter**. *J Microbiol Biotechnol* 2009, **19**:966-971.
 15. Chiruvolu V, Cregg JM, Meagher MM: **Recombinant protein production in an alcohol oxidase-defective strain of *Pichia pastoris* in fedbatch fermentations**. *Enzyme and Microb Technol* 1997, **21**:277-283.
 16. Kubler A, Schneider J, Thallinger GG, Anderl I, Wibberg D, Hajek T, Jaenicke S, Brinkrolf K, Goesmann A, Szczepanowski R, *et al*: **High-quality genome sequence of *Pichia pastoris* CBS7435**. *J Biotechnol* 2011, **154**:312-320.
 17. Swartz JR, Cooney CL: **Methanol Inhibition in Continuous Culture of *Hansenula-Polymorpha***. *Appl Environ Microbiol* 1981, **41**:1206-1213.
 18. Hazeu W, Donker RA: **A Continuous Culture Study of Methanol and Formate Utilization by the Yeast *Pichia-Pastoris***. *Biotechnol Lett* 1983, **5**:399-404.
 19. Kern A, Hartner FS, Freigassner M, Spielhofer J, Rumpf C, Leitner L, Frohlich KU, Glieder A: ***Pichia pastoris* "just in time" alternative respiration**. *Microbiology* 2007, **153**:1250-1260.
 20. Arnau C, Casas C, Valero F: **The effect of glycerol mixed substrate on the heterologous production of a Rhizopus oryzae lipase in *Pichia pastoris* system**. *Biochem Eng J* 2011, **57**:30-37.
 21. Jungo C, Marison I, von Stockar U: **Mixed feeds of glycerol and methanol can improve the performance of *Pichia pastoris* cultures: A quantitative study based on concentration gradients in transient continuous cultures**. *J Biotechnol* 2007, **128**:824-837.
 22. Zhang WH, Potter KJH, Plantz BA, Schlegel VL, Smith LA, Meagher MM: ***Pichia pastoris* fermentation with mixed-feeds of glycerol and methanol: growth kinetics and production improvement**. *J Ind Microbiol Biotechnol* 2003, **30**:210-215.
 23. Orman MA, Calik P, Ozdamar TH: **The influence of carbon sources on recombinant-human-growth-hormone production by *Pichia pastoris* is dependent on phenotype: a comparison of Mut(s) and Mut(+) strains**. *Biotechnol App Biochem* 2009, **52**:245-255.
 24. Ascacio-Martinez JA, Barrera-Saldana HA: **Production and secretion of biologically active recombinant canine growth hormone by *Pichia pastoris***. *Gene* 2004, **340**:261-266.
 25. Pla IA, Damasceno LM, Vannelli T, Ritter G, Batt CA, Shuler ML: **Evaluation of Mut(+) and Mut(S) *Pichia pastoris* phenotypes for high level extracellular scFv expression under feedback control of the methanol concentration**. *Biotechnol Prog* 2006, **22**:881-888.
 26. Lee B, Yurimoto H, Sakai Y, Kato N: **Physiological role of the glutathione-dependent formaldehyde dehydrogenase in the methylotrophic yeast *Candida boidinii***. *Microbiology-Sgm* 2002, **148**:2697-2704.
 27. Nakagawa T, Ito T, Fujimura S, Chikui M, Mizumura T, Miyaji T, Yurimoto H, Kato N, Sakai Y, Tomizuka N: **Molecular characterization of the glutathione-dependent formaldehyde dehydrogenase gene FLD1 from the methylotrophic yeast *Pichia methanolica***. *Yeast* 2004, **21**:445-453.
 28. Schroer K, Luef KP, Hartner FS, Glieder A, Pscheidt B: **Engineering the *Pichia pastoris* methanol oxidation pathway for improved NADH regeneration during whole-cell biotransformation**. *Metab Eng* 2010, **12**:8-17.
 29. Slekár KH, Kosman DJ, Culotta VC: **The yeast copper zinc superoxide dismutase and the pentose phosphate pathway play overlapping roles in oxidative stress protection**. *J Biol Chem* 1996, **271**:28831-28836.
 30. Dietzsch C, Spadiut O, Herwig C: **A dynamic method based on the specific substrate uptake rate to set up a feeding strategy for *Pichia pastoris***. *Microbial Cell Factories* 2011, **10**:14.
 31. Dietzsch C, Spadiut O, Herwig C: **A fast approach to determine a fed batch feeding profile for recombinant *Pichia pastoris* strains**. *Microbial Cell Factories* 2011, **10**:85.
 32. Morawski B, Lin ZL, Cirino PC, Joo H, Bandara G, Arnold FH: **Functional expression of horseradish peroxidase in *Saccharomyces cerevisiae* and *Pichia pastoris***. *Protein Engineering* 2000, **13**:377-384.
 33. Ohi H, Miura M, Hiramatsu R, Ohmura T: **The Positive and Negative Cis-Acting Elements for Methanol Regulation in the *Pichia-Pastoris* Aox2 Gene**. *Mol Gen Genet* 1994, **243**:489-499.
 34. van der Heijden RTJM, Romein B, Heijnen JJ, Hellinga C, Luyben KCAM: **Linear constraint relations in biochemical reaction systems: II. Diagnosis and estimation of gross errors**. *Biotechnol Bioeng* 1994, **43**:11-20.
 35. Abad S, Nahalka J, Bergler G, Arnold SA, Speight R, Fotheringham I, Nidetzky B, Glieder A: **Stepwise engineering of a *Pichia pastoris* D-amino acid oxidase whole cell catalyst**. *Microbial Cell Factories* 2010, **9**:24.
 36. Oka Y, Ishida H, Morioka M, Numasaki Y, Yamafuji T, Osono T, Umezawa H: **Combinicins, New Kanamycin Derivatives Bioconverted by Some Micromonosporas**. *J Antibiot* 1981, **34**:777-781.
 37. Wach A, Brachat A, Pohlmann R, Philippsen P: **New Heterologous Modules for Classical or Pcr-Based Gene Disruptions in *Saccharomyces-Cerevisiae***. *Yeast* 1994, **10**:1793-1808.
 38. Lin-Cereghino J, Wong WW, Xiong S, Giang W, Luong LT, Vu J, Johnson SD, Lin-Cereghino GP: **Condensed protocol for competent cell preparation and transformation of the methylotrophic yeast *Pichia pastoris***. *Biotechniques* 2005, **38**:44-48.
 39. Weis R, Luiten R, Skranc W, Schwab H, Wubbolts M, Glieder A: **Reliable high-throughput screening with *Pichia pastoris* by limiting yeast cell death phenomena**. *Fems Yeast Research* 2004, **5**:179-189.
 40. Zhang NY, Suen WC, Windsor W, Xiao L, Madison V, Zaks A: **Improving tolerance of *Candida antarctica* lipase B towards irreversible thermal inactivation through directed evolution**. *Protein Engineering* 2003, **16**:599-605.
 41. Abad S, Kitz K, Hormann A, Schreiner U, Hartner FS, Glieder A: **Real-time PCR-based determination of gene copy numbers in *Pichia pastoris***. *Biotechnol J* 2010, **54**:13-420.
 42. Hoffmann K, Onodera S, Noiva R: **Expression of recombinant human protein disulfide isomerase in the yeast *Pichia pastoris***. *Faseb J* 1996, **10**:677-677.
 43. Marchler-Bauer A, Bryant SH: **CD-Search: protein domain annotations on the fly**. *Nucleic Acids Res* 2004, **32**:W327-W331.
 44. Marchler-Bauer A, Anderson JB, Chitsaz F, Derbyshire MK, DeWeese-Scott C, Fong JH, Geer LY, Geer RC, Gonzales NR, Gwadz M, *et al*: **CDD: specific functional annotation with the Conserved Domain Database**. *Nucleic Acids Resh* 2009, **37**:D205-D210.
 45. Marchler-Bauer A, Lu SN, Anderson JB, Chitsaz F, Derbyshire MK, DeWeese-Scott C, Fong JH, Geer LY, Geer RC, Gonzales NR, *et al*: **CDD: a Conserved Domain Database for the functional annotation of proteins**. *Nucleic Acids Res* 2011, **39**:D225-D229.

doi:10.1186/1475-2859-11-22

Cite this article as: Krainer *et al*: Recombinant protein expression in *Pichia pastoris* strains with an engineered methanol utilization pathway. *Microbial Cell Factories* 2012 **11**:22.

- Chapter 8 -

Production of a recombinant peroxidase-protein G fusion protein in *Pichia pastoris*

Florian W. Krainer¹ and Anton Glieder^{1*}

¹ Graz University of Technology, Institute of Molecular Biotechnology, NAWI Graz, Petersgasse 14, 8010 Graz, Austria

* Corresponding author: Anton Glieder, Graz University of Technology, Institute of Molecular Biotechnology, NAWI Graz, Petersgasse 14, 8010 Graz, Austria; a.glieder@tugraz.at; Tel: +43 664 608734074; Fax: +43 316 873 4071

Abstract

Streptococcal protein G (SpG) binds immunoglobulin G from a broad range of mammalian species with high affinity. Chemical conjugations of SpG to the reporter enzyme horseradish peroxidase (HRP) are commonly used in immunohistochemical applications. However, commercial HRP preparations are typically isolated from horseradish roots as varying mixtures of HRP isoenzymes with different biochemical properties, and chemical conjugation procedures lead to heterogeneous HRP-SpG preparations, partially including inactivated enzyme. A recombinant process allows the production of a well-defined HRP isoenzyme fused to SpG at constant 1:1 stoichiometry in a single step without the need for laborious chemical conjugation. By using state-of-the-art biotechnological tools, we produced a recombinant HRP-SpG fusion protein in *P. pastoris* in a bioreactor cultivation. Purified HRP-SpG was tested successfully for functional binding of antibodies from different mammalian serums.

Keywords

Pichia pastoris, plant peroxidase, horseradish peroxidase, recombinant protein production, fusion protein, protein G, ELISA

Introduction

Staphylococcus and *Streptococcus* spp. produce surface proteins that bind tightly to the Fc region of immunoglobulin G (IgG) [1, 2]. One of these receptors is produced by *Streptococcus* spp. of the Lancefield group G, termed streptococcal protein G (SpG). SpG has been described to bind a broad range of mammalian IgGs [3, 4] via two [5] or three [6] IgG binding domains. A schematic overview of the domains of wildtype SpG is given in Figure 1.A.

The tight IgG binding capacity of SpG is commonly used for detection and quantification of antigens by coupling SpG to a reporter enzyme, *e.g.* in Western blots or enzyme-linked immunosorbent assays (ELISA). Owing to the tight binding of SpG to IgGs from a large variety of species, conjugates of a reporter enzyme with SpG were recently applied in studies on non-species dependent detection of antibodies against melioidosis-inducing *Burkholderia pseudomallei* [7], hantavirus [8], or Lyme borreliosis-inducing *Borrelia burgdorferi* s. l. [9]. Most commonly, reporter enzymes such as alkaline phosphatase or the heme-containing protein horseradish peroxidase (HRP) are coupled to SpG by chemical conjugation, *e.g.* [10, 11]. Unfortunately, chemical conjugation procedures are not only time- and labor-intensive but also bear the risk of inactivating the reporter enzyme and lead to heterogeneous conjugate preparations.

Whereas SpG is currently produced recombinantly, *e.g.* [12], HRP is still isolated from horseradish roots, introducing yet another potential source for heterogeneity. Until recently, yields of recombinant HRP were limited in the low mg/L range rendering a recombinant production process uncompetitive. However, in the face of the latest progress made in our lab using the methylotrophic yeast *Pichia pastoris* as host organism [Krainer *et al.*, manuscript in preparation, Chapter 5], recombinant HRP production has become a feasible alternative. As opposed to the isolation of HRP from its natural source, recombinant HRP production is independent from environmental influences and allows a steady enzyme supply at consistent quality. With regards to an immunohistochemical application, functional recombinant fusion proteins of staphylococcal protein A-eGFP [13] and anti-atrazine Fab-HRP [14] from *P. pastoris* have been described before. Recombinant fusion proteins allow stoichiometrically defined preparations and are thus more homogeneous and reproducible than chemical conjugates. Making use of our recombinant HRP production platform in *P. pastoris*, we produced more than 110 mg/L of functional recombinant HRP-SpG fusion protein in bioreactor cultivation.

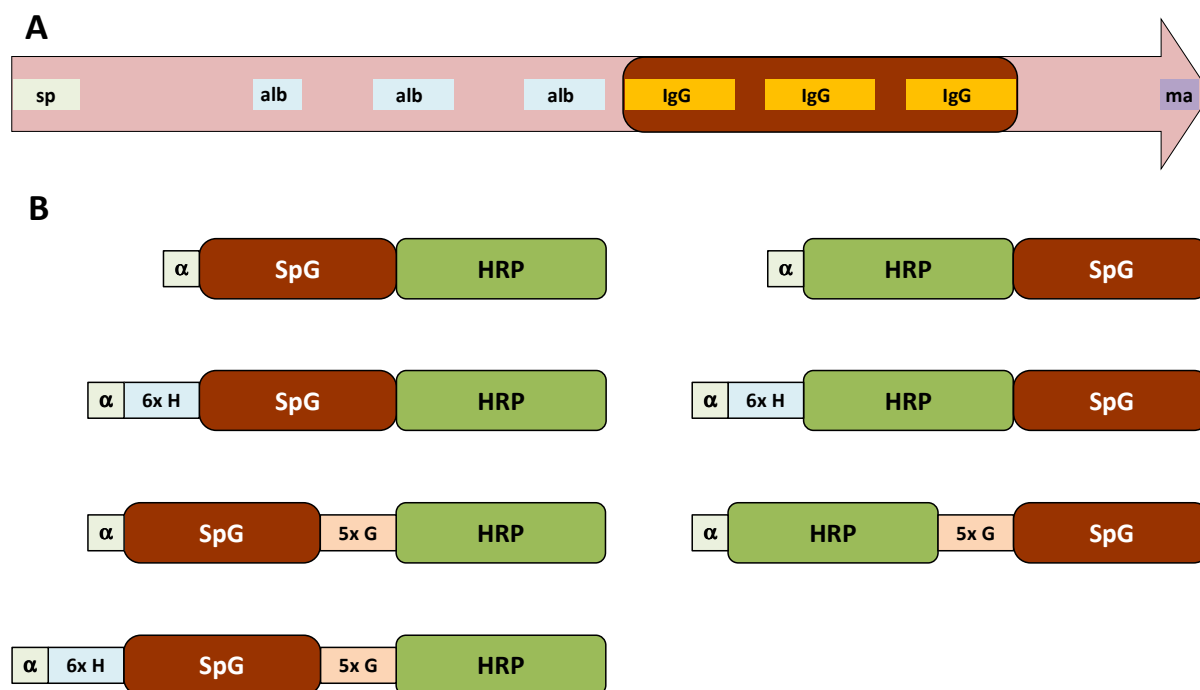


Figure 1. Schemes of SpG constructs. (A) Representation of wildtype SpG (based on UniProtID P19909) consisting of a signal peptide (sp), albumin and IgG binding domains (alb and IgG, respectively) and a membrane anchor (ma); recombinant SpG only consists of the three IgG binding domains. (B) Recombinant SpG-HRP fusion constructs with or without hexahistidine tag (6x H) or pentaglycine linker (5x G); left, N-terminal fusions of SpG to mature HRP; right, C-terminal fusions of SpG to mature HRP; the *S. cerevisiae* mating factor alpha prepro signal peptide (α) facilitates secretion of the recombinant fusion constructs and is cleaved off by the cells in the process.

Materials & methods

Strains and vectors

P. pastoris strains were based on the strain CBS 7435 (identical to NRRL Y-11430 and ATCC 76273) [15] with Mut^S phenotype [16, 17]. For recombinant protein production we used the previously described strain *PpFWK3* which facilitated the production of homogeneously glycosylated recombinant proteins due to the inactivation of the key mannosyltransferase Och1. [18]. Recombinant SpG based on [6, 12] comprising three IgG-binding sites (Figure 1.A) was codon-optimized [19] and ordered as gBlock (Integrated DNA Technologies, Belgium). Using the primers listed in Supplementary table 1, we assembled seven fusion constructs of SpG and HRP C1A with or without hexahistidine tag or pentaglycine linker (Figure 1.B). The *E.*

coli-P. pastoris shuttle vector pPpT4_alpha_S [16] was used for transformation to *PpFWK3* by electroporation [20] and heterologous expression by methanol induction.

Production, purification and characterization of HRP-SpG

Microscale cultivations were performed in DWPs as described previously [21, 22]. Bioreactor cultivation was performed in a BIOSTAT® B bioreactor (Sartorius, Germany). Concentrated cultivation supernatant of hexahistidine-tagged fusion proteins was loaded on a HisTrap FF column (GE Healthcare, Austria), bound protein was eluted with 100 mM imidazole. Polishing of elution fractions was performed by size exclusion chromatography (HiLoad™ 16/60 Superdex™ 200 prep grade column; GE Healthcare). Direct ELISA was done with human or rabbit IgG as antigens. HRP-SpG fusion protein was used at a concentration of 0.1 µg/mL. Detailed descriptions are given in the Supplementary information.

Results & discussion

Recombinant HRP-SpG fusion protein has a constant 1:1 stoichiometry and is thus more homogeneous and reproducible than chemical HRP-SpG conjugates, following quality-by-design principles. We assembled seven HRP-SpG fusion protein constructs (Figure 1.B) and screened for HRP activity from microscale cultivations. Previously, we found C-terminal fusions of tags to HRP to reduce or even abolish HRP activity, whereas N-terminal fusions did not result in such a detrimental effect [Vogl et al., manuscript in preparation]. In the case of a SpG-fusion however, three N-terminal fusions to HRP resulted in almost abolished HRP activity. The constructs 6xH-SpG-5xG-HRP and HRP-5xG-SpG (from N- to C-terminus) showed approximately the same activity as wildtype HRP. Intriguingly, transformation of constructs with SpG fused to the C-terminus of mature HRP without pentaglycine linker (*i.e.* HRP-SpG and 6xH-HRP-SpG) even resulted in *P. pastoris* strains producing three- to six-fold more HRP activity than strains producing wildtype HRP. Ultimately, we chose the construct 6xH-HRP-SpG for further experiments. At this point we do not have a rational explanation to interpret the distinct effect certain fusion setups had on HRP activity yields and additional studies will be necessary to draw non-speculative conclusions.

In order to produce sufficient amounts for functional tests of our HRP-SpG fusion protein, we cultivated the respective strain in a 1.2 L-bioreactor. After 160 h of total cultivation time (136 h of induction with methanol) we determined volumetric and specific HRP activities.

The volumetric activity was at 183 U/mL with a specific activity of 227 U/mg (Figure 2.A). Since both activity parameters were still increasing over time, even higher yields of target protein can be anticipated with prolonged cultivation time. Based on a specific activity of 1624 ± 175 U/mg of purified HRP-SpG fusion protein we produced approximately 113 mg/L of HRP-SpG fusion protein.

Following initial Ni^{2+} affinity purification, we performed size exclusion chromatography for polishing and followed the elution pattern of protein and heme via the absorbances at 280 and 403 nm, respectively. Interestingly, heme-containing protein eluted in a smaller leading peak and a more dominant main peak (Figure 2.B), presumably two different glycospecies of the same protein. The two species can be either combined in order to maximize the yields of functional HRP-SpG or the leading peak can be discarded in order to maximize homogeneity. To verify functional IgG binding of our HRP-SpG fusion protein we performed direct ELISA with immobilized IgG from either human or rabbit serum as antigens. In both cases, a concentration-dependent signal could be recorded (Figure 3), indicating binding of our recombinant HRP-SpG fusion protein to IgGs of the two tested species. Fusion proteins of both size exclusion peaks showed interchangeable HRP activity and IgG binding, indicating that both species were indeed functional HRP-SpG fusion proteins.

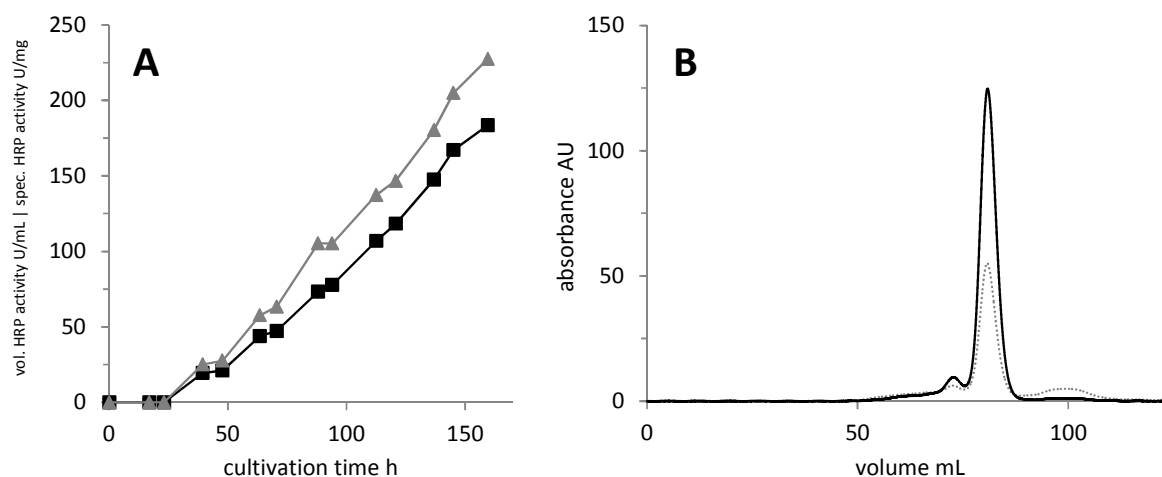


Figure 2. Production and purification of recombinant HRP-SpG fusion protein. A, Volumetric (black squares) and specific (gray triangles) HRP activities from bioreactor cultivation. B, Size exclusion chromatogram of HRP-SpG after Ni^{2+} affinity chromatography; black solid line, A403; gray dotted line, A280.

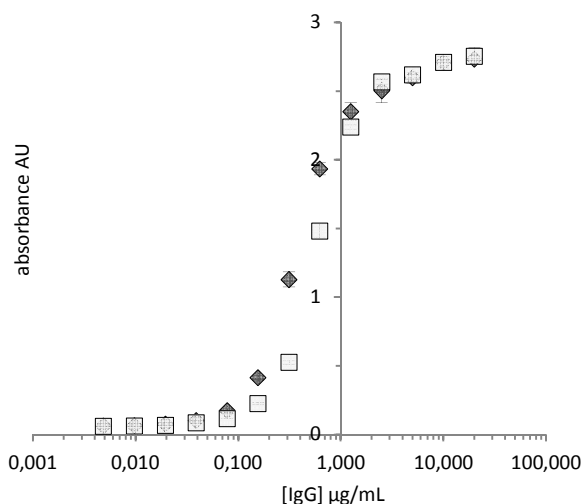


Figure 3. Antigen detection with recombinant HRP-SpG fusion protein in direct ELISA. IgGs from human and rabbit serums (dark gray diamonds and light gray squares, respectively) were used as antigens at concentrations ranging from 20 - 0.01953125 µg/mL. HRP-SpG was used at a concentration of 0.1 µg/mL. Error bars are standard deviations from triplicate measurements.

Conclusion

In contrast to the current methodology, the production of a recombinant HRP-SpG fusion protein is independent from the varying quality and isoenzyme content of common horseradish root isolates as well as from the pitfalls of chemical conjugation. In this study, we identified a particular fusion construct of HRP and SpG to be well secreted by *P. pastoris*. When produced in bioreactor cultivations, competitive yields of more than 110 mg/L were achieved. Direct ELISAs with IgGs from two mammalian species confirmed the applicability of the produced recombinant HRP-SpG fusion protein in immunohistochemistry.

Future studies will focus on using alternative HRP isoenzymes [23] as fusion partner with higher catalytic activity towards common ELISA substrates to increase assay sensitivity. Also, by performing directed evolution on the SpG fusion partner, tighter IgG binding and an even broader IgG range could be reached.

Acknowledgements

The authors gratefully acknowledge the excellent assistance of Carolin Kunz in the lab and the support from NAWI Graz and the Austrian Science Fund FWF project W901 "DK Molecular Enzymology". The authors declare that they have no conflict of interest.

References

1. Kronvall G: **A surface component in group A, C, and G streptococci with non-immune reactivity for immunoglobulin G.** *J. Immunol.* 1973, **111**:1401–6.
2. Myhre EB, Kronvall G: **Heterogeneity of nonimmune immunoglobulin Fc reactivity among gram-positive cocci: description of three major types of receptors for human immunoglobulin G.** *Infect. Immun.* 1977, **17**:475–82.
3. Björck L, Kronvall G: **Purification and some properties of streptococcal protein G, a novel IgG-binding reagent.** *J. Immunol.* 1984, **133**:969–74.
4. Akerström B, Brodin T, Reis K, Björck L: **Protein G: a powerful tool for binding and detection of monoclonal and polyclonal antibodies.** *J. Immunol.* 1985, **135**:2589–92.
5. Fahnestock SR, Alexander P, Nagle J, Filpula D: **Gene for an immunoglobulin-binding protein from a group G streptococcus.** *J. Bacteriol.* 1986, **167**:870–80.
6. Olsson A, Eliasson M, Guss B, Nilsson B, Hellman U, Lindberg M, Uhlén M: **Structure and evolution of the repetitive gene encoding streptococcal protein G.** *Eur. J. Biochem.* 1987, **168**:319–24.
7. Mekaprateep M, Tharavichitkul P, Srikitjakarn L: **Application of a non-species dependent ELISA for the detection of antibodies in sera of Burkholderia pseudomallei-immunized goats.** *J. Microbiol. Methods* 2010, **83**:266–9.
8. Lee B-H, Yoshimatsu K, Araki K, Ogino M, Okumura M, Tsuchiya K, Kariwa H, Arikawa J: **Detection of antibody for the serodiagnosis of hantavirus infection in different rodent species.** *Arch. Virol.* 2003, **148**:1885–97.
9. Stöbel K, Schönberg A, Staak C: **A new non-species dependent ELISA for detection of antibodies to Borrelia burgdorferi s. l. in zoo animals.** *Int. J. Med. Microbiol.* 2002, **291 Suppl** :88–99.
10. Avrameas S: **Coupling of enzymes to proteins with glutaraldehyde. Use of the conjugates for the detection of antigens and antibodies.** *Immunochemistry* 1969, **6**:43–52.
11. O’Sullivan MJ, Gnemmi E, Morris D, Chierigatti G, Simmons M, Simmonds AD, Bridges JW, Marks V: **A simple method for the preparation of enzyme-antibody conjugates.** *FEBS Lett.* 1978, **95**:311–3.
12. Goward CR, Murphy JP, Atkinson T, Barstow DA: **Expression and purification of a truncated recombinant streptococcal protein G.** *Biochem. J.* 1990, **267**:171–7.
13. Tang J-B, Zhu P, Yang H, Sun L-M, Song S, Ji A: **Expression and secretion of recombinant ZZ-EGFP fusion protein by the methylotrophic yeast Pichia pastoris.** *Biotechnol. Lett.* 2008, **30**:1409–14.
14. Koliassnikov O V, Grigorenko VG, Egorov AM, Lange S, Schmid RD: **Recombinant Production of Horseradish Peroxidase Conjugates with Fab Antibodies in Pichia pastoris for Analytical Applications.** *Acta Naturae* 2011, **3**:85–92.
15. Küberl A, Schneider J, Thallinger GG, Anderl I, Wibberg D, Hajek T, Jaenicke S, Brinkrolf K, Goesmann A, Szczepanowski R, Pühler A, Schwab H, Glieder A, Pichler H: **High-quality genome sequence of Pichia pastoris CBS7435.** *J. Biotechnol.* 2011, **154**:312–320.
16. Näätsaari L, Mistlberger B, Ruth C, Hajek T, Hartner FS, Glieder A: **Deletion of the Pichia pastoris KU70 Homologue Facilitates Platform Strain Generation for Gene Expression and Synthetic Biology.** *PLoS One* 2012, **7**:e39720.
17. Krainer FW, Dietzsch C, Hajek T, Herwig C, Spadiut O, Glieder A: **Recombinant protein expression in Pichia pastoris strains with an engineered methanol utilization pathway.** *Microb. Cell Fact.* 2012, **11**:22–35.
18. Krainer FW, Gmeiner C, Neutsch L, Windwarder M, Pletzenauer R, Herwig C, Altmann F, Glieder A, Spadiut O: **Knockout of an endogenous mannosyltransferase increases the homogeneity of glycoproteins produced in Pichia pastoris.** *Sci. Rep.* 2013, **3**:3279–91.
19. Abad S, Nahalka J, Bergler G, Arnold SA, Speight R, Fotheringham I, Nidetzky B, Glieder A: **Stepwise engineering of a Pichia pastoris D-amino acid oxidase whole cell catalyst.** *Microb. Cell Fact.* 2010, **9**:24.
20. Lin-Cereghino J, Wong WW, Xiong S, Giang W, Luong LT, Vu J, Johnson SD, Lin-Cereghino GP: **Condensed protocol for competent cell preparation and transformation of the methylotrophic yeast Pichia pastoris.** *Biotechniques* 2005, **38**:44–48.

21. Weis R, Luiten R, Skranc W, Schwab H, Wubbolts M, Glieder A: **Reliable high-throughput screening with *Pichia pastoris* by limiting yeast cell death phenomena.** *FEMS Yeast Res.* 2004, **5**:179–89.
22. Krainer FW, Capone S, Jäger M, Vogl T, Gerstmann M, Glieder A, Herwig C, Spadiut O: **Optimizing cofactor availability for the production of recombinant heme peroxidase in *Pichia pastoris*.** *Microb. Cell Fact.* 2015, **14**.
23. Näätäsaari L, Krainer FW, Schubert M, Glieder A, Thallinger GG: **Peroxidase gene discovery from the horseradish transcriptome.** *BMC Genomics* 2014, **15**:227.

Supplementary information

Materials and methods

Chemicals

2,2'-azino-bis(3-ethylbenzthiazoline-6-sulfonic acid) diammonium salt (ABTS), 3,3',5,5'-tetramethylbenzidine dihydrochloride hydrate (TMB), bovine serum albumin (BSA), D(+)-biotin, hemin, IgG from either human or rabbit serum and Tween® 20 were purchased from Sigma-Aldrich (Austria). Difco™ yeast nitrogen base w/o amino acids (YNB), Bacto™ tryptone and Bacto™ yeast extract (YE) were from Becton Dickinson (Austria). ACEPOL 83 E was from Lubrizol Additives (Ohio, USA). Zeocin™ was from InvivoGen (France). Other chemicals were obtained from Carl Roth (Germany).

Microscale cultivations

Strains were grown in 250 µL BMD1% minimal growth medium (11 g/L alpha-D(+)-glucose monohydrate, 13.4 g/L YNB, 0.4 mg/L D(+)-biotin, 0.1 M potassium phosphate buffer, pH 6.0) supplemented with 25 µM hemin at 28 °C, 320 rpm, 80% humidity. After approximately 60 h, recombinant expression was induced by additions of 250 µL BMM2 (1% v/v methanol, 13.4 g/L YNB, 0.4 mg/L, D(+)-biotin, 0.1 M potassium phosphate buffer, pH 6.0), followed by three additions of 50 µL BMM10 each (5% v/v methanol, 13.4 g/L YNB, 0.4 mg/L, D(+)-biotin, 0.1 M potassium phosphate buffer, pH 6.0) 10, 24 and 48 h after the first induction pulse. Cells were centrifuged at 3220 x g, 15 min, 72 h after the first induction pulse. HRP activity was determined by following an increase in absorbance at 405 nm upon mixing of 15 µL supernatant with 140 µL assay solution (1 mM ABTS, 0.9 mM H₂O₂, 50 mM sodium acetate, pH 4.5) in a microtiter plate.

Bioreactor cultivations

Media: Buffered minimal glycerol yeast medium (BMGY): 10 g/L YE, 13.4 g/L YNB, 20 g/L Bacto™ tryptone, 12.6 g/L glycerol, 0.4 mg/L D(+)-biotin, 100 mM potassium phosphate, pH 6. Trace element solution (PTM1): 5.99 g/L CuSO₄·5H₂O, 0.08 g/L KI, 3 g/L MnSO₄·H₂O, 0.2 g/L Na₂MoO₄·2H₂O, 0.02 g/L H₃BO₃, 0.92 g/L CoCl₂·6H₂O, 42.18 g/L ZnSO₄·7H₂O, 65 g/L FeSO₄·7H₂O, 5 mL/L 95-98% H₂SO₄. Basal salts medium (BSM): 40 g/L ≥98% glycerol, 4.25

mL/L 85% phosphoric acid, 0.17 g/L CaSO₄·2H₂O, 0.22 g/L NaCl, 0.64 g/L KOH, 2.86 g/L K₂SO₄, 14 g/L MgSO₄·7H₂O, 4.36 mL/L PTM1, 0.87 mg/L D(+)-biotin, 1 mL/L ACEPOL 83 E.

Cultivation procedure: Bioreactor cultivations were performed in a 1.2 L BIOSTAT® B bioreactor (Sartorius, Germany). NH₄OH was used as nitrogen source and to maintain pH 6. A dO₂ level of min. 30% was set under cascade control settings. A 50 mL preculture was grown for two days at 28 °C, 90 rpm, 80% humidity and used for inoculation to start a batch cultivation (450 mL autoclaved BSM, sterile addition of 2.18 mL PTM1 and 2.18 mL of 200 mg/L D(+)-biotin). Upon glycerol depletion (as indicated by a steady increase in dO₂), a glycerol fed-batch cultivation was started for 7 h with a total feed of 34.5 g glycerol. After addition of 30 µM hemin, 60.4 g methanol were fed over 136.6 h to induce PAOX1-regulated expression. Cells were harvested by centrifugation (17700 x g, 40 min) and the supernatant was filtered through 0.2 µm cellulose acetate filters (Sartorius, Germany).

Sample handling: Samples were taken regularly to determine dry cell weight (DCW), enzyme activity and total protein concentration. HRP activity was determined as described above. Protein concentration was determined with the Bio-Rad protein assay (Bio-Rad, Austria) based on a standard curve of different concentrations of BSA.

Protein purification

Protein concentration and buffer changes were done using Vivaflow® 50 cassettes (30 kDa MWCO) and Vivaspin® 20 centrifugal concentrators (3 kDa MWCO) (Sartorius). Prior to Ni²⁺ affinity chromatography on a HisTrap FF column (GE, Healthcare, Austria), the buffer was changed to calcium-supplemented tris-buffered saline (Ca-TBS; 1 mM CaCl₂, 150 mM NaCl, 50 mM Tris, pH 7.5 set with HCl). Washing was performed for at least five column volumes, elution was done with 100 mM imidazole in Ca-TBS. Elution fractions were pooled, concentrated to max. 1 mL and loaded on a HiLoad™ 16/60 Superdex™ 200 prep grade column (GE Healthcare) for size exclusion polishing at a flow of 0.3 mL/min with Ca-TBS.

ELISA

MICROLON® clear high-binding microplates (Greiner Bio-One, Austria) were coated with 100 µL IgG at concentrations from 20 - 0.01953125 µg/mL in coating buffer (150 mM NaCl, 50 mM Tris, pH 8.0) at 4 °C over night or at 37 °C, 2 h. Wells were washed three times (5 min, 600 rpm on a shaking platform) with 200 µL washing buffer (0.05% v/v Tween® 20, 150 mM

NaCl, 50 mM Tris, pH 7.5). Blocking was done by incubation with 200 μ L blocking buffer (1.5% w/v BSA in washing buffer), 37 $^{\circ}$ C, 1 h, followed by three washing steps. IgG binding with HRP-SpG fusions was done by addition of 100 μ L 0.1 μ g/mL HRP-SpG (diluted in blocking buffer) and incubation at 25 $^{\circ}$ C, 1 h, followed by six washing steps. Detection was performed by measuring the absorbance at 450 nm after 15 min incubation with 100 μ L detection solution (0.5 mM TMB, 2.9 mM H_2O_2 in 50 mM sodium citrate buffer, pH 5.5) followed by addition of 100 μ L 1 M H_2SO_4 .

Supplementary table 1. Oligonucleotide primers. Sequences are in 5'-3' orientation





name	sequence
mySpGfw	ATATCTCGAGAAGAGAGAGAGGCCGAAGCTACTTACAAGTTGATCCTGAACGGA
mySpG_NHISfw	ATATCTCGAGAAGAGAGAGAGGCCGAAG
mySpGrv1	CAAGAGTTATCGTAGAAGGTTGGAGTAAGTTGCTCGGTGACGGTGAAGGTCTTAG
mySpGrv2	CAAGAGTTATCGTAGAAGGTTGGAGTAAGTTG
oePCR_C1Afw	CAACTTACTCCAACCTTCTACGATAACTC
oePCR_C1Arv	ATATGCGGCCGCATTATGAGTTAGAG
C1Arv	TGAGTTAGAGTTGACAACACG
SpG5fw	CGTGTTGTCAACTCTAACTCAACTTACAAGTTGATCCTGAACGGA
SpG6fw	CGTGTTGTCAACTCTAACTCAGGAGGAGGTGGTGGAACTTACAAGTTGATCCTGAACGGA
SpGsCterm_rv	ATATGCGGCCGCATTACTCGGTGACGGTGAAGGTCTTA

- Chapter 9 -

Protocol for the production and purification of recombinant horseradish peroxidase from *Pichia pastoris*

Florian W. Krainer¹

¹ Graz University of Technology, Institute of Molecular Biotechnology, NAWI Graz, Petersgasse 14, 8010 Graz, Austria

Creation date: April 2015									
Validity: until revoked/cancelled									
This protocol replaces the version from: -									
Developed in project/working group: FWF project W901 "DK Molecular Enzymology"									
Notice of modification: -									
Written by: Florian W. Krainer									
Date/signature: 23.04.15 									
Checked:	<table border="1"> <tr> <td>Yes</td> <td><input checked="" type="checkbox"/></td> <td>Date/Signature:</td> <td>27.06.15 </td> </tr> <tr> <td>No</td> <td><input type="checkbox"/></td> <td></td> <td></td> </tr> </table>	Yes	<input checked="" type="checkbox"/>	Date/Signature:	27.06.15 	No	<input type="checkbox"/>		
Yes	<input checked="" type="checkbox"/>	Date/Signature:	27.06.15 						
No	<input type="checkbox"/>								
Approved by: UNABC PATRICIA									

1. Purpose and Field of Application

This protocol relates to the current methods for production and purification of recombinant horseradish peroxidase (HRP) from *Pichia pastoris*. The methods described here can be used to perform microscale screenings in 96-deep well plate (DWP) cultivations and production-scale cultivations in bioreactors using cofactor-supplemented growth media for augmented yields of any HRP isoenzyme. Also, a method for the purification of recombinant HRP, preferably isoenzyme C1A, from *P. pastoris* is described.

2. Principle

A *P. pastoris* strain producing recombinant HRP is cultivated in either DWPs or bioreactors. Supernatant from DWP cultivations can be used directly for HRP activity screenings. Supernatants from bioreactor cultivations are subjected to purification procedures

(immobilized metal affinity chromatography, optional ligand affinity chromatography, size exclusion chromatography) for the production of recombinant HRP preparations of high purity.

3. Keywords, Definitions & Abbreviations

Keywords

Plant peroxidase, horseradish peroxidase, recombinant protein production, protein purification, *Pichia pastoris*

Abbreviations

Abbreviation	Description
ABTS	2,2'-azino-bis(3-ethylbenzthiazoline-6-sulfonic acid) diammonium salt
AOX1	alcohol oxidase 1 gene
BHA	benzhydroxamic acid
BMD1%	buffered minimal dextrose medium
BMGY	buffered minimal glycerol yeast medium
BMM	buffered minimal methanol medium
BSM	basal salts medium
Ca-TBS	calcium-supplemented Tris-buffered saline
DCW	dry cell weight
DMSO	dimethyl sulfoxide
dO ₂	dissolved oxygen
DWP	96-deep well plate
EDAC	N-(3-Dimethylaminopropyl)-N'-ethylcarbodiimide hydrochloride
GAP	glyceraldehyde-3-phosphate dehydrogenase gene
HRP	horseradish peroxidase
IMAC	immobilized metal affinity chromatography
LAC	ligand affinity chromatography
MWCO	molecular weight cut off
NHA	naphthohydroxamic acid
PNP	5-nitrophenol
PTM1	trace element solution
SEC	size exclusion chromatography
YE	Bacto™ yeast extract
YNB	Difco™ yeast nitrogen base w/o amino acids

4. Methodology

4.1. Reagents

List of the chemicals and ingredients needed

Name	Formula	MW	Purity	Supplier	Order No.	Comments
2,2'-azino-bis(3-ethylbenzthiazoline-6-sulfonic acid) diammonium salt (ABTS)	$C_{18}H_{24}N_6O_6S_4$	548.68	≥98%	Sigma-Aldrich Handels GmbH	A1888	store at 4 °C
4-aminobenzoic acid	$C_7H_7NO_2$	137.14	99%	Sigma-Aldrich Handels GmbH	100536-250G	
5-nitrophenol (PNP)	$C_6H_5NO_3$	139.11	≥99%	Sigma-Aldrich Handels GmbH	241326-50G	hazardous
6-amino-2-naphthoic acid	$C_{11}H_9NO_2$	187.19	90%	Sigma-Aldrich Handels GmbH	512370-5G	
Acepol™ 83E				Lubrizol GmbH		turbid when autoclaved
alpha-(D+)-glucose monohydrate	$C_6H_{12}O_6 \cdot H_2O$	198.17	≥99.5%	Carl Roth GmbH	6780.2	
ammonium hydroxide	NH_4OH	17.03	25% (13.358 M)	Carl Roth GmbH	5460.2	hazardous
Bacto™ peptone				BD Biosciences	211820	
Bacto™ yeast extract (YE)				BD Biosciences	212720	
boric acid	H_3BO_3	61.83	≥99.8	Carl Roth GmbH	6943.2	
calcium sulfate dihydrate	$Ca_2SO_4 \cdot 2H_2O$	172.17	≥98	Carl Roth GmbH	P741.2	
calcium chloride dihydrate	$CaCl_2 \cdot 2H_2O$	147.01	≥99%	Carl Roth GmbH	5239.2	
cobalt chloride hexahydrate	$CoCl_2 \cdot 6H_2O$	237.93	≥99	Carl Roth GmbH	T889.1	
copper sulfate pentahydrate	$CuSO_4 \cdot 5H_2O$	249.69	≥99.5	Carl Roth GmbH	P024.1	
D(+)-biotin	$C_{10}H_{16}N_2O_3S$	244.31	≥98.5%	Carl Roth GmbH	3822.1	store at 4 °C
Difco™ yeast nitrogen base w/o amino acids (YNB)				BD Biosciences	291920	
dimethyl sulfoxid (DMSO)	$(CH_3)_2SO$	78.13	≥99.8%	Carl Roth GmbH	4720.4	
dipotassium hydrogen phosphate	K_2HPO_4	174.18	≥98%	Carl Roth GmbH	6875.1	
geneticin disulfate	$C_{20}H_{40}N_4O_{10} \cdot 2H_2SO_4$	692.70		Carl Roth GmbH	0239.4	antibiotic, store at 4 °C
glycerol	$C_3H_8O_3$	92.09	≥98%	Carl Roth GmbH	7530.4	
hydrochloric acid	HCl	36.46	37%	Carl Roth GmbH	9277.2	hazardous
hydrogen peroxide	H_2O_2	34.01	30% (9.7899 M)	Carl Roth GmbH	8070.2	store at 4 °C
hydroxylamine hydrochloride	$NH_2OH \cdot HCl$	69.49	99%	Sigma-Aldrich Handels GmbH	159417-500G	hazardous
imidazole	$C_3H_4N_2$	68.08	99%	Sigma-Aldrich Handels GmbH	I202-100G	
iron sulfate heptahydrate	$FeSO_4 \cdot 7H_2O$	278.02	≥99	Carl Roth GmbH	P015.1	

Chapter 9

magnesium sulfate heptahydrate	MgSO ₄ ·7H ₂ O	246.48	≥99	Carl Roth GmbH	P027.2	
manganese sulfate monohydrate	MnSO ₄ ·H ₂ O	169.02	≥99	Carl Roth GmbH	X890.1	
methanesulfonic acid	CH ₄ O ₃ S	96.11	≥99.5%	Sigma-Aldrich Handels GmbH	471356-25ML	hazardous
methanol	CH ₃ OH	32.04	≥99.9%	Carl Roth GmbH	4627.2	hazardous
N-(3-dimethylaminopropyl)-N'-ethylcarbodiimide hydrochloride (EDAC)	C ₈ H ₁₈ N ₃ Cl	191.70	≥98%	Sigma-Aldrich Handels GmbH	03450-5G	
kanamycin sulfate	C ₁₈ H ₃₆ N ₄ O ₁₁ ·H ₂ SO ₄	582.58	≥750 I.U./mg	Carl Roth GmbH	T832.4	antibiotic, store at 4 °C
N,N-dimethylformamide	C ₃ H ₇ NO	73.09	≥99%	Sigma-Aldrich Handels GmbH	D4551-500ML	hazardous
phosphoric acid	H ₃ PO ₄	98.01	85%	Carl Roth GmbH	6366.1	hazardous
potassium dihydrogen phosphate	KH ₂ PO ₄	136.09	≥99%	Carl Roth GmbH	3904.1	
potassium hydroxide	KOH	56.11	≥85%	Carl Roth GmbH	6751.1	hazardous
potassium iodide	KI	166.01	≥99.5	Carl Roth GmbH	6750.1	
potassium sulfate	K ₂ SO ₄	174.27	≥99	Carl Roth GmbH	P022.2	
sodium acetate	C ₂ H ₃ NaO ₂	82.03	≥99%	Carl Roth GmbH	6773.2	
sodium chloride	NaCl	58.44	≥99.5	Carl Roth GmbH	3957.1	
sodium molybdate dihydrate	Na ₂ MoO ₄ ·2H ₂ O	241.95	≥99.5	Carl Roth GmbH	0274.2	
succinic acid	C ₄ H ₆ O ₄	118.09	≥99%	Sigma-Aldrich Handels GmbH	S3674-100G	
sulfuric acid	H ₂ SO ₄	98.08	95.98%	Carl Roth GmbH	X944.2	hazardous
Tris	C ₄ H ₁₁ NO ₃	121.14	≥99.3%	Carl Roth GmbH	AE15.3	
zeocin™	C ₅₅ H ₈₅ O ₂₁ N ₂ OS ₂ Cu·HCl	1525.00	≥90	InvivoGen	ant-zn-5p	antibiotic, store at 4 °C
zinc sulfate heptahydrate	ZnSO ₄ ·7H ₂ O	287.54	≥99	Carl Roth GmbH	T884.1	

4.2. Solutions

List of the solutions needed to perform the method

Name	Ingredients	Comments
ABTS assay solution, 1x	1 mL 20.05 mM ABTS stock, 1.75 µL 30% H ₂ O ₂ , 19 mL 50 mM NaOAc, pH 4.5	prepare fresh, keep on ice, keep in dark place
ABTS stock, 20.05 mM	dissolve 440 mg 2,2'-azino-bis(3-ethylbenzthiazoline-6-sulfonic acid) diammonium salt in 40 mL NaOAc, pH 4.5	store at 4 °C
alpha-D(+)-glucose stock, 10x	220 g/L alpha-D(+)-glucose monohydrate	autoclave
BHAffi-A buffer	150 mM NaCl, 50 mM potassium phosphate, pH 7	0.2 µm filtration, store at 4 °C
BHAffi-B buffer	400 mM boric acid, set pH 9 with KOH	0.2 µm filtration, store at 4-10 °C, check for salt precipitation before use
BHAffi-S buffer	20% v/v ethanol, 20 mM potassium phosphate, pH 6	0.2 µm filtration
BMD1%	11 g/L alpha-D(+)-glucose monohydrate, 13.4 g/L YNB, 0.4 mg/L D(+)-biotin, 0.1 M potassium phosphate buffer, pH 6.0	prepare fresh with sterile solutions
BMGY	10 g/L YE, 13.4 g/L YNB, 20 g/L Bacto™ peptone, 12.6 g/L glycerol, 0.4 mg/L D(+)-biotin, 0.1 M potassium phosphate, pH 6	autoclave, addition of sterile D(+)-biotin afterwards
BMM2	1% v/v methanol, 13.4 g/L YNB, 0.4 mg/L, D(+)-biotin, 0.1 M potassium phosphate buffer, pH 6.0	prepare fresh with sterile solutions

Chapter 9

BMM10	5% v/v methanol, 13.4 g/L YNB, 0.4 mg/L, D(+)-biotin, 0.1 M potassium phosphate buffer, pH 6.0	prepare fresh with sterile solutions
BSM	40 g/L $\geq 98\%$ glycerol, 4.25 mL/L 85% phosphoric acid, 0.17 g/L $\text{CaSO}_4 \cdot 2\text{H}_2\text{O}$, 0.22 g/L NaCl, 0.64 g/L KOH, 2.86 g/L K_2SO_4 , 14 g/L $\text{MgSO}_4 \cdot 7\text{H}_2\text{O}$, 4.36 mL/L PTM1, 0.87 mg/L D(+)-biotin, 1 mL/L ACEPOL 83 E	autoclave, addition of sterile D(+)-biotin and PTM1 afterwards
Ca-TBS buffer	1 mM CaCl_2 , 150 mM NaCl, 50 mM Tris, pH 7.5 set with HCl	0.2 μm filtration
D(+)-biotin stock, 500x	200 mg/L D(+)-biotin	sterile filtration, store at 4 °C
glucose feed medium, 60% w/w	600 g/L $\geq 98\%$ α -D(+)-glucose monohydrate, 12 mL/L PTM1, 12 mL/L 500x D(+)-biotin stock, 976 mL/L dH_2O	autoclave, addition of sterile D(+)-biotin and PTM1 afterwards
glycerol feed medium, 50% w/w	500 g/L $\geq 98\%$ glycerol, 12 mL/L PTM1, 12 mL/L 500x D(+)-biotin stock, 476 mL/L dH_2O	autoclave, addition of sterile D(+)-biotin and PTM1 afterwards
hemin stock, 500 μM	either dissolve 16.3 mg hemin in 5 mL 100 mM KOH or dissolve 16.3 mg hemin in 1 mL 5% NH_4OH , then fill to 50 mL	sterile filtration, store at 4 °C
methanol feed medium, 50% v/v	500 mL/L $\geq 99.8\%$ methanol, 500 mL/L dH_2O	autoclave dH_2O , add methanol afterwards
potassium phosphate buffer, 10x (1 M)	30 g/L K_2HPO_4 , 118 g/L KH_2PO_4 , set pH 6 with KOH or phosphoric acid	autoclave
PTM1	5.99 g/L $\text{CuSO}_4 \cdot 5\text{H}_2\text{O}$, 0.08 g/L KI, 3 g/L $\text{MnSO}_4 \cdot \text{H}_2\text{O}$, 0.2 g/L $\text{Na}_2\text{MoO}_4 \cdot 2\text{H}_2\text{O}$, 0.02 g/L H_3BO_3 , 0.92 g/L $\text{CoCl}_2 \cdot 6\text{H}_2\text{O}$, 42.18 g/L $\text{ZnSO}_4 \cdot 7\text{H}_2\text{O}$, 65 g/L $\text{FeSO}_4 \cdot 7\text{H}_2\text{O}$, 5 mL/L 95-98% H_2SO_4	prepare fresh, sterile filtration, store at 4 °C
sodium acetate (NaOAc) buffer, 50 mM	4.1 g/L $\text{C}_2\text{H}_3\text{NaO}_2$, set pH 4.5 with sodium hydroxide or acetic acid	autoclave
YNB stock, 10x	134 g/L YNB	autoclave, store in dark place

4.3. Materials

Description of materials needed to perform the method

Name	Supplier	Order No.	Comments
96-deep-well plate	Bel-Art Products	F378600000	
Affi-Gel 10 gel agarose beads	Bio-Rad	153-6099	
baffled shake flasks, 300 mL	Bartelt GmbH		custom-made
Bio-Rad Protein Assay Dye Reagent Concentrate	Bio-Rad	500-0006	
cellulose acetate filter, 0.2 μm pore size	Sartorius GmbH		
HiLoad™ 16/60 Superdex™ 200 prep grade column	GE Healthcare GmbH	28-9893-35	
HisTrap FF column, 5 mL	GE Healthcare GmbH	17-5255-01	
Macrosep® advance centrifugal devices	Pall GmbH	MAP003C37	3 kDa MWCO
microcentrifuge tube, 1.5 mL	Greiner Bio-One	616201	
microplate, 96 well, PS, F-bottom, crystal-clear	Greiner Bio-One	655101	
Optifit tips, non filtered	Sartorius GmbH	791204	for multichannel pipettes
10 μL pipette tips	Biozym Scientific GmbH	720031	
200 μL pipette tips	Greiner Bio-One	739291	
1000 μL pipette tips	Greiner Bio-One	740290	
tube, 50 mL, PP, conical bottom, (skirt)	Greiner Bio-One	210261	
Vivaflow® 50 cross flow cassette	Sartorius GmbH	VF05P2	30 kDa MWCO
Vivaspin® 20 centrifugal concentrators	Sartorius GmbH	VS2091	3 kDa MWCO
XK 16/20 column	GE Healthcare GmbH	28-9889-37	

4.4. Apparatus

Description of the instruments needed to perform the test and specifications.

Name	Supplier	Comments
0.1-2.5 µL, 0.5-10 µL pipettes	Eppendorf AG	
2-20 µL, 20-200 µL, 100-1000 µL pipettes	Gilson Inc.	
5-100 µL, 50-1200 µL multichannel pipettes	Sartorius GmbH (formerly Biohit)	
ÄKTA pure / purifier	GE Healthcare GmbH	
BIOSTAT® B bioreactor	Sartorius GmbH	
centrifuge 5415 R + A-4-62 rotor	Eppendorf AG	
centrifuge Avanti® J-20 XP + JA-10 rotor	Beckman Coulter GmbH	
diaphragm pump	Vacuubrand GmbH + Co KG	
HT Multitron II shaker	Infors AG	
NanoDrop 2000c spectrophotometer	peqlab Biotechnologie GmbH	
SynergyMx platereader	BioTek Instruments, Inc.	

4.5. Software

List of the Software needed to perform the method

Name	Distributor
Gen5™	BioTek Instruments, Inc.
MFC SOPR Module Operator Service Program 3.0	Sartorius Stedim Systems
Unicorn 6.0	GE Healthcare GmbH

4.6. Procedure

4.6.1. Microscale cultivations in 96-deep well plates and screenings

Strains are inoculated to 250 µL/well of freshly prepared BMD1% minimal growth medium, supplemented with 25 µM hemin (from 500 µM hemin stock) in DWPs, similar to [1]. Addition of 25 µM hemin increases the volumetric activity yields in 96-DWPs up to 18-fold by efficiently saturating secreted apo-HRP, converting it to the active holo-enzyme. The addition of 1 mM FeSO₄ (instead of hemin) to BMD1% increases the volumetric activity yields up to 6-fold. Addition of d-aminolevulinic acid - as suggested in some publications, *e.g.* [2, 3] - does not increase the yields of active recombinant HRP from *P. pastoris* [4]. After approximately 60 h of growth (*e.g.* from Friday afternoon until Monday morning) at 28 °C, 320 rpm, 50-80% humidity, 250 µL/well of BMM2 are added. Alternatively, the production

protocol can be shortened by BMM2 addition already after approximately 48 h of growth (only recommendable for strains with intact *OCH1*). Approximately 10, 24 and 48 h after BMM2 addition, 50 μ L/well of BMM10 are added. Cells are harvested approximately 72 h after BMM2 addition by centrifugation at 3220 x *g*, 15 min. Supernatant aliquots are used for quantification of produced HRP activity with the ABTS assay (see chapter 4.6.4). If necessary, the induction protocol can be further shortened by BMM10 additions 10, 24, and 34 h after BMM2 addition and harvest 48 h after BMM2 addition (only strains with intact *OCH1*).

In contrast to the upper protocol for strains producing HRP under *PAOX1*-regulation, strains producing HRP under *PGAP*-regulation are fed with pulses of BMD1% instead of BMM2 and BMM10. Strains producing HRP from the *PHTX1* promoter are fed with pulses of BMG1% (1% w/v glycerol instead of alpha-D(+)-glucose monohydrate).

Note: Each plate should contain a negative growth control (*i.e.* not inoculated), a negative HRP activity control (typically the starting strain, *PpMutS* or *PpFWK3*), and a positive HRP activity control in replicates (strain producing reproducible amounts of HRP).

4.6.2. Bioreactor cultivations

Required media and solutions: BMGY, PTM1, BSM, 50% w/w glycerol feed medium, 50% v/v methanol feed medium, 60% w/v glucose feed medium. NH_4OH (10% v/v; dilute 25% v/v NH_4OH with sterile dH_2O) is used as nitrogen source and to set and maintain pH 5 or pH 6 (biomass growth and HRP production are alike at both pH values).

Note: The salts of PTM1 dissolve slowly and it is recommended to rather prepare two separate solutions, PTM1a (0.08 g/L KI, 0.2 g/L $\text{Na}_2\text{MoO}_4 \cdot 2\text{H}_2\text{O}$, 0.02 g/L H_3BO_3 , 0.92 g/L $\text{CoCl}_2 \cdot 6\text{H}_2\text{O}$) and PTM1b (5.99 g/L $\text{CuSO}_4 \cdot 5\text{H}_2\text{O}$, 3 g/L $\text{MnSO}_4 \cdot \text{H}_2\text{O}$, 65 g/L $\text{FeSO}_4 \cdot 7\text{H}_2\text{O}$, 42.18 g/L $\text{ZnSO}_4 \cdot 7\text{H}_2\text{O}$, 5 mL/L 95-98% H_2SO_4), which are added separately to the corresponding media after 0.2 μm filtration.

Strains: Both, a *P. pastoris* CBS 7435-based strain with Mut^{S} phenotype (*PpMutS*) [6] or a *P. pastoris* CBS 7435-based strain with Mut^{S} phenotype and *och1* deletion (*PpFWK3*) [7] can be cultivated using this protocol. However, only recombinant HRP from *PpFWK3* is homogeneously glycosylated and can thus be purified efficiently by SEC, whereas HRP from a *PpMutS* strain is heterogeneously hyperglycosylated and typically elutes as broad peak in SEC, containing adventitious protein contaminations. A histidine-tagged HRP should be produced in order to allow IMAC as convenient first purification step.

Currently, the highest yields of volumetric and specific HRP activities could be reached with a *PpFWK3* strain with *PHTX1*-regulated coproduction of HRP and Hac1, *i.e.* approximately 130 mg/L (based on a volumetric HRP activity of 266 U/mL) after 56 h of cultivation time.

Cultivation procedure for strains producing HRP under PAOX1-regulation: A map of the vector harboring the PAOX1-regulated expression cassette is shown in Figure 1.

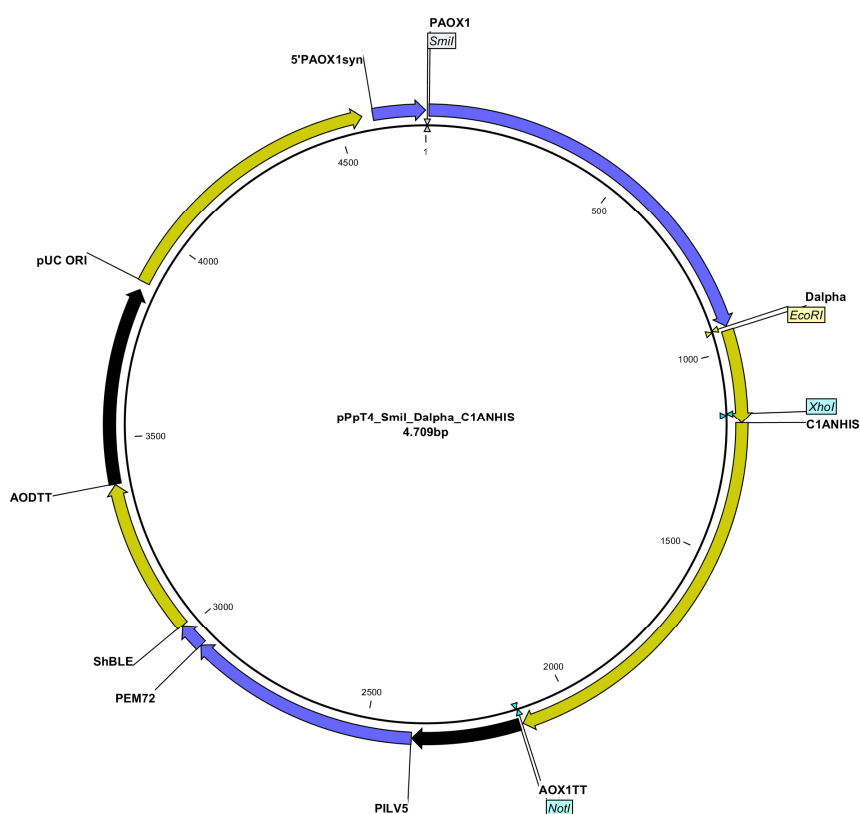


Figure 1: Vector map of pPpT4_Smil_Dalpha_C1ANHIS.

5'PAOX1syn, synthetic sequence upstream of PAOX1; AOX1TT, AOX1 transcription terminator; C1ANHIS, mature C1A gene with N-terminal hexahistidine tag; Dalpha, Δ N57-I70 mutant gene of the *S. cerevisiae* mating factor alpha prepro signal peptide [5]; PAOX1, methanol-inducible AOX1 promoter; PEM72, synthetic EM72 promoter; PILV5, *ILV5* promoter; pUC ORI, pUC origin of replication; ShBLE, *BLE* gene for zeocin™ resistance; [6].

Two precultures are grown in 50 mL BMGY in 300 mL baffled shake flasks for 1-2 d at 28 °C, 90 rpm, 50-80% humidity. The cells are harvested (500 x *g*, 5 min), resuspended in a combined total volume of 50 mL and transferred aseptically into a 1.2 L-BIOSTAT® B bioreactor vessel containing 450 mL sterile BSM. A constant airflow of 1 lpm is set (can be increased to the maximum of 1.5 lpm if necessary) and a minimum dO₂ of 30% is controlled by cascade setting, adjusting the stirrer speed. A glycerol batch cultivation is done until all glycerol is consumed as indicated by a constant increase in dO₂. Then, a growth-limiting

glycerol fedbatch cultivation is done with increasing glycerol medium feeds of 2.8 g/h for 4 h, followed by 5.1 g/h for 1 h, followed by 5.7 g/h for 2 h. Once the glycerol fedbatch is stopped and the cells go into starvation, a methanol induction fedbatch is started. At this point, sterile hemin is added aseptically from a 500 μM stock to a final hemin concentration of 40 μM in the culture broth through the septum [4]. Over the first 3 h of methanol induction, increase the methanol medium feed from 0.2 g/h to 1.0 g/h. A methanol feed of 1.0-1.8 g/h is maintained for approximately 130 h. The feed is regularly stopped to check for a dO_2 signal in order to avoid an overfeed with methanol and an accumulation thereof in the culture broth. The methanol feed should be reduced or temporarily stopped in case of methanol accumulation in the broth. Additionally, the culture's viability (*i.e.* metabolic activity) should be followed indirectly as a constant consumption of NH_4OH . If necessary, additional 1 mL aliquots of 1:10 diluted autoclaved antifoam are added aseptically.

At the end of the cultivation, the culture broth is centrifuged at 17700 x g , 45 min, 4 $^\circ\text{C}$ and the supernatant is filtered through 0.2 μm cellulose acetate filters using a diaphragm pump.

Samples are taken regularly throughout the cultivation to allow a determination of HRP activity and protein concentration with the ABTS assay and the Bio-Rad protein assay, respectively (see chapter 4.6.4 below). Only when the cultivation process is stopped, all samples should be measured on a single plate (due to a high plate-to-plate variability of up to 30%). Biomass is determined by centrifuging aliquots of 1 mL of culture broth (16100 x g , 5 min) in dried and preweighed microcentrifuge tubes. The pelleted biomass in preweighed tubes is then dried for at least 5 d at 95 $^\circ\text{C}$ and then weighed again to allow a calculation of the dry cell weight (DCW).

Cultivation procedure for strains producing HRP under PGAP-regulation: In contrast to the cultivation of strains producing HRP under PAOX1-regulation, neither glycerol fedbatch nor methanol induction fedbatch are performed. Instead, a fedbatch with 60% w/v glucose feed medium is done after the initial glycerol batch phase. In order to rapidly increase biomass, glucose feeds are set to 3.6 g/h for 5 h, followed by 4.3 g/h for 20 h. When the dO_2 signal starts to show a tendency to drop below 30% due to insufficient O_2 supply despite max. airflow and stirrer speed, reduce and maintain glucose feed between 1-4 g/h to a final cultivation time of 60-80 h. Similar to the regulation of the methanol feed described above, the glucose feed should be stopped regularly and the culture's response should be monitored. Hemin is added already at the stage of inoculation to 40 μM final concentration

in the culture broth [4]. A map of the vector harboring the *PGAP*-regulated expression cassette is shown in Figure 2.

Note: HRP production under *PAOX1*-regulation generally results in lower volumetric HRP activity yields than HRP production under *PGAP*-regulation and requires an induction phase with methanol. However, cultivation of strains with *PGAP*-regulated HRP production results in high biomass and thus higher cell lysis towards the end of the cultivation and contamination of HRP in the supernatant with adventitious cellular components that might impede downstream processing (*i.e.* repeated centrifugations are required to allow 0.2 μm filtration of the supernatant; seemingly turbid sample despite 0.2 μm filtration).

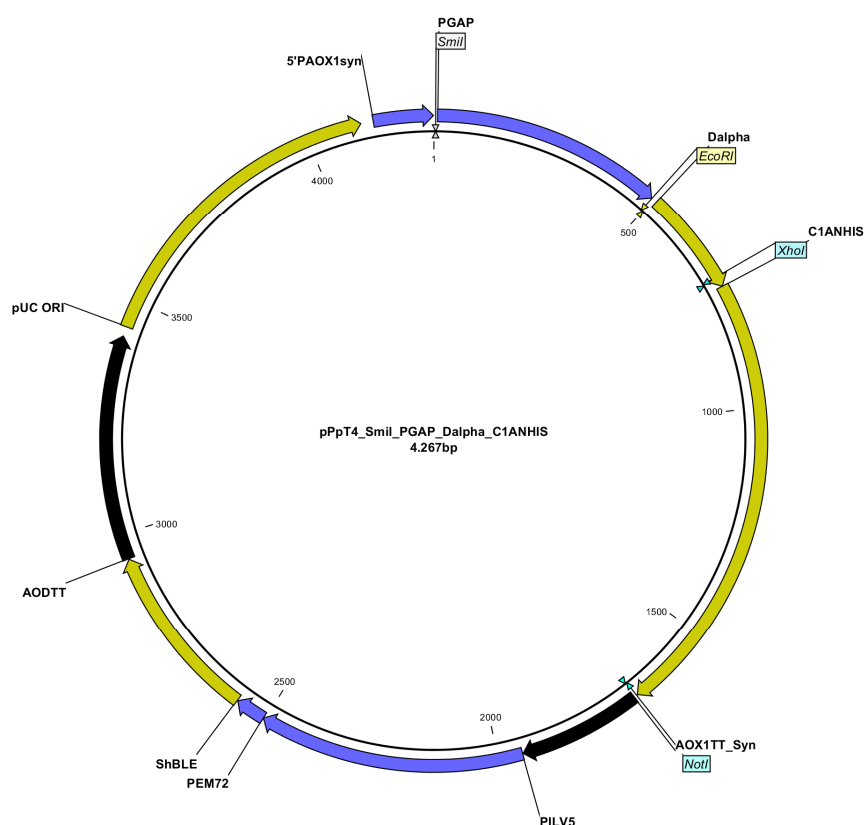


Figure 2: Vector map of pPpT4_Smil_PGAP_Dalpha_C1ANHIS.

5'PAOX1syn, synthetic sequence upstream of *PAOX1*; AOX1TT, AOX1 transcription terminator; C1ANHIS, mature C1A gene with N-terminal hexahistidine tag; Dalpha, $\Delta\text{N57-170}$ mutant gene of the *S. cerevisiae* mating factor alpha prepro signal peptide [5]; PEM72, synthetic EM72 promoter; PGAP, constitutive GAP promoter; PILV5, *ILV5* promoter; pUC ORI, pUC origin of replication; ShBLE, BLE gene for zeocin™ resistance; [6].

Cultivation procedure for strains producing HRP under PHTX1-regulation: Similar to the cultivation of a *PGAP*-regulated HRP production strain, methanol is not required for induction. After the initial glycerol batch cultivation, a feed with 50% w/w glycerol feed medium of 2.3-4.9 g/h is started for approximately 30 h. Hemin is added to the culture broth to a concentration of 40 μM at the stage of inoculation [4]. Again, the culture's viability

should be monitored throughout the whole cultivation. A map of the vector harboring the *PHTX1*-regulated coexpression cassette is shown in Figure 3.

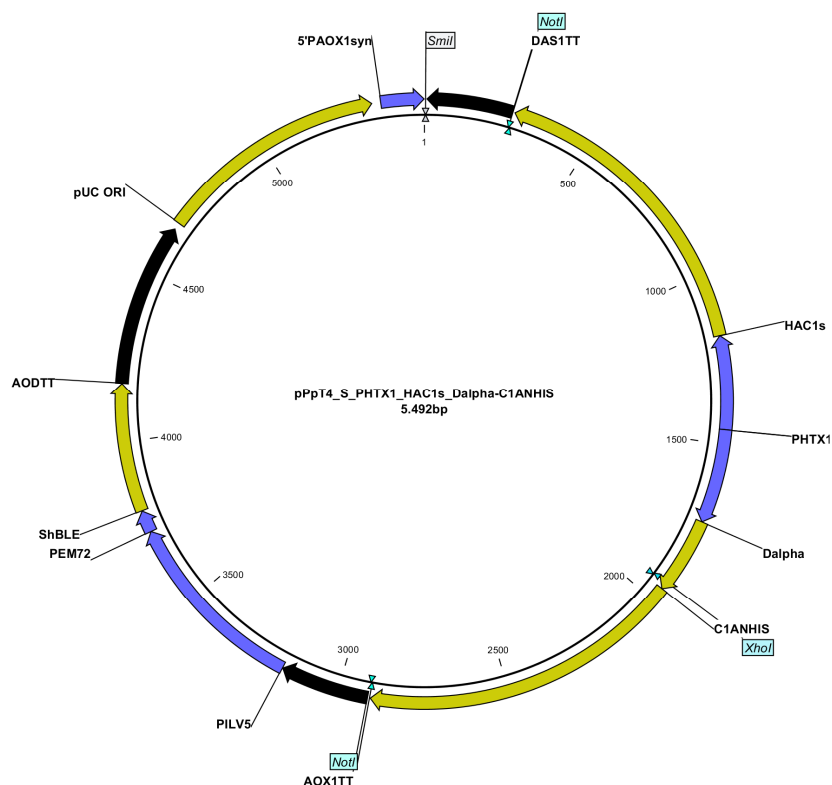


Figure 3: Vector map of pPpT4_SmI_PHTX1_HAC1s_C1ANHIS.

5'PAOX1syn, synthetic sequence upstream of PAOX1; AODTT, AOD transcription terminator; AOX1TT, AOX1 transcription terminator; C1ANHIS, mature C1A gene with N-terminal hexahistidine tag; Dalpha, Δ N57-I70 mutant gene of the *S. cerevisiae* mating factor alpha prepro signal peptide [5]; DAS1TT, DAS1 transcription terminator; HAC1s, active HAC1 gene; PEM72, synthetic EM72 promoter; PHTX1, bidirectional HTX1 promoter; PILV5, ILV5 promoter; pUC ORI, pUC origin of replication; ShBLE, BLE gene for zeocin™ resistance; [6].

4.6.3. Purification of recombinant horseradish peroxidase

After filtration of the cultivation supernatant through 0.2 μ m cellulose acetate filters, the total volume should be reduced below 100 mL using a Vivaflow® 50 cassette, and the buffer should be changed to Ca-TBS. Prior to column loading, all buffers used for purification and the concentrated sample should be filtered through 0.2 μ m filters. The sample is loaded onto a 5 mL HisTrap FF column for IMAC at a flowrate of 5-10 mL/min. All loading and washing fractions are collected and - if necessary - pooled and reloaded to minimize a loss of HRP activity. Elution of bound HRP is performed by washing the column with 200 mM imidazole-containing Ca-TBS. The absorbances at 403 nm (Soret band of HRP-bound heme) and 280 nm (mostly aromatic amino acids of proteins) are monitored. All fractions should be assayed for HRP activity using the ABTS assay (chapter 4.6.4). All elution fractions are

pooled, concentrated and the buffer is changed to the running buffer of the next purification step.

Note: In contrast to a N-terminal hexahistidine tag, a C-terminal hexahistidine tag greatly reduced HRP activity. However, an enzyme with C-terminal nonahistidine tag or a double-tagged enzyme with N-terminal hexahistidine and C-terminal nonahistidine tag did not show impaired activity. Nevertheless, recovery rates from IMAC were comparable for all constructs and the N-terminally hexahistidine-tagged variant should be used preferably.

A chromatogram of N-terminally hexahistidine-tagged HRP C1A loaded on a 5 mL HisTrap FF column is shown in Figure 4.

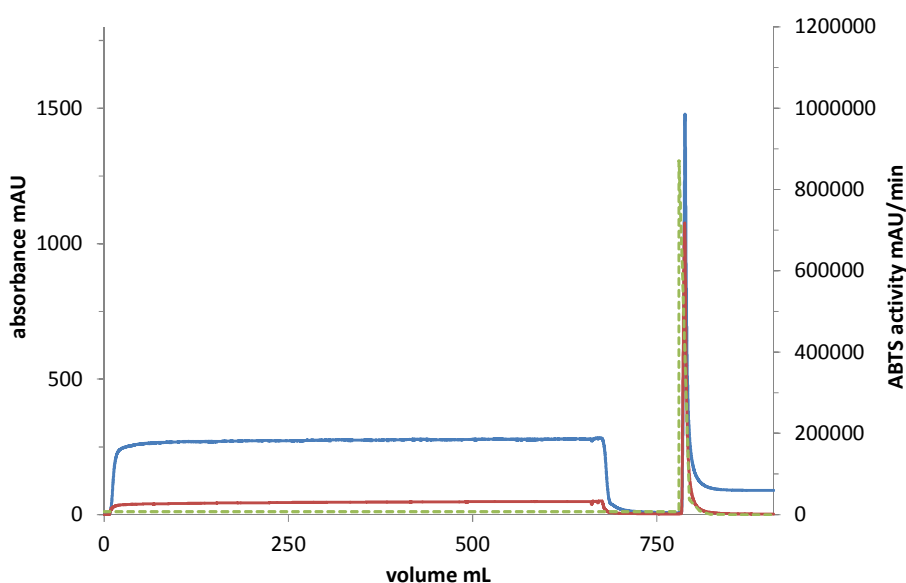


Figure 4: IMAC chromatogram of HRP C1A with N-terminal hexahistidine tag produced in *PpFWK3* under *PAOX1*-regulation.

Approximately 700 mL of HRP C1A containing culture supernatant was loaded on a 5 mL HisTrap FF column. The absorbances at 280 and 403 nm were recorded (blue and red solid lines, respectively). The HRP activities in the collected fractions were determined with the ABTS assay (dotted green line). The A403/A280 ratios may vary between runs, dependent on the cultivation conditions. Loss of HRP activity in load and wash fractions needs to be determined and these fractions can be reloaded if necessary. Enzyme recovery from elution fraction may vary and depends on yet unknown parameters.

In case of an excess of protein contaminants, SEC is not feasible, presumably due to aggregation effects. Thus, an optional ligand affinity chromatography (LAC) step can be performed for further removal of protein contaminants. HRP C1A binds with high affinity (*i.e.* K_d in lower μM range) to aromatic hydroxamic acids such as benzhydroxamic acid (BHA) or naphthohydroxamic acid (NHA) [8]. Either BHA or NHA can be immobilized on agarose gel beads (Affi-Gel 10) by a previously published protocol [8] using either 4-aminobenzoic acid (Figure 5) or 6-amino-2-naphthoic acid as starting molecule, respectively. This protocol provides a detailed step-by-step guide for the desired synthesis. HRP binding to BHA is

weaker than to NHA, however the precursor 4-aminobenzoic acid for immobilization is considerably cheaper than 6-amino-2-naphthoic acid (0.22-0.65 €/g vs. 34.40-53.40 €/g, respectively).

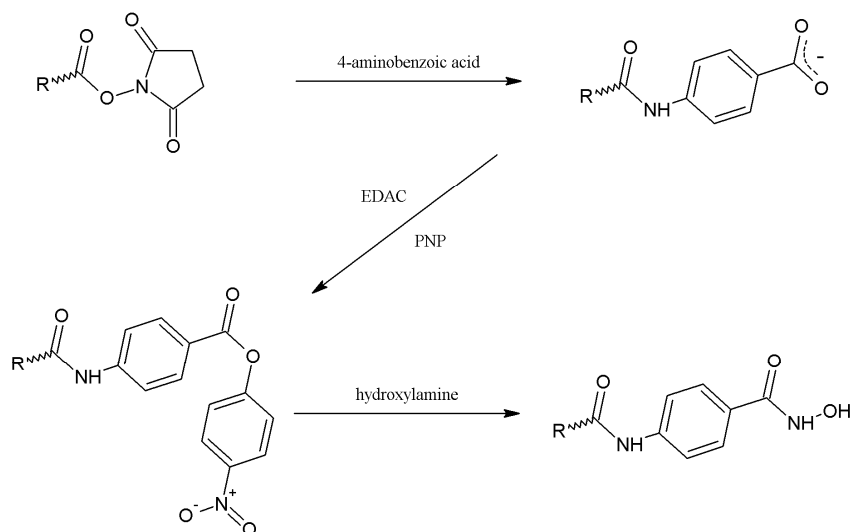


Figure 5: Synthesis of an immobilized aromatic hydroxamic acid for LAC.

In a first step, the N-hydroxysuccinimide group on Affi-Gel 10 agarose gel beads (shown as R~) is replaced by 4-aminobenzoic acid. In the presence of EDAC, PNP is esterified to the carboxylate group of the immobilized 4-aminobenzoic acid. The ester bond is broken by treatment with hydroxylamine, leaving immobilized BHA. When 6-amino-2-naphthoic acid is used instead of 4-aminobenzoic acid, NHA is immobilized on the agarose gel beads. Figure reproduced from [8].

The custom-made LAC matrix is filled into a XK 16/20 column. Chromatography is performed at a flow of <math><1 \text{ mL/min}</math>. Buffer BHAffi-A is used for loading and washing, BHAffi-B for elution, BHAffi-S for storage. Elution fractions are pooled and concentrated. LAC chromatograms look similar to IMAC chromatograms, see Figure 4.

Note: To the best of our current knowledge, LAC is only feasible for the HRP isoenzyme C1A. Recovery of C1A activity from elution fractions is slightly higher with immobilized NHA than with immobilized BHA, most probably due to the higher affinity of this isoenzyme to NHA than to BHA. The isoenzymes A2A and E5 did not bind to either of the immobilized ligands with sufficiently high affinity. Binding of other isoenzymes to immobilized BHA or NHA requires individual assessment.

Following either IMAC or LAC, a SEC step is performed on a HiLoad™ 16/60 Superdex™ 200 prep grade column for polishing. Ca-TBS is used for isocratic elution at a flow of 0.3 mL/min. Fractions containing HRP are easily identified by a dominant A403 peak (Figure 6). These fractions are again pooled and concentrated. They are of red-brownish color indicating a high relative heme content (*i.e.* Rz of 2-3, see chapter 4.6.4). Purified HRP samples can be stored at 4 °C without any detectable loss of activity for weeks (most probably for months).

Alternatively, aliquots can be stored at -20 °C or -80 °C. Two cycles of freeze-thawing did not result in any loss of activity. Also, lyophilization for long-term storage is feasible.

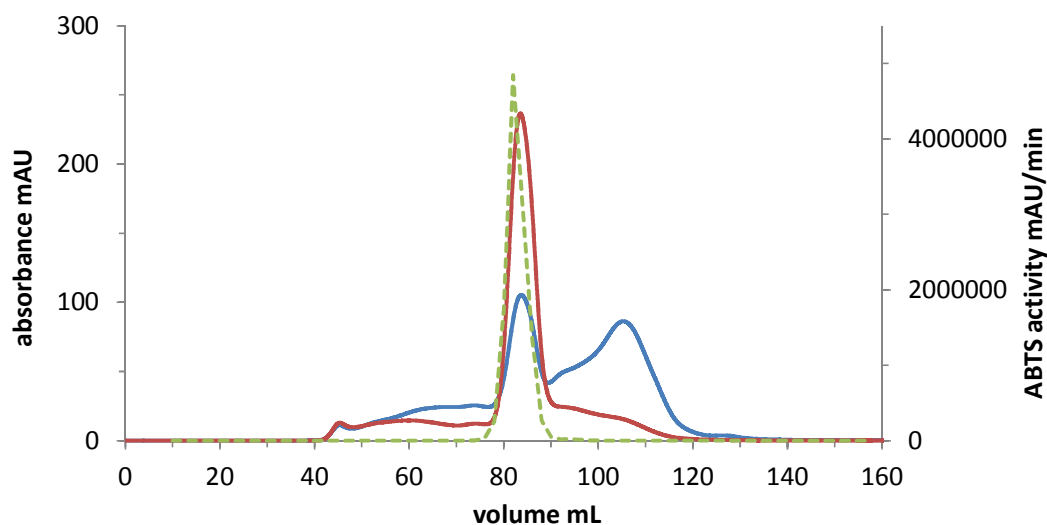


Figure 6: SEC chromatogram of HRP C1A with N-terminal hexahistidine tag produced in *PpFWK3* under *PAOX1*-regulation.

Max. 1.2 mL of concentrated HRP C1A solution after IMAC was loaded on a HiLoad 16/60 Superdex200 prep grade column. The absorbances at 280 and 403 nm were recorded (blue and red solid lines, respectively). The HRP activities in the collected fractions were determined with the ABTS assay (dotted green line). The A403/A280 ratios may vary, dependent on the cultivation conditions and preceding purification steps. The elution behavior of HRP C1A from a SEC column depends on the used production strain and promoter system. When produced in a strain with intact *OCH1*, HRP activity elutes as a broad peak, containing several adventitious protein contaminants. When produced under *PHTX1* control, HRP activity may elute later due to a lesser degree of glycosylation.

4.6.4. Characterization of horseradish peroxidase

In order to characterize HRP samples, enzyme activity is assayed using H₂O₂ as oxidizing substrate and ABTS as reducing substrate. The increase in A405 is followed on a SynergyMx platereader for 3 min upon mixing of 15 µL of HRP sample with 140 µL of freshly prepared ABTS assay solution.

Quantification of total protein in a sample is performed with the Bio-Rad protein assay using bovine serum albumin as standard at concentrations from 0.0625-1.0 mg/mL by mixing 5 µL of protein solution with 150 µL 1x Bio-Rad protein assay solution and measuring A595 on a SynergyMx platereader.

The absorbances at 403 nm and 280 nm can be determined easily on a NanoDrop 2000c spectrophotometer. The *Rz* value of a sample describes the ratio of heme absorbance at the Soret band (A403) over general protein absorbance (A280) [9]. A *Rz* value of ~3 is indicative of high relative heme content in a sample, *i.e.* high purity of the enzyme preparation.

4.7. Calculations

Volumetric HRP activity for ABTS as reducing substrate is calculated by using the extinction coefficient of oxidized ABTS at 405 nm, ϵ_{405} [3] (Equation 1):

$$\text{volumetric activity} = \frac{\Delta A_{405}/\text{min} * V * DF}{v * \epsilon * d}$$

Equation 1: Calculation of volumetric HRP activity in U/mL with ABTS as reducing substrate.

$\Delta A_{405}/\text{min}$, Change in absorbance at 405 nm in mAU/min; V, total reaction volume, 155 μL when measured in microtiter plate; DF, dilution factor, v, volume of enzyme sample, 15 μL when measured in microtiter plate; ϵ_{405} , extinction coefficient of oxidized ABTS at 405 nm, 34700 $\text{M}^{-1}.\text{cm}^{-1}$; d, distance in cm, 0.42 cm when measured in microtiter plate; 1 U converts 1 μmol ABTS in 1 min.

Specific HRP activity for ABTS as reducing substrate is calculated by combining Equation 1 with a protein concentration (Equation 2):

$$\text{specific activity} = \frac{\Delta A_{405}/\text{min} * V * DF}{v * \epsilon_{405} * d} * \frac{1}{[p]}$$

Equation 2: Calculation of specific HRP activity in U/mg with ABTS as reducing substrate.

[p], Protein concentration in mg/mL as determined with Bio-Rad protein assay; also see legend of Equation 1.

HRP concentration can be approximated by using the extinction coefficient of holo-HRP at 403 nm, ϵ_{403} * (Equation 3):

$$c = \frac{A_{403}}{\epsilon_{403} * d}$$

Equation 3: Calculation of HRP concentration in μM .

A_{403} , Absorbance at 403 nm in AU; ϵ_{403} , extinction coefficient of HRP at 403 nm, 0.1 $\mu\text{M}^{-1}.\text{cm}^{-1}$; d, distance in cm, 0.1 cm when measured on NanoDrop 2000c spectrophotometer.

The turnover number of HRP can be calculated using Equation 4:

$$k_{cat} = \frac{\Delta A_{405}/\text{min} * V * DF}{v * \epsilon_{405} * d * 60} * \frac{c}{1000}$$

Equation 4: Calculation of the turnover number k_{cat} in s^{-1} .

c, HRP concentration in μM ; also see legend of Equation 1.

* <http://www.sigmaldrich.com/life-science/metabolomics/enzyme-explorer/analytical-enzymes/peroxidase-enzymes.html> (accessed Apr 2015)

4.8. Troubleshooting

Trouble	Reason	Solution
conspicuously high HRP activity in wells on the edges and corners of a DWP	uneven medium evaporation due to insufficient humidity	cultivate DWPs in 28 °C room or use incubator with reliable 80% humidity
bioreactor vessel is rocking upon high stirrer speed	stirrer motor is not fixed properly onto the vessel	the stirrer motor is only fixed onto the vessel by a small screw; it is not possible to tell whether it is fixed properly without turning it on
dO ₂ drops below 30% in bioreactor cultivation despite max. stirrer speed	a) cell density too high b) blocked sparger	a) if possible increase air flow, otherwise stop feed/cultivation b) try unblocking sparger by increasing air flow, otherwise use so far unused inlet
no O ₂ consumption of bioreactor culture despite feed of C-source	a) dysfunctional dO ₂ probe b) the inlet of the feed line is blocked c) pump setting is below 1.1% of its capacity d) cells are dead (probably due to dysfunctional pH probe and overload with NH ₄ OH)	a) check reactivity of dO ₂ probe by altering air flow / stirrer speed b) try unblocking the feed line by shortly increasing the feed flow or use so far unused inlet c) the pump only works reliably when operated at >1.1% of its capacity and might otherwise not pump anything at all d) check reactivity of pH probe and restart cultivation
A405 does not increase in HRP activity ABTS assay	a) no HRP was present in the used sample b) too much HRP was present in the used sample and the reaction is already over or above the detection limit of the platereader	a) make sure to use the correct (<i>i.e.</i> HRP-containing) sample b) dilute sample
A595 signal >1.2 AU in Bio-Rad protein assay	too high protein concentration	dilute samples and make sure to get a signal that lies within the linear standard curve (typically 0.0625-1.0 mg/mL)

5. Safety Precautions

Please follow the instructions described in the laboratory guidelines ("Laborordnung") of the Institute of Molecular Biotechnology, Graz University of Technology.

6. Documentation

Documentation

Information	Location
collected manuscripts on recombinant HRP, strains and methods	PhD thesis of Florian W. Krainer Methods collection of Anton Glieder
step-by-step protocol for immobilization of BHA on agarose gel beads	Reimann L, Schonbaum GR: Purification of plant peroxidases by affinity chromatography. <i>Methods Enzymol.</i> 1978, 52:514–21.

7. References

1. Weis R, Luiten R, Skranc W, Schwab H, Wubbolts M, Glieder A: **Reliable high-throughput screening with *Pichia pastoris* by limiting yeast cell death phenomena.** *FEMS Yeast Res.* 2004, **5**:179–89.
2. Dietzsch C, Spadiut O, Herwig C: **A fast approach to determine a fed batch feeding profile for recombinant *Pichia pastoris* strains.** *Microb. Cell Fact.* 2011, **10**:85–94.
3. Morawski B, Lin Z, Cirino P, Joo H, Bandara G, Arnold FH: **Functional expression of horseradish peroxidase in *Saccharomyces cerevisiae* and *Pichia pastoris*.** *Protein Eng.* 2000, **13**:377–84.
4. Krainer FW, Capone S, Jäger M, Vogl T, Gerstmann M, Glieder A, Herwig C, Spadiut O: **Optimizing cofactor availability for the production of recombinant heme peroxidase in *Pichia pastoris*.** *Microb. Cell Fact.* 2015, **14**:4.
5. Lin-Cereghino GP, Stark CM, Kim D, Chang J, Shaheen N, Poerwanto H, Agari K, Moua P, Low LK, Tran N, Huang AD, Nattestad M, Oshiro KT, Chang JW, Chavan A, Tsai JW, Lin-Cereghino J: **The effect of α -mating factor secretion signal mutations on recombinant protein expression in *Pichia pastoris*.** *Gene* 2013, **519**:311–7.
6. Näätsaari L, Mistlberger B, Ruth C, Hajek T, Hartner FS, Glieder A: **Deletion of the *Pichia pastoris* KU70 Homologue Facilitates Platform Strain Generation for Gene Expression and Synthetic Biology.** *PLoS One* 2012, **7**:e39720.
7. Krainer FW, Gmeiner C, Neutsch L, Windwarder M, Pletzenauer R, Herwig C, Altmann F, Glieder A, Spadiut O: **Knockout of an endogenous mannosyltransferase increases the homogeneity of glycoproteins produced in *Pichia pastoris*.** *Sci. Rep.* 2013, **3**:3279–91.
8. Reimann L, Schonbaum GR: **Purification of plant peroxidases by affinity chromatography.** *Methods Enzymol.* 1978, **52**:514–21.
9. Theorell H, Maehly AC, Dam H, Kinell P-O: **Untersuchungen an künstlichen Peroxydasen.** *Acta Chem. Scand.* 1950, **4**:422–434.

- Conclusions and outlook -

Owing to the vast number of well-established applications for HRP in diagnostics and immunohistochemistry as well as to novel upcoming applications in biocatalysis, bioremediation and medicine, there is a considerable demand for large amounts of HRP preparations at consistent high quality. However, the current isolation protocol from plant roots can not meet these demands due to the large number of HRP isoenzymes whose expression regulation is poorly understood and non-adjustable, resulting in unsteady preparation quality. Here, a platform for the production of recombinant HRP using *P. pastoris* has been established and successfully applied.

By performing a two-step flowthrough purification protocol described in Chapter 2, HRP isoenzymes produced in wildtype-based Mut^S strains could be partially purified. This approach was shown to be particularly successful for isoenzymes with extensive hyperglycosylation such as C1A, C1C or A2A. For applications that do not require highly purified enzyme, the described protocol offers an easy-to-do approach for recombinant HRP preparations from wildtype-based *P. pastoris* strains. In order to reach high-end purity however, use of an engineered strain that enables homogeneous glycosylation and thus polishing by size exclusion chromatography is mandatory.

Inactivation of the *OCH1* encoded α -1,6-mannosyltransferase activity allowed the production of homogeneously glycosylated HRP in *P. pastoris* at similar yields as wildtype-based strains. However, the *och1* deletion strain exhibited a slow growth phenotype, presumably associated with the described rearrangement of cell wall components. The strain SuperM5 expressing an *OCH1* mutant variant and an α -1,2-mannosidase gene was described in a recent patent application (publication number: WO2014066479A1). In contrast to wildtype Och1, the described Och1 mutant lacked a N-terminal signal sequence targeting the enzyme to the Golgi apparatus. Similar to the *PpFWK3* strain described in chapter 3, the SuperM5 strain disclosed in the patent was described to be stable and robust in terms of genomic rearrangements which might reverse a disrupted *OCH1* gene back to the functional wildtype gene. However, the SuperM5 strain was also described to show a growth behavior similar to a wildtype strain while still allowing for the production of homogeneously glycosylated proteins. It thus seems, that catalytically active Och1 which is not targeted to

the Golgi apparatus is capable of preventing the rearrangement of cell wall components observed in the *PpFWK3* strain and thus a slow growth phenotype. In order to also achieve wildtype growth behavior in the *PpFWK3* strain, strain mutagenesis could be performed in order to select for a restored growth phenotype while keeping the desirable homogeneous N-glycosylation pattern on secreted target proteins. Also, alternative glycosyltransferases could be targeted to cellular compartments of *PpFWK3* other than the Golgi apparatus and evaluated for their potential to prevent cell wall rearrangements and the associated slow growth phenotype.

The insufficient supply with heme cofactor from the endogenous heme biosynthesis of *P. pastoris* described a major bottleneck in recombinant HRP production limiting the yields of active enzyme. Supplementation of cultivation media with a moderate excess of hemin could effectively saturate secreted apo-HRP in the culture broth. Cooverexpression of single genes of the heme biosynthesis pathway from either of the promoters *PAOX1*, *PGAP* or *PCAT1* however, did not lead to increased HRP activity yields. Simultaneous cooverexpressions of multiple *HEM* genes from differently regulated promoters of varying strengths might still be able to augment the endogenous heme production of *P. pastoris* and thus saturate HRP already at an intracellular level.

As described in Chapter 5, HRP production from *PGAP* or *PHTX1* resulted in high volumetric activities and the best space-time yields so far. Coproduction of active Hac1 with HRP enhanced specific HRP activities. In further studies, additional novel promoters and promoter combinations for coexpressions could be assessed to increase HRP yields even further, possibly in combination with recently described supersecretor strains, *e.g.* [1].

Comparative characterizations of the isoenzymes C1A, A2A and E5 revealed their distinct enzymatic features in terms of activity and stability under a range of conditions. Based on these data, E5 might be the isoenzyme of choice when resistance towards H₂O₂ inactivation is required whereas C1A might be more favorable for applications that require thermostability, for instance. In order to enhance the toolbox of available HRP isoenzymes [2] even further, additional isoenzymes could be produced in *P. pastoris* and characterized. Thereby, a broad range of natural HRP isoenzymes with individual advantages would be available for selection for any given application. In the long run, mutant isoenzymes with

custom characteristics could be designed based on the accumulated data on natural isoenzymes [2] and laboratory engineered variants, *e.g.* [3, 4].

Based on the data from *P. pastoris* strains with an engineered methanol utilization pathway, cooverexpression of either *FLD1* or *TKL1* was beneficial for specific and volumetric HRP productivities as well as for HRP production efficiency. With regard to the additional data using *Candida antarctica* lipase B as an alternative reporter enzyme, particularly *FLD1* cooverexpression turned out to be beneficial for the production parameters of target proteins in general.

In order to not only demonstrate the applicability of recombinant HRP as reporter enzyme in biotechnological strain engineering studies but also in immunohistochemical applications, a fusion protein with protein G was recombinantly produced in *P. pastoris*. The HRP-protein G fusion protein was shown to be functional in direct ELISAs using antibodies from either human or rabbit serum as antigens. By performing random mutagenesis, both HRP and protein G could be improved towards higher enzymatic activity and tighter binding, respectively, to enhance assay sensitivity. Also, alternative HRP isoenzymes with higher activity towards ELISA substrates could be fused to protein G instead of C1A. Moreover, the successful fusion strategy could be transferred to producing fusions of HRP with single domain antibodies that bind to tumor surface antigens for antibody-directed enzyme prodrug therapy [5].

In conclusion, the established *P. pastoris* production platform for recombinant HRP as demonstrated here describes a considerable improvement compared to the previous state-of-the-art, *i.e.* from yields in the lower mg/L range [6] to the 130 mg/L range. Additionally, recombinant HRPs from *P. pastoris* could be subjected to comprehensive enzymological characterizations and were successfully applied in a biotechnological strain engineering study as well as in a new and improved fusion protein of immunohistochemical relevance, demonstrating the broad applicability of the described system.

References

1. Larsen S, Weaver J, de Sa Campos K, Bulahan R, Nguyen J, Grove H, Huang A, Low L, Tran N, Gomez S, Yau J, Ilustrisimo T, Kawilarang J, Lau J, Tranphung M, Chen I, Tran C, Fox M, Lin-Cereghino J, Lin-Cereghino GP: **Mutant strains of *Pichia pastoris* with enhanced secretion of recombinant proteins.** *Biotechnol. Lett.* 2013, **35**:1925–1935.
2. Näätäsaari L, Krainer FW, Schubert M, Glieder A, Thallinger GG: **Peroxidase gene discovery from the horseradish transcriptome.** *BMC Genomics* 2014, **15**:227.
3. Loughran NB, O’Connell MJ, O’Connor B, O’Fágáin C: **Stability properties of an ancient plant peroxidase.** *Biochimie* 2014, **104**:156–9.
4. Kim SJ, Joo JC, Song BK, Yoo YJ, Kim YH: **Engineering a horseradish peroxidase C stable to radical attacks by mutating multiple radical coupling sites.** *Biotechnol. Bioeng.* 2015, **112**:668–76.
5. Folkes LK, Candeias LP, Wardman P: **Toward targeted “oxidation therapy” of cancer: peroxidase-catalysed cytotoxicity of indole-3-acetic acids.** *Int. J. Radiat. Oncol. Biol. Phys.* 1998, **42**:917–20.
6. Morawski B, Lin Z, Cirino P, Joo H, Bandara G, Arnold FH: **Functional expression of horseradish peroxidase in *Saccharomyces cerevisiae* and *Pichia pastoris*.** *Protein Eng.* 2000, **13**:377–84.

- Appendix -

Appendix table 1 summarizes the IP related to this doctoral thesis which was acquired either in the course of this thesis or in precedent studies.

In Appendix table 2, the extent of my contributions to the individual manuscripts that are part of this thesis is shown in percent and the nature of my contributions is stated.

Microorganism strains that were generated during this thesis were submitted to the in-house culture collection (CC). The corresponding CC numbers of these strains and of used preexisting strains are shown in Appendix table 3.

In the following, nucleotide sequences of genes that were used during this thesis but were not shown in either of the chapters above are shown here in FASTA format.

Appendix table 1: Intellectual property related to this thesis. The patents "Horseradish peroxidase isoenzymes" and "Degradation of hormones using recombinant HRP isoenzymes" were based on results generated by the listed inventors in studies prior to this doctoral thesis.

Patent title:	
Horseradish peroxidase isoenzymes	
Inventors: Florian Krainer, Laura Näätäsaari, Anton Glieder, Martin Kulterer, Victoria Reichel	
PCT number: PCT/EP2012/070751	Priority date: October 19, 2011
Abstract:	
The present invention relates to recombinant heme-containing horseradish peroxidase isoenzymes with improved properties. In particular, the present invention relates to a plant enzyme kit comprising recombinant peroxidase isoenzymes, preferably horseradish peroxidase isoenzymes.	
Patent title:	
Degradation of hormones using recombinant HRP isoenzymes	
Inventors: Martin Kulterer, Victoria Reichel, Volker Ribitsch, Anton Glieder, Florian Krainer	
PCT number: PCT/EP2013/052939	Priority date: February 15, 2012
Abstract:	
The present invention relates to the use of recombinant heme-containing horseradish peroxidase isoenzyme with improved technological properties such as altered glycosylation, improved catalytic properties or improved stability and different ranges of pH optima and improved surface interactions in the treatment of waste water.	

Appendix

Patent title:

Recombinant peroxidase-protein G fusion protein ("Rekombinantes Peroxidase-Protein G Fusionsprotein")

Inventor: Florian Krainer

Application submitted.

Appendix table 2: Contributions to the manuscripts of this thesis. The extent of my contributions to the manuscripts of this thesis is shown in % and the nature of the contribution is described.

An updated view on horseradish peroxidases: recombinant production and biotechnological applications	
Krainer FW, Glieder A. An updated view on horseradish peroxidases: recombinant production and biotechnological applications (2015). <i>Applied Microbiology and Biotechnology</i> 99: 1611-1625.	
% Contribution	Nature of contribution
90	Wrote the manuscript. Conceived of the study.
Purification and basic biochemical characterization of 19 recombinant plant peroxidase isoenzymes produced in <i>Pichia pastoris</i>	
Krainer FW, Pletzenauer R, Rossetti L, Herwig C, Glieder A, Spadiut O. Purification and basic biochemical characterization of 19 recombinant plant peroxidase isoenzymes produced in <i>Pichia pastoris</i> (2014). <i>Protein Expression and Purification</i> 95: 104-112.	
% Contribution	Nature of contribution
30	Designed and performed experiments, analyzed and interpreted data. Wrote the manuscript.
Knockout of an endogenous mannosyltransferase increases the homogeneity of glycoproteins produced in <i>Pichia pastoris</i>	
Krainer FW, Gmeiner C, Neutsch L, Windwarder M, Pletzenauer R, Herwig C, Altmann F, Glieder A, Spadiut O. Knockout of an endogenous mannosyltransferase increases the homogeneity of glycoproteins produced in <i>Pichia pastoris</i> (2013). <i>Scientific Reports</i> 3: 3279-3291.	
% Contribution	Nature of contribution
35	Designed and performed experiments, analyzed and interpreted data. Wrote the manuscript. Conceived of the study.
Optimizing cofactor availability for the production of recombinant heme peroxidase in <i>Pichia pastoris</i>	
Krainer FW, Capone S, Jäger M, Vogl T, Gerstmann M, Glieder A, Herwig C, Spadiut O. Optimizing cofactor availability for the production of recombinant heme peroxidase in <i>Pichia pastoris</i> (2015). <i>Microbial Cell Factories</i> 14: 4.	
% Contribution	Nature of contribution
30	Designed and performed experiments, analyzed and interpreted data. Wrote the manuscript. Conceived of the study.
Systematic assessment of strategies for improved production of recombinant plant peroxidase in <i>Pichia pastoris</i>	
Krainer FW, Gerstmann MA, Darnhofer B, Birner-Grünberger R, Glieder A. Systematic assessment of strategies for improved production of recombinant plant peroxidase in <i>Pichia pastoris</i> . In preparation.	
% Contribution	Nature of contribution
60	Designed and performed experiments, analyzed and interpreted data. Wrote the manuscript. Conceived of the study.

Characterization of recombinant horseradish peroxidase isoenzymes from *Pichia pastoris*

Krainer FW, McLean K, Hosford J, Wong LS, Darnhofer B, Birner-Grünberger R, Glieder A, Munro AW. Characterization of recombinant horseradish peroxidase isoenzymes from *Pichia pastoris*. In preparation.

% Contribution	Nature of contribution
50	Designed and performed experiments, analyzed and interpreted data. Wrote the manuscript. Conceived of the study.

Recombinant protein expression in *Pichia pastoris* strains with an engineered methanol utilization pathway

Krainer FW, Dietzsch C, Hajek T, Herwig C, Spadiut O, Glieder A. Recombinant protein expression in *Pichia pastoris* strains with an engineered methanol utilization pathway (2012). *Microbial Cell Factoris* 11: 22-35.

% Contribution	Nature of contribution
30	Designed and performed experiments, analyzed and interpreted data. Wrote the manuscript.

Biotechnological production of a peroxidase-protein G fusion protein in *Pichia pastoris*

Krainer FW, Glieder A. Biotechnological production of a peroxidase-protein G fusion protein in *Pichia pastoris*. In preparation.

% Contribution	Nature of contribution
90	Designed and performed experiments, analyzed and interpreted data. Wrote the manuscript. Conceived of the study.

Appendix table 3: Microorganism strains. Strains of *Escherichia coli* and *Pichia pastoris* that were generated or used during this thesis in the culture collection of the Institute of Molecular Biotechnology, Graz University of Technology. If not stated otherwise, *P. pastoris* strains produce the indicated target protein under PAOX1-regulation. By default, single overexpression is done using the pPpT4_S vector, cooverexpressions using the vectors pPpT4_S and the pPpKan_S.

CC #	organism	strain	description	comments
3090	<i>E. coli</i>	K12 Top10F'	pPpT4_S_alpha_C1A	PhD thesis of Laura Näätsaari
5827	<i>E. coli</i>	K12 Top10F'	pPpT4_S_alpha_A2A	Master's thesis of Florian Krainer
6588	<i>E. coli</i>	K12 Top10F'	pPpT4_S_alpha_A2ANHIS	N-terminal 6xH tag
6590	<i>E. coli</i>	K12 Top10F'	pPpT4_S_alpha_A2AnoSte13	
6858	<i>E. coli</i>	K12 Top10F'	pPpT4_S_alpha_05508NHIS	N-terminal 6xH tag
6859	<i>E. coli</i>	K12 Top10F'	pPpT4_S_alpha_06351NHIS	N-terminal 6xH tag
6860	<i>E. coli</i>	K12 Top10F'	pPpT4_S_alpha_17517.1NHIS	N-terminal 6xH tag
6861	<i>E. coli</i>	K12 Top10F'	pPpT4_S_alpha_22684.1NHIS	N-terminal 6xH tag
6862	<i>E. coli</i>	K12 Top10F'	pPpT4_S_alpha_C1ANHIS	N-terminal 6xH tag
6863	<i>E. coli</i>	K12 Top10F'	pPpT4_S_alpha_E5NHIS	N-terminal 6xH tag
6952	<i>E. coli</i>	K12 Top10F'	pPpKan_S_PAOX1_synPDI	
6954	<i>E. coli</i>	K12 Top10F'	pPpKan_S_PAOX1_eGFP	
6957	<i>E. coli</i>	K12 Top10F'	pPpKan_S_PCAT_eGFP	
6959	<i>E. coli</i>	K12 Top10F'	pPpKan_S_PGAP_synPDI	
6960	<i>E. coli</i>	K12 Top10F'	pPpKan_S_PGAP_eGFP	
6961	<i>E. coli</i>	K12 Top10F'	pPpKan_S_PAOX1_HEM1	
6962	<i>E. coli</i>	K12 Top10F'	pPpKan_S_PCAT_HEM1	
6963	<i>E. coli</i>	K12 Top10F'	pPpKan_S_PAOX1_HEM3	
6964	<i>E. coli</i>	K12 Top10F'	pPpKan_S_PCAT_HEM3	
7191	<i>E. coli</i>	K12 Top10F'	pPpT4_S_Dalpha_C1A	Δ57-70 signal peptide
7192	<i>E. coli</i>	K12 Top10F'	pJET1.2_SpG	
7193	<i>E. coli</i>	K12 Top10F'	pPpKan_S_PAOX1_KEX2	
7194	<i>E. coli</i>	K12 Top10F'	pPpKan_S_PAOX1_STE13	
7199	<i>E. coli</i>	K12 Top10F'	pPpT4_S_alpha_C1ASpG5	
7201	<i>E. coli</i>	K12 Top10F'	pPpT4_S_PGAP_alpha_C1A	

Appendix

7245	<i>E. coli</i>	K12 Top10F'	pPpKan_S_PAOX1_HAC1s	active Hac1
7246	<i>E. coli</i>	K12 Top10F'	pPpT4_S_Dalpha_C1ANHIS K174Q K241F	Δ57-70 signal peptide, N-terminal 6xH tag, Lys mutant
7247	<i>E. coli</i>	K12 Top10F'	pPpT4_S_Dalpha_C1ANHIS K174R K241N	Δ57-70 signal peptide, N-terminal 6xH tag, Lys mutant
7248	<i>E. coli</i>	K12 Top10F'	pPpT4_S_Dalpha_C1ANHIS K232N	Δ57-70 signal peptide, N-terminal 6xH tag, Lys mutant
7249	<i>E. coli</i>	K12 Top10F'	pPpT4_S_Dalpha_C1ANHIS K232N K241N	Δ57-70 signal peptide, N-terminal 6xH tag, Lys mutant
7250	<i>E. coli</i>	K12 Top10F'	pPpT4_S_Dalpha_C1ANHISSpG5	Δ57-70 signal peptide, N-terminal 6xH tag
7251	<i>E. coli</i>	K12 Top10F'	pPpT4_S_PGAP_Dalpha_C1A	Δ57-70 signal peptide
7252	<i>E. coli</i>	K12 Top10F'	pPpT4_S_PGAP_Dalpha_C1ANHIS	Δ57-70 signal peptide, N-terminal 6xH tag
7253	<i>E. coli</i>	K12 Top10F'	pPpT4_S_PHTX1_HAC1s_Dalpha- C1ANHIS	bidirectional expression, Δ57-70 signal peptide, N-terminal 6xH tag
7257	<i>E. coli</i>	K12 Top10F'	pPpT4_S_Dalpha_C1ASpG-9Hc	Δ57-70 signal peptide, C-terminal 9xH tag
7258	<i>E. coli</i>	K12 Top10F'	pPpT4_S_Dalpha_C1ASpG-6Hc	Δ57-70 signal peptide, C-terminal 6xH tag
7259	<i>E. coli</i>	K12 Top10F'	pPpT4_S_Dalpha_C1ANHIS-9Hc	Δ57-70 signal peptide, N-terminal 6xH tag, C-terminal 9xH tag
7260	<i>E. coli</i>	K12 Top10F'	pPpT4_S_Dalpha_C1A-9Hc	Δ57-70 signal peptide, C-terminal 9xH tag
7261	<i>E. coli</i>	K12 Top10F'	pPpT4_S_Dalpha_9Hn-C1A	Δ57-70 signal peptide, N-terminal 9xH tag
<hr/>				
3445	<i>P. pastoris</i>	PpMutS	Δaox1::FRT	PhD thesis of Laura Näätäsaari
3525	<i>P. pastoris</i>	PpMutS	A2A	
6624	<i>P. pastoris</i>	PpMutS	C1A	PhD thesis of Laura Näätäsaari
6815	<i>P. pastoris</i>	PpFWK3	Δaox1::FRT Δoch1::FRT	
6820	<i>P. pastoris</i>	PpFWK3	A2A	
6822	<i>P. pastoris</i>	PpMutS	A2ANHIS	N-terminal 6xH tag
6823	<i>P. pastoris</i>	PpMutS	A2AnoSte13	no C-terminal EAEA on signal peptide
6965	<i>P. pastoris</i>	PpFWK3	C1A	
6965	<i>P. pastoris</i>	PpFWK3	C1A	
6966	<i>P. pastoris</i>	PpFWK3	E5	
6967	<i>P. pastoris</i>	PpFWK3	22684.1	
6968	<i>P. pastoris</i>	PpFWK3	05508	
6969	<i>P. pastoris</i>	PpFWK3	06351	
6970	<i>P. pastoris</i>	PpFWK3	17517.2	

Appendix

6971	<i>P. pastoris</i>	PpMutS	C1A PCAT_HEM1	
6972	<i>P. pastoris</i>	PpMutS	C1A PCAT_HEM3	
6973	<i>P. pastoris</i>	PpMutS	C1A PCAT_eGFP	
6974	<i>P. pastoris</i>	PpMutS	C1A PGAP_HEM1	
6975	<i>P. pastoris</i>	PpMutS	C1A PGAP_HEM3	
6976	<i>P. pastoris</i>	PpMutS	C1A PGAP_eGFP	
6977	<i>P. pastoris</i>	PpMutS	C1A HEM1	
6978	<i>P. pastoris</i>	PpMutS	C1A HEM3	
6979	<i>P. pastoris</i>	PpMutS	C1A eGFP	
6980	<i>P. pastoris</i>	PpMutS	C1ANHIS	N-terminal 6xH tag
6981	<i>P. pastoris</i>	PpMutS	E5NHIS	N-terminal 6xH tag
6982	<i>P. pastoris</i>	PpMutS	22684.1NHIS	N-terminal 6xH tag
6983	<i>P. pastoris</i>	PpMutS	05508NHIS	N-terminal 6xH tag
6984	<i>P. pastoris</i>	PpMutS	06351NHIS	N-terminal 6xH tag
6985	<i>P. pastoris</i>	PpMutS	17517.2NHIS	N-terminal 6xH tag
6985	<i>P. pastoris</i>	PpMutS	17517.2NHIS	N-terminal 6xH tag
6986	<i>P. pastoris</i>	PpFWK3	C1ANHIS	N-terminal 6xH tag
6987	<i>P. pastoris</i>	PpFWK3	A2ANHIS	N-terminal 6xH tag
6988	<i>P. pastoris</i>	PpFWK3	E5NHIS	N-terminal 6xH tag
6989	<i>P. pastoris</i>	PpFWK3	22684.1NHIS	N-terminal 6xH tag
6990	<i>P. pastoris</i>	PpFWK3	05508NHIS	N-terminal 6xH tag
6992	<i>P. pastoris</i>	PpFWK3	17517.2NHIS	N-terminal 6xH tag
7228	<i>P. pastoris</i>	PpFWK3	C1ANHIS K174Q K241F	Δ 57-70 signal peptide, N-terminal 6xH tag, Lys mutant
7229	<i>P. pastoris</i>	PpFWK3	C1ANHIS K174R K241N	Δ 57-70 signal peptide, N-terminal 6xH tag, Lys mutant
7230	<i>P. pastoris</i>	PpFWK3	C1ANHIS K232N	Δ 57-70 signal peptide, N-terminal 6xH tag, Lys mutant
7231	<i>P. pastoris</i>	PpFWK3	C1ANHIS K232N K241N	Δ 57-70 signal peptide, N-terminal 6xH tag, Lys mutant
7232	<i>P. pastoris</i>	PpFWK3	C1ANHIS HAC1s	N-terminal 6xH tag
7233	<i>P. pastoris</i>	PpFWK3	C1ANHISSpG5	N-terminal 6xH tag
7234	<i>P. pastoris</i>	PpFWK3	C1ASpG5	
7235	<i>P. pastoris</i>	PpFWK3	PGAP_ C1ANHIS	Δ 57-70 signal peptide, N-terminal 6xH tag

Appendix

7236	<i>P. pastoris</i>	PpMutS	C1ANHIS K174Q K241F	Δ57-70 signal peptide, N-terminal 6xH tag, Lys mutant
7237	<i>P. pastoris</i>	PpMutS	C1ANHIS K174R K241N	Δ57-70 signal peptide, N-terminal 6xH tag, Lys mutant
7238	<i>P. pastoris</i>	PpMutS	C1ANHIS K232N	Δ57-70 signal peptide, N-terminal 6xH tag, Lys mutant
7239	<i>P. pastoris</i>	PpMutS	C1ANHIS K232N K241N	Δ57-70 signal peptide, N-terminal 6xH tag, Lys mutant
7240	<i>P. pastoris</i>	PpMutS	C1ANHIS <i>HAC1s</i>	N-terminal 6xH tag
7241	<i>P. pastoris</i>	PpMutS	C1ANHISSpG5	N-terminal 6xH tag
7242	<i>P. pastoris</i>	PpMutS	C1ASpG5	
7267	<i>P. pastoris</i>	PpFWK3	C1A-9Hc	Δ57-70 signal peptide, C-terminal 9xH tag
7268	<i>P. pastoris</i>	PpFWK3	<i>PHTX1_HAC1s_C1ANHIS</i>	bidirectional expression, Δ57-70 signal peptide, N-terminal 6xH tag
7269	<i>P. pastoris</i>	PpFWK3	C1ASpG-9Hc	Δ57-70 signal peptide, C-terminal 9xH tag
7270	<i>P. pastoris</i>	PpFWK3	C1ASpG-6Hc	Δ57-70 signal peptide, C-terminal 6xH tag
7271	<i>P. pastoris</i>	PpFWK3	C1A-9Hn	Δ57-70 signal peptide, N-terminal 9xH tag
7272	<i>P. pastoris</i>	PpFWK3	C1ANHIS-9Hc	Δ57-70 signal peptide, N-terminal 6xH tag, C-terminal 9xH tag

Appendix

>C1ANHIS

CACCATCACCACCATCACCAACTTACTCCAACCTTCTACGATAACTCTTGTCTAATGTGTCCAACATCGTTAGAGACACCAT
TGTCGAATGAATTGAGATCAGATCCACGATTTGCTGCATCTATCTTGAGACTTCACTTTCATGACTGCTTCGTCACCGTTGTG
ATGCTTCCATCTTGTGCGACAACACTACCTCTTTTCAAGAACTGAGAAGGACGCTTTTCGGTAATGCCAACTCTGCTAGAGGATTT
CCAGTCATTGACAGAATGAAGGCTGCCGTTGAATCTGCATGCTCTAGAACTGTGTCATGTGCTGACCTTCTGACTATTGCCGC
TCAGCAATCTGTTACCTTAGCTGGTGGACCATCCTGGAGAGTTCCATTGGGTGCTAGAGACTCCCTTCAAGCCTTTCTGGACC
TTGCAATGCTAACTTGCCTGCTCCATTCTTTACCTTACCTCAATTGAAAGACTCTTTCAGAAACGTTGGTCTTAACAGATCA
TCCGACTTGGTTGCCCTTATCTGGAGGTCACACCTTTGGTAAGAACCAATGTAGATTTCATCATGGATCGTCTGTACAACCTTCTC
TAACACCGGTTTGGCAGATCCTACTCTGAACACCCTTACTTGCAAACCTTAAGAGGTTTGTGCCACTTAAACGAAATCTGT
CTGCTCTGGTTGACTTCGATTTGCGTACTCCTACCATCTTCGACAACAAGTACTATGTCAACTTGGAGGAACAGAAGGGTCTT
ATCCAATCTGACCAGAGTTGTTCTCTCCTAACGCTACTGATACCATTCCATTGGTGAGATCCTTCGCAAACTCCACTCA
AACCTTCTTTAACGCTTTTCGTCGAGGCAATGGACAGAATGGGTAACATTACTCCTTTGACCGGTACTCAAGGACAGATTAGAT
TGAAGTGCCGTTGTGCAACTCTAACTCATAA

>C1ANHIS K232N

CACCATCACCACCATCACCAACTTACTCCAACCTTCTACGATCAACTTACTCCAACCTTCTACGATAACTCTTGTCTAATGT
GTCCAACATCGTTAGAGACACCATTGTCAATGAATTGAGATCAGATCCACGATTTGCTGCATCTATCTTGAGACTTCACTTTC
ATGACTGCTTTCGTCACCGTTGTGATGCTTCCATCTTGCTGGACAACACTACCTCTTTTCAAGAACTGAGAAGGACGCTTTTCGGT
AATGCCAACTCTGCTAGAGGATTTCCAGTCATTGACAGAATGAAGGCTGCCGTTGAATCTGCATGCTCTAGAACTGTGTCATG
TGCTGACCTTCTGACTATTGCCGCTCAGCAATCTGTTACCTTAGCTGGTGGACCATCCTGGAGAGTTCCATTGGGTGCTAGAG
ACTCCCTTCAAGCCTTCTGACCTTGCAATGCTAACTTGCCTGCTCCATTCTTTACCTTACCTCAATTGAAAGACTCTTTC
AGAAACGTTGGTCTTAACAGATCATCCGACTTGGTTGCCTTATCTGGAGGTCACACCTTTGGTAAGAACCAATGTAGATTCA
CATGGATCGTCTGTACAACCTTCTTAACACCGGTTTGGCAGATCCTACTCTGAACACCCTTACTTGCAAACCTTAAAGAGGTT
TGTGCCACTTAAACGAAATCTGTCTGCTCTGGTTGACTTCGATTTGGGTACTCCTACCATCTTCGACAACaAcTACTATGTC
AACTTGGAGGAACAGAAGGGTCTTATCCAATCTGACCAGGAGTTGTTCTCTCCTAACGCTACTGATACCATTCCATTGGT
GAGATCCTTCGCAAACTCCACTCAAACCTTCTTTAACGCTTTTCGTCGAGGCAATGGACAGAATGGGTAACATTACTCCTTTGA
CCGGTACTCAAGGACAGATTAGATTGAACTGCCGTTGTGCAACTCTAACTCATAA

>C1ANHIS K232N K241N

CACCATCACCACCATCACCAACTTACTCCAACCTTCTACGATCAACTTACTCCAACCTTCTACGATAACTCTTGTCTAATGT
GTCCAACATCGTTAGAGACACCATTGTCAATGAATTGAGATCAGATCCACGATTTGCTGCATCTATCTTGAGACTTCACTTTC
ATGACTGCTTTCGTCACCGTTGTGATGCTTCCATCTTGCTGGACAACACTACCTCTTTTCAAGAACTGAGAAGGACGCTTTTCGGT
AATGCCAACTCTGCTAGAGGATTTCCAGTCATTGACAGAATGAAGGCTGCCGTTGAATCTGCATGCTCTAGAACTGTGTCATG
TGCTGACCTTCTGACTATTGCCGCTCAGCAATCTGTTACCTTAGCTGGTGGACCATCCTGGAGAGTTCCATTGGGTGCTAGAG
ACTCCCTTCAAGCCTTCTGACCTTGCAATGCTAACTTGCCTGCTCCATTCTTTACCTTACCTCAATTGAAAGACTCTTTC
AGAAACGTTGGTCTTAACAGATCATCCGACTTGGTTGCCTTATCTGGAGGTCACACCTTTGGTAAGAACCAATGTAGATTCA
CATGGATCGTCTGTACAACCTTCTTAACACCGGTTTGGCAGATCCTACTCTGAACACCCTTACTTGCAAACCTTAAAGAGGTT
TGTGCCACTTAAACGAAATCTGTCTGCTCTGGTTGACTTCGATTTGCGTACTCCTACCATCTTCGACAACaAcTACTATGTC
AACTTGGAGGAACAGaaCGGTCTTATCCAATCTGACCAGGAGTTGTTCTCTCCTAACGCTACTGATACCATTCCATTGGT
GAGATCCTTCGCAAACTCCACTCAAACCTTCTTTAACGCTTTTCGTCGAGGCAATGGACAGAATGGGTAACATTACTCCTTTGA
CCGGTACTCAAGGACAGATTAGATTGAACTGCCGTTGTGCAACTCTAACTCATAA

>C1ANHIS K174R K241N

CACCATCACCACCATCACCAACTTACTCCAACCTTCTACGATCAACTTACTCCAACCTTCTACGATAACTCTTGTCTAATGT
GTCCAACATCGTTAGAGACACCATTGTCAATGAATTGAGATCAGATCCACGATTTGCTGCATCTATCTTGAGACTTCACTTTC
ATGACTGCTTTCGTCACCGTTGTGATGCTTCCATCTTGCTGGACAACACTACCTCTTTTCAAGAACTGAGAAGGACGCTTTTCGGT
AATGCCAACTCTGCTAGAGGATTTCCAGTCATTGACAGAATGAAGGCTGCCGTTGAATCTGCATGCTCTAGAACTGTGTCATG
TGCTGACCTTCTGACTATTGCCGCTCAGCAATCTGTTACCTTAGCTGGTGGACCATCCTGGAGAGTTCCATTGGGTGCTAGAG
ACTCCCTTCAAGCCTTCTGACCTTGCAATGCTAACTTGCCTGCTCCATTCTTTACCTTACCTCAATTGAAAGACTCTTTC
AGAAACGTTGGTCTTAAACAGATCATCCGACTTGGTTGCCTTATCTGGAGGTCACACCTTTGGTcgtAACCAATGTAGATTCA
CATGGATCGTCTGTACAACCTTCTTAACACCGGTTTGGCAGATCCTACTCTGAACACCCTTACTTGCAAACCTTAAAGAGGTT
TGTGCCACTTAAACGAAATCTGTCTGCTCTGGTTGACTTCGATTTGCGTACTCCTACCATCTTCGACAACAAGTACTATGTC
AACTTGGAGGAACAGaaCGGTCTTATCCAATCTGACCAGGAGTTGTTCTCTCCTAACGCTACTGATACCATTCCATTGGT
GAGATCCTTCGCAAACTCCACTCAAACCTTCTTTAACGCTTTTCGTCGAGGCAATGGACAGAATGGGTAACATTACTCCTTTGA
CCGGTACTCAAGGACAGATTAGATTGAACTGCCGTTGTGCAACTCTAACTCATAA

>C1ANHIS K174Q K241F

CACCATCACCACCATCACCAACTTACTCCAACCTTCTACGATCAACTTACTCCAACCTTCTACGATAACTCTTGTCTAATGT
GTCCAACATCGTTAGAGACACCATTGTCAATGAATTGAGATCAGATCCACGATTTGCTGCATCTATCTTGAGACTTCACTTTC
ATGACTGCTTTCGTCACCGTTGTGATGCTTCCATCTTGCTGGACAACACTACCTCTTTTCAAGAACTGAGAAGGACGCTTTTCGGT
AATGCCAACTCTGCTAGAGGATTTCCAGTCATTGACAGAATGAAGGCTGCCGTTGAATCTGCATGCTCTAGAACTGTGTCATG
TGCTGACCTTCTGACTATTGCCGCTCAGCAATCTGTTACCTTAGCTGGTGGACCATCCTGGAGAGTTCCATTGGGTGCTAGAG
ACTCCCTTCAAGCCTTCTGACCTTGCAATGCTAACTTGCCTGCTCCATTCTTTACCTTACCTCAATTGAAAGACTCTTTC
AGAAACGTTGGTCTTAAACAGATCATCCGACTTGGTTGCCTTATCTGGAGGTCACACCTTTGGTcagAACCAATGTAGATTCA
CATGGATCGTCTGTACAACCTTCTTAACACCGGTTTGGCAGATCCTACTCTGAACACCCTTACTTGCAAACCTTAAAGAGGTT
TGTGCCACTTAAACGAAATCTGTCTGCTCTGGTTGACTTCGATTTGCGTACTCCTACCATCTTCGACAACAAGTACTATGTC
AACTTGGAGGAACAGttCGGTCTTATCCAATCTGACCAGGAGTTGTTCTCTCCTAACGCTACTGATACCATTCCATTGGT
GAGATCCTTCGCAAACTCCACTCAAACCTTCTTTAACGCTTTTCGTCGAGGCAATGGACAGAATGGGTAACATTACTCCTTTGA
CCGGTACTCAAGGACAGATTAGATTGAACTGCCGTTGTGCAACTCTAACTCATAA

Appendix

>A2NHIS

CACCATCACCACCATCACCAATTGAATGCAACTTTCTATTCCGGAACCTGCCCAAACGCCTCTGCAATCGTTAGATCCACTAT
TCAACAGGCCCTTCCAATCAGACACTAGAATTGGTGCATCTTTGATTAGACTGCACCTTTCACGATTGTTTCGTGAACGGTTGTG
ACGCCCTCTATCTTGGTGGATGACTCAGGATCTATTAGTCAAGAGAAGATGCTGGTCCAAACGCCAATTCGGCTAGAGGTTTC
AATGTGGTTGATAACATCAAGACCGCTTTGGAAAACACTTGCCTGGTGTGGTTTCTTGTTCGACATCTTGGCTTTGGCATC
TGAAGCATCCGTTTCTTGGACTGGAGGTCCATCCTGGACTGTCTTATTGGGTAGACGTGACTCTCTTACCCTAAGTTAGCTG
GTGCCAACTCAGCTATTCCTTCCCCATTTGAAGGTCTTTCTAACATTACCTCTAAGTTCTCCGCTGTCCGACTGAACACCAAC
GACCTTGTGGACTGTCTGGTGGCCATACCTTTGGACGTGCTAGATGTGGTGTCTTCAACAATAGATTGTTCAACTTTTTCTGG
AACTGGTAACCCAGACCCTACCTTGAACCTCACTTTGCTGTCTTCTTGCAGCAACTTTGTCCACAGAACGGTTCTGTCTCAA
CTATCACTAACCTGGACTTATCTACCCCTGACGCTTTGACAACAATACTTTGCCAACCTTCAATCTAACACCGGTTTGTTA
CAATCCGATCAAGAGTTGTTCTCTACCACTGGTTCTGCTACTATCGCAGTTGTACCTCTTTCGCTTCAACCAACTTTGTT
CTTTCAAGCCTTCGCTCAATCAATGATCAACATGGGTAAACATTTCTCTTTGACCGGTTCTAACGGTGAGATTAGACTTGATT
GCAAGAAAGTTAACGGATCCTAA

>E5NHIS

CACCATCACCACCATCACCAATTGGCTCCCGACTTTTACTCCAGGACGTGTCCGTGAGTTTCAACATTATCAAAAACGTCAT
CGTCGATGAAGTGCAGACTGATCCTAGAAATAGCTGCCTCCATCTTGGAGACTGCATTTTTCACGACTGTTTCGTAGAGGTTGCG
ATGCTTCAATTTCTACTCGATAACAAGCAAGAGTTTTCAGAACTGAGAAGGACGACGCTCCTAATGTTAACTCTGCTAGGGGCTTC
AACGTGATTGACAGGATGAAAACAGCCCTTGAAGAGCATGTCCACGTACTGTCTTGTGTCAGATATACTCACCATCGCATC
ACAAATCTCCGTTTACTGTCCGGTGGTCCATCTTGGGCTGTTCATTAGGTGCTAGAGATTTCGGTTGAGGCTTTTTCTGACT
TGGCTAATACAGCTTACCTAGTCCCTTTTTACATTAGCACAAATGAAAAGGCATTGCTGATGTGGGATTGAATAGGCCA
TCTGACCTAGTCCGATTGTCTGGAGGTCATACTTTCCGTAGAGCTAGATGTTTGTTCGTAACAGCAAGATTGTATAACTTCAA
TGGTACAAACAGACCGGATCAACCCCTGAATCCTTCTACCTGGCTGACCTTCGTAGATTATGCCCTCGTAATGGTAATGGTA
CGGTGTTGGTGAACCTTGTATGTAATGACGCCAAATACTTTTGACAACCAGTTCTACACCAATCTTAGAAATGGAAAAGGCTTG
ATTGAGTCAAGAGTTGTTTTGACTCCTGGTCCGACACAATTCACCTTGTGAATCTGTATAGTAGCAACACTCTTTC
CTTTTTCGGAGCTTTTGCAGACGCTATGATTAGAATGGGAAATCTTAGACCTTTGACAGGAACACAGGGTGAATCCGTCAAA
ACTGCCGTGTTGCTCAATAGCAGGTGA

>05508NHIS

CACCATCACCACCATCACACCATCAGAATTGGTTTTCTACCTTACTACCTGTCTACTGCCGAGATCATTGTTAGAAATGCAGT
TAGAGCTGGTTTTCACTCTGACCCAAGAATTGCACCAGGTATCCTTAGAATGCACCTTTCACGACTGTTTTGTTACAGGTTGTG
ACGGTTCTGTCTGATTTTCAAGATCTAACACCGAGAGAACCGCAGTTCCAAACTTGTCTCTTAGAGGATTTGAAGTTATCGAA
AACGTAAGACCCAATTGGAAGCAGCTTGCCAGGAGTTGTTTCTGTGCTGACATCTTGGCCTTAGCTGCTAGAGATACTGT
TGTCTGACCCGTGGTATTGGTTGGCAGGTCCCAACCGGAAGAAGAGACGGTCTGTCTCCGTTGGCCTCCAATGCAAACAACT
TGCCCTGGTCTAGAGACTCCGTTGTCTTCAACAGCAAAAAGTTTTCTGCCCTTGGATTGAATACCAGAGACTTGGTCTGTTCTG
GCTGGTGGTCACTTTGGGTACTGCTGGTTGCGGTGTCTTTCAGAGATAGACTGTTCAACAACACTGACCCAAACGTTGGACCA
ACCTTCTTAAACCCAGTTGCAAACCTAAGTGCACGTAATGGTGATGGTTCCGTTAGAGTGGACTTAGATACTGGTTCTGGTA
CTACCTTCGATAACTCTTACTTCACTCAACTTGTCCAGAGGTAGAGGTGTTTTGGAATCTGACCACGTTCTTTGGACTGACCCCT
GCCACCAGACCTATTGTCCAACAACCTATGTCTTCTCTGGTAACCTTCAACGCAGAGTTTGTAGATCAATGGTGAAGATGTC
TAACATCGGAGTTGCTACTGGAACCTAACGGTGAGATTAGAAAAGTCTGTTTACGCTATCAACTAA

>22684.1NHIS

CACCATCACCACCATCACCAATTGAATGCAACTTTCTATTCCGGAACCTGCCCAAACGCCTCTGCAATCGTTAGATCCACTAT
TCAACAGGCCCTTCCAATCAGACACTAGAATTGGTGCATCTTTGATTAGACTGCACCTTTCACGATTGTTTCGTGAACGGTTGTG
ACGCCCTCTATCTTGGTGGATGACTCAGGATCTATTAGTCAAGAGAAGATGCTGGTCCAAACGCCAATTCGGCTAGAGGTTTC
AATGTGGTTGATAACATCAAGACCGCTTTGGAAAACACTTGCCTGGTGTGGTTTCTTGTTCGACATCTTGGCTTTGGCATC
TGAAGCATCCGTTTCTTGGACTGGAGGTCCATCCTGGACTGTCTTATTGGGTAGACGTGACTCTCTTACCCTAAGTTAGCTG
GTGCCAACTCAGCTATTCCTTCCCCATTTGAAGGTCTTTCTAACATTACCTCTAAGTTCTCCGCTGTCCGACTGAACACCAAC
GACCTTGTGGACTGTCTGGTGGCCATACCTTTGGACGTGCTAGATGTGGTGTCTTCAACAATAGATTGTTCAACTTTTTCTGG
AACTGGTAACCCAGACCCCTACCTTGAACCTCACTTTGCTGTCTTCTTGCAGCAACTTTGTCCACAGAACGGTTCTGTCTCAA
CTATCACTAACCTGGACTTATCTACCCCTGACGCTTTCGACAACAATACTTTGCCAACCTTCAATCTAACACCGGTTTGTTA
CAATCCGATCAAGAGTTGTTCTCTACCACTGGTTCTGCTACTATCGCAGTTGTACCTCTTTCGCTTCAACCAACTTTGTT
CTTTCAAGCCTTCGCTCAATCAATGATCAACATGGGTAAACATTTCTCTTTGACCGGTTCTAACGGTGAGATTAGACTTGATT
GCAAGAAAGTTAACGGATCCTAA

>06351NHIS

CACCATCACCACCATCACTTCCCATTCCACGCCAGAGGTTTGTCCATGACTTACTACATGATGTCCTGCCCTATGGCAGAACA
GATCGTCAAGAACTCTGTCAACAATGCCTTGAAGCTGATCCTACCTTGGCTGCTGGATTGATTGATGCTTTTCCACGATT
GCTTCATCGAGGGTTGCGACGCCTCTATTCTGTTGGATTCTACCAAAGACAATACCGCTGAGAAAGACTCTCCAGCCAACCTG
TCCCTGAGAGGATATGAGATCATTGACGATGCTAAGGAAAAGGTTGAGAACATGTGTCCAGGAGTTGTGCTTGTGACAGACAT
TGTGGCTATGGCTGCCAGAGACGCTGTTTTCTGGGCTGGTGGACCTTACTATGACATTTCCAAAGGGTAGATTTCGACGGTAAGC
TTTCAAAGATCGAAGACACTAGAAACTTGCCCTTCTCATCTCTGAATGCCTCTCAACTGATTCAAACCTTTGGAACCGTGGT
TCTCTCCACAAGATGTTGTCGCTTTGTCTGGTGTCACTACTTTGGTGTGGTGTGCTAGATGTTCTTCAATCAAGCTCGTCTGAC
CACTCTGACTCTTCTTGGACTCTACTTTTGCACAACCCCTTACCAGAACCTGTAACGCTGGTGATAACGCTGAGCAGCCTT
TTGATGCAACTAGAAACGATTTTCGACAACGCCTACTTCAACGCACCTTCAAAGAAAGTCTGGTGTCTTGTTTTCCGACCAACT
TTGTTCAACACCCCTAGAACTCGTAACCTTAGTCAATGGTTACGCATTGAACCAGGCAAAGTTCTTCTTTGACTTTTCAGCAAGC
TATGAGAAAGATGTCAAACCTTACGTTAAGTTGGGTTCTCAAGGTGAGATCAGACAGAATTGTAGAACCATCAACTAA

Appendix

>17517.2NHIS

```
CACCATCACCACCATCACAGACCTAGAGTTGGTTTCTACGGTAACAGATGCAGAAAGGTCGAGTCAATTGTCAGATCCGTTGT
GAGATCCCACCTTCAGATGCAACCCCTGCAAAATGCTCCAGGTATTCTGAGAATGCACCTTCACGACTGTTTCGTTGAACGGTTGTG
ATGGTTCAATCTTACTTGCTGGAAACACTTCTGAGAGAACCCTGGTCTTAACAGATCCTTGAGAGGATTCGAAGCTATTGAG
GAAGCAAAGACTCGTTTAGAGAACGCTTGTCTTAACACCGTCTCTTGCCTGACATCTTGACCTTGGCTGCCAGAGACGCAGT
GGTTTGGACTGGTGGTAAAGGTTGGTCTGTCCCTTTAGGTAGATTGGACGGAAGACGTTCTGAAGCCTCAGATGTTAACTTGC
CAGGTCCTTCTGACCCAGTTGCAAAACAGAAGCAAGACTTCGCTGCCAAGAACCTGAACACTTTAGACTTGGTTACCCTGGTT
GGAGGTCATACCATTGGTACTGCCGGTTGTGGTTTGTAGTCAGAGGTCGTTTCTTCAACTTCAACGGTACTGGTCAACCAGACCC
ATCTATTGACCCATCTTTTGTTCCTTTGGTGCAGGCTCGTTGCCACAAAACGGTAACGCTACTACTAGAGTTCGATTTGGATA
CTGGATCTGTGGTACTTCGATACCTCTTACCTTTCCAACGTCAGATCCTCTCGTGTGTCTTGCAGTCTGATTTGGTTCTT
TGGAAGGACACCGAAACTAGAGCCATCATTGAGAGATTGTTGGGCTTAGACGTCAGTGTAAAGATTTGGATCTGAGTTCGG
TAAGTCTATGACCAAGATGTCCCTTATCGAAGTTAAGACCAGATTGTCTGACGGTGGATTCGTAGAGTTTGTTCGCCATCA
ACTAA
```

>SpG_ordered gBlock

```
CTCGAGAAGAGAGAGGCGCAAGCTCACCATCACCACCATCACACTTACAAGTTGATCCTGAACGGAAAGACCTTGAAGGGAGA
AACCACTACTGAGGCTGTCGATGCTGCCACTGCCGAAAAGGCTTCAAGCAGTATGCCAACGACAACGGTGTGACGGTGGT
GGACCTACGACGATGCCACAAAACCTTCACTGTCACTGAGAAGCCTGAAGTCATTGATGCTTCTGAGTTAACCCCTGCTGTG
ACTACCTACAAGTTGGTTATCAACGGAAAAGACTTTGAAGGGTGAACCACCCTGAAGCCGTTGATGCTGCAACTGCCGAAAA
GGTCTCAAGCAATACGCTAAtGATAACGGAGTTGACGGAGAGTGGACTTACGATGACGCTACTAAGACTTCACTGTTACTG
AGAAGCCAGAGGTTATCGACGCTTCAGAGTTGACTCCAGCAGTTACTACTTACAAGTTAGTCATCAACGGAAAAGACCTTGAAG
GGTGAAGACTACTACCAAGGCTGTGGATGCCGAAAACCGCAGAAAAGGCCCTTCAAGCAGTACGCTAACGACAATGGTGTGGATGG
TGTTTGGACCTACGATGATGCTACTAAGACCTTACCCTCACCAGGGAGGAGGTGGTGGACAACCTTACTCCAACCTTCTACG
ATAACTCTTG
```

>C1ANHISSpG5

```
CACCATCACCACCATCACCACCTTCTACGATAACTCTTGTCTTAATGTGTCCAACATCGTTAGAGACACCAT
TGTCATGAATGAGATCAGATCCACGTATTGCTGCATCTATCTTGAGACTTCACTTTCATGACTGCTTCGTCACCGTTGTG
ATGCTTCCATCTGCTGGCAACACTACCTCTTTCAGAAGTGAAGGACGCTTTCGGTAATGCCAACCTCTGCTAGAGGATTT
CCAGTCTATTGACGAAATGAAGGCTGCCGTTGAATCTGCATGCTCCTAGAAGTGTGTCATGTGCTGACCTTCTGACTATTGCCG
TCAGCAATCTGTTACCTTAGCTGGTGGACCATCCTGGAGAGTTCCATTGGGTCGTAGAGACTCCCTTCAAGCCTTCTGACCC
TTGCAAAATGCTAACTTGCCTGCTCCATTCTTTACCTTACCTCAATTGAAAGACTCTTTCAGAAAAGCTTGGTCTTAACAGATCA
TCCGACTTGGTTGCCTTATCTGGAGGTCACACCTTTGGTAAGAACCAATGTAGATTTCATCATGGATCGTCTGTACAACCTTCTC
TAACACCGGTTTGGCAGATCCTACTCTGAACACCCTTACTTGCAAAACCTTAAAGAGGTTTGTGCCCACTTAAACGAAAATCTGT
CTGCTCTGGTTGACTTCGATTTGCGTACTCCTACCATCTTCGACAACAAGTACTATGTCAACTTGGAGGAAACAGAAGGGTCTT
ATCCAATCTGACCAGGAGTTGTTCTCCTCTCCTAACGCTACTGATACCATTCCATTGGTGAGATCCTTCGAAAACCTCACTCA
AACCTTCTTTAACGCTTTCGTCGAGGCAATGGACAGAATGGGTAACATTACTCCTTTGACCGGTACTCAAGGACAGATTAGAT
TGAAGTGCCTGTTGTCAACTCTAACTCAACTTACAAGTTGATCCTGAACGGAAAGACCTTGAAGGGAGAAACCACTACTGAG
GCTGTGATGCTGCCACTGCCGAAAAGGCTTCAAGCAGTATGCCAACGACAACGGTGTGACGGTGGTGGACCTACGACGA
TGCCACAAAACCTTCACTGTCACTGAGAAGCCTGAAGTCATTGATGCTTCTGAGTTAACCCCTGCTGTGACTACCTACAAGT
TGTTTATCAACGGAAAAGACTTTGAAGGGTGAACCACCCTGAAGCCGTTGATGCTGCAACTGCCGAAAAGGCTTCAAGCAA
TACGCTAAtGATAACGGAGTTGACGGAGAGTGGACTTACGATGACGCTACTAAGACTTCACTGTTACTGAGAAGCCAGAGGT
TATCGACGCTTCAGAGTTGACTCCAGCAGTTACTACTTACAAGTTAGTCATCAACGGAAAAGACCTTGAAGGGTGAAGCTACTA
CCAAGGCTGTGGATGCCGAAAACCGCAGAAAAGGCCCTTCAAGCAGTACGCTAACGACAATGGTGTGGATGGTGTGGACCTAC
GATGATGCTACTAAGACCTTACCCTCACCAGGATAA
```

>Dalphi_d57-70 signal peptide mutant

```
ATGAGATTCCCATCTATTTTACCAGCTGTCTTGTTCGCTGCCTCCTCTGCATTGGCTGCCCTGTAACTACTACCCTGAAGA
CGAGACTGCTCAAATTCAGCTGAAGCAGTTATCGGTTACTCTGACCTTGAAGGATGATTCGACGTCGCTGTTTGCCTTCTC
TGCTTCCATTGCTGCTAAGGAAGAGGGTGTCTCTCAGAGAAGAGAGAGGCCGAAGCT
```

>PpKEX2

```
ATGTATTTGCCAGCACTTCGCTTAGCATGCTGGATCTTAATTGGTCTTAGGTCTACGGAGGCTTTGGAGACTTCCGAGAGAGA
GATCTTTGCTCTCAAGCTGGATAAATCCTGGCTTCCACGTTTCTAGAAAACGTTCCAAGATAAGTTCAAGGATGAAAGACAGA
TCAACGGTTTGGATGACTACCATGTTTTTTCACACAGTAAGAACGAAGAGTTTCAGTTAGAGAACTTTAAAGTGAAGACTCTT
TTGACGCGAGACAACGCCAATCTTCACTCCGAAGTATTCCCACAATGTGGACGAGGTTACATGCTAAGGCCCTCTCATA
TTTGATAAACCAGCTCCTGTTGTGATGGACAAGTCAGAGGAATTAAGAGAACAATAAGCGAAGGATTTGACATTGATGACC
CTTTATTTGCTAAACAGTGGCATCTATTTAATCCTCGTTACCCAGGACACGACGTGAACGTTGTCGAAGTTTGGTACGATGGT
ATCACTGGAAAAGGTGATGAGTACCAGCCATAGTTGATGACGGACTAGATATGGACAGTAAAGATCTCAAAGAATCTTTTTGTGA
GGAAGGATCTTGGGATTTCAATGCCAACACTAGACTACCCAAACCAAGACTTAGAGACGATCACCACGGAACCAGATGTGCAG
CGGAGATTGCAGCTAAGAAGGGAAATAAATACTGTGGAGTTGGTGTGGCATATGATTCAAAGGTTTCTGGCATCAGGATCTT
AGTGATAAATAACACACAGAGGATGAAGCTCTCTCCTAATCTACGGTCTTGTGATGTCACGACATTTATTCATGTTTATGGGG
GCCAGCAGACAATGGAAATCACAATGCAAGGTCACGCTGCTTAGTCAAGAAGCCATGCTTAAAGGAGTTCAAGATGGAAGAA
AGGGTAAAGGTTGCGCTGTATGTATTGCCAGTGGAAACGGAGCATCTTCTGGTGTAACTGCAATTTTACGGGTACACCAAT
AGCATTTATTCATAACAGTTGGGGCAATTGATATTTAAAGGGCTTCACTCCACCATACGCTGAGGCTTGTCTGCTGTGATGAC
TGTCACATACAGTTCTGGATCGGGTGGACACATACACAACCGACATCAACGATAAATGTTCTGATACCCATGGAGGAACAT
CCGCTGCTGCACCTTTAGCGGCTGGTCTTTATTCCTTTGGTTTATCAGGCTAATCCGGACTGACTTGGCGAGATATTCATGG
CTGACTGTTTTAACAGCCGTTCTGTAAACGAACAGGAGCCTGGCTGGCAGAAGACTGCTATCGGTAAGATGTATTCTCATAA
ATACGGATATGGCAAGATCGATGCATATGCACTGGTCAATCTAGCAAGATCTCCAGACTTCCCGTATCTCAAACCACAAGCT
GGATTTATGGCACTGAGGTTACGAAAAGCTTGAATACTTCCGAAGCTAACGGTGTGCTGACATCCAAGTATGAATTGACCCAG
```

Appendix

GAGGCCAAAGATCTAATGAACTTTGAAAAAATTGAGCATGTTACGGTACTGTAGATATAAAGGCGGCGGAAAGAGGTAAAGT
TCTTGTGTGAGTTGATCTCCCCTTCAGGTGTTGTCTAGTGAATTGGCTCCCTATCGAAGAATGGACAAGGATAAGGAAGGATTC
CAAATTGGACGTTTCATGTCTAGTGCATTCATTGGGGTGAAGACGGGTTAGGAGAGTGGATATGAAAATCACTAACAAAGAAGGA
AATTCGTGGTGCCTTAACCTCGGCAATAAAAATCTTTGGAGAAAAGTCAAGACCCTGAAAAGGCTGAAAATTTCTCTTTAAC
TAAGAAATATGACGAAATATTAGTCAACCCTCCATCTTCATCTACTTCCACGACAGTGGACACCTCATCTACAGAAGCCACTT
TTTCGTCTTCTCTGTTTCAGAGGCTTCAGCCACGGAAACGGATGTAAGAGAGACTTCTACAACCGGTGATGAAGATTTTGAG
AATGAGGAGGGCTCCTACAAGCATTCTAACTCCTCTCATATTACTGAATATTTAGCTTTCCTTCTCGGGCTTGGATTTTTGAT
CTGTATCATTTTTCTGTTTCAAAAATAGGAACAAGCTAGAGAGAAGACAGAGAAGAAATCGAAGAGATGAATACGAGTTTGATC
TCATCCCAGCCGATGACGACTTTGATACTGAAGAAGATCAAGAAGCCAATAGTCAATTCACCTTGGATTCCGATGCAGAAATG
ATGTTTGAGGACACATCTCAAAGAGAGGCTAGCCACATGAGTACCAAGACAGCTTAGGTTCTAATGAACATCCCAAACGTGC
GCATTGTAA

>PpSTE13

ATGACATCTCGGACAGCTGAGAACCCTTCGATATAGAGCTTCAAGAGAATCTAAGTCCACGTTCTTCCAATTCGTCATATT
GGAAAACATTAATGAGTATGCTAGAAGACATCGCAATGATTTCGCTTTCCCAAGAATGTGATAATGAAGATGAGAACGAAAATC
TCAATTATACTGATAACTTGGCCAAGTTTTCAAAGTCTGGAGTATCAAGAAAGAGCTGATGCTAATATTTGGTATTTGCTTT
GTTATCTGGCTGTTTCTTCTTTCCTTGTATGCGAGGACAATCGATTTTCCAATTTGAACGAGTACGTTCCAGATTCAAAACAG
CCACGGAACTGCTTCTGCCACCACGTCTATCGTTGAACCAAAAACAGACTGAATTACCTGAAAGCAAAGATTCTAACACTGATT
ATCAAAAAGGAGCTAAAATTGAGCCTTAGCGGCTGGAGATCAGGTCTGTACAATGTCTATCCAAAACCTGATCTCTCGTGGTGAA
GATGACATATACTATGAACACAGTTTTTCATCGTATAGATGAAAAGAGGATTACAGACTCTCAACACGGTCAACTGTATTTAA
CTATGAGAAAATTGAAGTAAATGGAATCACGTATACAGTGTCAATTTGTCACCATTTCTCTTACGATTCGCCAAATTCCTAG
TCGCATGCGACTATGAAAACACTGGAGACATTTCTACGTTTGCAAAAATATTTTCATATATGATAAGGAAAAGCCAAAGAGGAT
AGCTTTGTACCTGTCTACGATGACAAGGCATTGAGCTTCGTTGAATGGTTCGCCCTCAGGTGATCATGTAGTATTCGTTTTTGA
AAACAATGTATACCTCAAACAACCTCAACTTTAGAGGTTAAGCAGGTAACTTTTGATGGTGTAGAGATATTTACAATGGTA
AGCCTGACTGGATCTATGAAGAGGAAGTTTTAAGTAGCGACAGAGCCATATGGTGAATGACGATGGATCGTACTTTACGTTT
TTGAGACTTGATGACAGCAATGTCCCAACCTTCAACTTGCAGCATTTTTTTGAAGAAACAGGCTCTGTGTGCAAAATATCCGGT
CATTGATCGATTGAAATATCCAAAACAGGATTTGACAACCCCTGGTTTCTTTGTTTAGTTACAACGTGCCAAGCAAAGT
TAGAAAAGCTAAATATTGGAGCAGCAGTTTTCTTTGGGAGAAGACTTCGTGCTTTACAGTTTAAAATGGATAGACAATCTTTT
TTCTTGTGCAAGTTACAGACCGCACTTCGAAAAAATGGAAGTTACTCTAGTGGACATTGAAGCCAATTTCTGCTCGGTGGT
GAGAAAACATGATGCAACTGAGTATAACGGCTGGTCTACTGGAGAAATTTCTGTTTATCTGTGGAGATACCATTGGTT
ACATTGATGTAATCTATTATGAGGACTACGATCACTTGGCTTATTATCCAGACTGCACATCCGATAAGTATATTTGCTTACA
GATGGTTTCATGGAATGTTGTTGGACCTGGAGTTTTAGAAAGTGTGTTGAAGATAGAGTCTACTTTATCGGCACCAAAGAATCATC
AATGGAACATCACTTGTATTATACATCATTAAACGGGACCCAAGGTTAAGGCTGTTATGGATATCAAAGAACCTGGGTACTTTG
ATGTAACATTAAGGAAAATATGCTTTACTATCTTACAGAGGCCCAAACCTCCATACCAGAAATTTATGATCTTTCTGAC
CCTAGTACAACAAGTCTTGATGACATTTTATCGTCTAATAGAGGAATGTGCGAGGTTAGTTTAGCAACTCACAGCGTTCTCTGT
TTCTACCTATACTAATGTAACACTTGAGGACGGCGTACACTGGAACATGATTGAAGTGTGCTGCTGCAATTTTAACTCTAGCA
AGAAGTACCACGTGTTGGTCAACATTTATGGTGGACGGGCTCCAGAAAGTATAGATGTGCAAGTCAACATTTGGGTTTGAGCAT
ATTTATTTCTTCTGCTCACTGGATGCAATAGTGTCTTACATAGATCCGAGAGGTAAGGAGTAAAAGCTGGGCTTTTAAATCTTA
CGCTACAGAGAAAATAGGCTACTGGGAACCACGAGACATCACTGCAGTAGTTTCCAAGTGGATTTTCCAGTCACTCATTGTGA
ATCCTGACAAAACCTGCGATATGGGGTGGTCTTACGGTGGGTTCACTACGCTTAAAGCATTGGAATATGATTCTGGAGAGGTT
TTCAAATATGGTATGGCTGTTGCTCCAGTAACATAATGGCTTTTGTATGACTCCATCTACACTGAAAGATACATGAACCTTCC
AAAGGACAATGTTGAAGGCTACAGTGAACACAGCGTCATTAAGAAGGTTTCCAATTTTAAAGATGTAACCCGATTCTTGGTTT
GTCACGGGACTAGTATGATAACGTGCATTTTTCAGAACACACTAACCTTACTGGACCAGTTCAATATTAATGGTGTGTGAAT
TACGATCTTACGGTGTATCCCGACAGTGAACATAGCATTGCCATCAACAACGCAAATAAAGTGATCTACGAGAGGTTATTCAA
GTGGTTAGAGCGGGCATTTAACGATAGATTTTTGTAA

>PpHAC1s

ATGCCCGTAGATTCTTCTCATAAGACAGCTAGCCCACTTCCACCTCGTAAAAGAGCAAAGACGGAAGAAGAAAAGGAGCAGCG
TCGAGTGAACGATCTCCTACGTAATAGGAGAGCGGCCATGCTTCCAGAGAGAAGAAACGAAGACACGTTGAATTTCTGGAAA
ACCACGTCGTCGACCTGGAATCTGCCTTCAAGAATCAGCCAAAGCCACTAACAAGTTGAAAGAAAATACAAGATATCATTGTT
TCAAGGTTGGAAGCCTTAGGTGGTACCGTCTCAGATTTGGATTTAACAGTTCGGAAGTCGATTTTTCCCAAATCTTCTGATTT
GGAACCCATGTCTGATCTCTCAACTTCTTCGAAATCGGAGAAAGCATCTACATCCACTCGCAGATCTTTGACTGAGGATCTGG
ACGAAGATGACGTCGTTGAATATGACGACGAAGAAGAGGACGAAGAGTTACCCAGGAAAATGAAAGTCTTAAACGACAAAAAC
AAGAGCACATCTATCAAGCAGGAGAAGTTGAATGAACCTCCATCTCCTTTGTCATCCGATTTTTTCAGACGTAGATGAAGAAAA
GTCAACTCTCACACATTTAAAGTTGCAACAGCAACAACAACACAGTAGACAATATGTTTCTACTCCTTTGAGTCTTCCGG
AGGATTCAGTTGATTTTATTAACCCAGGTAACCTAAAAATAGAGTCCGATGAGAATCTTGTGTTGATTCAAATACTTTACAA
ATAAAACACGAAAATGACACCGACTACATTACTACAGCTCCATCAGGTTCCATCAATGATTTTTTTAAATCTTATGACATTAG
CGAGTCGAATCGGTTGCATCATCCAGCAGCACCATTTACCCTAATGCATTTGATTTGAAAGTACTTTGTATTCTTCCAGGAAAT
AA

- Curriculum vitae -

Personal data

Name: Florian Wolfgang Krainer
Date of birth: May 5th, 1986
Place of birth: Graz, Austria
Nationality: Austria

Education

Sep 2011 - Jul 2015 Graz University of Technology, Austria:
PhD program "DK Molecular Enzymology".
Oct 2008 - Aug 2011 University of Graz, Austria:
MSc studies "Molecular Microbiology" passed with distinction.
Nov 2010 Bielefeld University, Germany:
International late autumn school on advanced techniques in bacterial genome
research.
April 2010 Polytechnic University of Valencia, Spain:
Summer course on Synthetic Biology.
Sep 2008 - Dec 2008 University of Basel, Switzerland:
Erasmus studentship.
Oct 2005 - Jul 2008 University of Graz, Austria:
BSc studies "Molecular Biology" passed with distinction.
Oct 1996 - Jul 2004 BG / BRG Lichtenfels, Graz:
A levels: Biology (A), Informatics (A), Maths (A), English (A).

Research experience

Aug 2015 - Graz University of Technology, Austria: Institute of Molecular Biotechnology:
Postdoctoral fellow AWS "PRIZE" prototype funding project P1404401:
"Recombinant horseradish peroxidases".
Sep 2011 - Jul 2015 Graz University of Technology, Austria: Institute of Molecular Biotechnology:
PhD thesis "Production and characterization of recombinant plant peroxidases in
Pichia pastoris".
Oct 2013 - Apr 2014 University of Manchester, UK: Manchester Institute of Biotechnology:
Research stay in the laboratory of Professor Andrew W. Munro.
Jan 2010 - Aug 2011 Graz University of Technology, Austria: Institute of Molecular Biotechnology:
Master's thesis "Recombinant Horseradish Peroxidases".
Aug 2009 - Sep 2009 Annikki GmbH, Graz, Austria:
Summer internship.
Apr 2009 - Jun 2009 Graz University of Technology, Austria: Institute of Molecular Biotechnology:
Research fellowship.
Jul 2008 - Aug 2008 University of Graz, Austria: Institute of Molecular Biosciences:
Summer internship.
Jul 2007 - Aug 2007 University state hospital, Graz, Austria: Pediatric Hematology & Oncology:
Summer internship.

Teaching experience

- 2013 NAWI Graz Doctoral Schools Molecular Biology and Biochemistry & Molecular Biosciences and Biotechnology, Graz, Austria: Organization of 9th Doc Day.
- 2012 Austrian Centre of Industrial Biotechnology (ACIB GmbH), Graz, Austria: Teaching assistant in "Hands-on Pichia course".
- 2011 - 2013 Graz University of Technology, Austria: Teaching assistant in "Analysis of DNA- and Protein Sequences" (MOL.504).
- 2011 - 2015 Supervision and tutoring of master's and project students.
- 2010 - 2015 Graz University of Technology, Austria: Tutor in "Laboratory Course Bioinformatics" (MOL.923).

Publications

Patents

- Krainer F. Recombinant peroxidase-protein G fusion protein. Submitted.
- Krainer F, Näätäsaari L, Glieder A, Kulterer M, Reichel V. Horseradish peroxidase isoenzymes. PCT/EP2012/070751.
- Kulterer M, Reichel V, Ribitsch V, Glieder A, Krainer F. Degradation of hormones using recombinant HRP isoenzymes. PCT/EP2013/052939.

Papers

- Krainer FW, Glieder A. Biotechnological production of a peroxidase-protein G fusion protein in *Pichia pastoris*. In preparation.
- Krainer FW, McLean K, Hosford J, Wong LS, Darnhofer B, Birner-Grünberger R, Glieder A, Munro AW. Characterization of recombinant horseradish peroxidase isoenzymes from *Pichia pastoris*. In preparation.
- Krainer FW, Gerstmann MA, Darnhofer B, Birner-Grünberger R, Glieder A. Systematic assessment of strategies for improved production of recombinant plant peroxidase in *Pichia pastoris*. In preparation.
- Vogl T, Ahmad M, Krainer FW, Schwab H, Glieder A. Restriction site free cloning (RSFC) plasmid family for seamless, sequence independent cloning in *Pichia pastoris*. Submitted to *Microbial Cell Factories*.
- Krainer FW, Capone S, Jäger M, Vogl T, Gerstmann M, Glieder A, Herwig C, Spadiut O. Optimizing cofactor availability for the production of recombinant heme peroxidase in *Pichia pastoris* (2015). *Microbial Cell Factories* 14: 4.
- Krainer FW, Glieder A. An updated view on horseradish peroxidases: recombinant production and biotechnological applications (2015). *Applied Microbiology and Biotechnology* 99:1611-1625.
- Krainer FW, Pletzenauer R, Rossetti L, Herwig C, Glieder A, Spadiut O. Purification and basic biochemical characterization of 19 recombinant plant peroxidase isoenzymes produced in *Pichia pastoris* (2014). *Protein Expression and Purification* 95: 104-112.
- Näätäsaari L, Krainer FW, Schubert M, Glieder A, Thallinger GG. Peroxidase gene discovery from the horseradish transcriptome (2014). *BMC Genomics* 15: 227-242.
- Spadiut O, Capone S, Krainer F, Glieder A, Herwig C. Microbials for the production of monoclonal antibodies and antibody fragments (2014). *Trends in Biotechnology* 32: 54-60.
- Krainer FW, Gmeiner C, Neutsch L, Windwarder M, Pletzenauer R, Herwig C, Altmann F, Glieder A, Spadiut O. Knockout of an endogenous mannosyltransferase increases the homogeneity of glycoproteins produced in *Pichia pastoris* (2013). *Scientific Reports* 3: 3279-3291.
- Krainer FW, Dietzsch C, Hajek T, Herwig C, Spadiut O, Glieder A. Recombinant protein expression in *Pichia pastoris* strains with an engineered methanol utilization pathway (2012). *Microbial Cell Factories* 11: 22-35.

Posters and presentations

Jul 2014	OxiZymes 2014, Vienna, Austria.
Jun 2014	EMBO Conference Enzyme mechanisms by biological systems, Manchester, UK.
2011 - 2014	Doc Days, NAWI Graz Doctoral Schools Molecular Biology and Biochemistry & Molecular Biosciences and Biotechnology, Graz, Austria.
2011 - 2014	Graduate Seminars, PhD program "DK Molecular Enzymology", Graz, Austria.
Dec 2012	Zing Biocatalysis conference 2012, Xcaret, Mexico.
Sep 2012	OxiZymes 2012, Marseille, France.
Jul 2012	ACIB Science Days 2012, Vienna, Austria.
Feb 2012	Pichia 2012, Alpbach, Austria.
Nov 2010	ESF-Bielefeld-CeBiTec Conference Microbes and Industrial Biotechnology, Bielefeld Germany.

Grants and awards

2015	"Ideenwettbewerb 2015" (innovation competition) of the Science Park Graz, 3rd place: 1,500.00 €.
2014	"PRIZE" Prototypenförderung (prototype funding) of the AWS (Austrian federal promotional bank): 100,000.00 €.
2014	Merit scholarship of the Graz University of Technology, Austria.
2007	Merit scholarship of the University of Graz, Austria.
2006	Merit scholarship of the University of Graz, Austria.